UNIVERSITÀ DEGLI STUDI DI PALERMO
Dottorato di Ricerca in Scienze Chimiche
Dipartimento di Fisica e Chimica
S.S.D. – CHIM/06

LIQUIDI IONICI E FULLERENI: PIATTAFORME PER NUOVI MATERIALI

IONIC LIQUIDS AND FULLERENES: PLATFORMS FOR NEW MATERIALS

IL DOTTORE
Vincenzo Campisciano

IL COORDINATORE
Prof. Paolo Lo Meo

IL TUTOR
Prof. Michelangelo Gruttadauria

IL CO-TUTOR
Dr. Francesco Giacalone

CICLO XXVI
2016

Riassunto

Il fullerene C_{60} è stato modificato covalentemente, mediante reazione di Bingel, con diversi esteri malonici, dando origine sia a derivati monoaddotti che a derivati esaaddotti altamente simmetrici caratterizzati da una simmetria di tipo ottaedrico. L'ulteriore funzionalizzazione di tutti i derivati ottenuti con 1-metilimidazolo, 1,2-dimetilimidazolo o 1-butilimidazolo ha portato alla formazione di nuovi sistemi ibridi fullerene C_{60}-liquidi ionico (IL) aventi peculiari proprietà come l'elevata solubilità in acqua (superiore a 800 mg/mL in alcuni casi). Uno dei sistemi ibridi C_{60}-IL è stato usato come supporto per nanoparticelle di palladio, procedendo dapprima allo scambio anionico con gli ioni tetracloropalladato usati come precursori delle nanoparticelle metalliche generate mediante riduzione con sodio boroidruro. In seguito al processo di riduzione, si è avuta la formazione di alcune nanostrutture carboniose, compresi dei *carbon nanoonions*. Il materiale così ottenuto è stato ampiamente caratterizzato mediante diverse tecniche quali l'analisi termogravimetrica (TGA), la spettroscopia fotoelettronica a raggi X (XPS), la microscopia elettronica a scansione accoppiata con l'analisi a raggi X a dispersione di energia (SEM-EDAX) e la microscopia elettronica a trasmissione ad alta risoluzione (HR-TEM). Questo nuovo materiale è stato usato con successo come catalizzatore nelle reazioni di accoppiamento C–C di Suzuki e di Heck con un carico dello 0,2 mol%. Inoltre, è stato possibile riciclare il catalizzatore usato nella reazione di Suzuki fino a cinque volte senza perdita di attività catalitica (Capitolo 1, *C_{60}-IL hybrids*).

Sulla base dei buoni risultati ottenuti con il catalizzatore basato sul sistema ibrido C_{60}-IL, si è pensato di sviluppare una nuova procedura sintetica al fine di ancorare tale sistema catalitico su diversi supporti quali la silice amorfa, la silice mesostrutturata SBA-15 e nanoparticelle paramagnetiche di maghemite (γ-Fe_2O_3) ricoperte di silice. Tutti i nuovi materiali sintetizzati, così come i sistemi catalitici, ottenuti in seguito all'immobilizzazione di nanoparticelle di palladio, sono stati caratterizzati tramite TGA, fisisorbimento di azoto (BET, BJH), scattering di raggi X a basso angolo (SAXS), diffrazione di raggi X (XRD), XPS e HR-TEM. Questi sistemi catalitici si sono mostrati attivi nella catalisi delle reazioni di Heck e di Suzuki, raggiungendo, nel caso della reazione di Suzuki, elevati valori di TON (100.000) e di TOF (2.000.000 h^{-1}). Inoltre, sono stati condotti dei test per verificare la riciclabilità di tali materiali catalitici, riuscendo a utilizzare il catalizzatore supportato su

silice amorfa per dieci cicli consecutivi, sia nella reazione di Heck che in quella di Suzuki (Capitolo 1, *Supported C_{60}-IL hybrids*).

I nanotubi di carbonio a parete singola (SWCNTs) sono stati usati, in unione a dendrimeri poliammidoamminici (PAMAM) di generazione 2.5 e 3 caratterizzati dalla presenza di un *core* cistaminico, per la sintesi convergente di diversi materiali ibridi SWCNT-PAMAM ottenuti per reazione diretta dei nanotubi con i dendrimeri in toluene a riflusso. In seguito, l'immobilizzazione delle specie di palladio(II) ($PdCl_4^{2-}$) nella *shell* dendrimerica e la loro successiva riduzione con sodio boroidruro hanno portato alla produzione di nanoparticelle di palladio di piccole dimensioni, omogeneamente disperse su tutta la lunghezza dei nanotubi. Uno dei materiali sintetizzati si è rivelato attivo nelle reazioni di Suzuki e di Heck riuscendo a promuovere il primo processo anche con un carico molto basso dello 0,005 mol%, mostrando un TON di 20.000 e un valore di TOF corrispondente a 240.000 h^{-1}. È stato possibile, inoltre, recuperare e riciclare il materiale catalitico fino a sette volte. In aggiunta, ulteriori esperimenti hanno permesso di dimostrare come, in entrambi i processi catalitici, sia coinvolto un meccanismo di tipo "*release and catch*" sebbene, durante la reazione di Heck, specie cataliticamente attive del palladio possono essere stabilizzate dalla presenza del solvente e della base e quindi essere rilasciate in soluzione. Nella reazione di Suzuki, invece, non è stata rilevata la presenza di specie del palladio rilasciate in soluzione in seguito al processo catalitico (Capitolo 2).

L'ottimizzazione delle procedure sintetiche, mediante irraggiamento con microonde, dei principali derivati del fullerene C_{60} e C_{70} (PCBM, DPM6, BHN e ICBA), usati come specie accettrici nelle celle solari organiche a eterogiunzione *bulk*, ha portato all'ottenimento di risultati migliori rispetto a quelli riportati in letteratura, sia in termini di resa che di tempo di reazione. Tali risultati rappresentano un passo avanti verso la produzione di celle solari organiche sempre più economiche grazie all'abbattimento dei costi di produzione delle specie accettrici, sintetizzate con alte rese e con brevi tempi di reazione che portano a un notevole risparmio energetico (Capitolo 3).

Abstract

The synthesis of innovative catalysts based on different carbon nanoforms (CNFs), namely fullerene C_{60} and carbon nanotubes (CNTs), and their application in Suzuki and Heck C–C coupling reactions, constitutes the common thread of the first part (Chapter 1 and 2) of this thesis. C_{60} and CNTs were functionalized with ionic liquids (ILs) and poly-amidoamine (PAMAM) dendrimers, respectively, and used as supports for palladium nanoparticles (PdNPs). Moreover, additional supported catalytic systems based on one of the synthesized C_{60}-IL hybrids were prepared and successfully employed in the title coupling reactions.

The final part (Chapter 3) of the thesis deals on the microwave-mediated synthesis optimization of some fullerene-based acceptors species for organic photovoltaics (OPV). In such a way, the main C_{60}- and C_{70}-based acceptor derivatives for organic solar cells, such as PCBM, DPM6, BHN and ICBA, were obtained in higher yields and shorter reaction times with respect to the data reported in literature. These findings represent a step forward toward the wide production of cheaper organic solar cells as a consequence of the cost abatement of the acceptors given by higher yields, lower waste production, and reduced reaction time which means a strong energy saving.

Acknowledgements

I would first of all like to thank my tutor Prof. Michelangelo Gruttadauria and my co-tutor Dr. Francesco Giacalone for their fundamental contribution to my scientific growth. The continuous exchange of views and all the constructive dialogues engaged with them constituted for me a great motivation to increase my enthusiasm for research and to go forward in my PhD experience. I want also to thank Dr. Leonarda Francesca Liotta and Dr. Valeria La Parola of Centro Nazionale delle Ricerche – Istituto per lo Studio dei Materiali Nanostrutturati (CNR-ISMN) for their precious collaboration for the characterization of some materials by means TGA, XRD, SAXS, XPS and MP-AES experiments. I am also grateful to Prof. Carmela Aprile who supervised me during my period abroad at University of Namur (Belgium), where I was warmly welcomed by her research group (Dr. Luca Fusaro, Dr. Esther Carbonell, Dr. Mireia Buaki-Sogo, Dr. Xavier Collard, Lucia Anna Bivona and Alvise Vivian) to which I am very grateful for the interesting scientific experience.

Contents

Chapter 1

Synthesis and Catalytic Activity in Suzuki and Heck reactions of new Fullerene-Ionic Liquids Conjugates

Part of this chapter has been published in Chem. Eur. J. **2015**, *21*, 3327-3334.

1.1 Introduction

In the last decades, ionic liquids (ILs) have experienced a growing interest in their study and applications.[1] Nowadays ILs constitute an interdisciplinary research topic that link different scientific fields like chemistry, biology and engineering.[2] According to their definition, ILs are materials composed of ions and with a melting point below 100 °C. However, behind this simple definition hides a class of compounds with unique features. The reasons of the huge potential of ILs must be seek in the possibility of tune their physical and chemical properties depending on the nature of the cations or anions. A very low vapour pressure, wide liquid range, high ionic conductivity and excellent thermal and chemical stability are some of these properties that makes ionic liquids an alternative green media to common organic solvents.[3] ILs find applications in several fields such as synthesis and catalysis,[1a, 4] biotechnology,[5] separation science,[6] energy storage,[7] electrochemistry, and sensing,[8] among others. In addition, the scope of application of ILs can be further extended by the introduction of specific functional moieties leading to the so-called task specific ionic liquids (TSILs).[9] According to the definition proposed by Davis,[9c] TSILs are a particular class of ILs that, after the covalent modification of the cation and/or anion with a functional group, can exert a specific action. Such materials find application in a wide range of processes like catalysis,[10] CO_2 capture,[11] extraction of metal ions,[12] and also preparation of carbon based materials and zeolites.[13]

Another important application of ILs concerns their use as dispersion media and stabilizers of metal nanoparticles (MNPs). Transition MNPs have received great attention owing to their unique properties related to their small size and consequent large surface to volume ratio. The preparation of MNPs with high surface area and small size distribution is fundamental both for the field of catalysis[14] and also for a wide range of applications, such as photoluminescence, optical sensors, etc.[15] Small-size MNPs are fairly unstable and they will tend to combine into thermodynamically stable larger particles via agglomeration.[16] The agglomeration process is driven by the energetically favored formation of larger particles. This phenomenon rests on the principle that coordinatively unsaturated surface atoms of a particle have a higher energy than the fully coordinated and well-ordered inner atoms. Since the system will tend to reduce its overall energy, there will be a decrease in the number of small particles with respect to the number of the larger ones. Usually, the synthesis of small sized nanoparticles requires the use of stabilizing agents like surfactants

or also capping agents that form a kind of layer that provide protection against the agglomeration. ILs constitute a unique media that thanks to their intrinsic features provide both an electrostatic and steric stabilization of MNPs. The exact stabilization mode of MNPs by ILs is still matter of discussion.[17]

Early studies, directed towards understanding the type of interaction between ILs and MNPs, were carried out using X-ray photoelectron spectroscopy (XPS) and are based on the DLVO (Derjaguin-Landau-Verwey-Overbeek) model.[18] XPS analysis revealed that stabilization of MNPs was essentially given by counterion of imidazolium based ILs. The results obtained suggested that anions interacted with the surface of MNPs forming a negatively charged layer, which, in turn, is covered by a layer of cations (imidazolium moiety). In such a way, the stabilization of MNPs was achieved *via* the creation of coulombic repulsion between NPs (**Figure 1a**).

Finke *et al.* studied the iridium NPs catalyzed hydrogen-deuterium exchange at all aromatic positions of the 1-butyl-3-methylimidazolium cation. Results confirmed the at least transiently formation of *N*-heterocyclic carbene (NHC)-type that can interact and stabilize MNPs (**Figure 1b**).[19]

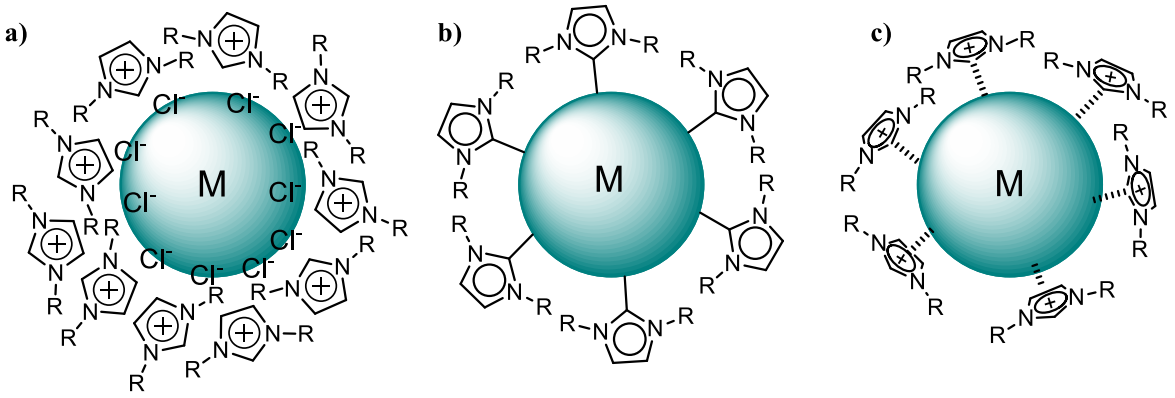

Figure 1. *Different stabilization modes of metal nanoparticles in ionic liquids.*

However, other studies, by Dupont *et al.*, using an ether modified imidazolium species revealed a direct interaction between gold NPs and imidazolium cation (**Figure 1c**).[20] The establishment of the interaction between IL and gold NPs was pointed out by means of a surface-enhanced Raman spectroscopy (SERS) study. Raman spectra revealed that imidazolium ring vibrational modes of 1-triethylene glycol monomethyl ether-3-methylimidazolium methanesulfonate were enhanced and shifted to lower wavenumbers in comparison with the spectrum of neat imidazolium methanesulfonate. In addition, the Raman study revealed no interaction of the methanesulfonate anion with gold NPs. In

another study, Chun *et al.* also claimed that palladium NPs deposited on the surface of IL modified carbon nanotubes were stabilized by a coordination involving the imidazolium cation.[21]

Therefore, given the elevated number of studies reported in literature dealing with ILs-MNPs interaction, the real stabilization mode of MNPs by ILs may depend on the experimental conditions of considered system.

An alternative to the use of ILs as homogeneous dispersion media and stabilizers of MNPs is their heterogenization to give a supported ionic liquid phase (SILP).[22] ILs can be physisorbed[23] or covalently[24] attached to an inert support material (**Figure 2**). Although the heterogenization of the catalyst lead to active sites that can be poorly accessible and usually less active than in a homogeneous system, the advantage of an easily recoverable and reusable catalyst is the reason why to point towards heterogeneous systems.

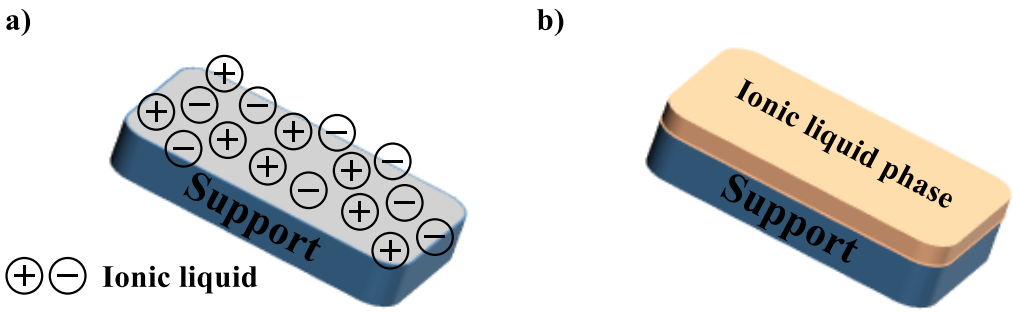

Figure 2. *Representation of a) physisorbed and b) covalently attached ionic liquid on support material.*

The most used support materials for SILP are usually commercially available silica gels but also MCM-41 and SBA-15 in addition to zeolites, clays, carbon nanotubes (CNTs), metal oxide nanoparticles etc.[25] A good support material must have some important features such as a large surface area, high chemical and thermal stability and also a good mechanical strength. Among support materials, magnetic nanoparticles have an intrinsic advantage owing to their paramagnetic nature that allow an easily recover of the catalyst by an external magnet avoiding centrifugation or filtration process. During the years, SILPs have found a wide range of applications.[25a, 26] The great importance of SILP is due to the synergistic effect between the IL and the support material. In such a way, it is possible to obtain a material with an improved recover ability compared with homogeneous IL phase and, above all, it is also possible to lower costs reducing the amount of employed IL. Furthermore, another key point is the possibility to transfer the IL properties to the heterogeneous material. Therefore, the SILP can constitute a heterogeneous phase in which dissolve a homogeneous

catalyst[23, 24b, 27] or also stabilize MNPs.[28]

Lately, ILs have begun to find application in combination with carbon nanomaterials. ILs were used as reaction media with the purpose to achieve the functionalization of carbon nanoforms (CNFs) such as fullerene C_{60}[29] or CNTs.[29a, 30] An interesting example of this application of ILs is that reported by Prato *et al.*[29a, b] in which the microwave mediated functionalization of C_{60} by 1,3-dipolar cycloaddition of azomethine ylides in high yield and in few minutes, using a 1:3 octyl methylimidazolium tetrafluoroborate ([omim]BF_4)-oDCB mixture, was achieved (**Scheme 1**).

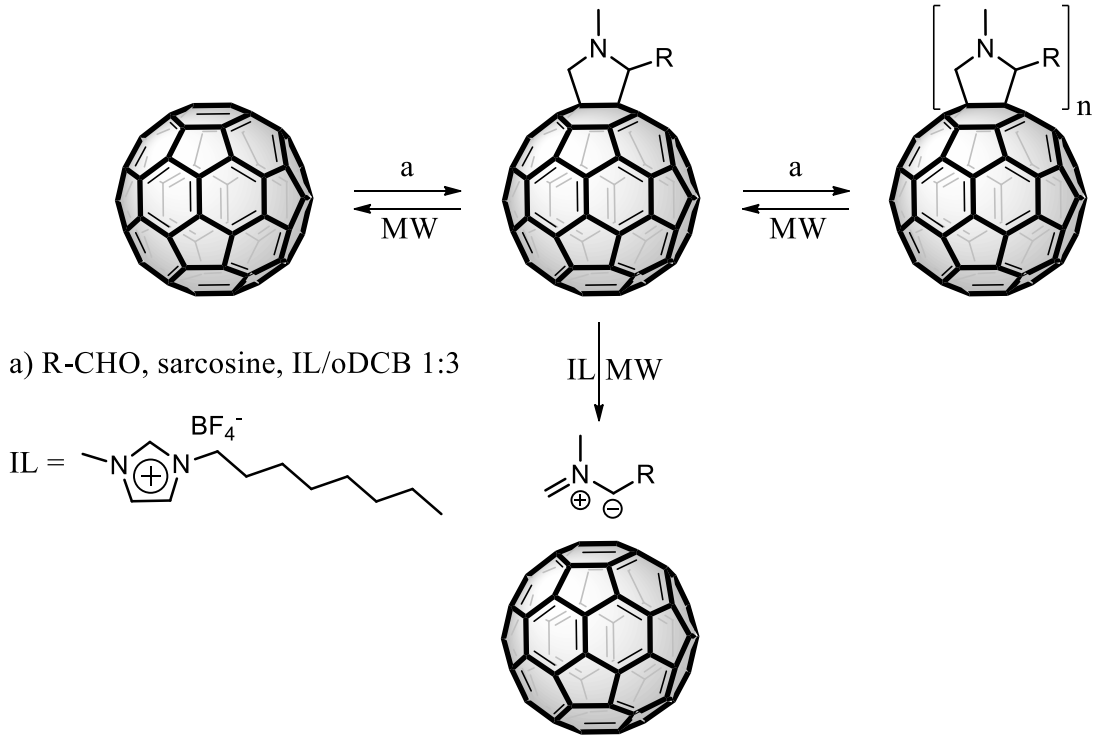

Scheme 1. *Functionalization of fullerene C_{60} in ionic liquid under microwave irradiation.*

Conversely, microwave irradiation of the solution of the so-formed fulleropyrrolidines in neat [omim]BF_4 lead to the cycloreversion originating the starting insoluble C_{60} (**Scheme 1**). The role of ILs is not only limited to that of reaction media for the functionalization of CNFs. In 2003, Fukushima *et al.*[31] found that the simple mixing and subsequent grinding of an imidazolium based IL with pristine single walled carbon nanotubes (SWCNTs) gave rise to physical gels, the so-called bucky gels. Both Raman and IR studies in conjunction with DFT calculation have established that no strong interaction such as cation-π interaction are present between SWCNTs and imidazolium cation.[32] The dispersion of SWCNTs in ILs is probably due to their shielding effect on the π-π stacking interaction of SWCNTs. It is for

this reason that the mixing of ILs with SWCNTs causes the debundling of entangled nanotubes. In addition, the specific interactions between ILs and nanocarbons afford to the hybrids unique properties as well as improved dispersibility in various media that can be employed in electrochemical and energy-storage devices or as supports for catalysis.[33]

ILs have been also used for the covalent modification of the surface of CNFs (single- and multiwalled nanotubes, nanohorns, and graphene) and several examples of this type of functionalization were reported.[25e, 34]

Despite the large number of examples for CNF-IL hybrids, just few reports deal with the chemical functionalization of fullerene C_{60} with ILs. C_{60} was modified to obtain a series of fulleropyrrolidine–imidazolium[35] and pyridinium[36] salts and to study their solubility profiles. Furthermore, two more examples were reported in which covalently modified C_{60}-IL hybrids were used for interesting application. More deeply, a Eu(III) complex was successfully encapsulated in CNTs using a C_{60}-IL hybrid as nano-carrier.[37] Moreover, Nierengarten, Stoddardt *et al.*[38] synthesized a C_{60} bearing twelve 4,4'-bipyridinium subunits which can undergo a redox-switchable π-dimerization of bipyridinium moieties. Fullerene C_{60}–IL hybrids will doubtless constitute a new class of materials that could find applications in several fields. In this regard, fullerene C_{60}–IL mixtures have been successfully employed as glucose sensors[39] or in the preparation of stationary phases for gas chromatography.[40] Analogously, zwitterionic multicharged fullerene derivatives have been used for gene delivery[41] or in medicinal chemistry.[42]

1.2 Aim of the Chapter

A series of fullerene C_{60}-IL hybrids have been synthesized and fully characterized by means of thermogravimetric analysis (TGA), XPS, X-ray diffraction (XRD), scanning electron microscopy/energy-dispersive X-ray analysis (SEM-EDAX), and high-resolution transmission electron microscopy (HR-TEM). The number of ILs moieties of such hybrids, as well as anions and cations have been varied.

In the light of the above considerations, taking into account the possibility to achieve a good MNPs stabilization using ILs, one of these hybrids has been used for the immobilization of palladium nanoparticles and used as catalyst for C–C coupling reactions (Suzuki and Mizoroki–Heck reactions).

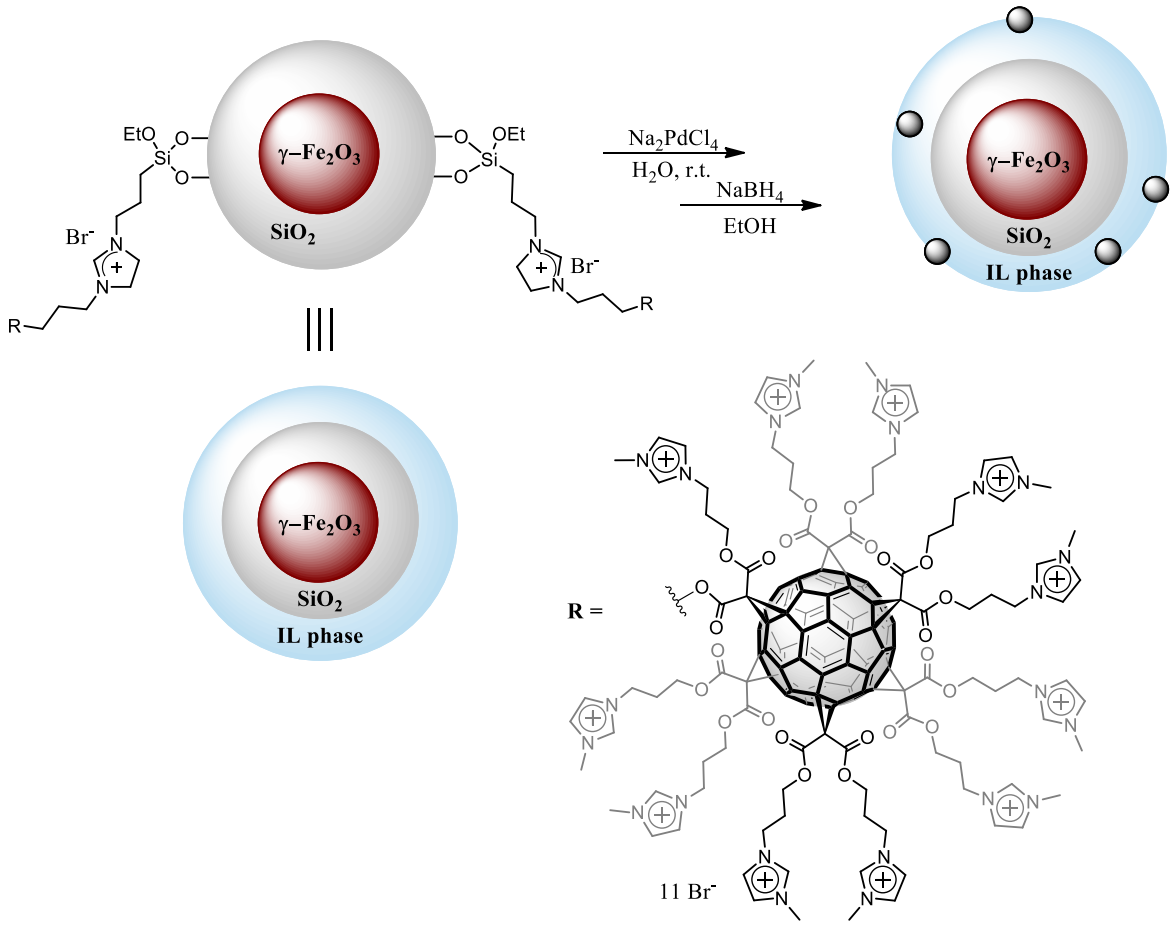

Scheme 2. *Schematic representation of one of the synthesized supported catalysts.*

In such a way fullerene C_{60} was used as molecular scaffold for ILs that, in turn, stabilize PdNPs, obtaining a recyclable and reusable catalyst by means of simple centrifugation processes. A similar use of C_{60} was reported only in one case in which a

biguanide(metformine)-functionalized fullerene C_{60} was used as support for palladium and the so-obtained catalyst used for the catalysis of Suzuki reaction.[43]

Encouraged by results obtained, the covalent immobilization of C_{60}-based catalyst on several supports such as silica, SBA-15 and silica-coated maghemite (γ-Fe_2O_3@SiO_2) by following a new synthetic strategy has been also carried out. Surprisingly, catalytic tests showed that the supported catalysts (**Scheme 2**) are more active than the unsupported one, both in the Suzuki and in Heck reaction. The higher catalytic activity of the supported catalyst could be ascribed to the benefit arising from the optimal dispersion of the C_{60}-IL moiety on the support materials and probably to the higher stability of PdNPs with respect to unsupported catalyst. In this way, the supported C_{60}-IL moiety forms a kind of monolayer of IL in which immobilize PdNPs. The optimal dispersion of the catalytic sites and their stability are key points in heterogeneous catalysis and this could be the reason of this unprecedented high catalytic activity.

C_{60}-IL hybrids
1.3 Results and Discussion

The synthesis of the novel C_{60}-IL derivatives starts, firstly, from the preparation of malonates **1a-c**[44] that were obtained starting from the malonyl chloride and the properly substituted propanol. Hence, the fullerene-derivatives endowed with two moieties of IL **3a** and **3b** have been obtained through Bingel cyclopropanation[45] reaction followed by nucleophilic substitution with 1-butylimidazole in quantitative yields (**Scheme 3**).

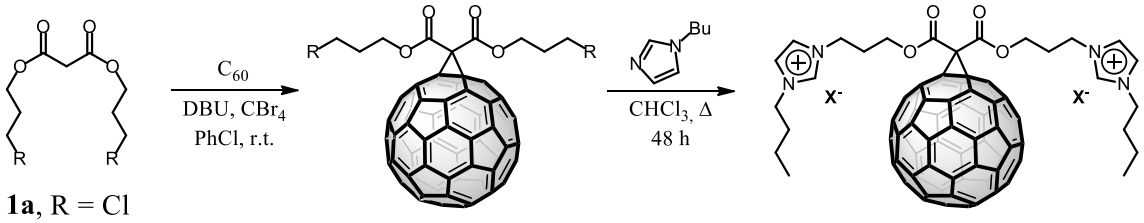

1a, R = Cl
1b, R = Br
1c, R = N_3

2a, R = Cl, 45%
2b, R = Br, 41%

3a, X = Cl, quant. from **2a**
3b, X = Br, quant. from **2b**

Scheme 3. *Synthesis of C_{60}–IL **3a** and **3b** (DBU=1,8-diazabicyclo[5.4.0]undec-7-ene).*

Next, the syntheses of C_{60}-IL conjugates bearing twelve ionic liquid moieties arranged in an octahedral addition pattern have been carried out by following the protocol of Sun *et al.*[46]

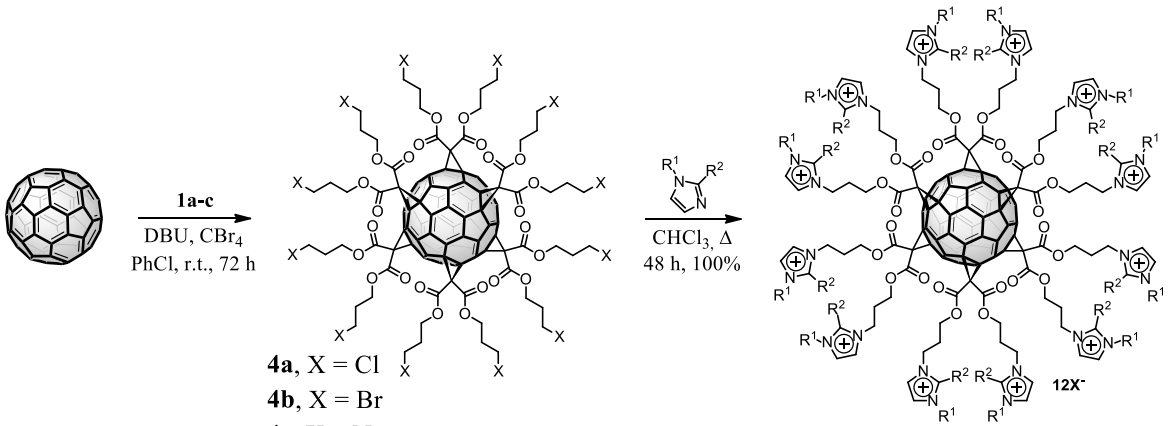

4a, X = Cl
4b, X = Br
4c, X = N_3

5a, R^1 = Me; R^2 = H; X = Br, quant. from **4b**
5b, R^1 = Me; R^2 = Me; X = Br, quant. from **4b**
5c, R^1 = Bu; R^2 = H; X = Br, quant. from **4b**
5d, R^1 = Bu; R^2 = H; X = Cl, quant. from **4a**

Scheme 4. *Synthetic route of the C_{60}-IL conjugates **5a-d**.*

In this way it has been possible to access highly symmetric hexakis-adducts **4a-c** with

satisfactory yields (**Scheme 4**). Then the octahedral intermediate **4b** has been in turn reacted with 1-methylimidazole, 1,2-dimethylimidazole and 1-butylimidazole, and **4a** with 1-butylimidazole in refluxing chloroform to afford the hexakis C_{60}-IL hybrids **5a-d** in quantitative yields. Recently, the synthesis of several fullerene hexakis-adducts through the copper(I)-catalyzed alkyne-azide cycloaddition (CuAAC) "click" reaction[47] that employed a C_{60} dodecakis-alkyne[41b, 48] or the dodecakis-azido derivative **4c**[44a, 49] has been reported. Hence, a different strategy to obtain access to C_{60}-IL conjugate with a different cation has been designed.

As a matter of fact, taking inspiration from the seminal work of Nierengarten and co-workers, derivative **4c** could be employed to build, through the CuAAC approach, a known dodecakis-triazole hybrid.[44a] This could then be easily transformed into the corresponding triazolium salt **6** with benzyl bromide in 80% yield over two steps (**Scheme 5**).

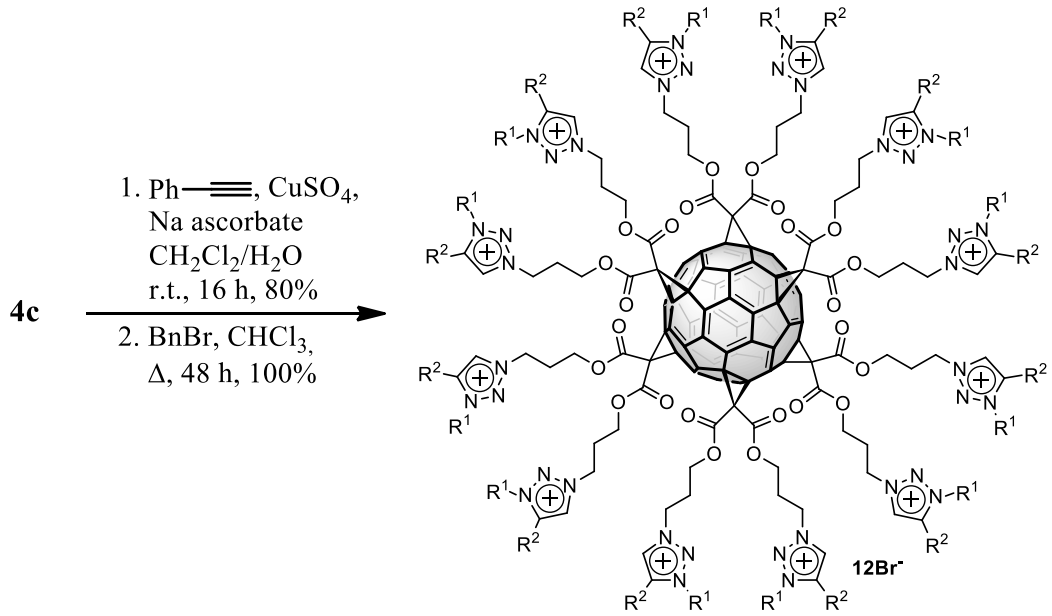

Scheme 5. *Synthetic route of the C_{60}-IL conjugate **6**.*

All the fullerene-IL hybrids were thoroughly characterized and their spectroscopic data are in agreement with the proposed structures. Mono-adduct precursors **2a** and **2b**[44b] showed in the ^{13}C NMR spectra 15 sp^2 signals typical of C_{2v} fullerene derivatives[50] along with the signals at δ = 71 ppm and 52 ppm that belong to the two sp^3 carbons of C_{60} and the carbon atom labelled with the number one (**Figure 3**), respectively.

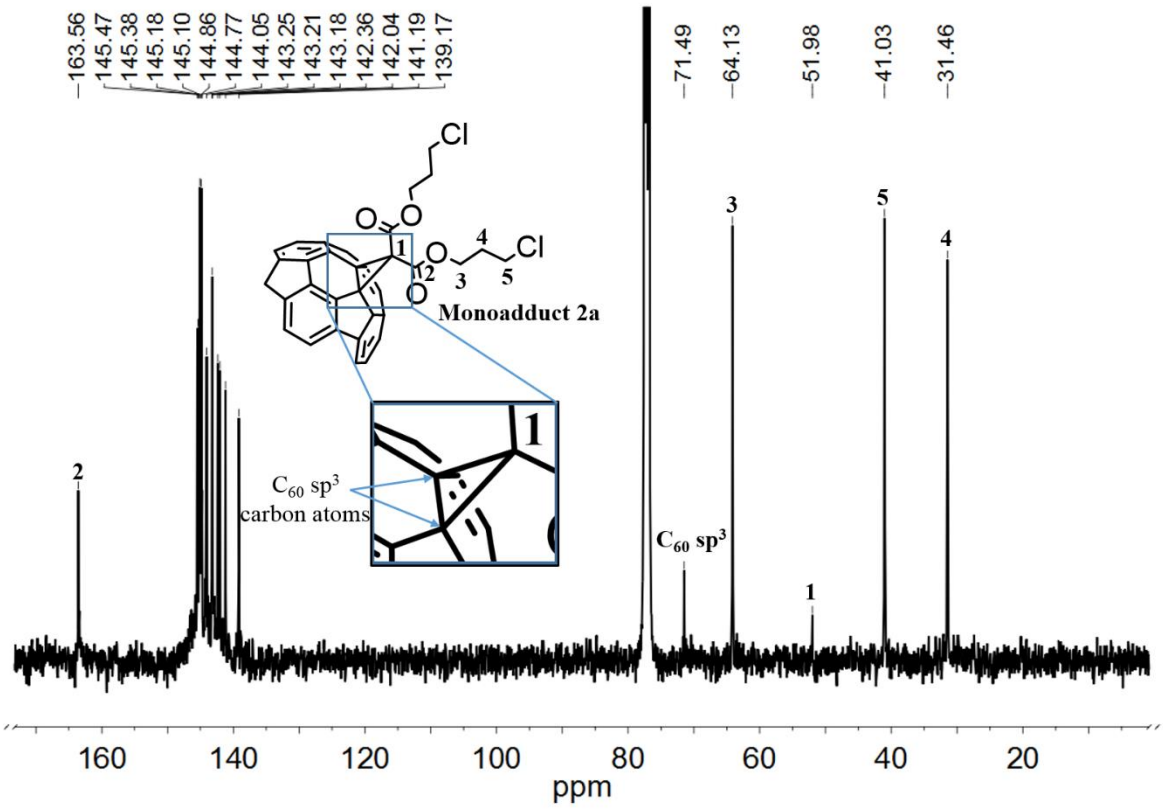

Figure 3. *^{13}C NMR spectrum of compound **2a**.*

The NMR spectra of hybrid derivatives **3a** and **3b** were more complicated, probably owing to strong intermolecular interactions (**Figures E2** and **E3** in the Experimental Section ***1.6***). On the contrary, ^{1}H and ^{13}C NMR spectra of hexakis-adduct are simpler (**Figures E4** and **E5** in the Experimental Section ***1.6***). In the proton spectra of **4a** and **4b** the multiplicity of the three methylenic groups is clearly visible even if the signals are slightly broadened, whereas in the carbon spectra the octahedral substitution pattern of the C_{60} gives rise to two sp^2 signals at δ = 146 and 141 ppm along with an sp^3 signal at δ = 69 ppm. Interestingly, in the ^{1}H NMR spectra of 1-substituted imidazolium C_{60}-IL **5a**, **5c** and **5d** the proton at the C2 position of the imidazolium ring disappears after exchange with the deuterated solvent (compare **Figures 4** and **E8** with **Figure E9** in the Experimental Section ***1.6***). The ^{1}H NMR spectrum of **5c** shows the presence of all the expected signals with their corresponding integrals indicating the good outcome of the reaction (**Figure 4**).

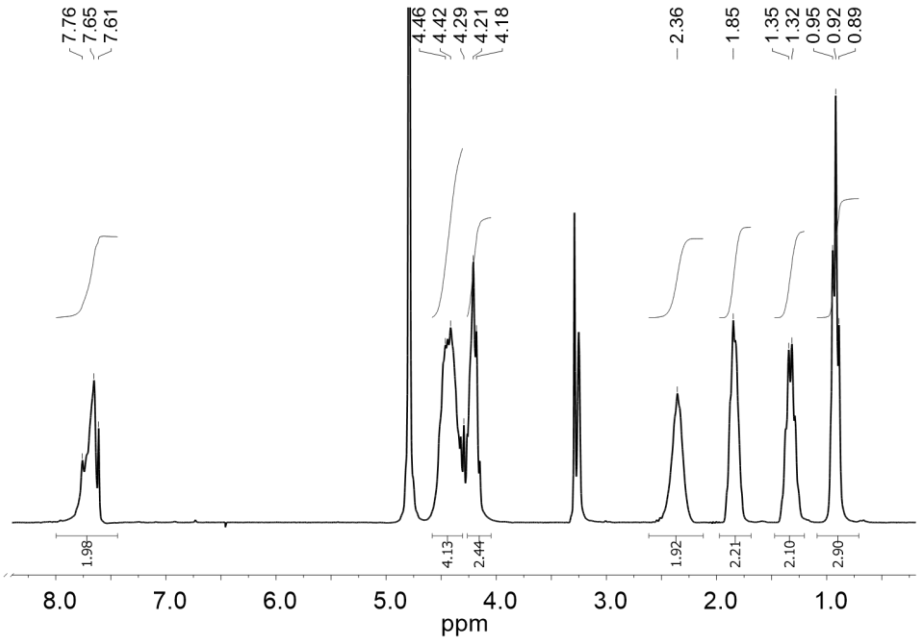

Figure 4. *^{1}H NMR spectrum of compound **5c**.*

The ^{1}H NMR spectrum of the triazolium adduct **6** presents all the signals including ten aromatic protons in the δ = 7.0–8.0 ppm region plus the triazole proton at δ = 9.6 ppm, whereas in its ^{13}C NMR spectra (see **Figure E10** in the Experimental Section ***1.6***) the peaks of the benzyl moiety appear in the δ = 127–132 ppm region along with those of the parent triazole.[44a]

Unfortunately, owing to their highly charged nature, we were unable to get good high-resolution (HR) ESI spectra of the imidazolium-based fullerene-IL hybrids. However, the HR-ESI spectrum of **6** clearly showed the presence of multicharged species with 3, 5 and 6 positive charges (**Figure 5**).

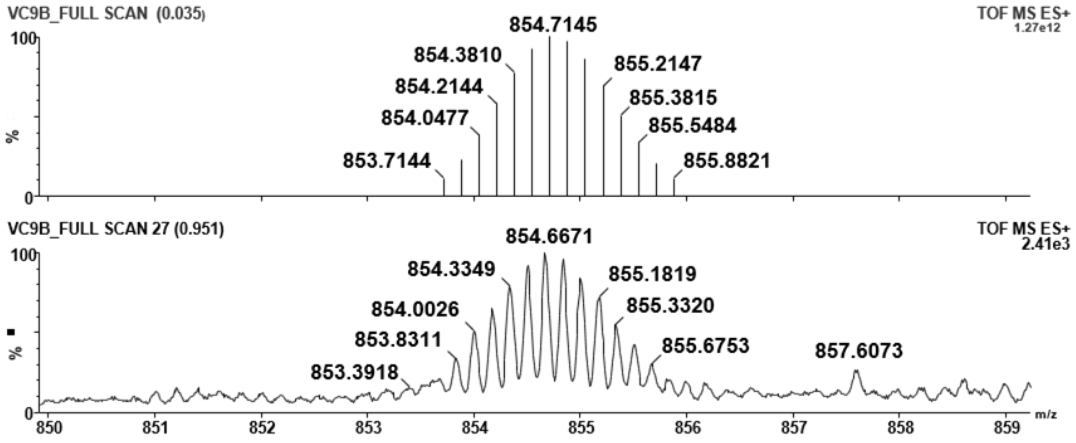

Figure 5. *Simulated (top) and experimental (bottom) HRMS (ESI-TOF) spectrum of [**6**-6Br^{-}]$^{6+}$.*

The presence of the IL moieties on the fullerene cage affords to these hybrids an excellent solubility in polar solvents such as methanol and water. Although several examples of water soluble fullerene mono-adducts[51] and polymers[52] have been described so far, only a few water-soluble octahedral hexakis-adducts have been reported.[53] This is particularly important given that these easily accessible multicharged molecules may find application in gene delivery.[41a, 41c, 42b, 54]

The UV/Vis spectra of **5a-d** recorded in water and in methanol are reported in **Figure 6**. The spectra show no aggregation in water with three transitions at about 240, 275 and 335 nm. Most interestingly, **5a-d** display an outstanding solubility in water at room temperature and pH 7 higher than 800 mg mL^{-1} (0.19–0.21 mol L^{-1}) to form solutions that were stable for months; these are probably the highest values of solubility for fullerene derivatives reported so far.[51-52, 55] The same concentration could be achieved by dissolving hybrid **6** in methanol.

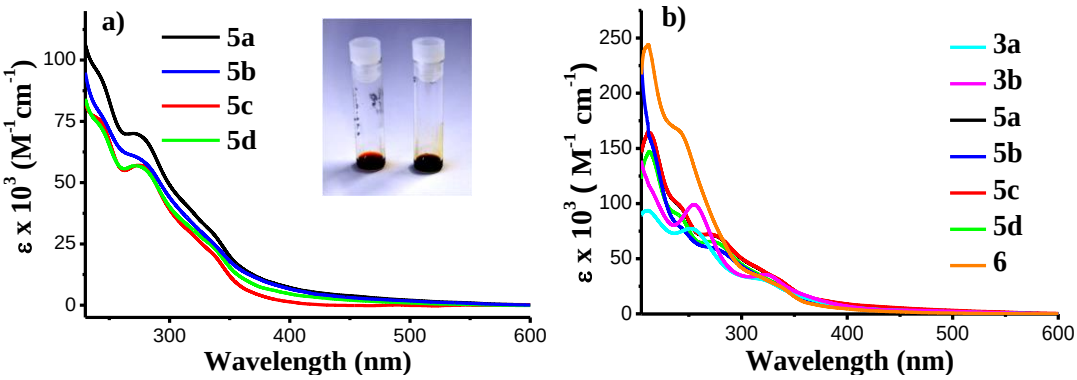

Figure 6. *UV/Vis spectra of C_{60}-IL conjugates **5a-d** a) in water and b) of **3a-b**, **5a-d** and **6** in methanol. The inset in the figure a) shows a picture of 100 mg/mL water solutions of **5c** (left) and **5d** (right).*

With the hybrid C_{60}-IL systems in hand, their possible practical application as support for catalysts was explored. In this regard, palladium nanoparticles were immobilized to prepare a new catalyst for C–C coupling reactions by using our systems as a kind supported ionic liquid-like phase (SILLP)[56] on the fullerene sphere. The synthesis of the catalytic material was accomplished in two steps, as reported in **Scheme 6**. First, tetrachloropalladate ions (10 wt%) were immobilized onto C_{60}-IL **5a** through anion metathesis, hence the supported $PdCl_4^{2-}$ species was reduced with $NaBH_4$ in ethanol.[57] The purification of material **8** from inorganic salts was achieved by means of dialysis using a membrane with a cutoff of 1000 Da to afford a finely dispersed insoluble black powder.

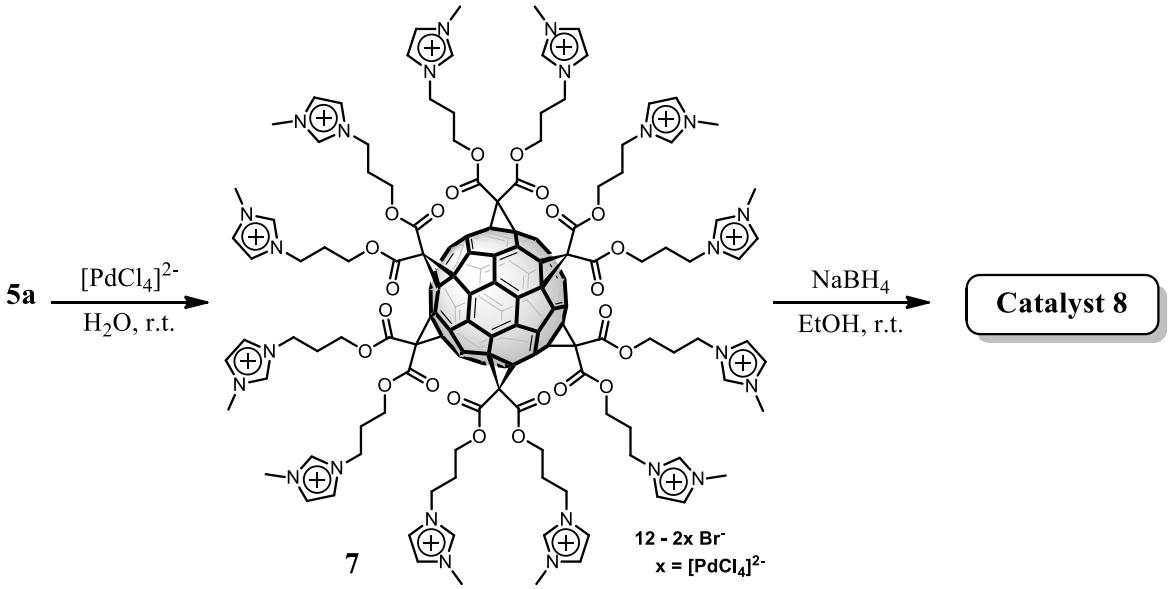

Scheme 6. *Synthesis of catalyst* ***8****.*

Catalyst **8** was characterized by means of several analytical and spectroscopic techniques. Thermogravimetric analysis was performed under oxygen flow from 100 to 1000 °C with a heating rate of 10 °C/min to determine the total amount of Pd species present in the sample and the degradation temperature range (**Figure 7**).

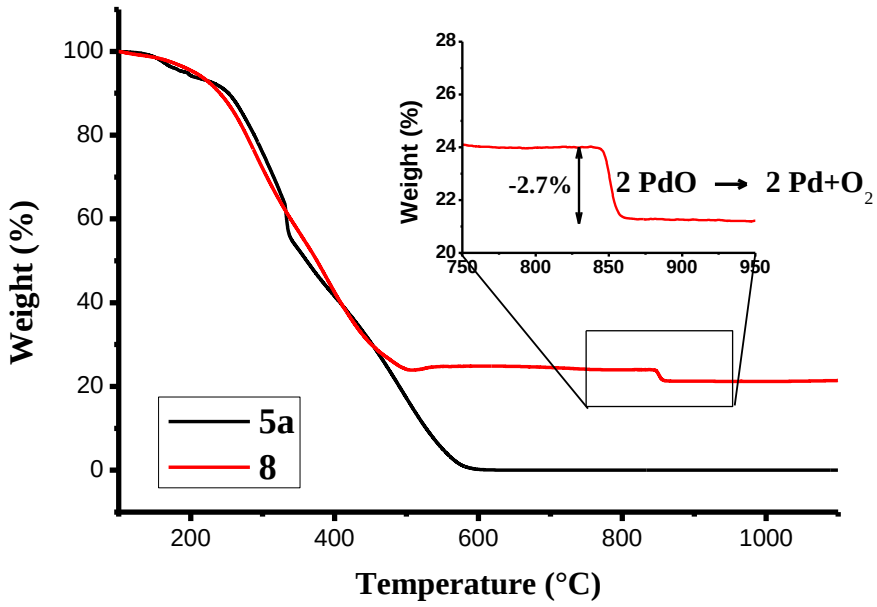

Figure 7. *TGA of* ***5a*** *and* ***8*** *under oxygen flow.*

As expected, the TGA trace of **5a** shows a continuous weight loss in the 140–590 °C range, the temperature at which the combustion is completed and no residue was detected. Conversely, TGA of **8** presents a weight loss with the same slope of **5a** up to approximately

500 °C, after which no additional loss was observed up to 840 °C. Hence, a new small weight loss of 2.7% can be accounted for by the quantitative transformation of PdO to Pd since the former species is not stable over 800 °C.[58] By this last weight loss, the Pd content in sample **8** was calculated, resulting in a loading of 18% as metallic Pd.

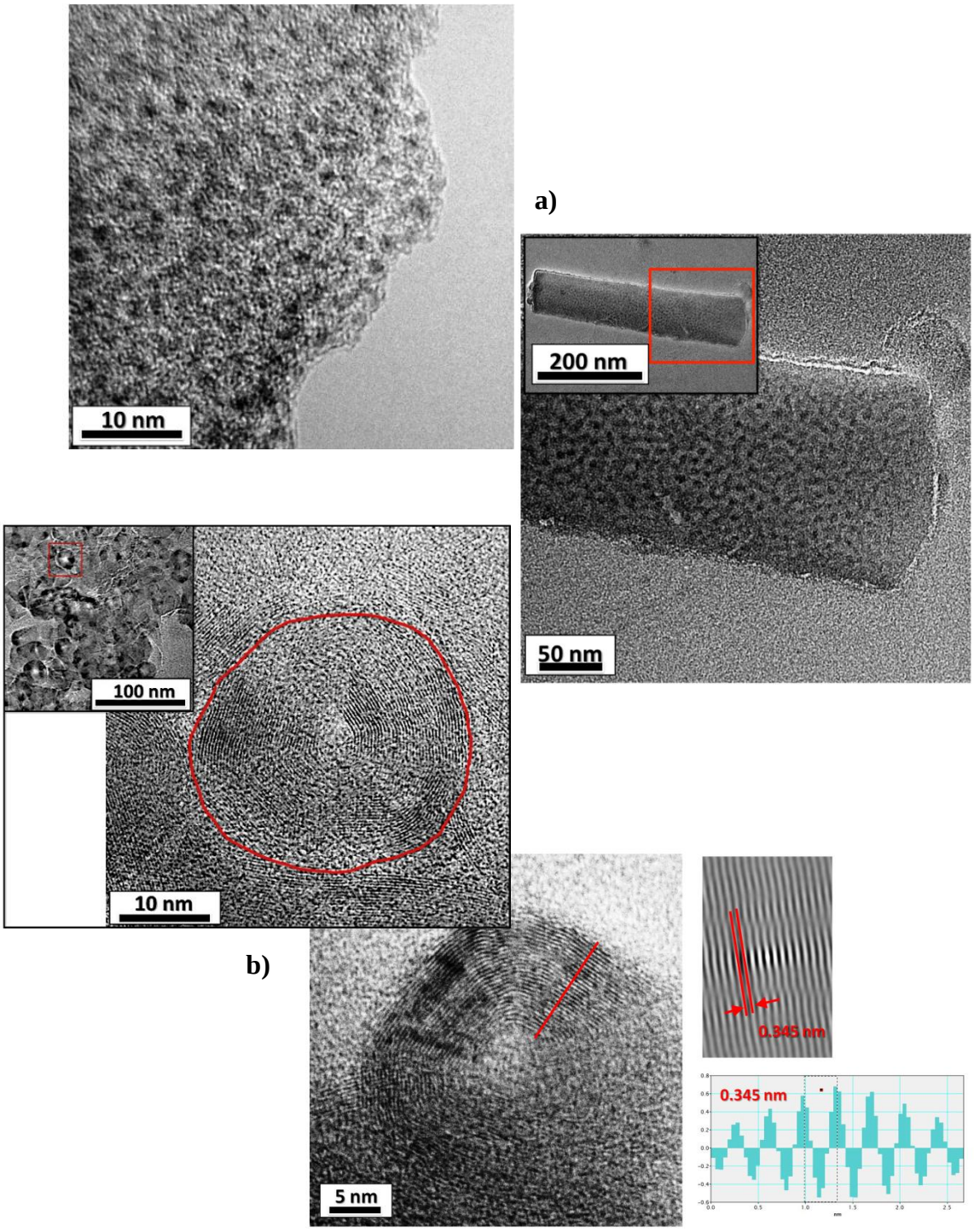

Figure 8. *HR-TEM images of a)* ***7*** *and b)* ***8****.*

The morphologic characterization of hybrids **7** and **8** was carried out by means of HR-TEM. The analysis of TEM images helps to shed light on the organization of the hybrids, and in particular it can provide useful information about the presence and dimension of palladium nanoparticles. Interestingly, **7** shows both organized and amorphous nano-objects in which ionic-liquid-like speckled domains are discernible (**Figure 8a**).[59] Small-sized palladium-rich aggregates are clearly visible and uniformly distributed with a mean diameter of 1.4 ± 0.5 nm. It is likely that the repulsive action of the positive charge of imidazolium groups prevents their agglomeration into larger domains.[60] Nevertheless, TEM analysis of **7** also displayed the presence of few larger Pd aggregates. However, the TEM analysis of **8** was very surprising owing to the presence of a number of organized carbon nanostructures with large graphitic domains as well as to several carbon nano-onions with diameters in the 20–30 nm range (**Figure 8b**).

In all cases, the interplane distance estimated after noise reduction and calculating the intensity profile was 0.345 nm. This value, slightly higher than that of d_{002} value of graphite (0.335 nm), clearly indicates a local structure similar to turbostratic graphite (d_{002}= 0.344 nm).[61]

In accordance with the X-ray diffraction data (see below), the palladium nanoparticles are highly dispersed throughout the sample and large aggregates were not detected by TEM. Nevertheless, the presence of these kind of carbon nanoforms in the sample raise the question on how these nanostructures were formed. Per the data, carbon nano-onions can be prepared through different methods such as electron irradiation,[62] ion implantation,[63] plasma-enhanced chemical vapor deposition,[64] high-temperature annealing[65] or plasma spraying of nanodiamonds,[66] chemical vapor deposition using transition metal catalyst,[67] counter-flow diffusion flames, [68] underwater arc discharge,[69] the latter being the preferred one to produce bulk amounts. However, all the above techniques usually require high doses of energy, whereas in our case the reduction of Pd(II) to Pd(0), which seems to be the step in which the nanocarbons are formed, is carried out at room temperature. To shed light on this process, we carried out a blank experiment by treating C_{60}-IL **5a** with $NaBH_4$ in ethanol, but this reaction only resulted in the hydrolysis of the hybrid, thus giving rise to the formation of 3-(3-hydroxypropyl)-1-methyl-imidazolium bromide, in accord with other reported Bingel adducts in presence of hydride ions/alcohol.[45b, 70] This latter result justifies the higher Pd-content (18 wt%) with respect to the anticipated one (10 wt%). Unfortunately, SEM analyses carried out on **8** (**Figure 9**) did not help to add conclusive data. On the basis of these findings, an explanation for the formation of the experimentally observed carbon

nanostructures cannot be proposed and more in-depth studies will be carried out in due course to completely reveal the mechanism of formation of such nanocarbons.

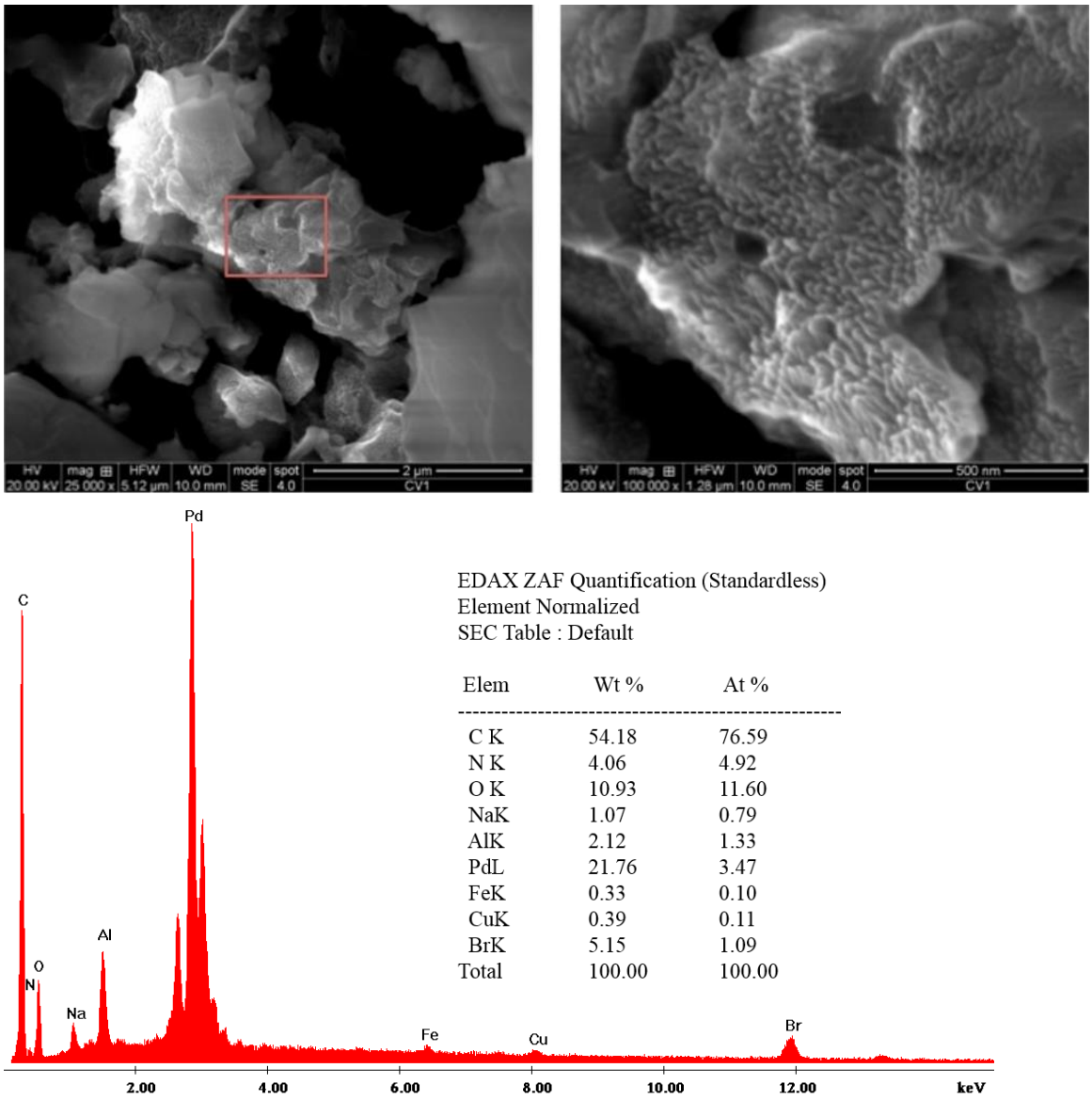

Figure 9. *Top: SEM images of* ***8*** *at different magnifications; bottom: EDAX analysis of* ***8*** *with the semiquantitative atomic composition.*

The XRD data of **8** (**Figure 10**) show a very broad peak at approximately 40° 2θ owing to metallic Pd (PDF number 180870). Metallic Pd particles smaller than 2 nm were found by applying the Scherrer equation that evaluates the full width at half maximum (FWHM) of the reflection line at approximately 40° 2θ. Such a result is in good agreement with the particles size estimated by TEM analysis.

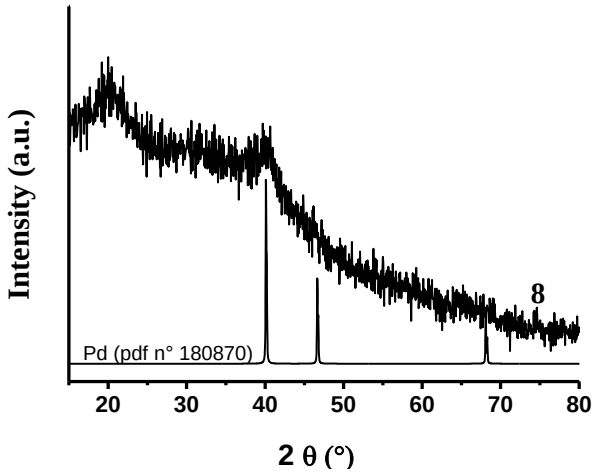

Figure 10. *X-ray diffraction pattern of catalyst **8**.*

The broad peak at approximately 20° 2θ is attributed to a poor ordering of graphene sheets.[71] As a matter of fact, reduced graphite oxide or reduced graphene oxide might exhibit a peak in the range between 20 and 25° owing to restacking. In that case, no graphitic stacking is achieved owing to lattice mismatch, structural defects or to the presence of residual functional groups.[72] XPS analysis was used to analyze the outer part of the materials. **Figure 11** shows the survey spectra of samples **7** and **8**.

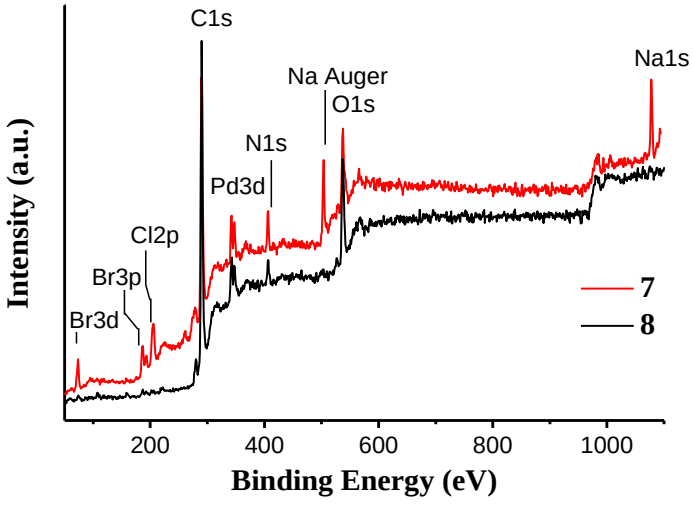

Figure 11. *XPS survey spectra of **7** and **8**.*

The comparison of the two spectra proved that dialysis purification of the final product was successful in eliminating the Na, Br and Cl present in the precursor **7**, as confirmed by SEM-EDAX analysis (**Figure 9**: bottom). The final product **8** shows, along with carbon, the

presence of O, N, and Pd.

The results obtained by the analysis of the region of C1s, O1s N1s and Pd3d are summarized in **Table 1**. The C1s peak shows for both samples three components at 284.4, 286.3, and 288.3 eV owing to sp^2 graphitic carbon, to sp^3 C–C bond and C–O, and to C=O bond, respectively.[73] The main difference in the carbon region between samples **7** and **8** is that, after reducing treatment in $NaBH_4$, the increase in the graphitic component with respect to the others occurs, as evidenced by **Figure 12a** and **Table1**.

Table 1. *XPS binding energies (eV) and atomic ratios of elements constituting samples **7** and **8**.*

Sample	C1s	$Pd3d_{5/2}$	Pd/C	O/C	N/C
7	284.6 (67%) 286.3 (30%) 288.3 (3%)	337.1	0.018	0.13	0.07
8	284.6 (85%) 286.2 (13%) 288.5 (2%)	335.6 (35%) 337.3 (65%)	0.016	0.14	0.04

Oxygen and nitrogen regions show binding energy values of 532 and 401 eV, respectively (see **Figure 11**), typical of C–O and aromatic nitrogenated species.

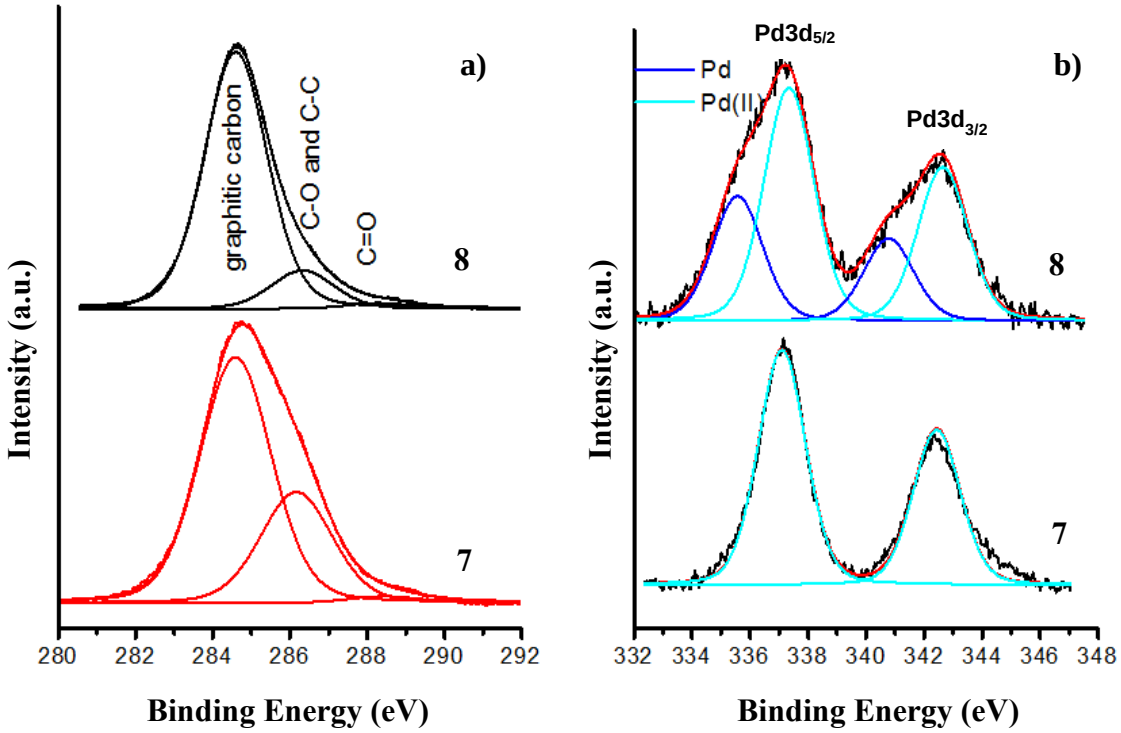

Figure 12. *High-resolution XPS of a) C1s and b) Pd3d of **7** and **8**.*

However, the Pd3d spectra, shown in **Figure 12b**, are characterized by the typical two spin-

orbit components $Pd3d_{5/2}$ and $Pd3d_{3/2}$ separated by approximately 5.4 eV. The spectrum relative to **7** is typical of Pd(II) with a binding energy centered at 337.1 eV. The spectrum of **8** exhibits two doublets attributed to two different chemical species: Pd(0) and Pd(II), respectively.[74] The relative amount of the two components indicated a degree of reduction of 35% after treatment with $NaBH_4$. It is worth noting that XPS is a surface-sensitive technique; this means that the surface signal weight much more than bulk, and this phenomenon is particularly important in the case of very small nanoparticles like the ones that have been found in this sample. For that reason, the real degree of reduction could probably be higher than 35%.

Material **8**, which contained highly dispersed Pd nanoparticles, thus constitutes a good candidate for a catalyst in Pd-mediated cross-coupling reactions given that metal nanoparticles are known to be more active than their particulate metal counterparts in catalytic reactions.[75]

Table 2. *Suzuki–Miyaura reactions catalyzed by* ***8****.*[a]

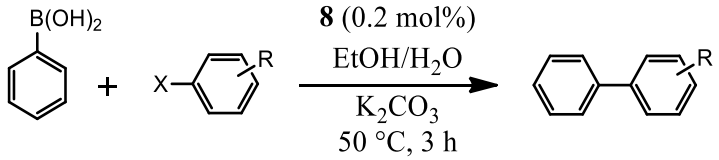

Entry	Substrate	Product	Conv.[b] (%)	Yield (%)
1	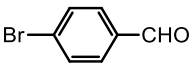	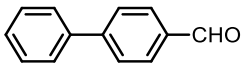	>95	99
2	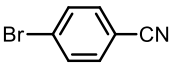	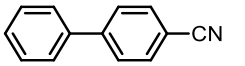	>95	99
3	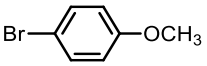	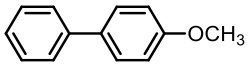	88	87
4	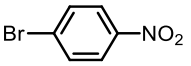	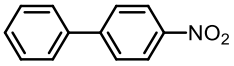	>95	99
5	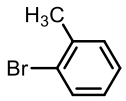	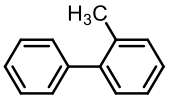	87	68
6	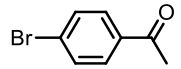	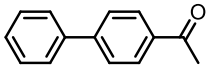	>95	99
7[c]	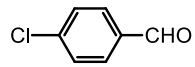	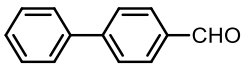	–[d]	–[d]
8[e]	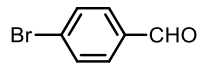	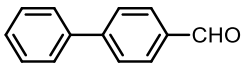	>95	99

[a] Reaction conditions: Phenylboronic acid (1.1 mmol), aryl halide (1 mmol), K_2CO_3 (1.2 mmol), EtOH (1.2 mL), H_2O (1.2 mL), catalyst (0.2 mol%, 1 mg), reaction time 3 h. [b] Determined by ^1H NMR. [c] Reaction time: 19 h. [d] No reaction. [e] Reaction conditions: Phenylboronic acid (3.3 mmol), aryl halide (3 mmol), K_2CO_3 (3.6 mmol), EtOH (1.8 mL), H_2O (1.8 mL), catalyst (0.02 mol%), reaction time 4 h.

Moreover, since metal nanoparticles are thermodynamically unstable, the synergistic effect of coordination, steric, and electrostatic interactions can be exploited in the present approach, thereby preventing nanoparticle coalescence and percolation.[60b] In this regard, **8** was used as catalyst in the Suzuki reaction between phenylboronic acid and a set of aryl bromides in ethanol/water at 50 °C in the presence of K_2CO_3 as base. All the reactions were carried out for 3 h using the catalyst in a 0.2 mol% loading (**Table 2**). Conversions were often quantitative with isolate yields ranged from 68 to 99%. The catalyst was shown to be inactive toward aryl chlorides, given that 4-chlorobenzaldehyde gave no reaction under the common reaction conditions (**Table 2**, entry 7).

In addition, the recyclability of the catalyst was checked for the reaction between 4-bromobenzaldehyde and phenylboronic acid (0.2 mol%, 3 h). After easy recover of **8** by centrifugation, it was used for five consecutive runs to give rise to complete conversion and yield, thus showing no loss in catalytic activity. Moreover, by lowering the catalyst loading to just 0.02 mol%, the biphenyl-4-carboxaldehyde was formed quantitatively with a turnover number (TON; moles of desired product/moles of catalyst) of 5,000 (**Table 2**, entry 8). All the above results make this catalyst a good candidate for further tests under continuous-flow conditions.[76]

These promising results prompted us to explore the catalytic activity of material **8** in another Pd-promoted C-C coupling process such as the Mizoroki-Heck reaction (**Table 3**).

Table 3. *Mizoroki–Heck reactions catalyzed by* ***8****.*[a]

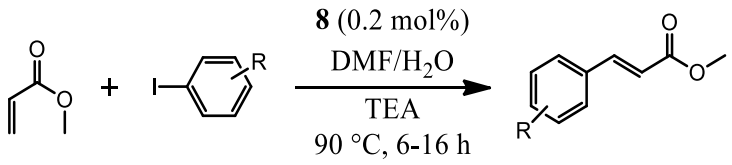

Entry	Substrate	Product	Conv.[b] (%)	Yield (%)
1[c]	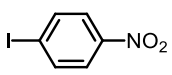	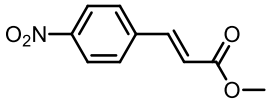	>95	99
2[d]	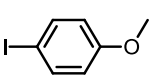	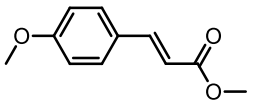	>95	99
3[d]	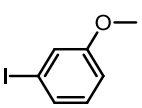	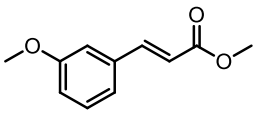	>95	89
4[c]	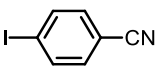	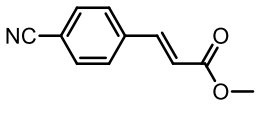	>95	99

[a] Reaction conditions: Methyl acrylate (1.5 mmol), aryliodide (1 mmol), triethylamine (TEA; 2 mmol), DMF (4 mL), H_2O (1 mL), catalyst (0.2 mol%, 1 mg). [b] Determined by ^1H NMR. [c] Reaction time: 6 h. [d] Reaction time: 16 h.

Reaction between a set of four aryliodides and methyl acrylate in DMF/water at 90 °C in the presence of trimethylamine (TEA) as base gave the corresponding alkenes in high yields and excellent selectivity, with the expected *trans* isomer as the only product, once again by employing just 0.2 mol% of catalyst **8**.

Supported C_{60}-IL hybrids
1.4 Results and Discussion

Encouraged by the good results obtained and with the aim to improve the already good catalytic activity of the material **8**, we developed a new synthetic strategy of a series of supported catalysts based on the previously studied C_{60}-IL moiety employed to stabilize PdNPs. These new heterogeneous catalytic systems were anchored onto inert support materials such as amorphous silica gel, mesoporous SBA-15 and silica-coated maghemite (γ-Fe_2O_3@SiO_2) obtaining easily recoverable catalysts by means of centrifugation or, in the case of the paramagnetic support, by means of magnetic decantation with an external magnet.

The synthesis of these supported catalysts, depicted in the **Scheme 7**, starts from the reaction between triethoxy-3-(2-imidazolin-1-yl)propylsilane and the C_{60} hexakis-adducts **4b**[77] to give compound **9**. Grafting of **9** onto the different supports gave materials **10a-c** that reacted with 1-methylimidazole allowing obtaining materials **11a-c**. The supported C_{60}-IL hybrids **11a-c** were used for the immobilization of palladium nanoparticles through anion metathesis with tetrachloropalladate ions and the subsequent reduction with $NaBH_4$ obtaining supported catalysts **13a-c**. Palladium loading of the catalytic systems **13a-c** was determined by means of microwave plasma - atomic emission spectrometry (MP-AES) and was found to be 2.3, 1.5 and 2.1 wt%, respectively.

Materials **10a-c** and **11a-c** were analyzed by means of thermogravimetric analysis performed under oxygen flow from 100 to 1000 °C with a heating rate of 10 °C/min (**Figure 13**). From the net weight losses (calculated considering the weight losses of the pristine support materials) at 800 °C for materials **10a-b** and at 900 °C for material **10c**, it was possible to determine the degree of functionalization with the C_{60} derivative **9** of the different support materials that resulted 0.081, 0.057 and 0.083 mmol/g, respectively. Conversely, IL loading of compounds **11a-c** was determined by comparing the weight losses of such materials at 800 and 900 °C with those of their precursor materials **10a-c**.

From the analysis of TG profiles, it was possible to prove that materials **10a** and **10c** were almost quantitatively functionalized with 1-methylimidazole giving rise to values of IL loading of 0.970 and 0.987 mmol/g for materials SiO_2-C_{60}-IL **11a** and γ-Fe_2O_3@SiO_2-C_{60}-IL **11c**, respectively.

On the other hand, the functionalization of material SBA15-C_{60} **10b** was not likewise

efficient. The estimated IL loading of **11b** was 0.387 mmol/g that revealed, based on the loading of the precursor material **10b**, a partial functionalization (56.6%) of such a material with 1-methylimidazole.

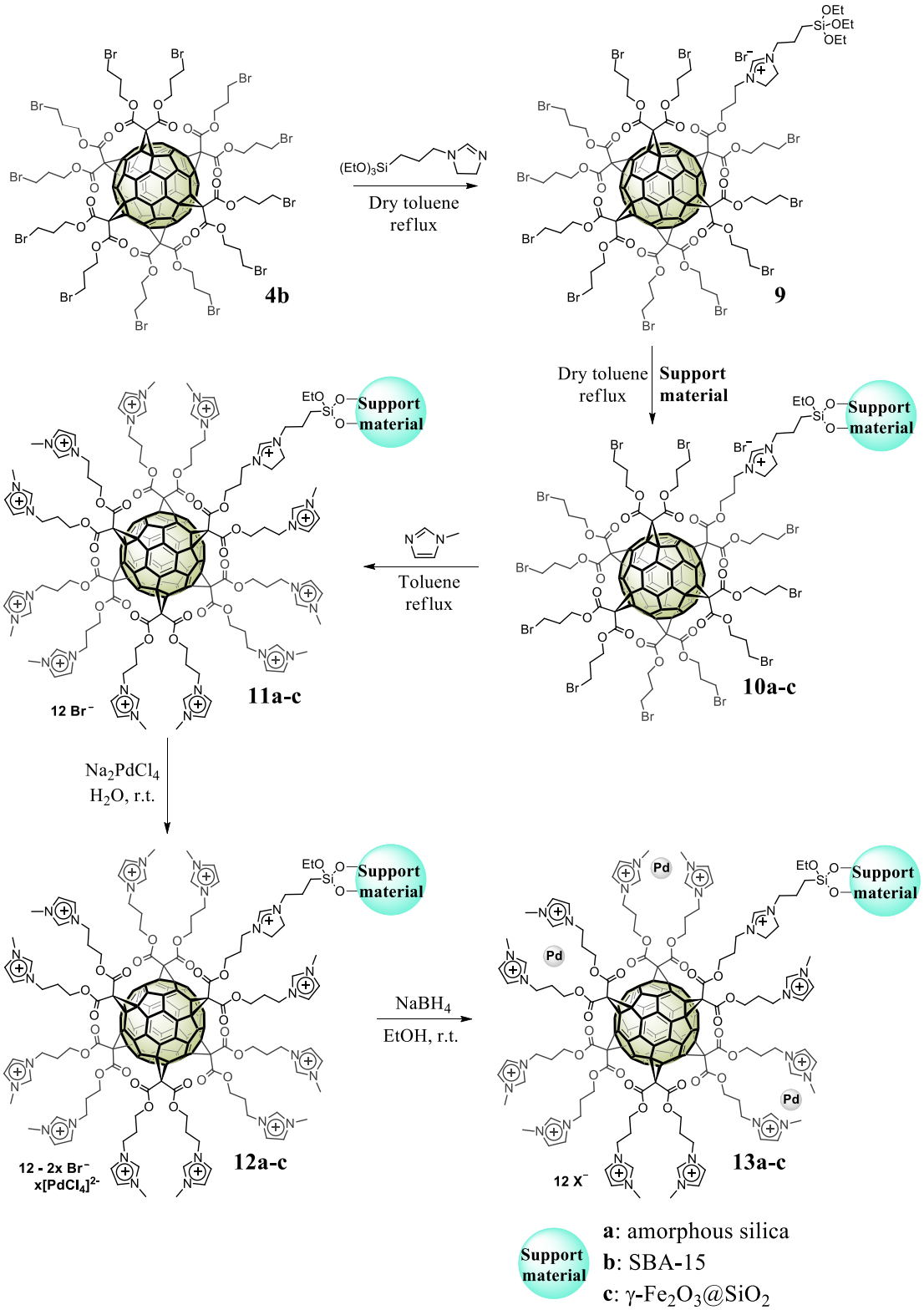

Scheme 7. *Synthesis of catalysts **13a-c**.*

This different behaviour could be ascribed to the nature of the support material, namely

mesoporous SBA-15. The grafting of bulky compound **9** on the mesostructured SBA-15 could partial block the access to the pores of silica, avoiding the functionalization of molecules grafted into the inner surface of SBA-15 channels.

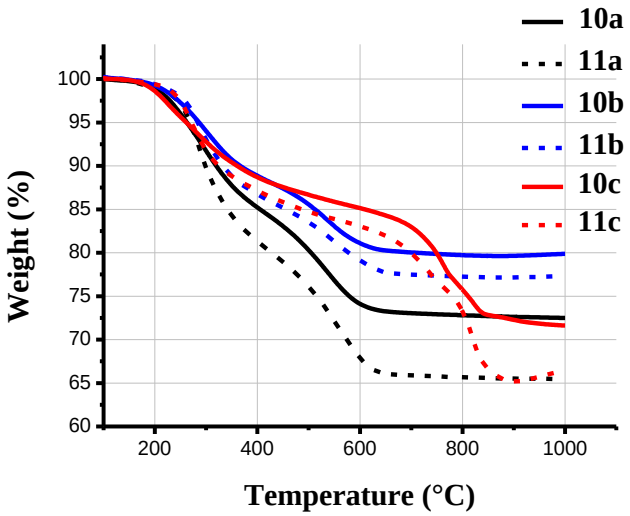

Figure 13. *TGA of materials **10a-c** and **11a-c** under oxygen flow.*

The morphological properties, in terms of specific surface area (SSA), pores volumes and pore size distribution, of materials **11a-b** and that of their pristine support materials, namely amorphous silica and SBA-15, were investigated by means of nitrogen adsorption/desorption measurements (**Table 4**).

Table 4. *N_2 physisorption analysis of **11a**, **11b** and of their support materials.*

Material	BET[a] (m^2g^{-1})	Mean pore size distribution[b] (BJH) (nm)	Cumulative pore volume (cm^3g^{-1})
SiO_2	416.0	5.3	0.57
11a	171.5	5.5	0.27
SBA-15	569.5	11.6	1.04
11b	315.0	10.8	0.76

[a] BET: range p/p_0: 0.05-0.3
[b] Pore size distribution (BJH method) calculated on the adsorption curve in the range p/p_0 : 0.05-0.3

Conversely, silica-coated γ-Fe_2O_3 support materials are characterized by a low SSA < 70 m^2g^{-1}.[78] Brunauer–Emmett–Teller (BET) equation was applied to determine the specific surface area, whereas the Barrett-Joyner-Halenda (BJH) method was applied to determine the volume and the diameter of the pores using the adsorption isotherm. The functionalization of the support materials, namely amorphous silica and SBA-15 with a starting surface area corresponding to 416.0 and 569.5 m^2g^{-1}, respectively, led to decreased values of surface area corresponding to 171.5 and 315.0 m^2g^{-1}, respectively. Furthermore, a decrease of the pores diameter was also observed in the case of material **11b**.

Figure 14 shows the small-angle X-ray scattering (SAXS) patterns of pristine SBA-15, SBA15-C_{60}-IL **11b** and amorphous silica. No reflections were detected for silica gel confirming its amorphous nature. Conversely, SAXS pattern confirmed the ordered mesostructure of SBA-15 with the characteristic scattering pattern showing a peak at 0.75° 2θ and two peaks, not well resolved, at 1.32° and 1.6° 2θ corresponding to *d* spacings of 11.6, 6.7, and 5.8 nm, respectively. The ratios of the *d* spacing values correspond exactly to 1:1/√3:1/2 then it is possible to index the corresponding peaks as (100), (110) and (200) scattering reflections associated with a 2D-hexagonal mesostructure (space group *p6mm*).[79]

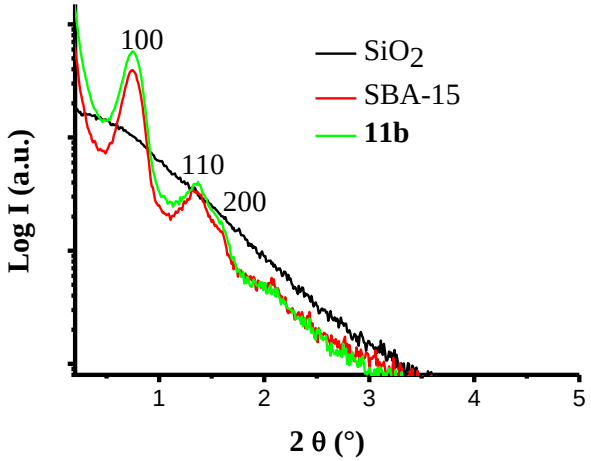

Figure 14. *SAXS patterns of SiO_2, SBA-15 and material **11b**.*

From the main *d* spacing (100), it was possible to calculate the pore-to-pore distance a_0 ($2d_{100}/\sqrt{3}$) corresponding to 13.4 nm. Moreover, the SAXS pattern of material **11b** showed that SBA-15 structure was maintained unaltered after its functionalization.

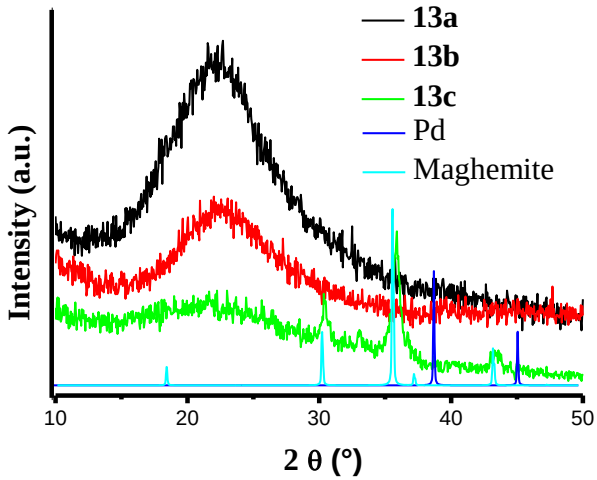

Figure 15. *Experimental X-ray diffraction pattern of materials **13a-c** and simulated diffraction pattern of palladium and maghemite.*

The wide-angle XRD patterns of the catalysts **13a-c** are reported in **Figure 15**.

For all materials a very broad diffraction peak typical of silica at around 23° 2θ is present. In addition, the typical diffraction peaks due to the presence of the maghemite core of γ-Fe_2O_3@SiO_2-C_{60}-IL-Pd catalyst **13c** are clearly visible as showed in **Figure 15**. However, no peaks belonging to the diffraction planes of metallic palladium are visible, suggesting the presence of highly dispersed PdNPs.

Further investigations on catalysts **13a** and **13b** were carried out by means of HR-TEM. TEM images confirmed XRD data showing a uniform distribution of PdNPs, well dispersed throughout both catalysts. SiO_2-C_{60}-IL-Pd **13a** exhibited the presence of small PdNPs with a narrow size distribution of 1.85 ± 0.38 nm (n = 295) (**Figure 16a**).

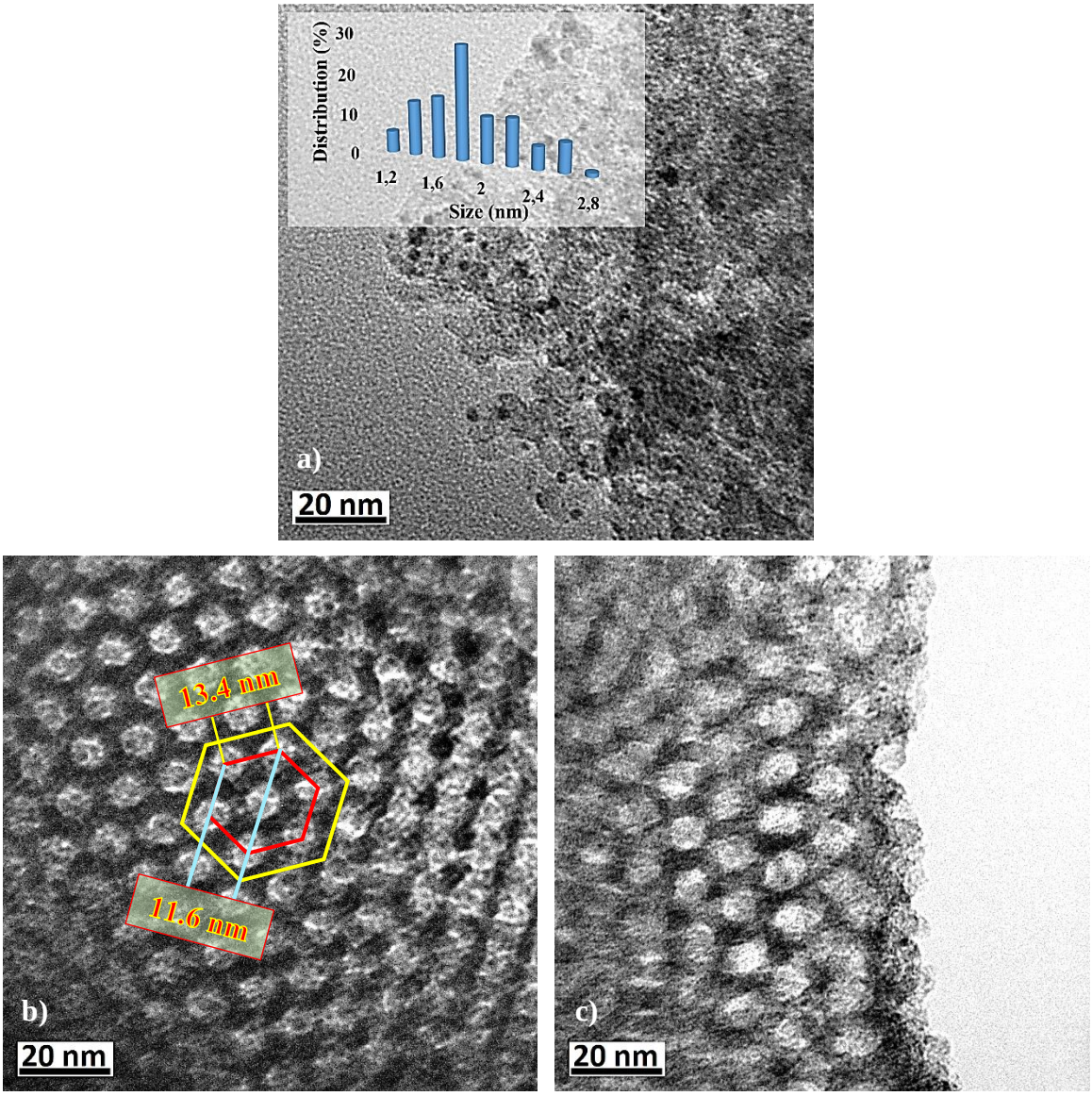

Figure 16. *HR-TEM pictures of materials a)* ***13a****, b)* ***11b*** *and c)* ***13b****.*

In addition, TEM analysis of the catalyst SBA15-C_{60}-IL-Pd **13b** and its precursor **11b** (before Pd immobilization) was very useful to obtain information about the structure of these materials. First of all, it was possible to see, as also proved by SAXS measurements, how the structure of SBA-15 support remained unchanged after chemical functionalization. In fact, TEM images (**Figures 16b-c**) show the bidimensional hexagonal mesostructure typical of SBA-15 present in both materials **11b** and **13b**. Furthermore, catalyst **13b** is characterized by the presence of small-sized PdNPs (< 1 nm) not clear discernible from the TEM images (**Figure 16c**).

The exceptionally small dimensions of such NPs makes their identification in the micrograph very difficult. However, it is possible to affirm that NPs are very well dispersed throughout the sample and this could explain their lack of detection by XRD analysis. Moreover, by the measure of the centre-to-centre distance of the pores of material **11b** it was possible to confirm the a_0 value (13.4 nm) and the interplanar spacing d_{100} (11.6 nm) previously estimated by means of SAXS measurements.

XPS analysis was used to collect information about the surface composition of the as-synthesized catalytic systems **13a-c** and to evaluate the reduction degree of the supported palladium species. **Figure 17** shows the survey spectra of catalyst **13a-c**, whereas **Table 5** reports the surface composition of such materials expressed as atomic ratios.

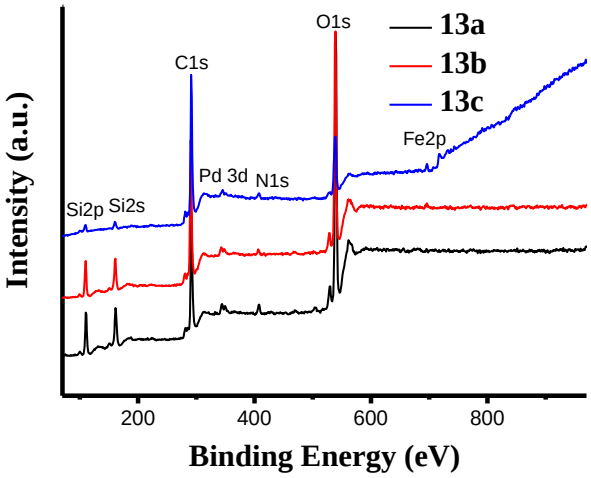

Figure 17. *XPS survey spectra of materials* ***13a-c****.*

According to the values of N/C atomic ratios of materials **13a-c**, a possible partial loss of the IL moiety, as previously reported in the case of the unsupported catalytic system **8**, seems to have occurred.

Table 5. *XPS Pd $3d_{5/2}$ binding energies (eV), Pd/Si, Pd/C, N/Si and N/C surface atomic ratios. The relative percentages are given in parentheses.*

Material	Pd $3d_{5/2}$	Pd/Si	Pd/C	N/Si	N/C
13a	334.9 (42), 336.9 (58)	0.025	0.010	0.1082	0.045
13b	334.9 (46), 337 (54)	0.024	0.008	0.0838	0.029
13c	335.3 (37), 337.6(63)	0.094	0.005	0.5193	0.027

Figure 18 shows the Pd3d region of materials **13a-c** with the peaks centred at 335.0 ($3d_{5/2}$) and 340.0 ($3d_{3/2}$) eV corresponding to Pd(0) and those at 337.0 ($3d_{5/2}$) and 342.2 ($3d_{3/2}$) eV corresponding to Pd(II).[80] In all materials, palladium is therefore present both in the metallic and ionic form. The calculated percentages of Pd(0) present in the catalysts **13a**, **13b** and **13c** were 42, 46 and 37%, respectively, proving that there was an incomplete reduction of the Pd(II) species or, as already reported, a possible air oxidation of the surface of PdNPs.[81] However, it is important to consider that XPS is a surface sensitive technique, hence, the measured degree of reduction is considerably more affected by the signals arising from the surface than those of the bulk. For this reason, is extremely difficult to know with accuracy the exact chemical state composition of palladium by means of this technique.

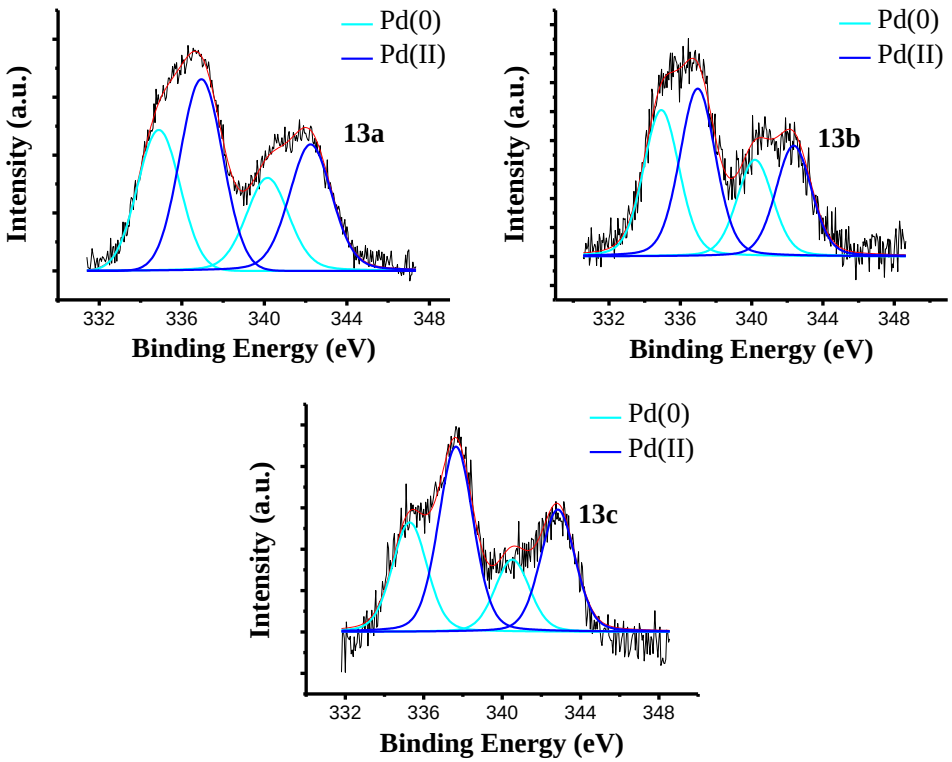

Figure 18. *High-resolution XPS of Pd3d region of materials **13a-c**.*

Moreover, further investigations on the SiO_2-C_{60}-IL-Pd material **13a** by means of solid-state ^{13}C NMR were carried out. In **Figure 19** the solid-state ^{13}C NMR spectrum of material **13a** and the ^{13}C NMR spectrum in the liquid-state of the hexakis-adduct C_{60}-IL **5a** are compared. It is possible to see how there is an almost perfect overlapping of the two NMR spectra thus proving the good outcome of chemical functionalization of such a material.

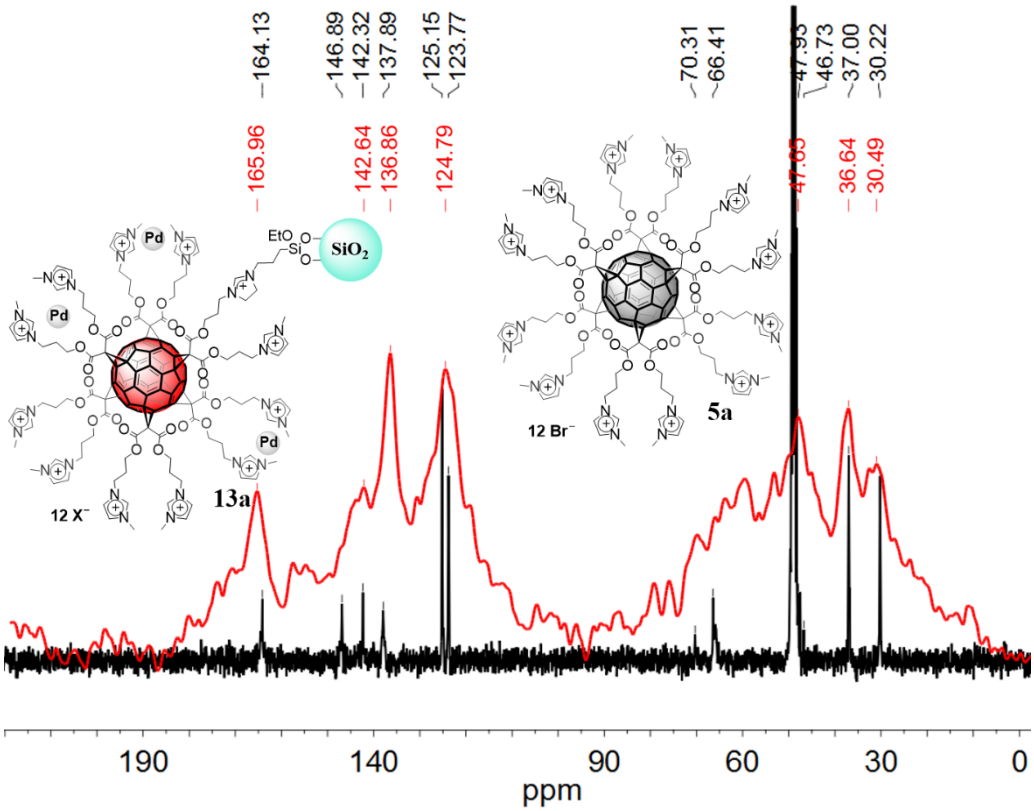

Figure 19. *Solid-state ^{13}C NMR of material **13a** (red) and ^{13}C NMR of compound **5a** in CD_3OD (black).*

Materials **13a-c** were tested as catalysts in the C–C coupling reactions of Heck and Suzuki. Heck reactions were carried out using various aryl iodides coupled with methyl acrylate, styrene or 4-chlorostyrene. Catalysts were used at 0.1 mol% loading using DMF as solvent and triethylamine as base at 120 °C for 4 h (**Table 6**).

Table 6. *Mizoroki–Heck reactions catalyzed by materials* ***13a-c****.*[a]

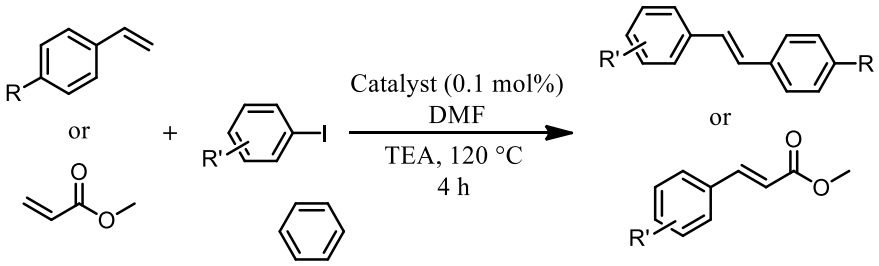

Entry	Product	Catalyst 13a		Catalyst 13b		Catalyst 13c	
		t (h)	Conv.[b] (%)	t (h)	Conv.[b] (%)	t (h)	Conv.[b] (%)
1	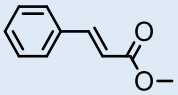	4	>95 (97)	4	>95 (98)	4	>95 (97)
2	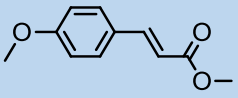	4	>95 (99)	4	>95 (99)	4	>95 (99)
3	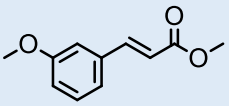	4	>95 (99)	4	>95 (99)	4	>95 (96)
4	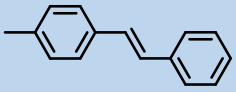	4	>95 (97)	4	>95 (97)	4	>95 (98)
5	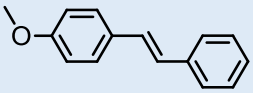	4	88	4	83 [96][c]	4	94 [93][c]
6	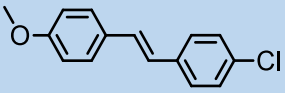	4	84 [88][c]	4	82 [88][c]	4	84 [88][c]

[a] Reaction conditions: methyl acrylate, styrene or 4-chlorostyrene (0.75 mmol), aryliodide (0.5 mmol), triethylamine (1 mmol), DMF (1 mL), catalyst (0.1 mol%). [b] Conversion determined by ^{1}H NMR, yield reported in parentheses. [c] Selectivity toward *trans*-alkene, determined by ^{1}H NMR.

High yields were obtained with all the catalysts **13a-c**. Regioselectivities of the tested Heck reactions were excellent with almost all substrates with the expected *trans* isomer as the only product. However the coupling reactions of 4-iodoanisole with styrene and 4-chlorostyrene gave not complete regioselectivity, affording also the gem-alkene product formed during the catalytic cycle as a result of the α-migration of R- group during the alkene insertion step as shown in **Figure 20**.

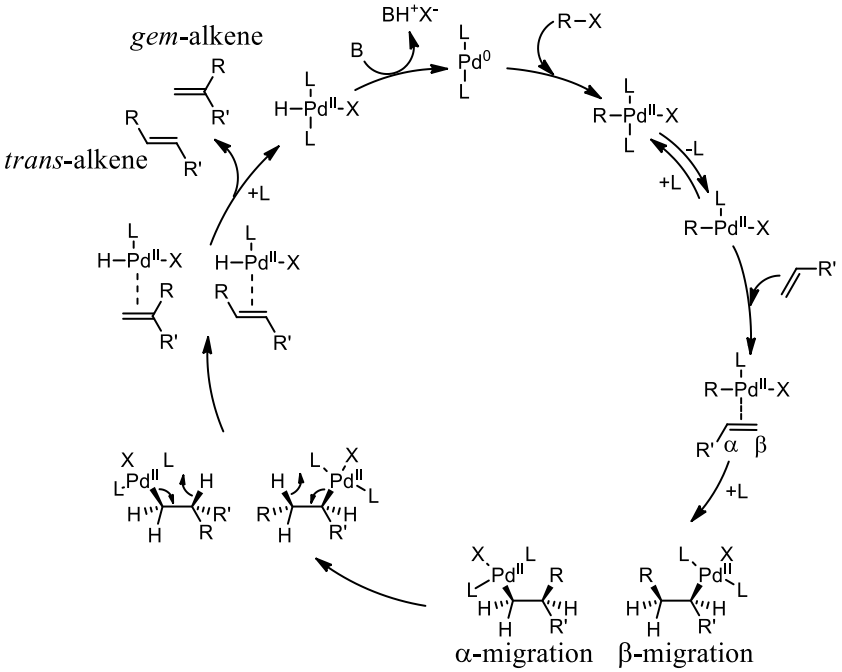

Figure 20. *Heck reaction mechanism showing the formation of both gem- and trans-alkene.*

Furthermore, catalysts SiO_2-C_{60}-IL-Pd **13a** and SBA15-C_{60}-IL-Pd **13b** were chosen to assess their recyclability in the reaction between 4-iodoanisole and methyl acrylate (see Experimental Section ***1.7*** for more details).

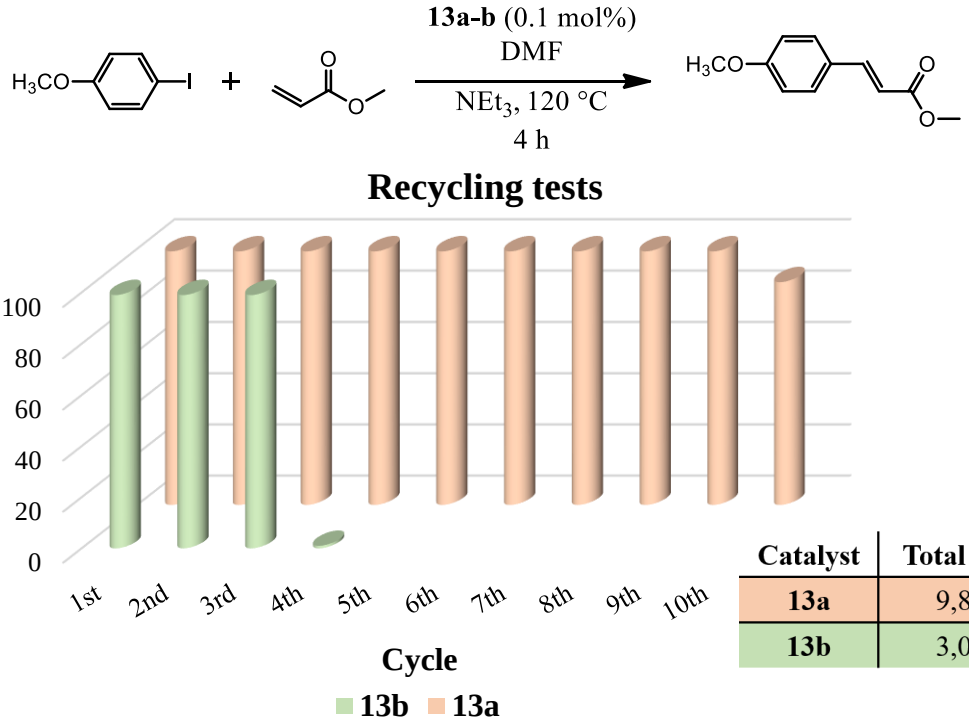

Catalyst	Total TON
13a	9,870
13b	3,000

Figure 21. *Recycling tests of catalysts **13a-b** in the Heck reaction.*

Catalyst **13a** showed to be a good candidate for the recycling experiments in the Heck reaction. In fact, it was possible to carry out up to ten catalytic cycles with a slight decrease of catalytic activity in the tenth cycle that afforded the desired product in 87% yield (**Figure 21**). Conversely, catalyst **13b** proved to be a less recyclable catalytic system in the light of the fact that it was possible to use the catalyst only three times with a net drop of catalytic activity in the fourth cycle that gave rise to no reaction (**Figure 21**).

Catalysts **13a-c** were also tested at 0.01 mol% loading in another Pd-mediated C–C coupling process such as the Suzuki reaction carried out between various aryl bromides and phenylboronic acid at 50 °C in a mixture of ethanol and water (1:1) using K_2CO_3 as base (**Table 7**).

Table 7. *Suzuki-Miyaura reactions catalyzed by materials* ***13a-c****.*[a]

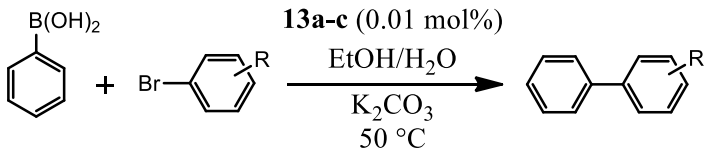

Entry	Product	Catalyst 13a		Catalyst 13b		Catalyst 13c	
		t (h)	Conv.[b] (%)	t (h)	Conv.[b] (%)	t (h)	Conv.[b] (%)
1	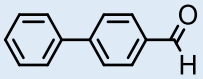	5	82 (80)	2	>95 (98)	2	>95 (98)
2	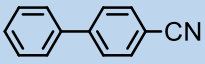	2	>95 (99)	1.5	>95 (99)	1.5	>95 (99)
3	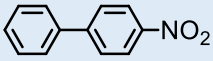	2	>95 (98)	1	>95 (97)	1	>95 (99)
4	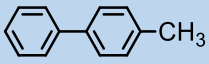	2.5	>95 (69)	1	>95 (76)	1	>95 (75)
5	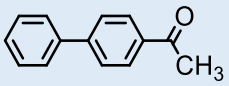	3	>95 (96)	1	>95 (98)	1	>95 (99)
6	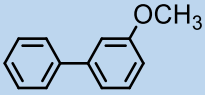	3	>95 (99)	1.5	>95 (98)	1.5	>95 (99)

[a] Reaction conditions: aryl halide (0.5 mmol), phenylboronic acid (0.55 mmol), K_2CO_3 (0.6 mmol), EtOH/H_2O (1:1, 0.4 mL), catalyst (0.01 mol%). [b] Determined by ^{1}H NMR, yield reported in parentheses.

In almost all cases, high yields were obtained in a short time ranging from 1 to 2 h, only in some cases, in which silica based catalyst **13a** was used, the reaction required more time.

From the analysis of the results reported in **Table 7**, it is possible to see how silica supported catalyst **13a** seems to be less active than the corresponding SBA and γ-Fe_2O_3@SiO_2 based catalysts **13b** and **13c**. For example taking into account the reaction between 4-bromobenzaldehyde and phenylboronic acid, quantitative yields were obtained in just 2 h when catalysts **13b** and **13c** were used. Conversely, the use of catalyst **13a** required more

time (5 h) to reach 80% yield (**Table 7**, entry 1).

Additionally, Pd-leaching in solution and in the isolated products, both in the Heck and in the Suzuki reaction catalyzed by catalyst **13a** at 0.1 and 0.01 mol%, respectively, was determined by MP-AES analysis. However, no Pd leached species were detected.

In the light of the good results obtained in the Suzuki couplings, further experiments with a decreased catalytic loading (0.001 mol%) were carried out (**Table 8**).

Table 8. *Suzuki-Miyaura reaction catalyzed by materials **13a-c** at 0.001 mol% loading.*[a]

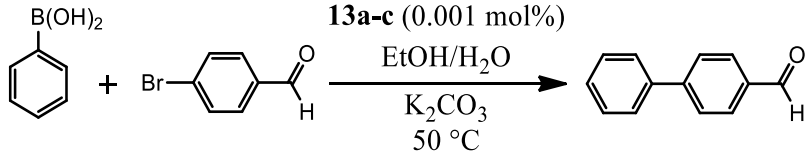

Entry	Catalyst	t (h)	Conv.[b] (%)	TON[c]	TOF[d] (h^{-1})
1	**13a**	16	83	83,000	5,187
2	**13b**	6	88	88,000	14,667
3	**13c**	6	81	81,000	13,500

[a] Reaction conditions: 4-bromobenzaldehyde (2 mmol), phenylboronic acid (2.2 mmol), K_2CO_3 (2.4 mmol), EtOH/H_2O (1:1, 1.6 mL), catalyst (0.001 mol%). [b] Determined by ^1H NMR. [c] TON defined as mol of product/mol of catalyst. [d] Turnover frequency (TOF = TON/h).

Catalysts were tested at 0.001 mol% loading and, once again, materials **13b** and **13c** revealed to be the best catalytic systems displaying a remarkable activity under the reaction conditions adopted. Despite the low catalytic loading, very high yields of the desired biphenyl-4-carboxaldehyde product, TON up to 88,000 and good values of TOF up to 14,667 h^{-1} were obtained. In the same conditions, catalyst SiO_2-C_{60}-IL-Pd **13a** required more time (16 h) to reach a good conversion, approaching a TOF value of 5,187 h^{-1}.

Moreover, the catalysts **13a** and **13b** were chosen to carry out some experiments at higher temperature (120 °C) both under microwave (MW) irradiation and under conventional heating. MW-mediated palladium catalysed cross coupling reactions are known to be a valid alternative to the traditional reactions carried out by conductive heating with an external heat source. Many benefits, arising from reduced time of reaction and improved yields toward the coupled products, were attributed to MW-assisted heating mode.[82] Therefore, the reactions between aryl bromides with electron-withdrawing or electron-rich substituents (4-bromoacetophenone or 3-bromoanisole) and phenylboronic acid were carried out using catalysts **13a** and **13b** at 0.001 mol% loading and at 120 °C to assess the presence of any beneficial effect of MW irradiation on such reactions and to evaluate the real performances of such catalytic systems (**Table 9**).

Table 9. *Suzuki-Miyaura reaction catalyzed by material* ***13a-b*** *at 120 °C.*[a]

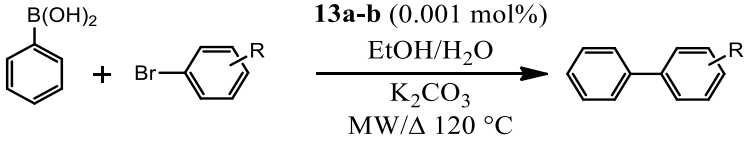

Entry	Catalyst	R	T	t (min)	Conv.[b] (%)	TON[c]	TOF[d] (h^{-1})
1	**13b**	4-$COCH_3$	120 °C (MW)	10	>95	100,000	600,000
2	**13b**	4-$COCH_3$	120 °C (Δ)	10	>95	100,000	600,000
3	**13b**	4-$COCH_3$	120 °C (MW)	3	>95	100,000	2,000,000
4	**13b**	4-$COCH_3$	120 °C (Δ)	3	88	88,000	1,760,000
5	**13a**	4-$COCH_3$	120 °C (MW)	3	>95	100,000	2,000,000
6	**13b**	3-OCH_3	120 °C (MW)	3	73	73,000	1,460,000
7	**13b**	3-OCH_3	120 °C (Δ)	10	56	56,000	336,000

[a] Reaction conditions: Phenylboronic acid (2.2 mmol), 4-bromoacetophenone or 3-bromoanisole (2 mmol), K_2CO_3 (2.4 mmol), EtOH (0.8 mL), H_2O (0.8 mL), catalyst (0.001 mol%) were stirred under microwave irradiation (11 W) or under conventional heating for the indicated time. [b] Determined by ^1H NMR. [c] TON defined as mol of product/mol of catalyst. [d] TOF = TON/h.

From the comparison of the results obtained under MW irradiation and with conventional heating, no specific MW effect seems to be involved in the formation of 4-phenylacetophenone product when the reaction was carried out for 10 minutes (**Table 9**, entries 1 and 2). MW irradiation allows reaching a faster and uniform heating of the reaction mixture compared to conventional heating; in such a way, it is possible to explain the small differences in terms of yield obtained toward the desired product when a very short time (3 minutes) was adopted (**Table 9**, entries 3 and 4) compared to the quantitative yields obtained when a longer reaction time (10 minutes) was adopted (**Table 9**, entries 1 and 2). In more detail, in the first case, the higher heating ability of the MW irradiation is the discriminating factor that led to a quantitative yield in such short time when MW heating was applied (compare **Table 9**, entries 3 and 4). Conversely, 10 minutes were sufficient to mitigate any difference with MW irradiation leading to quantitative yield also in the case in which conventional heating was adopted (**Table 9**, entries 1 and 2). Furthermore, catalyst SiO_2-C_{60}-IL-Pd **13a** was also employed in the coupling reaction between 4-bromoacetophenone and phenylboronic acid affording the corresponding coupled product in quantitative yield in 3 minutes under MW irradiation (**Table 9**, entry 5). On the other hand, as already reported for electron-rich aryl bromides,[83] the MW-assisted reaction of the less reactive 3-bromoanisole substrate for 3 minutes at 120 °C led to improved conversions compared to the same reaction carried out with conventional heating for 10 minutes, proving that, in this case, there was a beneficial MW effect (**Table 9**, entries 6 and 7).

High values of TON up to 100,000 were obtained when 4-bromoacetophenone was used as

substrate. However, heterogeneous catalysts, used in the Suzuki coupling, with even higher TONs were reported.[84] On the other hand, despite these high values of TON up to 3,570,000, as reported by Yamada *et al.*,[84b] the coupling reactions required several hours giving rise to a TOF value of 119,000 h^{-1}. To the best of our knowledge, the highest TOF reported for supported palladium catalysts reached a value of $1.4 \cdot 10^6$ h^{-1}[85] therefore lower than that herein reported (TOF $2.0 \cdot 10^6$ h^{-1}) (**Table 9**, entries 3 and 5). In summary, the combined values of TON and TOF obtained with the catalyst under investigation, prove its good stability and high efficiency in the catalysis of the Suzuki reaction with a very low loading of 0.001 mol%.

Furthermore, in the light of the use of palladium-based catalysts in the synthesis of pharmaceuticals, the possibility of metal contamination of the as-synthesized drugs has to be taken into account. For this reason, it is extremely important to avoid or limit the metal leaching from the catalyst. However, the high activity of the catalytic systems herein considered, allows working with a very low catalytic loading (down to 0.001 mol%). The implications related to this possibility lead to interesting considerations. As a matter of fact, even if there was the leaching of the total amount of palladium present in the heterogeneous catalyst, there would be a metal contamination of the final product (in the case of 4-bromoacetophenone couplings with quantitative conversions; **Table 9**, entries 1-4) amounting to approximately 5.4 ppm. Such a value is just slightly higher than the allowable palladium residual amount in active pharmaceutical ingredients required by government regulations (< 5 ppm).[86]

In summary, the supported catalysts **13a-c** possess a very impressive catalytic activity not shown by the corresponding unsupported catalyst **8**. In literature very few examples in which the solid-supported Pd catalyst is more active than the homogeneous counterpart are reported.[87] This phenomenon was explained taking into account the possible improved stability of the active Pd species in the heterogeneous catalyst compared to the homogeneous catalyst. For this reason, the adopted synthetic strategy of materials **13a-c** was chosen with the aim to achieve an optimal dispersion of the C_{60}-IL moiety on the support materials in which PdNPs can be efficiently stabilized. These considerations could eventually explain the reason of this high catalytic activity.

Finally, the recyclability of the catalytic systems **13a-c** (see Experimental Section ***1.7*** for more details), used at 0.1 mol% loading, was evaluated in the coupling reaction between 4-bromobenzaldehyde and phenylboronic acid (**Figure 22**). Catalysts **13b** and **13c** were used up to five and six times, respectively, with a loss of activity in the last cycles. On the other

hand, silica supported catalyst **13a**, which showed to be less active (see **Table 6**, entry 1) than other catalysts, revealed to be a more robust catalyst. In fact, with this catalyst it was possible to run up to ten cycles without loss of activity.

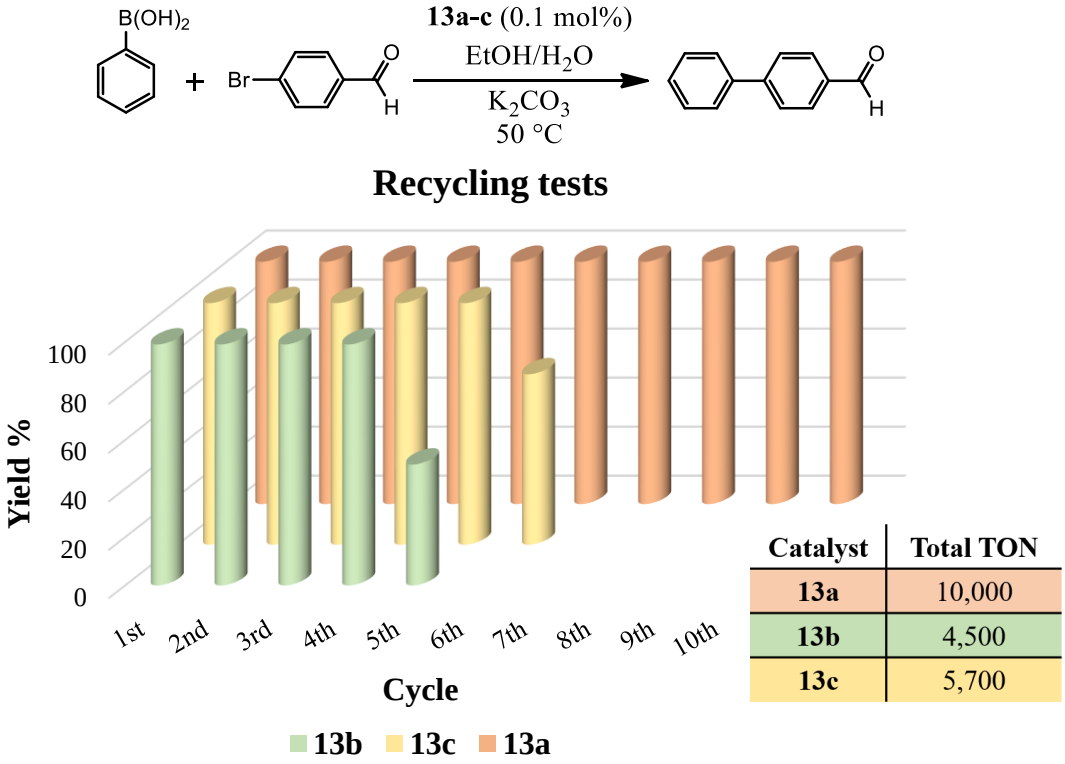

Figure 22. *Recycling tests of catalysts **13a-c** in the Suzuki reaction.*

To understand the reasons of such great longevity of the catalyst **13a**, TEM analysis of the spent catalyst after ten cycles was carried out.

TEM images revealed only a little increase of PdNPs dimensions (2.65 ± 0.50 nm; n = 222) (compare **Figure 23** with **Figure 16a**). These findings could furnish the reason of the constant catalytic activity over ten cycles of catalyst **13a** that is able to stabilize effectively the metal NPs limiting their agglomeration.

Furthermore, regarding the recycling experiments of catalysts **13b** (Suzuki and Heck reactions) and **13c** (Suzuki reaction), it is possible to affirm that despite their great catalytic activity, they suffer of intrinsic drawbacks owing to the difficult handling of the support materials, namely SBA-15 and γ-Fe_2O_3@SiO_2, compared to amorphous silica.

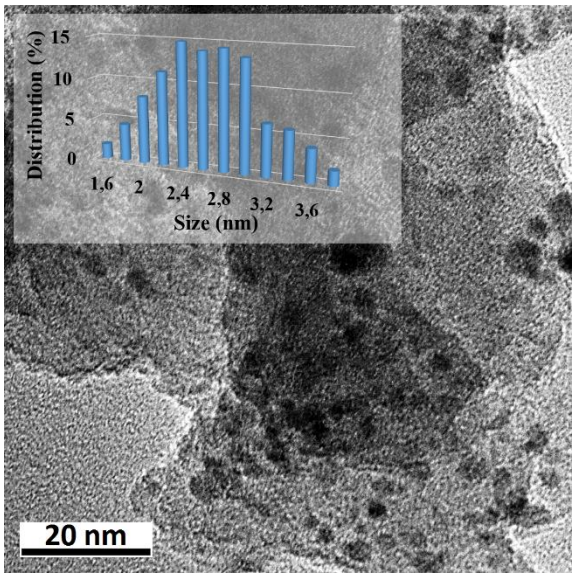

Figure 23. *HR-TEM picture of catalyst* ***13a*** *after ten cycles in the Suzuki reaction.*

In more detail, during the sonication and centrifugation processes involved in the work up procedures after each catalytic cycle, both catalysts **13b** and **13c** were reduced to a fine powder difficult to handle and this can lead to the loss of catalytic material. It is for this reason that catalyst **13a** is a more promising catalytic material for its possible use in continuous flow reactors[76] owing to its greater resistance to mechanical stress conferred to it by the amorphous silica support.

1.5 Conclusions

A set of several C_{60}-IL conjugates were synthesized and thoroughly characterized. Both anions and cations as well as side chain were varied, giving rise to new hybrids with outstanding solubility profiles in classically non-C_{60}-friendly solvents such as water and methanol in which imidazolium-based hexakis-adducts show solubilities higher than 800 mg/mL. This unprecedented solubility can be exploited in several key fields such as medicinal chemistry for gene delivery, photodynamic cancer therapy, and DNA photocleavage, but also in materials chemistry, catalysis, analytical, and coordination chemistry, among others. With this in mind, one of the C_{60}–IL hybrids was used for the immobilization of palladium nanoparticles through ion exchange with $PdCl_4^{2-}$ followed by reduction with sodium borohydride. Surprisingly, during reduction, several carbon nanostructures were formed that comprised nano-onions and nanocages displaying few-layers graphene sidewalls. The so-obtained nanomaterial was successfully applied as a recyclable catalyst in Suzuki and Heck reactions with a 0.2 mol% loading. In the former process, the catalyst was recycled for five consecutive runs with no loss in catalytic activity. In the light of the good results obtained, we developed a new synthetic strategy to anchor the previously tested catalyst on different supports, namely amorphous silica, SBA-15 and silica-coated maghemite. This approach led to extremely active catalytic systems employed in the Heck and Suzuki couplings. The catalytic performances of these materials were very impressive reaching a high TON (100,000) and a remarkable value of TOF (2,000,000 h^{-1}) that probably, to the best of our knowledge, represents the highest value ever reported for the Suzuki coupling mediated by heterogeneous palladium catalysts. Furthermore, silica supported catalyst proved to be highly recyclable, up to ten cycles, both in Suzuki and Heck reactions with only a slight decrease of catalytic activity in the tenth cycle of Heck reaction.

C_{60}-IL hybrids

1.6 Experimental Section

General: Chemicals and solvents were purchased from commercial suppliers or purified by standard techniques. For thin-layer chromatography (TLC), silica gel plates (Merck 60 F254) were used and compounds were visualized by irradiation with UV light and/or by treatment with a $KMnO_4$ solution. Flash chromatography was carried out using Macherey–Nagel silica gel (0.04–0.063 mm). Petroleum ether refers to the fraction with the boiling range 40–60 °C. ^1H and ^{13}C NMR spectra were recorded with a Bruker 250, Bruker 300 MHz or Bruker Avance II 400 MHz spectrometers. Solid-state ^{13}C CP-MAS NMR was recorded on a Bruker AV 2, 400 MHz spectrometer with samples packed in zirconia rotors spinning at 15 kHz. The specific surface areas were determined by applying the BET method[88] to the nitrogen adsorption isotherm registered at -196 °C using Sorptomatic 1900 (Carlo Erba) instrument. FTIR spectra were registered with a Shimadzu FTIR 8300 infrared spectrophotometer. UV-vis spectra were recorded with a Bechmann-Coulter DU 800 spectrophotometer thermostated at 20 °C. Thermogravimetric analysis (TGA) was performed under oxygen flow from 100 to 1000 °C with a heating rate of 10 °C/min in a Mettler Toledo TGA/DSC STAR System. Elemental analysis was performed through Thermo Finnigan Flash EA 1112 analyzer. XRD measurements were carried out with a Bruker D 5000 diffractometer equipped with a Cu *Kα* anode and a graphite monochromator. A proportional counter and a 0.05° step size in 2*θ* were used. The assignment of the various crystalline phases in 2*θ* was based on the JCPDS powder diffraction file cards (JCPDS Powder Diffraction File, International Centre for Diffraction Data, Swarthmore, PA, USA, 1989.). The particle size (*d*) was estimated as volume-average crystallite dimension, through the line-broadening (LB) of the available reflection peaks, using the Scherrer equation.[89] The instrumental broadening was determined by collecting the diffraction pattern of the standard, lanthanum hexaboride LaB_6. The X-ray photoelectron spectroscopy (XPS) analyses were performed with a VGMicrotech ESCA 3000Multilab, equipped with a dual Mg/Al anode. The spectra were excited by the unmonochromatized Al Kα source (1486.6 eV) run at 14 kV and 15 mA. The analyzer was operated in the constant analyzer energy (CAE) mode. For the individual peak energy regions, a pass energy of 20 eV set across the hemispheres was used. Survey spectra were measured at 50 eV pass energy. The sample powders were mounted on a double-sided adhesive tape. The pressure in the analysis chamber was in the range of 10^{-8}

Torr during data collection. The constant charging of the samples was removed by referencing all the energies to the C1s set at 284.6 eV. The invariance of the peak shapes and widths at the beginning and at the end of the analyses ensured absence of differential charging. Analyses of the peaks were carried out with the software provided by VG, based on non-linear least squares fitting program using a weighted sum of Lorentzian and Gaussian component curves after background subtraction according to Shirley and Sherwood.[90] Atomic concentrations were calculated from peak intensity using the sensitivity factors provided with the software. The binding energy values are quoted with a precision of ±0.15 eV and the atomic percentage with a precision of ±10%. TEM micrographs were recorded on a high-resolution transmission electron microscope (HR-TEM) JEOL JEM-2100 operating at 200 kV accelerating voltage. Samples were dispersed in water and drop cast onto carbon coated copper TEM grids for HR-TEM analysis. The imaging conditions were carefully tuned by lowering the accelerating voltage of the microscope and reducing the beam current density to a minimum in order to minimize the electron beam induced damage of the sample. SEM analyses were carried out on a FEI Quanta 200 FEG instrument equipped with Edax probe. MW-assisted catalytic tests were carried out with a CEM DISCOVER monomode system in closed vessel in manual mode (no remote PC control) with infrared sensor for temperature control and with no pressure control. Microwave Plasma - Atomic Emission Spettroscopy (MP-AES) analyses were carried out with a 4200 MP-AES, Agilent. Analyses were conducted using a calibration curve, obtained by dilution.

- **General procedure for preparation of compounds 1a-c**

Malonyl dichloride (1 eq.) was added to a solution of the appropriate alcohol (2 eq.) and pyridine (2 eq.) in 1,2-dichloroethane at 0 °C under Ar atmosphere. After 1 h, the mixture was allowed to warm up to room temperature, then stirred overnight. The reaction mixture was washed with a solution of 5% HCl (50 mL x 2) and a saturated solution of $NaHCO_3$ (60 mL x 2). The organic layer was dried over anhydrous sodium sulfate, filtered and evaporated. The products were purified by flash chromatography (SiO_2, CH_2Cl_2/petroleum ether).

Compound 1a. This compound was prepared from malonyl dichloride (9.00 mmol), 3-chloro-1-propanol (18.00 mmol) and pyridine (18.00 mmol) in 1,2-dichloroethane (60 mL). Purification by flash column chromatography (SiO_2, CH_2Cl_2/petroleum ether 60/40) gave **1a** (1.898 g, 61%) as a pale yellow oil. IR (neat): 1734 (C=O) cm^{-1}; ^1H NMR ($CDCl_3$, 250 MHz): δ = 4.33 (t, *J* = 6.0 Hz, 4H, OC***H***$_2$), 3.62 (t, *J* = 6.2 Hz, 4H, ClC***H***$_2$), 3.41 [s, 2H,

C***H***$_2$(COO)$_2$], 2.13 (quint, *J* = 6.1 Hz, 4H, ClCH$_2$C***H***$_2$) ppm; ^{13}C NMR ($CDCl_3$, 62.5 MHz): δ = 166.2 [2C, CH$_2$(***C***OO)$_2$], 62.2 (2C, O***C***H$_2$), 41.4 (2C, Cl***C***H$_2$), 40.8 [1C, ***C***H$_2$(COO)$_2$], 31.3 (2C, ClCH$_2$***C***H$_2$) ppm.

Compound 1b. This compound was prepared from malonyl dichloride (9.00 mmol), 3-bromo-1-propanol (18.00 mmol) and pyridine (18.00 mmol) in 1,2-dichloroethane (60 mL). Purification by flash column chromatography (SiO_2, CH_2Cl_2/petroleum ether 60/40) gave **1b** (1.684 g, 54%) as a pale yellow oil. ^{1}H NMR ($CDCl_3$, 250 MHz): δ = 4.32 (t, *J* = 6.1 Hz, 4H, OC***H***$_2$), 3.48 (t, *J* = 6.3 Hz, 4H, BrC***H***$_2$), 3.42 [s, 2H, C***H***$_2$(COO)$_2$], 2.21 (quint, *J* = 6.2 Hz, 4H, BrCH$_2$C***H***$_2$) ppm. Spectroscopic data of compound **2b** are in agreement with those reported in literature.[44b]

Compound 1c. This compound was prepared from malonyl dichloride (9.00 mmol), 3-azido-1-propanol (18.00 mmol) and pyridine (18.00 mmol) in 1,2-dichloroethane (60 mL). Purification by flash column chromatography (SiO_2, CH_2Cl_2/petroleum ether 80/20) gave **2c** (2.090 g, 86%) as a pale yellow oil. ^{1}H NMR ($CDCl_3$, 250 MHz): δ = 4.26 (t, *J* = 6.3 Hz, 4H, OC***H***$_2$), 3.42 [m, 6H, N$_3$C***H***$_2$ and, C***H***$_2$(COO)$_2$], 1.94 (quint, *J* = 6.2 Hz, 4H, N$_3$CH$_2$C***H***$_2$) ppm. Spectroscopic data of compound **1c** are in agreement with those reported in literature.[44a]

- **General procedure for preparation of compounds 2a-b**

The appropriate malonic ester **1a-c** (1 eq.), CBr_4 (2 eq.), and DBU (4 eq.) were added to a solution of C_{60} (1.5 eq.) in chlorobenzene. The reaction mixture was stirred for 24 h at room temperature and then was directly poured in the chromatographic column (SiO_2, toluene/hexane). The obtained compound was solubilized in a small amount of chloroform, precipitated with methanol and then centrifuged.

Compound 2a. This compound was prepared from **1a** (0.67 mmol), CBr_4 (1.34 mmol), DBU (2.68 mmol) and C_{60} (1.00 mmol) in chlorobenzene (105 mL). Purification by flash column chromatography (SiO_2, toluene/hexane 60/40) and subsequent precipitation gave **2a** (0.296 g, 45%) as a brown solid. IR (neat): 2961 (C–H), 1749 (C=O), 1460 (C–H bending) cm^{-1}; ^{1}H NMR ($CDCl_3$, 300 MHz): δ = 4.69 (t, *J* = 6.0 Hz, 4H, OC***H***$_2$), 3.74 (t, *J* = 6.3 Hz, 4H, ClC***H***$_2$), 2.33 (quint, *J* = 6.2 Hz, 4H, ClCH$_2$C***H***$_2$) ppm; ^{13}C NMR ($CDCl_3$, 100 MHz): δ = 163.56 (2C, C_{60}=C***C***OO), 145.47, 145.38, 145.18, 145.10, 144.86, 144.77, 144.05, 143.25,

143.21, 143.18, 142.36, 142.04, 141.19, 139.17, 71.49 (2C, C_{60} sp^3), 64.13 (2C, O***C***H_2), 51.98 [1C, C_{60}=C(***C***$OO)_2$], 41.03 (2C, Cl***C***H_2), 31.46 (2C, ClCH_2***C***H_2) ppm.

Compound 2b. This compound was prepared from **1b** (0.67 mmol), CBr_4 (1.34 mmol), DBU (2.68 mmol) and C_{60} (1.00 mmol) in chlorobenzene (105 mL). Purification by flash column chromatography (SiO_2, toluene/hexane 60/40) and subsequent precipitation gave **2b** (0.291 g, 41%) as a brown solid. Spectroscopic data of compound **2b** are in agreement with those reported in literature.[44b]

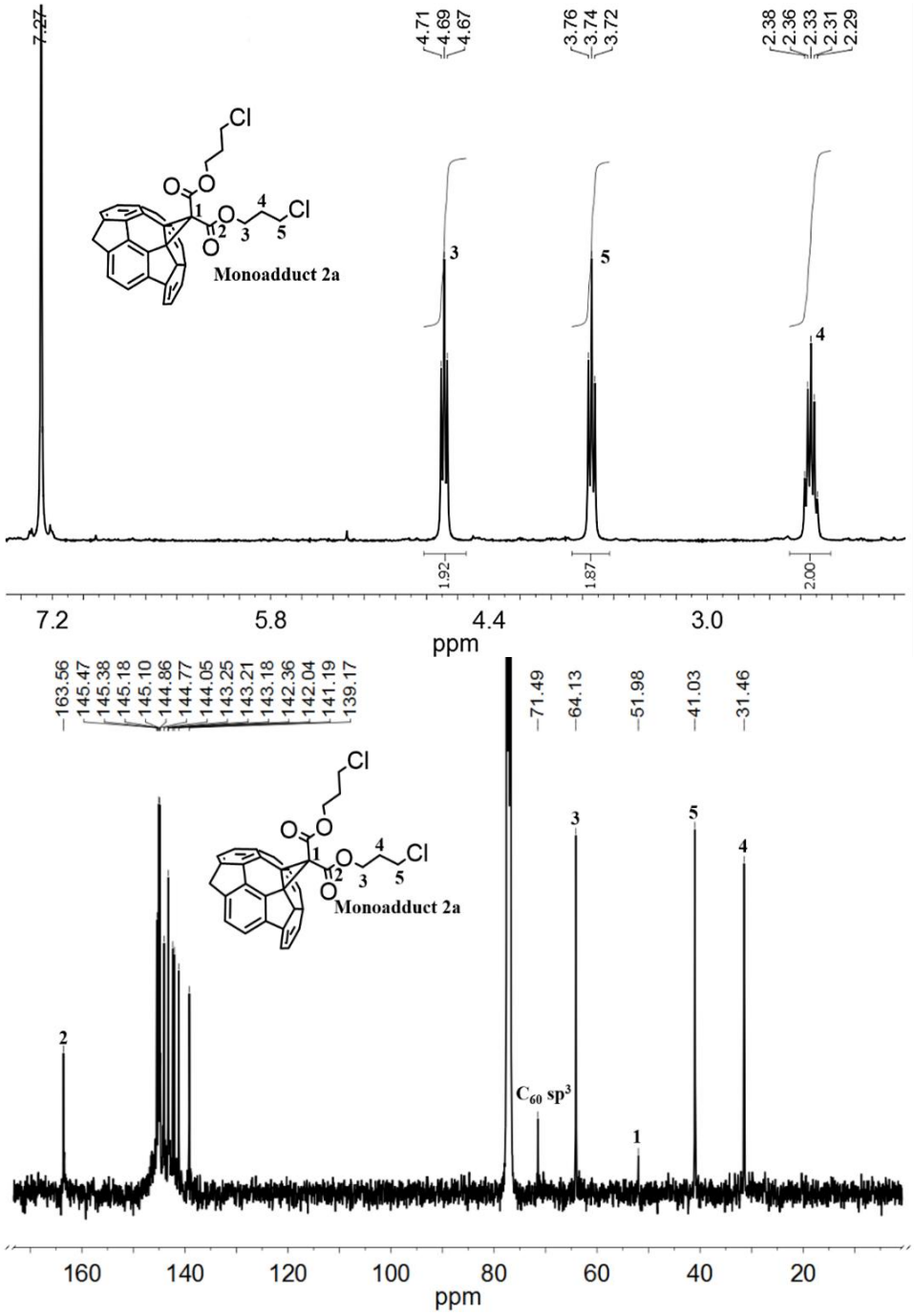

Figure E1. *^{1}H (top) and ^{13}C NMR (bottom) of compound **2a**.*

- **General procedure for preparation of compounds 3a-b**

1-butylimidazole (20 eq.) was added to a solution of the appropriate monoadduct (1 eq.) in chloroform. The reaction mixture was refluxed for 48 h. The solvent was evaporated and the remaining oil was solubilized in a small amount of methanol, precipitated with diethyl ether and then centrifuged. The supernatant was removed and the whole procedure of precipitation was repeated two times using first diethyl ether and then methanol.

Compound 3a. This compound was prepared from **2a** (0.10 mmol) and 1-butylimidazole (2.00 mmol) in chloroform (3.0 mL). After precipitation, **3a** was obtained in quantitative yield as a brown solid. IR (KBr): 3133 (C–H ring), 2955, 2928 (C–H) 1737 (C=O), 1625 (C=C, C=N), 1562 (C–C, C–N), 1460 (C–H alkyl bending), 1160 (C–H ring bending), 526 cm^{-1}; ^{1}H NMR (CD_3OD, 300 MHz): δ = 9.27 (m, 2H, 2***H***-imidazolium), 7.76 (m, 4H, 4***H*** and 5***H***-imidazolium), 4.29-4.80 (br, 12H, OC***H***$_2$, NC***H***$_2CH_2CH_2O$ and NC***H***$_2CH_2CH_2CH_3$), 2.53 (br, 4H, NCH_2C***H***$_2CH_2O$), 1.91 (br, 4H, NCH_2C***H***$_2CH_2CH_3$), 1.40 (br, 4H, NCH_2CH_2C***H***$_2CH_3$), 0.98 (br, 6H, $NCH_2CH_2CH_2C$***H***$_3$) ppm; ^{13}C NMR (CD_3OD, 100 MHz): δ = 164.46 (2C, C_{60}=C***C***OO), 146.56, 146.38, 146.09, 145.97, 145.48, 145.16, 144.36, 143.88, 143.51, 143.33, 143.10, 142.28, 141.62, 140.29, 140.13, 137.55, 124.06, 123.98, 72.91 (2C, C_{60} sp^3), 65.73 (2C, O***C***H_2), 51.96 [1C, C_{60}=C(***C***OO)$_2$], 50.86 (4C, N***C***$H_2CH_2CH_2CH_3$), 48.13 (4C, N***C***$H_2CH_2CH_2O$), 33.09 (4C, NCH_2***C***$H_2CH_2CH_3$), 30.35 (4C, NCH_2***C***H_2CH_2O), 20.58 (4C, NCH_2CH_2***C***H_2CH_3), 13.86 (4C, $NCH_2CH_2CH_2$***C***H_3) ppm.

Compound 3b. This compound was prepared from **2b** (0.10 mmol) and 1-butylimidazole (2.00 mmol) in chloroform (3.0 mL). After precipitation, **3b** was obtained in quantitative yield as a brown solid. IR (KBr): 3130 (C–H ring), 2955, 2928 (C–H) 1739 (C=O), 1625 (C=C, C=N), 1564 (C–C, C–N), 1460 (C–H alkyl bending), 1160 (C–H ring bending), 526 cm^{-1}; ^{1}H NMR (DMSO-d_6, 300 MHz): δ = 9.29 (s, 2H, 2***H***-imidazolium), 7.85 (s, 4H, 4***H*** and 5***H***-imidazolium), 4.56 (t, 4H), 4.36 (t, 4H), 4.17 (t, 4H), 2.37 (br, 4H, NCH_2C***H***$_2CH_2O$), 1.80 (quint, 4H, NCH_2C***H***$_2CH_2CH_3$), 1.27 (sext, 4H, NCH_2CH_2C***H***$_2CH_3$), 0.90 (t, 6H, $NCH_2CH_2CH_2C$***H***$_3$) ppm; ^{13}C NMR (CD_3OD, 100 MHz): δ = 164.37 (2C, C_{60}=C***C***OO), 146.58, 146.31, 146.19, 146.00, 145.90, 144.81, 144.78, 144.65, 144.57, 144.44, 143.49, 143.14, 142.28, 140.52, 140.31, 137.35, 124.04, 123.98, 72.83 (2C, C_{60} sp^3), 65.84 (2C, O***C***H_2), 52.02 [1C, C_{60}=C(***C***OO)$_2$], 50.86 (4C, N***C***$H_2CH_2CH_2CH_3$), 48.19 (4C, N***C***$H_2CH_2CH_2O$), 33.09 (4C, NCH_2***C***$H_2CH_2CH_3$), 30.76 (4C, NCH_2***C***H_2CH_2O), 20.60 (4C, NCH_2CH_2***C***H_2CH_3), 13.97 (4C, $NCH_2CH_2CH_2$***C***H_3) ppm.

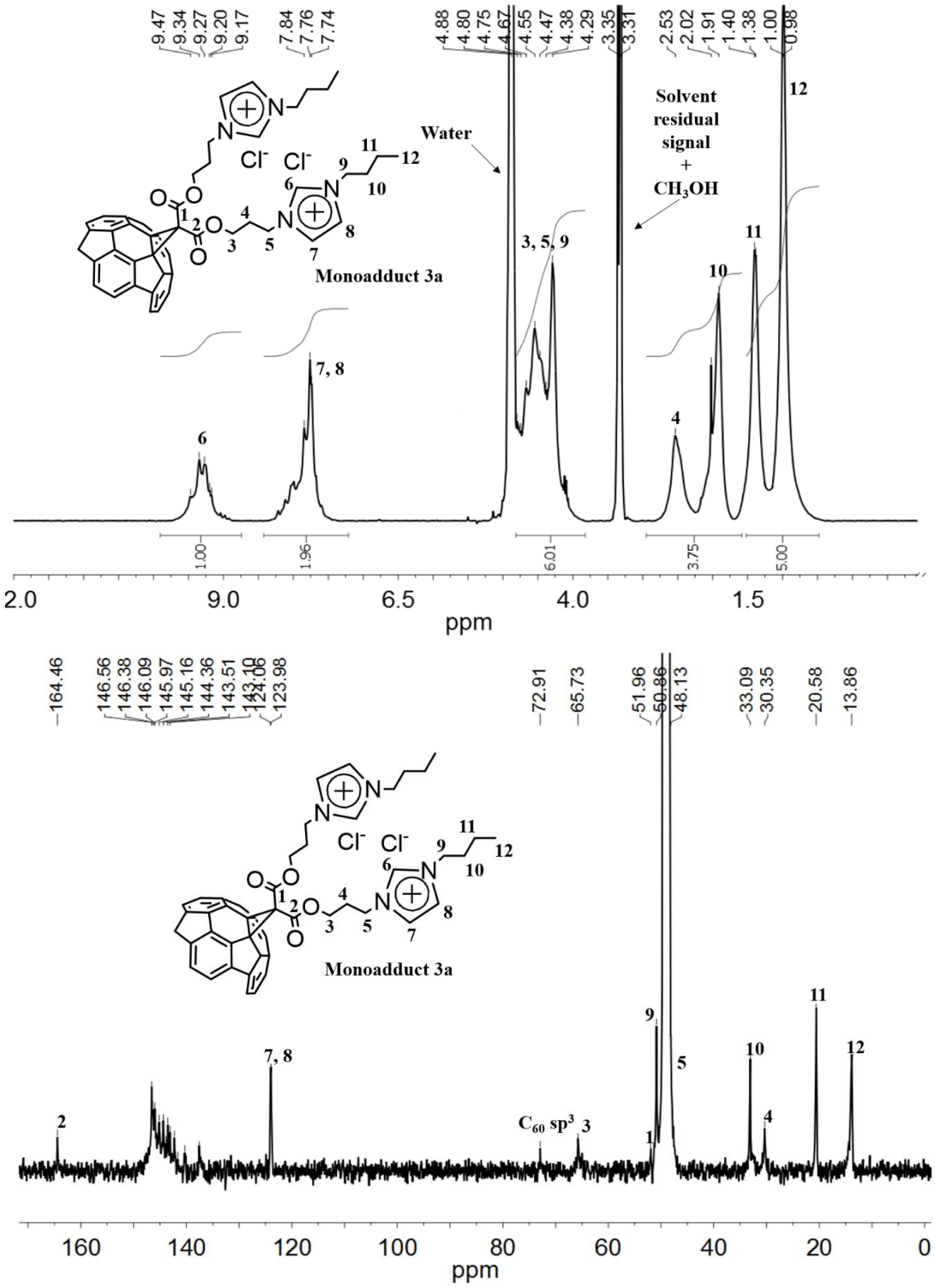

Figure E2. *^{1}H (top) and ^{13}C NMR (bottom) of compound **3a**.*

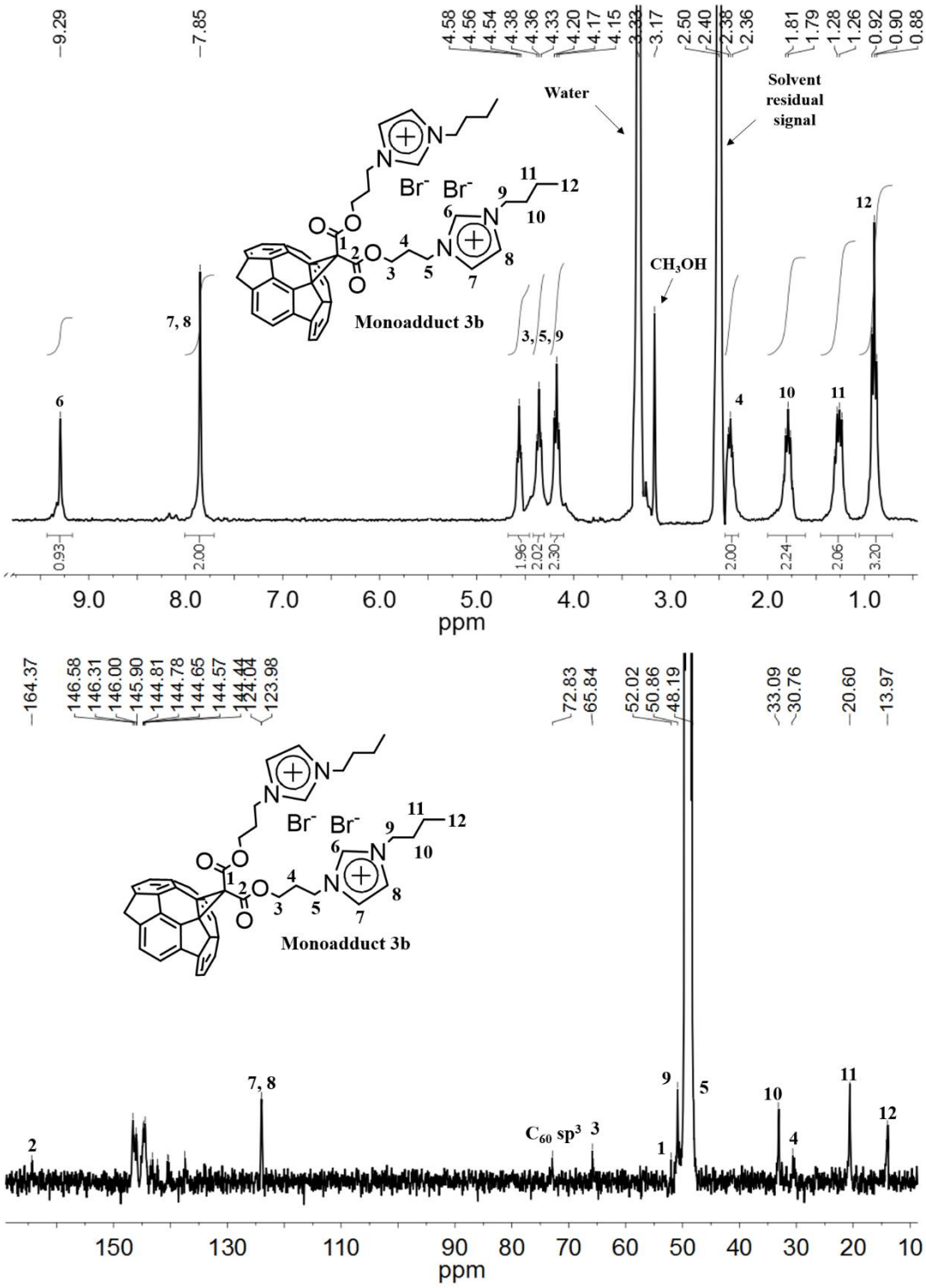

Figure E3. *^{1}H (top) and ^{13}C NMR (bottom) of compound **3b**.*

- **General procedure for preparation of compounds 4a-c**

The appropriate malonic ester (10 eq.), CBr_4 (50 eq.), and DBU (20 eq.) were added to a solution of C_{60} (1 eq.) in chlorobenzene. The reaction mixture was stirred for 72 h at room temperature and then was directly poured in the chromatographic column (SiO_2, CH_2Cl_2/hexane). The obtained compound was solubilized in a small amount of dichloromethane, precipitated with hexane and then centrifuged. The supernatant was removed and the whole procedure of precipitation was repeated two times using first hexane and then methanol.

Compound 4a. This compound was prepared from **1a** (5.00 mmol), CBr_4 (25.00 mmol), DBU (10.00 mmol) and C_{60} (0.50 mmol) in chlorobenzene (110 mL). Purification by flash column chromatography (SiO_2, CH_2Cl_2/petroleum ether 85/15) and subsequent precipitation gave **4a** (0.563 g, 50%) as a red glassy solid. 2967 (C–H) 1747 (C=O), 1448 (C–H bending) cm^{-1}; ^1H NMR ($CDCl_3$, 250 MHz): δ = 4.45 (t, *J* = 6.3 Hz, 24H, OC***H***$_2$), 3.61 (t, *J* = 6.4 Hz, 24H, ClC***H***$_2$), 2.18 (quint, *J* = 6.2 Hz, 24H, $ClCH_2C$***H***$_2$), ppm; ^{13}C NMR ($CDCl_3$, 62.5 MHz): δ = 163.5 (12C, C_{60}=C***C***OO), 145.8 (24C, C_{60} sp^2), 141.1 (24C, C_{60} sp^2), 69.1 (12C, C_{60} sp^3), 63.7 (24C, O***C***H_2), 45.3 [6C, C_{60}=C(***C***$OO)_2$], 40.9 (12C, Cl***C***H_2), 31.3 (12C, $ClCH_2$***C***H_2) ppm. MS (APCI) Calcd. 2244.0676, found 2244.1836.

Compound 4b. This compound was prepared from **1b** (5.00 mmol), CBr_4 (25.00 mmol), DBU (10.00 mmol) and C_{60} (0.50 mmol) in chlorobenzene (110 mL). Purification by flash column chromatography (SiO_2, CH_2Cl_2/petroleum ether 90/10) and subsequent precipitation gave **4b** (0.810 g, 58%) as a red glassy solid. IR (neat): 2965 (C–H) 1745 (C=O), 1460 (C–H bending) cm^{-1}; ^1H NMR ($CDCl_3$, 250 MHz): δ = 4.45 (t, *J* = 6.3 Hz, 24H, OC***H***$_2$), 3.45 (t, *J* = 6.6 Hz, 24H, BrC***H***$_2$), 2.26 (quint, *J* = 6.4 Hz, 24H, $BrCH_2C$***H***$_2$), ppm; ^{13}C NMR ($CDCl_3$, 62.5 MHz): δ = 163.5 (12C, C_{60}=C***C***OO), 145.8 (24C, C_{60} sp^2), 141.1 (24C, C_{60} sp^2), 69.1 (12C, C_{60} sp^3), 64.7 (24C, O***C***H_2), 45.3 [6C, C_{60}=C(***C***$OO)_2$], 31.3 (12C, Br***C***H_2), 29.0 (12C, $BrCH_2$***C***H_2) ppm. MS (APCI) Calcd. 2785.6330, found 2785.7178.

Compound 4c. This compound was prepared from **1c** (5.00 mmol), CBr_4 (25.00 mmol), DBU (10.00 mmol) and C_{60} (0.50 mmol) in chlorobenzene (110 mL). Purification by flash column chromatography (SiO_2, CH_2Cl_2/petroleum ether 90/10) and subsequent precipitation gave **5c** (0.493 g, 42%) as an orange glassy solid. ^1H NMR ($CDCl_3$, 300 MHz): δ = 4.30 (t, *J* = 6.0 Hz, 24H, OC***H***$_2$), 3.34 (t, *J* = 6.1 Hz, 24H, N_3C***H***$_2$), 1.89 (quint, *J* = 6.0 Hz, 24H, N_3CH_2C***H***$_2$) ppm; ^{13}C NMR ($CDCl_3$, 75 MHz): δ = 163.5 (12C, C_{60}=C***C***OO), 145.8 (24C,

C_{60} sp^2), 141.1 (24C, C_{60} sp^2), 69.1 (12C, C_{60} sp^3), 63.7 (24C, O***C***H_2), 47.8 (12C, N_3***C***H_2), 45.0 [6C, C_{60}=C(***C***$OO)_2$], 28.0 (12C, $BrCH_2$***C***H_2) ppm. Spectroscopic data of compound **4c** are in agreement with those reported in literature.[44a].

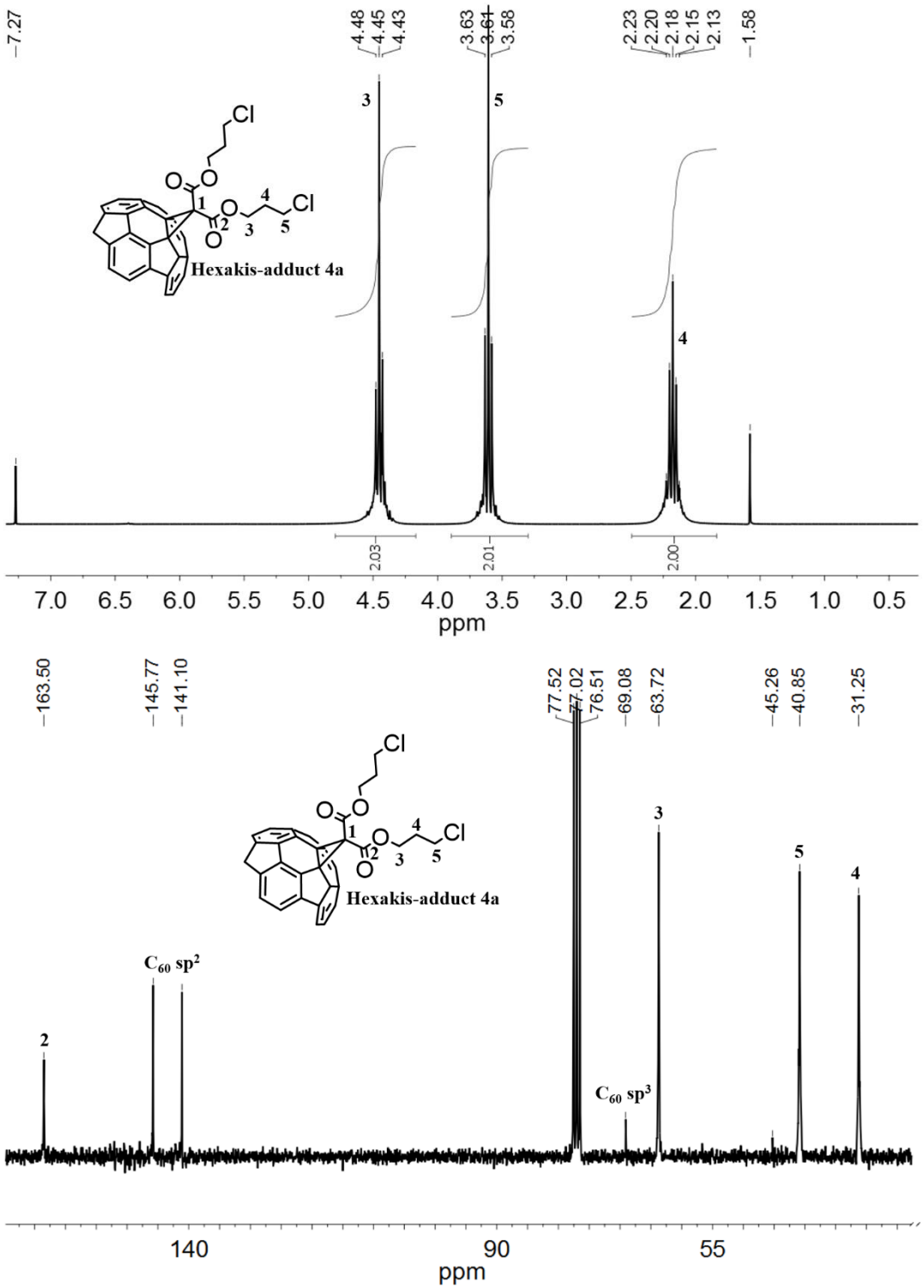

Figure E4. *^1H (top) and ^{13}C NMR (bottom) of compound **4a**.*

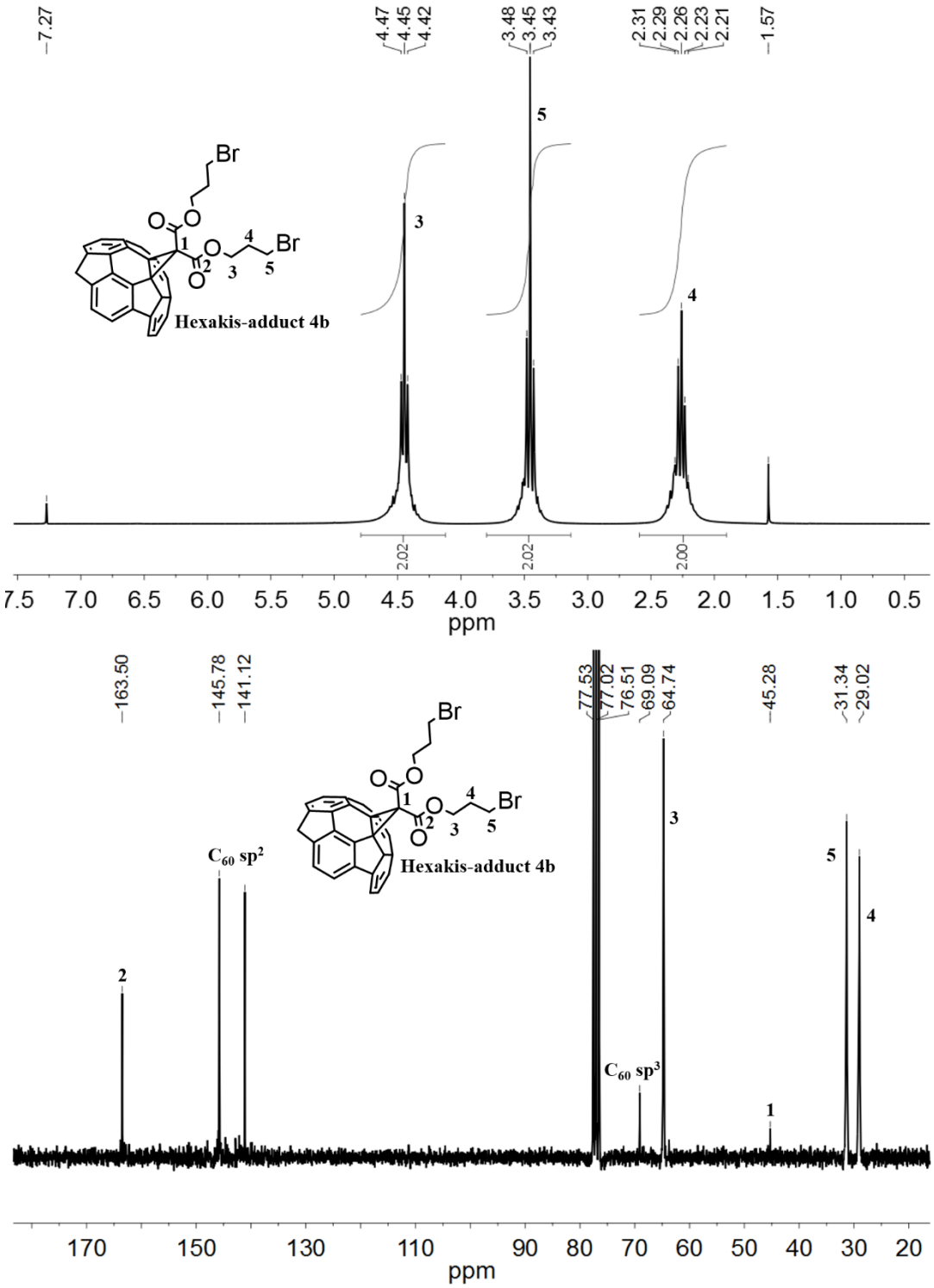

Figure E5. *^{1}H (top) and ^{13}C NMR (bottom) of compound* ***4b****.*

- **General procedure for preparation of compounds 5a-d**

1-methylimidazole, 1-butylimidazole or 1,2-dimethylimidazole (120 eq.) were added to a solution of the appropriate hexakis adduct (1 eq.) in chloroform. The reaction mixture was refluxed for 48 h. The solvent was evaporated and the obtained oil was solubilized in a small amount of methanol, precipitated with diethyl ether and then centrifuged. The supernatant was removed and the whole procedure of precipitation was repeated two times using first diethyl ether and then methanol.

Compound 5a. This compound was prepared from **4b** (0.04 mmol) and 1-methylimidazole (4.80 mmol) in chloroform (2.5 mL). After the precipitation, **5a** was obtained in quantitative yield as a brown viscous oil. IR (neat): 3151 (C–H ring), 3093, 2959 (C–H) 1741 (C=O), 1632 (C=C, C=N), 1571 (C–C, C–N), 1459 (C–H alkyl bending), 1168 (C–H ring bending) cm^{-1}; ^{1}H NMR (CD_3OD, 400 MHz): δ = 7.97-7.77 (m, 24H, 4***H*** and 5***H***-imidazolium), 4.63 (br, 48H, $NCH_2CH_2C\boldsymbol{H}_2O$ and , $NC\boldsymbol{H}_2CH_2CH_2O$), 4.12 (br, 36H, $NC\boldsymbol{H}_3$), 2.55 (br, 24H, $NCH_2C\boldsymbol{H}_2CH_2O$) ppm; ^{13}C NMR (CD_3OD, 100 MHz): δ = 164.13 (12C, C_{60}=C***C***OO), 146.89 (24C, C_{60} sp^2), 142.32 (24C, C_{60} sp^2), 137.89 (12C, 2***C***-imidazolium), 125.15 (12C, ***C***-imidazolium), 123.77 (12C, ***C***-imidazolium), 70.31 (12C, C_{60} sp^3), 66.41 (12C, O***C***H_2), 47.93 (24C, N***C***$H_2CH_2CH_2O$), 46.73 [6C, C_{60}=C(***C***$OO)_2$], 37.00 (12C, N***C***H_3), 30.22 (24C, $NCH_2\boldsymbol{C}H_2CH_2O$) ppm. Elem. Anal. Calcd for $C_{162}H_{144}Br_{12}N_{24}O_{24}$•$18H_2O$: C, 47.52; H, 4.43; N, 8.21. Found: C, 47.42; H, 4.65; N, 8.37.

Compound 5b. This compound was prepared from **4b** (0.04 mmol) and 1,2-dimethylimidazole (4.80 mmol) in chloroform (2.5 mL). After the precipitation, **5b** was obtained in quantitative yield as a brown viscous oil. IR (neat): 3137 (C–H ring), 3078, 2961 (C–H) 1739 (C=O), 1628 (C=C, C=N), 1589 (C–C, C–N), 1464 (C–H alkyl bending), 1180 (C–H ring bending) cm^{-1}; ^{1}H NMR (CD_3OD, 400 MHz): δ = 7.84-7.72 (m, 24H, 4***H*** and 5***H***-imidazolium), 4.72-4.53 (m, 48H, $NCH_2CH_2C\boldsymbol{H}_2O$ and , $NC\boldsymbol{H}_2CH_2CH_2O$), 4.00 (s, 36H, $NC\boldsymbol{H}_3$), 2.88 (s, 36H, $CC\boldsymbol{H}_3$), 2.48 (m, 24H, $NCH_2C\boldsymbol{H}_2CH_2O$) ppm; ^{13}C NMR (CD_3OD, 100 MHz): δ = 164.13 (12C, C_{60}=C***C***OO), 146.92 (24C, C_{60} sp^2), 146.16 (12C, 2***C***-imidazolium), 142.37 (24C, C_{60} sp^2), 124.02 (12C, 2***C***-imidazolium), 122.24 (12C, 2***C***-imidazolium), 70.40 (12C, C_{60} sp^3), 65.98 (12C, O***C***H_2), 46.77 (24C, N***C***$H_2CH_2CH_2O$), 46.39 [6C, C_{60}=C(***C***$OO)_2$], 36.03 (12C, N***C***H_3), 29.75 (24C, $NCH_2\boldsymbol{C}H_2CH_2O$), 10.56 (12C, C***C***$H_3$) ppm. Elem. Anal. Calcd for $C_{174}H_{168}Br_{12}N_{24}O_{24}$•$20H_2O$: C, 48.62; H, 4.88; N, 7.82. Found: C, 48.60; H, 5.17; N, 7.78.

Compound 5c. This compound was prepared from **4b** (0.04 mmol) and 1-butylimidazole (4.80 mmol) in chloroform (2.5 mL). After the precipitation, **5c** was obtained in quantitative yield as a red viscous oil. IR (neat): 3139 (C–H ring), 3079, 2961, 2873 (C–H) 1742 (C=O), 1636 (C=C, C=N), 1564 (C–C, C–N), 1463 (C–H alkyl bending), 1164 (C–H ring bending) cm^{-1}; ^{1}H NMR (CD_3OD, 400 MHz): δ = 7.73 (m, 24H, 4***H*** and 5***H***-imidazolium), 4.54-4.26 (br, 72H, OC***H***$_2$, NC***H***$_2CH_2CH_2O$ and NC***H***$_2CH_2CH_2CH_3$), 2.44 (br, 24H, NCH_2C***H***$_2CH_2O$), 1.92 (br, 24H, NCH_2C***H***$_2CH_2CH_3$), 1.41 (br, 24H, NCH_2CH_2C***H***$_2CH_3$), 1.00 (br, 36H, $NCH_2CH_2CH_2C$***H***$_3$) ppm; ^{13}C NMR (CD_3OD, 75 MHz): δ = 164.3 (12C, C_{60}=C***C***OO), 147.0 (24C, C_{60} sp^2), 142.4 (24C, C_{60} sp^2), 137.2 (12C, 2***C***-imidazolium), 123.9 (12C, ***C***-imidazolium), 123.7 (12C, ***C***-imidazolium), 70.3 (12C, C_{60} sp^3), 65.9 (12C, O***C***H_2), 50.9 (24C, N***C***$H_2CH_2CH_2CH_3$), 48.1 (24C, N***C***$H_2CH_2CH_2O$), 33.5 (24C, NCH_2***C***$H_2CH_2CH_3$), 30.2 (24C, NCH_2***C***H_2CH_2O), 20.5 (24C, NCH_2CH_2***C***H_2CH_3), 13.9 (24C, $NCH_2CH_2CH_2$***C***H_3) ppm. Elem. Anal. Calcd for $C_{198}H_{216}Br_{12}N_{24}O_{24}$•$12H_2O$: C, 52.95; H, 5.39; N, 7.49. Found: C, 53.18; H, 5.40; N, 7.12.

Compound 5d. This compound was prepared from **4a** (0.04 mmol) and 1-butylimidazole (4.80 mmol) in chloroform (2.5 mL). After the precipitation, **5d** was obtained in quantitative yield as a brown viscous oil. IR (neat): 3139 (C–H ring), 3077, 2962, 2873 (C–H) 1741 (C=O), 1637 (C=C, C=N), 1562 (C–C, C–N), 1460 (C–H alkyl bending), 1165 (C–H ring bending) cm^{-1}; ^{1}H NMR (CD_3OD, 400 MHz): δ = 9.21 (m, 12H, 2***H***-imidazolium), 7.73 (m, 24H, 4***H*** and 5***H***-imidazolium), 4.49-4.26 (m, 72H, OC***H***$_2$, NC***H***$_2CH_2CH_2O$ and NC***H***$_2CH_2CH_2CH_3$), 2.41 (m, 24H, NCH_2C***H***$_2CH_2O$), 1.91 (m, 24H, NCH_2C***H***$_2CH_2CH_3$), 1.40 (m, 24H, NCH_2CH_2C***H***$_2CH_3$), 0.99 (m, 36H, $NCH_2CH_2CH_2C$***H***$_3$) ppm; ^{13}C NMR (CD_3OD, 62.5 MHz): δ = 165.3 (12C, C_{60}=C***C***OO), 147.9 (24C, C_{60} sp^2), 143.3 (24C, C_{60} sp^2), 138.2 (12C, 2***C***-imidazolium), 124.9 (24C, 4***C*** and 5***C***-imidazolium), 71.0 (12C, C_{60} sp^3), 66.6 (12C, O***C***H_2), 51.7 (24C, N***C***$H_2CH_2CH_2CH_3$), 48.6 (24C, N***C***$H_2CH_2CH_2O$), 33.9 (24C, NCH_2***C***$H_2CH_2CH_3$), 31.1 (24C, NCH_2***C***H_2CH_2O), 21.4 (24C, NCH_2CH_2***C***H_2CH_3), 14.8 (24C, $NCH_2CH_2CH_2$***C***H_3) ppm. Elem. Anal. Calcd for $C_{198}H_{216}Cl_{12}N_{24}O_{24}$•$30H_2O$: C, 55.54; H, 6.50; N, 7.85. Found: C, 55.61; H, 6.54; N, 7.47.

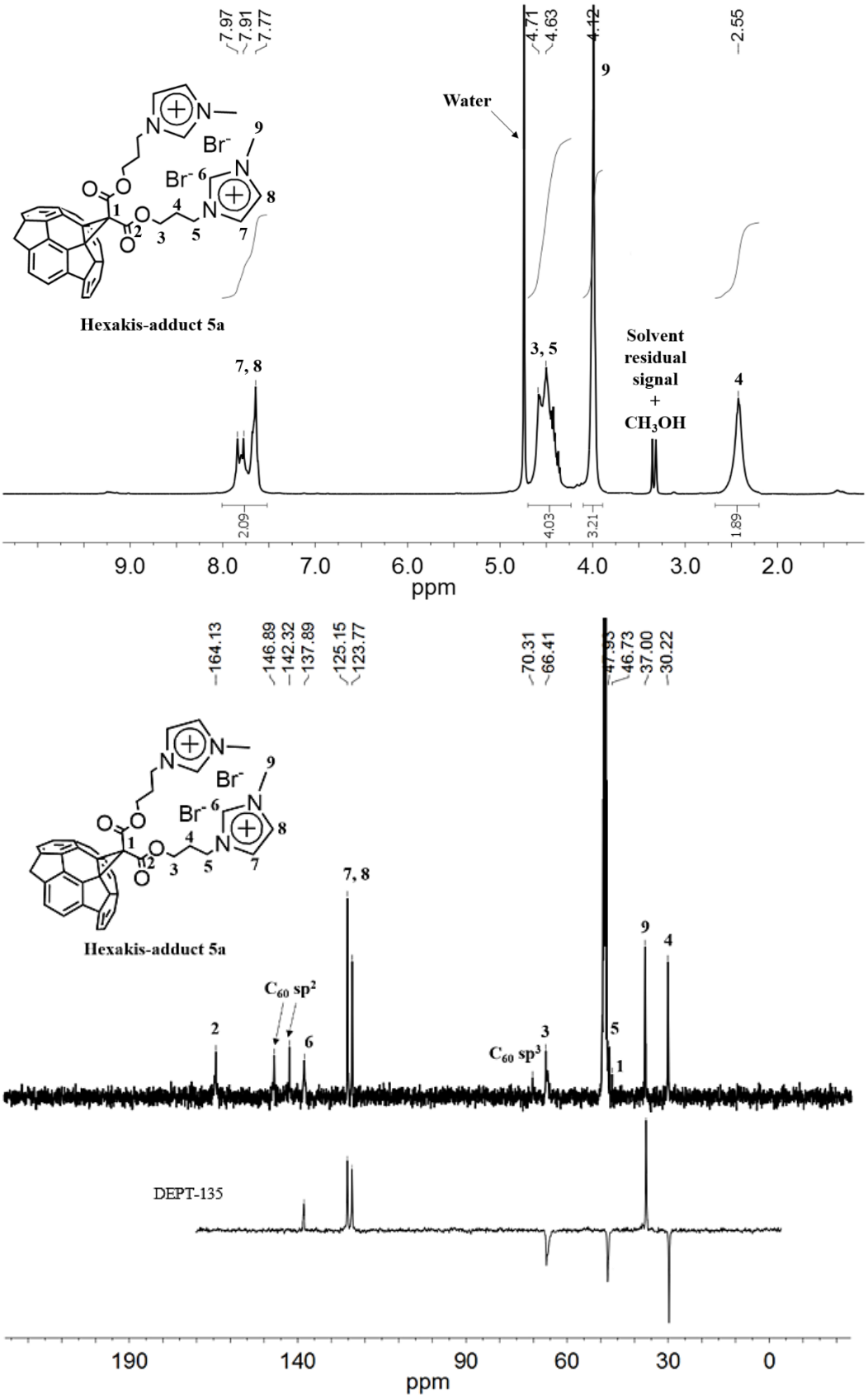

Figure E6. *^{1}H NMR (top), ^{13}C NMR and DEPT-135 (bottom) of compound **5a**.*

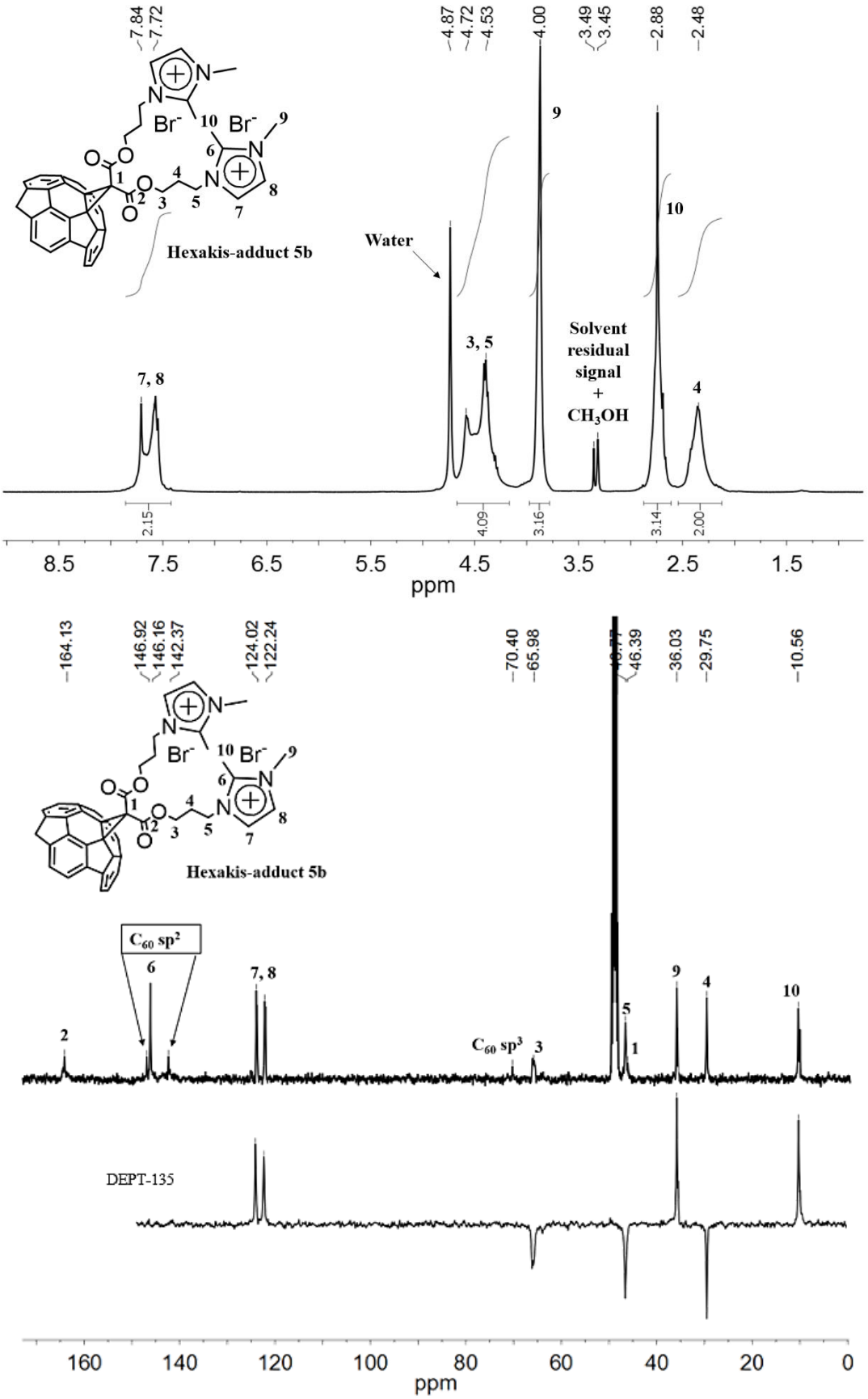

Figure E7. *^{1}H NMR (top), ^{13}C NMR and DEPT-135 (bottom) of compound* ***5b****.*

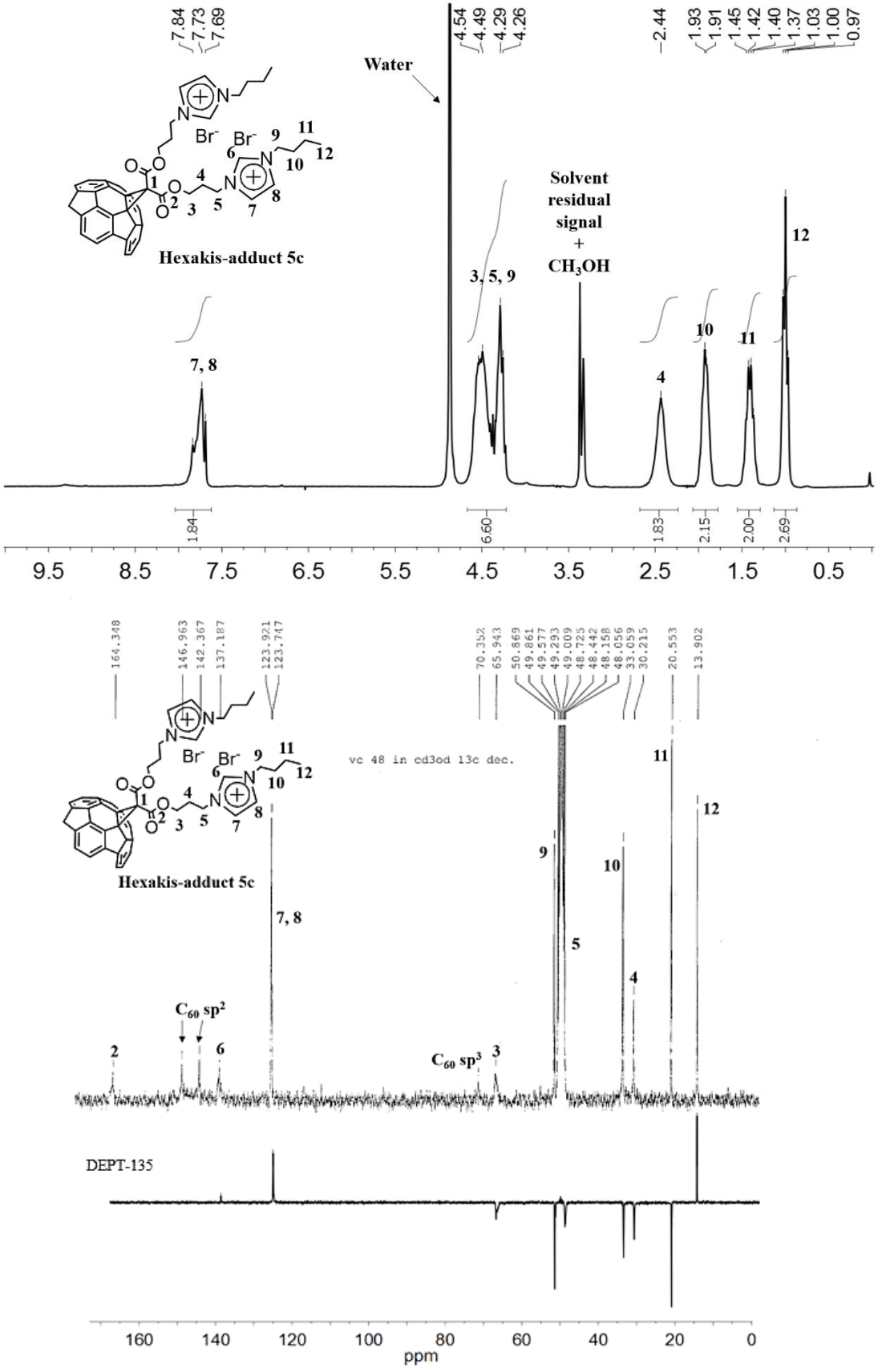

Figure E8. *^{1}H NMR (top), ^{13}C NMR and DEPT-135 (bottom) of compound* ***5c****.*

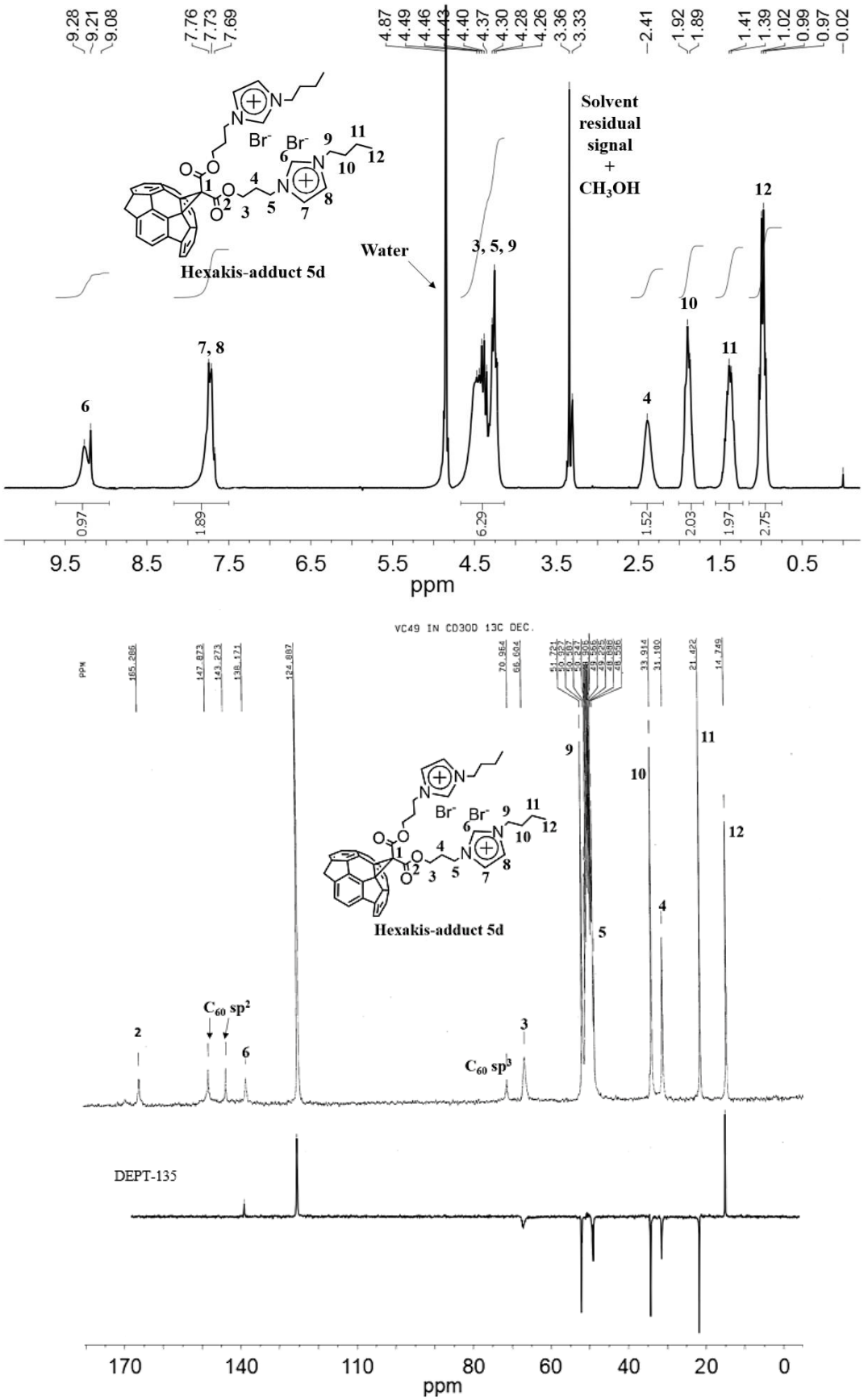

Figure E9. *^{1}H NMR (top), ^{13}C NMR and DEPT-135 (bottom) of compound* ***5d****.*

- **Synthesis of compound 6**

$CuSO_4 \cdot 5H_2O$ (0.012 mmol) and sodium ascorbate (0.036 mmol) were added to a mixture of **4c** (0.12 mmol) and phenylacetylene (1.83 mmol) in CH_2Cl_2/H_2O (1:1) (8 mL). The reaction mixture was stirred overnight at room temperature under argon atmosphere. The organic layer was diluted with CH_2Cl_2, washed with water, dried over Na_2SO_4, filtered and evaporated. Purification by flash column chromatography (SiO_2, 1% of methanol in dichloromethane) gave the desired product (340 mg, 80%) as an orange glassy solid. Spectroscopic data are in agreement with those reported in literature.[44a]

A solution of the obtained product (0.02 mmol) in chloroform (2 mL) was reacted with benzyl bromide (2.4 mmol). The reaction mixture was refluxed for 48 h. The solvent was evaporated and the obtained oil was solubilized in a small amount of dichloromethane, precipitated with hexane and then centrifuged. The supernatant was removed and the whole procedure of precipitation was repeated three times using diethyl ether. Compound **6** was obtained in quantitative yield as an orange/red glassy solid. IR (neat): 3053 (C–H arom), 2964 (C–H) 1743 (C=O), 1613 (C=C, C=N), 1494 (N=N), 1455 (C–H alkyl bending) cm^{-1}; ^1H NMR ($CDCl_3$, 250 MHz): δ = 9.64 (m, 12H, 5***H***-triazolium), 8.04-7.02 (m, 120H, ***H*** arom), 5.78 (m, 24H, NC***H***$_2$Ph), 5.03 (m, 24H), 4.49 (m, 24H), 2.57 (m, 24H, $NCH_2C\boldsymbol{H}_2CH_2O$) ppm; ^{13}C NMR ($CDCl_3$, 62.5 MHz): δ = 163.0 (12C, C_{60}=C***C***OO), 145.7 (12C, C_{60} sp^2), 142.8 (12C, 4***C***-triazolium), 140.9 (12C, C_{60} sp^2), 131.5, 129.8, 129.3, 129.1, 128.9, 128.6, 128.2, 127.3, 121.9, 69.0 (12C, C_{60} sp^3), 64.1 (12C, O***C***H_2), 55.7 (24C, N***C***H_2Ph), 51.2 (24C, N***C***$H_2CH_2CH_2O$), 28.5 (24C, $NCH_2\boldsymbol{C}H_2CH_2O$) ppm.

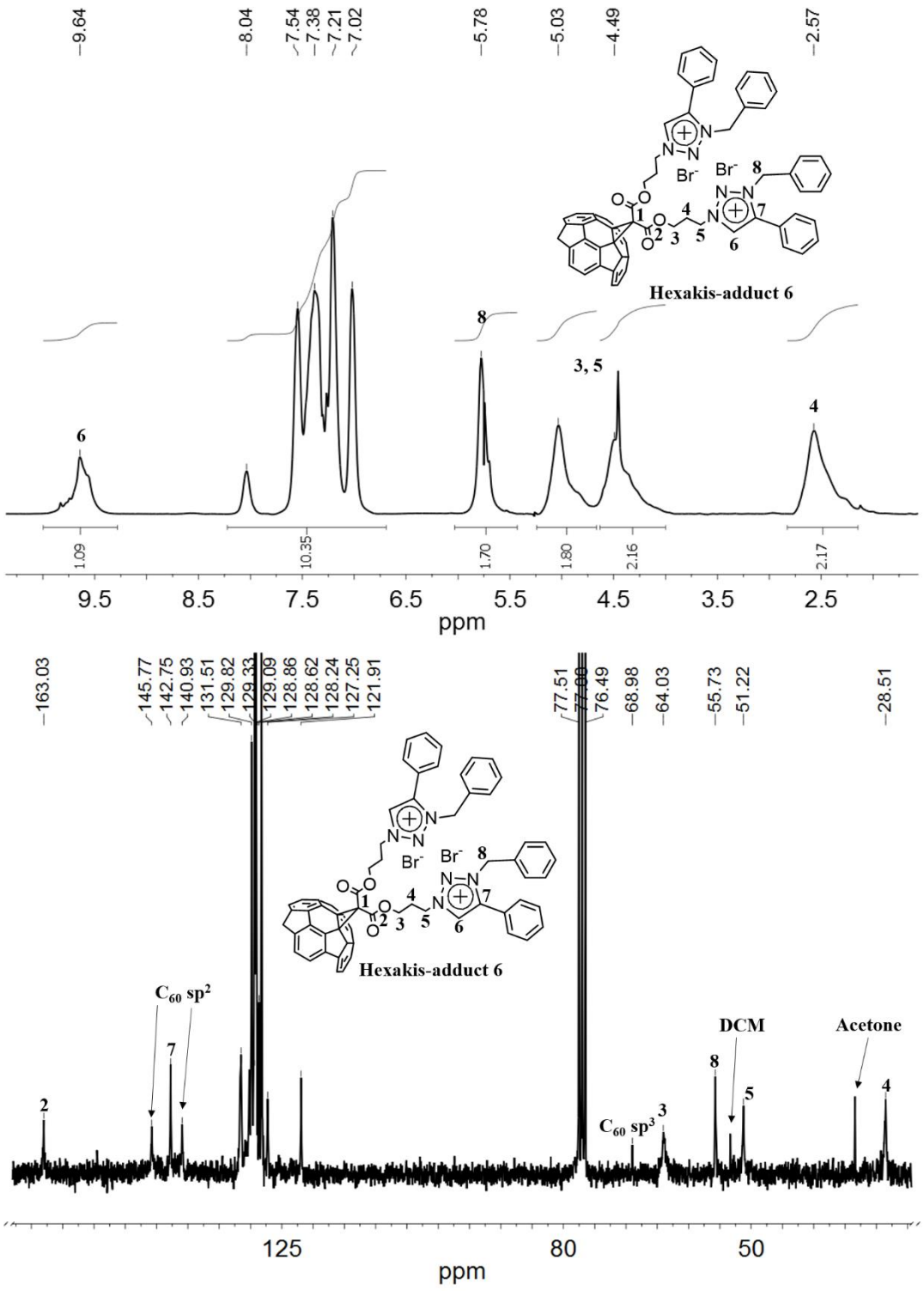

Figure E10. *^{1}H NMR (top) and ^{13}C NMR (bottom) of compound **6**.*

- **General Procedure for the Synthesis of Palladium Catalyst 8.**

$PdCl_2$ (37 mg, 0.209 mmol) and NaCl (246 mg, 4.18 mmol, 20 eq.) in water (5.3 mL) were heated at 80 °C until the $PdCl_2$ was dissolved. The obtained clear reddish solution was cooled at room temperature. A solution in water (1.8 mL) of compound **5a** (200 mg) was added dropwise to the previous solution. The obtained brown suspension was stirred at room temperature for 20 h, then solvent was removed under vacuum and the sticky brown residue was dried overnight under reduced pressure at room temperature affording **7**. The brown solid **7** was suspended in ethanol (4.8 mL) and to this suspension a solution of $NaBH_4$ (57 mg, 1.46 mmol, 7 equiv.) in ethanol (4.8 mL) was added dropwise. The suspension turned black and was stirred at room temperature for 6 h. After removal of water under vacuum, the obtained black residue was suspended in 30 mL of water and dialyzed by dialysis tubing (molecular weight cutoff 1000 Da) for 3 days. After removal of water under vacuum and drying at 40 °C overnight, catalyst **8** (93 mg) was obtained as a dark powder.

- **General Procedure for the Suzuki Reaction with catalyst 8**

In a round-bottom flask catalyst **8** (0.2 mol%, 1 mg), phenylboronic acid (138 mg, 1.1 mmol), K_2CO_3 (167 mg, 1.2 mmol), aryl bromide (1 mmol), ethanol (1.2 mL) and water (1.2 mL) were placed and stirred at 50 °C for 3 h. Then, the reaction mixture was allowed to cool down at room temperature, diluted with water, extracted three times with dichloromethane and dried over Na_2SO_4. The organic phase was evaporated under vacuum and the residue was purified by a short flash column chromatography (SiO_2, petroleum ether/ethyl acetate). Conversions were determined by ^1H NMR. Spectroscopic data are in agreement with those reported in literature.[91]

- **Recycling procedure of catalyst 8 in the Suzuki reaction**

Recycling tests were performed in a test tube in which catalyst **8** (0.2 mol%, 3 mg), phenylboronic acid (415 mg, 3.3 mmol), K_2CO_3 (503 mg, 3.6 mmol), 4-bromobenzaldehyde (561 mg, 3 mmol), ethanol (3.6 mL) and water (3.6 mL) were placed. The reaction was carried out at 50 °C for 3 h. The reaction mixture was allowed to cool down to room temperature and was directly centrifuged in the test tube. The supernatant was removed and collected. The centrifugation was repeated after the addition of ethanol and then two times using dichloromethane. The collected organic layers were washed with water and the

aqueous phase was further extracted two times with dichloromethane. The organic layers were dried over anhydrous sodium sulfate, filtered and evaporated. The product was purified by flash column chromatography (SiO_2, petroleum ether/ethyl acetate).

- **General Procedure for the Heck Reaction with catalyst 8**

In a round-bottom flask catalyst **8** (0.2 mol%, 1 mg), methyl acrylate (1.5 mmol), aryliodide (1 mmol), triethylamine (2 mmol) and DMF/H_2O (4 mL + 1 mL) were placed and heated at 90 °C for the appropriate time. Then, the reaction was allowed to cool down to room temperature, diluted with water and extracted with dichloromethane. The organic phase was evaporated under vacuum and the residue was purified by a short flash column chromatography (SiO_2, petroleum ether/ethyl acetate). Conversions were determined by ^1H NMR. Spectroscopic data are in agreement with those reported in literature.[92]

Supported C_{60}-IL hybrids
1.7 Experimental Section

- **Preparation of the support materials**

SBA-15. Mesoporous SBA-15 was prepared starting from tetraethyl orthosilicate (TEOS), as silica source and using a triblock poly(ethylene oxide)-poly(propylene oxide)-poly(ethylene oxide) ($EO_{20}PO_{70}EO_{20}$, Pluronic P123), as template, according to a published procedure.[79b]

γ-Fe_2O_3@SiO_2. 14 wt% silica-coated Fe_2O_3 were prepared by flame spray pyrolysis (FSP) of iron(III) acetylacetonate in xylene–acetonitrile solution and the resulting aerosol was *in situ* coated with SiO_2 using hexamethyldisiloxane (HMDSO) vapour as silica source.[93]

- **General procedure for the synthesis of materials 10a-c**

In a two-necked round bottom flask C_{60}-IL-hexakis-adduct **8**[77] (1 eq.) and triethoxy-3-(2-imidazolin-1-yl)propylsilane (1.5 eq.) in anhydrous toluene were placed. The reaction mixture was refluxed under stirring and in Argon atmosphere for 24 h (intermediates **9a-c** were not isolated). Afterwards, to the reaction mixture, the appropriate amount of support material was added and the obtained suspension was refluxed under Argon atmosphere for 72 h. The obtained materials (**10a-c**) were washed following the procedures described in the text below.

SiO_2-C_{60} 10a. This material was prepared from C_{60}-IL-hexakis-adduct **8** (500 mg, 0.180 mmol) and triethoxy-3-(2-imidazolin-1-yl)propylsilane (75 μL, 0.270 mmol) in anhydrous toluene (15 mL). After refluxing for 24 h, 1 g of amorphous silica was added and the obtained suspension was refluxed for a further 72 h. Then the suspension was filtered under reduced pressure by a sintered glass funnel, washed with toluene, dichloromethane and diethyl ether and the recovered solid was dried in an oven overnight at 40 °C obtaining material **10a** as a brown powder (1.4 g).

SBA15-C_{60} 10b. This material was prepared from C_{60}-IL-hexakis-adduct **8** (250 mg, 0.090 mmol) and triethoxy-3-(2-imidazolin-1-yl)propylsilane (36 μL, 0.135 mmol) in anhydrous toluene (8 mL). After refluxing for 24 h, 500 mg of SBA-15 were added and the obtained

suspension was refluxed for a further 72 h. Then the suspension was filtered under reduced pressure by a sintered glass funnel, washed with toluene, ethyl acetate and diethyl ether and the recovered solid was dried in an oven overnight at 40 °C obtaining material **10b** as a light brown powder (565 mg).

γ-Fe_2O_3@SiO_2-C_{60} 10c. This material was prepared from C_{60}-IL-hexakis-adduct **8** (514 mg, 0.278 mmol) and triethoxy-3-(2-imidazolin-1-yl)propylsilane (78 μL, 0.278 mmol) in anhydrous toluene (15 mL). After refluxing for 24 h, 514 mg of silica-coated maghemite (γ-Fe_2O_3@SiO_2) were added and the obtained suspension was refluxed for a further 72 h. Then the suspension was magnetically decanted with the aid of an external magnet, washed with toluene and diethyl ether and the recovered solid was finally dried in an oven overnight at 40 °C obtaining material **10c** as a brown powder (786 mg).

- **General procedure for the synthesis of materials 11a-c**

To a suspension of the indicated amount of materials **10a-c** in toluene, 1-methylimidazole (15 eq. with respect to propyl bromide moieties as determined by TG analysis of material 10a-c) was added. The reaction mixture was refluxed under stirring for 72 h. The obtained materials (**11a-c**) were washed following the procedures described in the text below.

SiO_2-C_{60}-IL 11a. This material was prepared from 1-methylimidazole (1.39 mL 17.35 mmol) and 1.3 g of material **10a** in toluene (40 mL). After refluxing for 72 h, the suspension was filtered under reduced pressure by a sintered glass funnel, washed with toluene, ethyl acetate and diethyl ether and the recovered solid was finally dried in an oven overnight at 40 °C obtaining material **11a** as a brown powder (1.390 g).

SBA15-C_{60}-IL 11b. This material was prepared from 1-methylimidazole (405 μL, 5.05 mmol) and 537 mg of material **10b** in toluene (20 mL). After refluxing for 72 h, the suspension was filtered under reduced pressure by a sintered glass funnel, washed with toluene, ethyl acetate and diethyl ether and the recovered solid was finally dried in an oven overnight at 40 °C obtaining material **11b** as a light brown powder (545 mg).

γ-Fe_2O_3@SiO_2-C_{60}-IL 11c. This material was prepared from 1-methylimidazole (830 μL, 10.36 mmol) and 757 mg of material **10c** in toluene (20 mL). After refluxing for 72 h, the suspension was magnetically decanted with the aid of an external magnet, washed with toluene, ethyl acetate and diethyl ether and the recovered solid was finally dried in an oven

overnight at 40 °C obtaining material **11b** as a brown powder (761 mg).

- **General procedure for the synthesis of materials 12a-c**

$PdCl_2$ (10.40 mg, 0.058 mmol) and NaCl (68.13 mg, 1.16 mmol) in water (4 mL) were heated at 80 °C until the $PdCl_2$ was dissolved. The obtained clear reddish solution of sodium tetrachloropalladate(II) was cooled at room temperature and added dropwise to a suspension of materials (**11a-c**, 300 mg) in water (2 mL). The reaction mixture was stirred overnight at room temperature. The obtained materials (**12a-c**) were washed following the procedures described in the text below.

SiO_2-C_{60}-IL-Pd(II) 12a. After the ion metathesis reaction of material **11a** with tretrachloropalladate anions, the obtained suspension was filtered under reduced pressure by a sintered glass funnel, washed with water, methanol and diethyl ether and the recovered solid was finally dried in an oven overnight at 40 °C obtaining material **12a** as a brown powder (252 mg).

SBA15-C_{60}-IL-Pd(II) 12b. After the ion metathesis reaction of material **11b** with tretrachloropalladate anions, the obtained suspension was filtered under reduced pressure by a sintered glass funnel, washed with water, methanol and diethyl ether and the recovered solid was finally dried in an oven overnight at 40 °C obtaining material **12b** as a light brown powder (290 mg).

γ-Fe_2O_3@SiO_2-C_{60}-IL-Pd(II) 12c. After the ion metathesis reaction of material **11c** with tretrachloropalladate anions, the obtained suspension was magnetically decanted with the aid of an external magnet, washed with water, methanol and diethyl ether and the recovered solid was finally dried in an oven overnight at 40 °C obtaining material **12c** as a brown powder (761 mg).

- **General procedure for the synthesis of materials 13a-c**

To a suspension of materials **12a-c** in ethanol a solution of $NaBH_4$ in ethanol was added dropwise. The reaction mixture was stirred at room temperature for 6 h. The obtained catalysts **13a-c** were washed following the procedures described in the text below.

SiO_2-C_{60}-IL-Pd 13a. The suspension of 240 mg of material **12a** in ethanol (5 mL) was reduced with a solution of $NaBH_4$ (12.16 mg, 0.315 mmol, 7 eq.) in ethanol (2 mL). Then the reaction mixture was filtered under reduced pressure by a sintered glass funnel, washed with water, methanol and diethyl ether and the recovered solid was finally dried in an oven overnight at 40 °C obtaining material **13a** as a brown powder (238 mg).

SBA15-C_{60}-IL-Pd 13b. The suspension of 280 mg of material **12b** in ethanol (5 mL) was reduced with a solution of $NaBH_4$ (14.20 mg, 0.368 mmol, 7 eq.) in ethanol (2 mL). Then the reaction mixture was filtered under reduced pressure by a sintered glass funnel, washed with water, methanol and diethyl ether and the recovered solid was finally dried in an oven overnight at 40 °C obtaining material **13a** as a brown powder (278 mg).

γ-Fe_2O_3@SiO_2-C_{60}-IL-Pd 13c. The suspension of 243 mg of material **12c** in ethanol (5 mL) was reduced with a solution of $NaBH_4$ (12.35 mg, 0.320 mmol, 7 eq.) in ethanol (2 mL). Then the reaction mixture was magnetically decanted with the aid of an external magnet, washed with water, methanol and diethyl ether and the recovered solid was finally dried in an oven overnight at 40 °C obtaining material **12c** as a brown powder (761 mg).

- **General Procedure for the Heck Reaction with catalysts 13a-c**

In a 3 mL glass vial with screw cap catalyst (**13a-c**, 0.1 mol%), aryliodide (0.5 mmol), alkene (0.75 mmol), triethylamine (1 mmol) and DMF (1 mL) were placed and stirred at 120 °C for the appropriate time. Then the reaction mixture was allowed to cool down to room temperature, poured in 20 mL of water and extracted with diethyl ether (3 x 20 mL). The combined organic layers were dried over Na_2SO_4 filtered and evaporated under vacuum. Conversions were determined by ^1H NMR. Spectroscopic data are in agreement with those reported in literature.[92a, b, 94]

- **Recycling procedure of catalyst 13a-b in the Heck reaction**

In a 10 mL glass vial with screw cap catalysts (**13a-b**, 0.1 mol%), 4-iodoanisole (477.61 mg, 2 mmol), methyl acrylate (272 μL, 3 mmol), triethylamine (560 μL, 4 mmol) and DMF (4 mL) were placed and stirred at 120 °C for 4 h. Then the reaction mixture was allowed to cool down to room temperature and centrifuged removing the supernatant. Catalyst was washed, sonicated and centrifuged with ethyl acetate, methanol and diethyl ether and then dried in an oven at 40 °C before using it for the next cycle. The recovered organic layers

were collected and evaporated under reduced pressure to remove volatiles then poured in 20 mL of water and extracted with diethyl ether (3 x 20 mL). The combined organic layers were dried over Na_2SO_4 filtered and evaporated under vacuum. Conversions were determined by ^{1}H NMR.

- **General Procedure for the Suzuki Reaction with catalysts 13a-c (0.01 mol%)**

In a 3 mL glass vial with screw cap catalyst (**13a-c**, 0.01 mol%), aryl bromide (0.5 mmol), phenylboronic acid (0.55 mmol), K_2CO_3 (0.6 mmol) and a mixture of EtOH/H_2O 1:1 (0.4 mL) were placed and stirred at 50 °C for the appropriate time. The reaction mixture was diluted with water, extracted three times with dichloromethane and the combined organic layers dried over Na_2SO_4. The organic phase was evaporated under vacuum and the residue was purified by a short flash column chromatography (SiO_2, petroleum ether/ethyl acetate). Conversions were determined by ^{1}H NMR. Spectroscopic data are in agreement with those reported in literature.[91, 95]

- **General Procedure for the Suzuki Reaction with catalysts 13a-c (0.001 mol%)**

In a 3 mL glass vial with screw cap catalyst (**13a-c**, 0.001 mol%), 4-bromobenzaldehyde (2 mmol), phenylboronic acid (2.2 mmol), K_2CO_3 (2.4 mmol) and a mixture of EtOH/H_2O 1:1 (1.6 mL) were placed and stirred at 50 °C for the appropriate time. The reaction mixture was diluted with water, extracted three times with dichloromethane and the combined organic layers dried over Na_2SO_4. The organic phase was evaporated under vacuum and the residue was purified by a short flash column chromatography (SiO_2, petroleum ether/ethyl acetate). Conversions were determined by ^{1}H NMR.

- **Suzuki reaction with catalyst 13b under microwave irradiation**

In a microwave glass tube 4-bromoacetophenone (406.20 mg, 2.0 mmol), phenylboronic acid (276.54 mg, 2.2 mmol), K_2CO_3 (335.05 mg, 2.4 mmol) and the appropriate amount of catalyst **13b** were placed. Then, water (0.8 mL) and ethanol (0.8 mL) were added. The reaction mixture was sonicated for a short time and heated under microwave irradiation (11 W) at 120 °C for 3 minutes. Then, the reaction mixture was cooled at room temperature and, after confirming the complete conversion by TLC, the crude was poured into water and extracted with diethyl ether. The organic layers were dried over Na_2SO_4 and the solvent

evaporated under vacuum to afford the desired product in 100% yield (confirmed by TLC and GC-MS).

- **Recycling procedure of catalysts 13a and 13b in the Suzuki reaction**

In a 3 mL glass vial with screw cap catalyst (**13a** or **13b**, 0.1 mol%), 4-bromobenzaldehyde (93.44 mg, 0.5 mmol), phenylboronic acid (70.59 mg, 0.55 mmol), K_2CO_3 (82.93 mg, 0.6 mmol) and a mixture of EtOH/H_2O 1:1 (1.2 mL) were placed and stirred at 50 °C. Reaction times were 2 h when catalyst **13a** was used or 40 minutes in the case of catalyst **13b**. The reaction mixture was diluted with ethyl acetate and centrifuged removing the supernatant. Catalyst was washed, sonicated and centrifuged with dichloromethane, methanol and diethyl ether and then dried in an oven at 40 °C before using it for the next cycle. The recovered organic layers were collected and evaporated under reduced pressure. The obtained residue was taken up in dichloromethane, poured in water and extracted three times with dichloromethane. The combined organic layers were dried over Na_2SO_4 filtered and evaporated under vacuum. The residue was purified by a short flash column chromatography (SiO_2, petroleum ether/ethyl acetate). Conversions were determined by ^{1}H NMR.

- **Recycling procedure of catalysts 13c in the Suzuki reaction**

In a 10 mL glass vial with screw cap catalyst **13c** (0.1 mol%), 4-bromobenzaldehyde (467.22 mg, 2.5 mmol), phenylboronic acid (352.95 mg, 2.75 mmol), K_2CO_3 (414.63 mg, 3.0 mmol) and a mixture of EtOH/H_2O 1:1 (6 mL) were placed and mechanically stirred at room temperature for 3 h. The reaction mixture was diluted with ethyl acetate and centrifuged removing the supernatant. Catalyst was washed, sonicated and centrifuged with dichloromethane, methanol and diethyl ether and then dried in an oven at 40 °C before using it for the next cycle. The recovered organic layers were collected and evaporated under reduced pressure. The obtained residue was taken up in dichloromethane, poured in water and extracted three times with dichloromethane. The combined organic layers were dried over Na_2SO_4 filtered and evaporated under vacuum. The residue was purified by a short flash column chromatography (SiO_2, petroleum ether/ethyl acetate). Conversions were determined by ^{1}H NMR.

1.8 References

[1] (a) P. Wasserscheid, W. Keim, *Angew. Chem. Int. Ed.* **2000**, *39*, 3773-3789; (b) N. V. Plechkova, K. R. Seddon, *Chem. Soc. Rev.* **2008**, *37*, 123-1560; (c) J. S. Wilkes, *Green Chem.* **2002**, *4*, 73-80; (d) C. Chiappe, D. Pieraccini, *J. Phys. Org. Chem.* **2005**, *18*, 275-297; (e) R. D. Rogers, K. R. Seddon, *Science* **2003**, *302*, 792-793.

[2] M. Smiglak, J. M. Pringle, X. Lu, L. Han, S. Zhang, H. Gao, D. R. MacFarlane, R. D. Rogers, *Chem. Commun.* **2014**, *50*, 9228-9250.

[3] F. Pena-Pereira, A. Kloskowski, J. Namiesnik, *Green Chem.* **2015**, *17*, 3687-3705.

[4] (a) R. Sheldon, *Chem. Commun.* **2001**, 2399-2407; (b) J. P. Hallett, T. Welton, *Chem. Rev.* **2011**, *111*, 3508-3576.

[5] (a) S. N. Riduan, Y. Zhang, *Chem. Soc. Rev.* **2013**, *42*, 9055-9070; (b) P. Domínguez de María, Z. Maugeri, *Curr. Opin. Chem. Biol.* **2011**, *15*, 220-225.

[6] (a) V. Pino, A. M. Afonso, *Anal. Chim. Acta* **2012**, *714*, 20-37; (b) C. F. Poole, S. K. Poole, *J. Sep. Sci.* **2011**, *34*, 888-900; (c) M. D. Joshi, J. L. Anderson, *RSC Adv.* **2012**, *2*, 5470-5484.

[7] (a) D. R. MacFarlane, N. Tachikawa, M. Forsyth, J. M. Pringle, P. C. Howlett, G. D. Elliott, J. H. Davis, M. Watanabe, P. Simon, C. A. Angell, *Energy Environ. Sci.* **2014**, *7*, 232-250; (b) B. Scrosati, J. Hassoun, Y.-K. Sun, *Energy Environ. Sci.* **2011**, *4*, 3287-3295; (c) G. Gebresilassie Eshetu, M. Armand, B. Scrosati, S. Passerini, *Angew. Chem. Int. Ed.* **2014**, *53*, 13342-13359.

[8] (a) M. J. A. Shiddiky, A. A. J. Torriero, *Biosens. Bioelectron.* **2011**, *26*, 1775-1787; (b) K. Fujita, K. Murata, M. Masuda, N. Nakamura, H. Ohno, *RSC Adv.* **2012**, *2*, 4018-4030.

[9] (a) R. Giernoth, *Angew. Chem. Int. Ed.* **2010**, *49*, 2834-2839; (b) S. G. Lee, *Chem. Commun.* **2006**, 1049-1063; (c) J. H. Davis Jr, *Chem. Lett.* **2004**, *33*, 1072-1077; (d) C. Chiappe, C. S. Pomelli, *Eur. J. Org. Chem.* **2014**, *2014*, 6120-6139.

[10] (a) J. Sun, W. Cheng, W. Fan, Y. Wang, Z. Meng, S. Zhang, *Catal. Today* **2009**, *148*, 361-367; (b) F.-L. Yu, Y.-Y. Wang, C.-Y. Liu, C.-X. Xie, S.-T. Yu, *Chem. Eng. J.* **2014**, *255*, 372-376.

[11] (a) E. D. Bates, R. D. Mayton, I. Ntai, J. H. Davis, *J. Am. Chem. Soc.* **2002**, *124*, 926-927; (b) X. Zhang, X. Zhang, H. Dong, Z. Zhao, S. Zhang, Y. Huang, *Energy Environ. Sci.* **2012**, *5*, 6668-6681; (c) I. Niedermaier, M. Bahlmann, C. Papp, C. Kolbeck, W. Wei, S. Krick Calderón, M. Grabau, P. S. Schulz, P. Wasserscheid, H. P. Steinrück, F. Maier, *J. Am. Chem. Soc.* **2014**, *136*, 436-441.

[12] (a) A. E. Visser, R. P. Swatloski, W. M. Reichert, R. Mayton, S. Sheff, A. Wierzbicki, J. J. H. Davis, R. D. Rogers, *Chem. Commun.* **2001**, 135-136; (b) A. Stojanovic, B. K. Keppler, *Sep. Sci. Technol.* **2012**, *47*, 189-203.

[13] (a) J. S. Lee, X. Wang, H. Luo, G. A. Baker, S. Dai, *J. Am. Chem. Soc.* **2009**, *131*, 4596-4597; (b) P. S. Wheatley, P. K. Allan, S. J. Teat, S. E. Ashbrook, R. E. Morris, *Chem. Sci.* **2010**, *1*, 483-487.

[14] D. Astruc, F. Lu, J. R. Aranzaes, *Angew. Chem. Int. Ed.* **2005**, *44*, 7852-7872.

[15] (a) D. Astruc, *Nanoparticles and Catalysis*, Wiley-VCH Verlag GmbH & Co. KGaA, Weinheim, Germany, **2008**; (b) B. Corain, G. Schmid, N. Toshima, *Metal Nanoclusters in Catalysis and Materials Sciences: The Issue of Size Control*, Elsevier Science, Amsterdam, Netherlands, **2007**; (c) G. Schmid, *Nanoparticles: From Theory to Application, 2nd, Completely Revised and Updated Edition*, Wiley-VCH Verlag GmbH & Co. KGaA, Weinheim, Germany, **2010**.

[16] M. Kim, V. N. Phan, K. Lee, *CrystEngComm* **2012**, *14*, 7535-7548.

[17] (a) C. J. Serpell, J. Cookson, A. L. Thompson, C. M. Brown, P. D. Beer, *Dalton Trans.* **2013**, *42*, 1385-1393; (b) M.-A. Neouze, *J. Mater. Chem.* **2010**, *20*, 9593-9607.

[18] (a) S. Özkar, R. G. Finke, *J. Am. Chem. Soc.* **2002**, *124*, 5796-5810; (b) S. W. Kang, K. Char, Y. S. Kang, *Chem. Mater.* **2008**, *20*, 1308-1311; (c) G. S. Fonseca, G. Machado, S. R. Teixeira, G. H. Fecher, J. Morais, M. C. M. Alves, J. Dupont, *J. Colloid Interface Sci.* **2006**, *301*, 193-204; (d) C. W. Scheeren, G. Machado, S. R. Teixeira, J. Morais, J. B. Domingos, J. Dupont, *J. Phys. Chem. B* **2006**, *110*, 13011-13020; (e) L. S. Ott, R. G. Finke, *Coord. Chem. Rev.* **2007**, *251*, 1075-1100.

[19] L. S. Ott, M. L. Cline, M. Deetlefs, K. R. Seddon, R. G. Finke, *J. Am. Chem. Soc.* **2005**, *127*, 5758-5759.

[20] H. S. Schrekker, M. A. Gelesky, M. P. Stracke, C. M. L. Schrekker, G. Machado, S. R. Teixeira, J. C. Rubim, J. Dupont, *J. Colloid Interface Sci.* **2007**, *316*, 189-195.

[21] Y. S. Chun, J. Y. Shin, C. E. Song, S.-g. Lee, *Chem. Commun.* **2008**, 942-944.

[22] (a) R. Fehrmann, A. Riisager, M. Haumann, *Supported Ionic Liquids: Fundamentals and Applications*, Wiley-VCH Verlag GmbH & Co., Weinheim, Germany, **2014**; (b) B. Xin, J. Hao, *Chem. Soc. Rev.* **2014**, *43*, 7171-7187.

[23] (a) A. Riisager, K. M. Eriksen, P. Wasserscheid, R. Fehrmann, *Catal. Lett.* **2003**, *90*, 149-153; (b) C. P. Mehnert, E. J. Mozeleski, R. A. Cook, *Chem. Commun.* **2002**, 3010-3011; (c) A. Riisager, P. Wasserscheid, R. van Hal, R. Fehrmann, *J. Catal.* **2003**, *219*, 452-455.

[24] (a) M. H. Valkenberg, C. deCastro, W. F. Holderich, *Green Chem.* **2002**, *4*, 88-93; (b) C. P. Mehnert, R. A. Cook, N. C. Dispenziere, M. Afeworki, *J. Am. Chem. Soc.* **2002**, *124*, 12932-12933.

[25] (a) T. Selvam, A. Machoke, W. Schwieger, *Appl. Catal. A-Gen.* **2012**, *445–446*, 92-101; (b) B. Gadenne, P. Hesemann, J. J. E. Moreau, *Chem. Commun.* **2004**, 1768-1769; (c) O. C. Vangeli, G. E. Romanos, K. G. Beltsios, D. Fokas, E. P. Kouvelos, K. L. Stefanopoulos, N. K. Kanellopoulos, *J. Phys. Chem. B* **2010**, *114*, 6480-6491; (d) W. Zhang, H. Wang, J. Han, Z. Song, *Appl. Surf. Sci.* **2012**, *258*, 6158-6168; (e) L. Rodriguez-Perez, E. Teuma, A. Falqui, M. Gomez, P. Serp, *Chem. Commun.* **2008**, 4201-4203.

[26] (a) H. Li, P. S. Bhadury, B. Song, S. Yang, *RSC Adv.* **2012**, *2*, 12525-12551; (b) C. Van Doorslaer, J. Wahlen, P. Mertens, K. Binnemans, D. De Vos, *Dalton Trans.* **2010**, *39*, 8377-8390; (c) L. J. Lozano, C. Godínez, A. P. de los Ríos, F. J. Hernández-Fernández, S. Sánchez-Segado, F. J. Alguacil, *J. Membr. Sci.* **2011**, *376*, 1-14.

[27] (a) M. Gruttadauria, S. Riela, C. Aprile, P. L. Meo, F. D'Anna, R. Noto, *Adv. Synth. Catal.* **2006**, *348*, 82-92; (b) C. Aprile, F. Giacalone, M. Gruttadauria, A. M. Marculescu, R. Noto, J. D. Revell, H. Wennemers, *Green Chem.* **2007**, *9*, 1328-1334.

[28] (a) M. Gruttadauria, L. F. Liotta, A. M. P. Salvo, F. Giacalone, V. La Parola, C. Aprile, R. Noto, *Adv. Synth. Catal.* **2011**, *353*, 2119-2130; (b) J. Huang, T. Jiang, H. Gao, B. Han, Z. Liu, W. Wu, Y. Chang, G. Zhao, *Angew. Chem. Int. Ed.* **2004**, *43*, 1397-1399; (c) S. Miao, Z. Liu, B. Han, J. Huang, Z. Sun, J. Zhang, T. Jiang, *Angew. Chem. Int. Ed.* **2006**, *45*, 266-269; (d) M. A. Gelesky, S. S. X. Chiaro, F. A. Pavan, J. H. Z. dos Santos, J. Dupont, *Dalton Trans.* **2007**, 5549-5553; (e) Y. Kume, K. Qiao, D. Tomida, C. Yokoyama, *Catal. Commun.* **2008**, *9*, 369-375; (f) H. Hagiwara, T. Nakamura, T. Hoshi, T. Suzuki, *Green Chem.* **2011**, *13*, 1133-1137; (g) L. Luza, A. Gual, D. Eberhardt, S. R. Teixeira, S. S. X. Chiaro, J. Dupont, *ChemCatChem* **2013**, *5*, 2471-2478.

[29] (a) I. Guryanov, F. M. Toma, A. Montellano López, M. Carraro, T. Da Ros, G. Angelini, E. D'Aurizio, A. Fontana, M. Maggini, M. Prato, M. Bonchio, *Chem. Eur. J.* **2009**, *15*, 12837-12845; (b) I. Guryanov, A. Montellano Lopez, M. Carraro, T. Da

Ros, G. Scorrano, M. Maggini, M. Prato, M. Bonchio, *Chem. Commun.* **2009**, 3940-3942; (c) Z. Yinghuai, S. Bahnmueller, C. Chibun, K. Carpenter, N. S. Hosmane, J. A. Maguire, *Tetrahedron Lett.* **2003**, *44*, 5473-5476; (d) Z. Yinghuai, *J. Phys. Chem. Solids* **2004**, *65*, 349-353; (e) R. R. Deshmukh, J. W. Lee, U. S. Shin, J. Y. Lee, C. E. Song, *Angew. Chem. Int. Ed.* **2008**, *47*, 8615-8617; *Angew. Chem.* **2008**, *120*, 8743-8745; (f) E. Vázquez, F. Giacalone, M. Prato, *Chem. Soc. Rev.* **2014**, *43*, 58-69.

[30] (a) B. K. Price, J. L. Hudson, J. M. Tour, *J. Am. Chem. Soc.* **2005**, *127*, 14867-14870; (b) M. L. Polo-Luque, B. M. Simonet, M. Valcárcel, *TrAC, Trends Anal. Chem.* **2013**, *47*, 99-110.

[31] T. Fukushima, A. Kosaka, Y. Ishimura, T. Yamamoto, T. Takigawa, N. Ishii, T. Aida, *Science* **2003**, *300*, 2072-2074.

[32] J. Wang, H. Chu, Y. Li, *ACS Nano* **2008**, *2*, 2540-2546.

[33] (a) M. Tunckol, J. Durand, P. Serp, *Carbon* **2012**, *50*, 4303-4334; (b) J. Lee, T. Aida, *Chem. Commun.* **2011**, *47*, 6757-6762; (c) T. Fukushima, T. Aida, *Chem. Eur. J.* **2007**, *13*, 5048-5058.

[34] (a) A. P. Saxena, M. Deepa, A. G. Joshi, S. Bhandari, A. K. Srivastava, *ACS Applied Materials and Interfaces* **2011**, *3*, 1115-1126; (b) S. Guo, S. Dong, E. Wang, *Adv. Mater.* **2010**, *22*, 1269-1272; (c) Y. Zhang, Y. Shen, J. Yuan, D. Han, Z. Wang, Q. Zhang, L. Niu, *Angew. Chem. Int. Ed.* **2006**, *45*, 5867-5870; *Angew. Chem.* **2006**, *118*, 5999-6002; (d) Y. Zhang, Y. Shen, D. Han, Z. Wang, J. Song, F. Li, L. Niu, *Biosens. Bioelectron.* **2007**, *23*, 438-443; (e) N. Karousis, S. P. Economopoulos, E. Sarantopoulou, N. Tagmatarchis, *Carbon* **2010**, *48*, 854-860; (f) P. Bhunia, E. Hwang, M. Min, J. Lee, S. Seo, S. Some, H. Lee, *Chem. Commun.* **2012**, *48*, 913-915; (g) H. Yang, C. Shan, F. Li, D. Han, Q. Zhang, L. Niu, *Chem. Commun.* **2009**, 3880-3882; (h) B. Yu, F. Zhou, G. Liu, Y. Liang, W. T. S. Huck, W. Liu, *Chem. Commun.* **2006**, 2356-2358; (i) M. J. Park, J. K. Lee, B. S. Lee, Y.-W. Lee, I. S. Choi, S.-g. Lee, *Chem. Mater.* **2006**, *18*, 1546-1551; (j) N. Karousis, T. Ichihashi, S. Chen, H. Shinohara, M. Yudasaka, S. Iijima, N. Tagmatarchis, *J. Mater. Chem.* **2010**, *20*, 2959-2964; (k) B. Wang, X. Wang, W. Lou, J. Hao, *J. Phys. Chem. C* **2010**, *114*, 8749-8754; (l) L. Rodríguez-Pérez, R. García, M. Á. Herranz, N. Martín, *Chem. Eur. J.* **2014**, *20*, 7278-7286.

[35] T. Itoh, M. Mishiro, K. Matsumoto, S. Hayase, M. Kawatsura, M. Morimoto, *Tetrahedron* **2008**, *64*, 1823-1828.

[36] C. M. Tollan, J. A. Pomposo, D. Mecerreyes, *Nano* **2009**, *04*, 299-302.

[37] L. Maggini, M.-E. Fustos, T. W. Chamberlain, C. Cebrian, M. Natali, M. Pietraszkiewicz, O. Pietraszkiewicz, E. Szekely, K. Kamaras, L. De Cola, A. N. Khlobystov, D. Bonifazi, *Nanoscale* **2014**, *6*, 2887-2894.

[38] J. Iehl, M. Frasconi, H.-P. Jacquot de Rouville, N. Renaud, S. M. Dyar, N. L. Strutt, R. Carmieli, M. R. Wasielewski, M. A. Ratner, J.-F. Nierengarten, J. F. Stoddart, *Chem. Sci.* **2013**, *4*, 1462-1469.

[39] W. Zhilei, L. Zaijun, S. Xiulan, F. Yinjun, L. Junkang, *Biosens. Bioelectron.* **2010**, *25*, 1434-1438.

[40] (a) C. D. Tran, S. Challa, *Analyst* **2008**, *133*, 455-464; (b) A. Speltini, D. Merli, A. Profumo, *Anal. Chim. Acta* **2013**, *783*, 1-16.

[41] (a) C. Klumpp, L. Lacerda, O. Chaloin, T. D. Ros, K. Kostarelos, M. Prato, A. Bianco, *Chem. Commun.* **2007**, 3762-3764; (b) D. Sigwalt, M. Holler, J. Iehl, J. F. Nierengarten, M. Nothisen, E. Morin, J. S. Remy, *Chem. Commun.* **2011**, *47*, 4640-4642; (c) R. Maeda-Mamiya, E. Noiri, H. Isobe, W. Nakanishi, K. Okamoto, K. Doi, T. Sugaya, T. Izumi, T. Homma, E. Nakamura, *Proc. Natl. Acad. Sci.* **2010**, *107*, 5339-5344.

[42] (a) T. Da Ros, M. Prato, *Chem. Commun.* **1999**, 663-669; (b) R. Bakry, R. M. Vallant, M. Najam-ul-Haq, M. Rainer, Z. Szabo, C. W. Huck, G. K. Bonn, *Int. J. Nanomedicine* **2007**, *2*, 639-649; (c) N. Tagmatarchis, H. Shinohara, *Mini Rev. Med. Chem.* **2001**, *1*, 339-348.

[43] H. Veisi, R. Masti, D. Kordestani, M. Safaei, O. Sahin, *J. Mol. Catal. A: Chem.* **2014**, *385*, 61-67.

[44] (a) J. Iehl, R. Pereira De Freitas, B. Delavaux-Nicot, J. F. Nierengarten, *Chem. Commun.* **2008**, 2450-2452; (b) M. Rae, F. Perez-Balderas, C. Baleizão, A. Fedorov, J. A. S. Cavaleiro, A. C. Tomé, M. N. Berberan-Santos, *J. Phys. Chem. B* **2006**, *110*, 12809-12814.

[45] (a) C. Bingel, *Chem. Ber.* **1993**, *126*, 1957-1959; (b) A. Hirsch, I. Lamparth, T. Grosser, H. R. Karfunkel, *J. Am. Chem. Soc.* **1994**, *116*, 9385-9386; (c) A. Hirsch, I. Lamparth, H. R. Karfunkel, *Angew. Chem. Int. Ed.* **1994**, *33*, 437-438; (d) X. Camps, A. Hirsch, *J. Chem. Soc., Perkin Trans. 1* **1997**, 1595-1596; (e) J.-F. Nierengarten, V. Gramlich, F. Cardullo, F. Diederich, *Angew. Chem. Int. Ed.* **1996**, *35*, 2101-2103.

[46] (a) H. Li, S. A. Haque, A. Kitaygorodskiy, M. J. Meziani, M. Torres-Castillo, Y.-P. Sun, *Org. Lett.* **2006**, *8*, 5641-5643; (b) H. Li, A. Kitaygorodskiy, R. A. Carino, Y.-P. Sun, *Org. Lett.* **2005**, *7*, 859-861.

[47] J. F. Nierengarten, *Pure Appl. Chem.* **2012**, *84*, 1027-1037.

[48] (a) J. Luczkowiak, A. Muñoz, M. Sánchez-Navarro, R. Ribeiro-Viana, A. Ginieis, B. M. Illescas, N. Martín, R. Delgado, J. Rojo, *Biomacromolecules* **2013**, *14*, 431-437; (b) P. Compain, C. Decroocq, J. Iehl, M. Holler, D. Hazelard, T. M. Barragán, C. O. Mellet, J. F. Nierengarten, *Angew. Chem. Int. Ed.* **2010**, *49*, 5753-5756; (c) J. F. Nierengarten, J. Iehl, V. Oerthel, M. Holler, B. M. Illescas, A. Muñoz, N. Martín, J. Rojo, M. Sánchez-Navarro, S. Cecioni, S. Vidal, K. Buffet, M. Durka, S. P. Vincent, *Chem. Commun.* **2010**, *46*, 3860-3862; (d) J. Lehl, J. F. Nierengarten, *Chem. Eur. J.* **2009**, *15*, 7306-7309; (e) R. Rísquez-Cuadro, J. M. García Fernández, J. F. Nierengarten, C. Ortiz Mellet, *Chem. Eur. J.* **2013**, *19*, 16791-16803.

[49] (a) J. Iehl, J. F. Nierengarten, *Chem. Commun.* **2010**, *46*, 4160-4162; (b) S. Cecioni, V. Oerthel, J. Iehl, M. Holler, D. Goyard, J. P. Praly, A. Imberty, J. F. Nierengarten, S. Vidal, *Chem. Eur. J.* **2011**, *17*, 3252-3261.

[50] X. Camps, A. Hirsch, *J. Chem. Soc., Perkin Trans. 1* **1997**, 1595-1596.

[51] (a) M. Brettreich, A. Hirsch, *Tetrahedron Lett.* **1998**, *39*, 2731-2734; (b) S. Filippone, F. Heimann, A. Rassat, *Chem. Commun.* **2002**, 1508-1509; (c) K. Kokubo, K. Matsubayashi, H. Tategaki, H. Takada, T. Oshima, *ACS Nano* **2008**, *2*, 327-333; (d) A. B. Kornev, E. A. Khakina, S. I. Troyanov, A. A. Kushch, A. Peregudov, A. Vasilchenko, D. G. Deryabin, V. M. Martynenko, P. A. Troshin, *Chem. Commun.* **2012**, *48*, 5461-5463; (e) A. M. López, F. Scarel, N. R. Carrero, E. Vázquez, A. Mateo-Alonso, T. D. Ros, M. Prato, *Org. Lett.* **2012**, *14*, 4450-4453; (f) A. B. Kornev, A. S. Peregudov, V. M. Martynenko, G. V. Guseva, T. E. Sashenkova, A. Y. Rybkin, I. I. Faingold, D. V. Mishchenko, R. A. Kotelnikova, N. P. Konovalova, J. Balzarini, P. A. Troshin, *Mendeleev Commun.* **2013**, *23*, 323-325.

[52] (a) F. Giacalone, N. Martín, *Adv. Mater.* **2010**, *22*, 4220-4248; (b) Z. Yao, K. C. Tam, *Macromol. Rapid Commun.* **2011**, *32*, 1863-1885.

[53] (a) M. Brettreich, S. Burghardt, C. Böttcher, T. Bayerl, S. Bayerl, A. Hirsch, *Angew. Chem. Int. Ed.* **2000**, *39*, 1845-1848; (b) M. Braun, U. Hartnagel, E. Ravanelli, B. Schade, C. Böttcher, O. Vostrowsky, A. Hirsch, *Eur. J. Org. Chem.* **2004**, 1983-2001; (c) N. Chronakis, U. Hartnagel, M. Braun, A. Hirsch, *Chem. Commun.* **2007**, 607-609; (d) P. Witte, F. Hörmann, A. Hirsch, *Chem. Eur. J.* **2009**, *15*, 7423-7433; (e) F. Hörmann, A. Hirsch, *Chem. Eur. J.* **2013**, *19*, 3188-3197.

[54] (a) E. Nakamura, H. Isobe, *Acc. Chem. Res.* **2003**, *36*, 807-815; (b) H. Isobe, W. Nakanishi, N. Tomita, S. Jinno, H. Okayama, E. Nakamura, *Chem. Asian. J.* **2006**, *1*, 167-175; (c) B. Sitharaman, T. Y. Zakharian, A. Saraf, P. M. J. Ashcroft, S. Pan, Q. P. Pham, A. G. Mikos, L. J. Wilson, D. A. Engler, *Mol. Pharm.* **2008**, *5*, 567-578.

[55] C. F. Richardson, D. I. Schuster, S. R. Wilson, *Org. Lett.* **2000**, *2*, 1011-1014.

[56] (a) A. Riisager, R. Fehrmann, S. Flicker, R. van Hal, M. Haumann, P. Wasserscheid, *Angew. Chem. Int. Ed.* **2005**, *44*, 815-819; (b) C. P. Mehnert, *Chem. Eur. J.* **2005**, *11*, 50-56.

[57] (a) S. Kidambi, M. L. Bruening, *Chem. Mater.* **2005**, *17*, 301-307; (b) Y. M. A. Yamada, Y. Uozumi, *Tetrahedron* **2007**, *63*, 8492-8498; (c) J. Zhang, L. Meng, D. Zhao, Z. Fei, Q. Lu, P. J. Dyson, *Langmuir* **2008**, *24*, 2699-2704; (d) F. Durap, Ö. Metin, M. Aydemir, S. Özkar, *Appl. Organomet. Chem.* **2009**, *23*, 498-503.

[58] S. Eriksson, M. Boutonnet, S. Järås, *Appl. Catal. A-Gen.* **2006**, *312*, 95-101.

[59] (a) S. Chen, K. Kobayashi, R. Kitaura, Y. Miyata, H. Shinohara, *ACS Nano* **2011**, *5*, 4902-4908; (b) S. Chen, S. Zhang, X. Liu, J. Wang, J. Wang, K. Dong, J. Sun, B. Xu, *PCCP* **2014**, *16*, 5893-5906.

[60] (a) D. Zhao, Z. Fei, T. J. Geldbach, R. Scopelliti, P. J. Dyson, *J. Am. Chem. Soc.* **2004**, *126*, 15876-15882; (b) L. Li, J. Wang, T. Wu, R. Wang, *Chem. Eur. J.* **2012**, *18*, 7842-7851.

[61] (a) O. Zhou, R. M. Fleming, D. W. Murphy, C. H. Chen, R. C. Haddon, A. P. Ramirez, S. H. Glarum, *Science* **1994**, *263*, 1744-1747; (b) H. Takuya, S. D. Mildred, K. Yoong Ahm, T. Mauricio, E. Morinobu, *Carbon Nanotubes and Other Carbon Materials* in *Dekker Encyclopedia of Nanoscience and Nanotechnology, Second Edition - Six Volume Set (Print Version)*, CRC Press, **2008**, pp. 691-706.

[62] (a) D. Ugarte, *Nature* **1992**, *359*, 707-709; (b) F. Banhart, T. Füller, P. Redlich, P. M. Ajayan, *Chem. Phys. Lett.* **1997**, *269*, 349-355.

[63] E. Thune, T. Cabioc'h, P. Guérin, M. F. Denanot, M. Jaouen, *Mater. Lett.* **2002**, *54*, 222-228.

[64] X. H. Chen, F. M. Deng, J. X. Wang, H. S. Yang, G. T. Wu, X. B. Zhang, J. C. Peng, W. Z. Li, *Chem. Phys. Lett.* **2001**, *336*, 201-204.

[65] (a) V. L. Kuznetsov, A. L. Chuvilin, Y. V. Butenko, I. Y. Mal'kov, V. M. Titov, *Chem. Phys. Lett.* **1994**, *222*, 343-348; (b) E. Thune, T. Cabioc'h, M. Jaouen, F. Bodart, *Phys. Rev. B* **2003**, *68*, 115434.

[66] A. V. Gubarevich, J. Kitamura, S. Usuba, H. Yokoi, Y. Kakudate, O. Odawara, *Carbon* **2003**, *41*, 2601-2606.

[67] C. He, N. Zhao, X. Du, C. Shi, J. Ding, J. Li, Y. Li, *Scripta Mater.* **2006**, *54*, 689-693.

[68] S.-S. Hou, D.-H. Chung, T.-H. Lin, *Carbon* **2009**, *47*, 938-947.

[69] (a) N. Sano, H. Wang, M. Chhowalla, I. Alexandrou, G. A. J. Amaratunga, *Nature* **2001**, *414*, 506-507; (b) N. Sano, H. Wang, I. Alexandrou, M. Chhowalla, K. B. K. Teo, G. A. J. Amaratunga, K. Iimura, *J. Appl. Phys.* **2002**, *92*, 2783-2788.

[70] (a) I. Lamparth, C. Maichle–Mössmer, A. Hirsch, *Angew. Chem. Int. Ed.* **1995**, *34*, 1607-1609; (b) J. Cerar, M. Pompe, M. Guček, J. Cerkovnik, J. Škerjanc, *J. Chromatogr. A* **2007**, *1169*, 86-94.

[71] (a) S. P. Dubey, A. D. Dwivedi, I.-C. Kim, M. Sillanpaa, Y.-N. Kwon, C. Lee, *Chem. Eng. J.* **2014**, *244*, 160-167; (b) Y. Kim, Y. Noh, E. J. Lim, S. Lee, S. M. Choi, W. B. Kim, *J. Mater. Chem. A* **2014**, *2*, 6976-6986.

[72] (a) S. Park, J. An, J. R. Potts, A. Velamakanni, S. Murali, R. S. Ruoff, *Carbon* **2011**, *49*, 3019-3023; (b) Z. Bo, X. Shuai, S. Mao, H. Yang, J. Qian, J. Chen, J. Yan, K. Cen, *Sci. Rep.* **2014**, *4*.

[73] (a) Z. Syrgiannis, V. La Parola, C. Hadad, M. Lucío, E. Vázquez, F. Giacalone, M. Prato, *Angew. Chem. Int. Ed.* **2013**, *52*, 6480-6483; (b) K. Flavin, K. Lawrence, J. Bartelmess, M. Tasior, C. Navio, C. Bittencourt, D. F. O'Shea, D. M. Guldi, S. Giordani, *ACS Nano* **2011**, *5*, 1198-1206; (c) M. Liu, Y. Yang, T. Zhu, Z. Liu, *Carbon* **2005**, *43*, 1470-1478; (d) A. Jung, R. Graupner, L. Ley, A. Hirsch, *Phys. Stat. Sol. (B)* **2006**, *243*, 3217-3220.

[74] G. Z. Hu, F. Nitze, X. Jia, T. Sharifi, H. R. Barzegar, E. Gracia-Espino, T. Wagberg, *RSC Adv.* **2014**, *4*, 676-682.

[75] (a) B. M. Choudary, S. Madhi, N. S. Chowdari, M. L. Kantam, B. Sreedhar, *J. Am. Chem. Soc.* **2002**, *124*, 14127-14136; (b) M. Moreno-Mañas, R. Pleixats, *Acc. Chem. Res.* **2003**, *36*, 638-643; (c) D. Astruc, F. Lu, J. R. Aranzaes, *Angew. Chem. Int. Ed.* **2005**, *44*, 7852-7872; (d) L. S. Ott, R. G. Finke, *Inorg. Chem.* **2006**, *45*, 8382-8393; (e) Z. Hou, N. Theyssen, W. Leitner, *Green Chem.* **2007**, *9*, 127-132; (f) C. Ornelas, L. Salmon, J. Ruiz Aranzaes, D. Astruc, *Chem. Commun.* **2007**, 4946-4948; (g) Y. Tsuji, T. Fujihara, *Inorg. Chem.* **2007**, *46*, 1895-1902; (h) J. Durand, E. Teuma, M. Gómez, *Eur. J. Inorg. Chem.* **2008**, 3577-3586; (i) J. N. Park, A. J. Forman, W. Tang, J. Cheng, Y. S. Hu, H. Lin, E. W. McFarland, *Small* **2008**, *4*, 1694-1697; (j) J. Dupont, J. D. Scholten, *Chem. Soc. Rev.* **2010**, *39*, 1780-1804; (k) M. Lamblin, L. Nassar-Hardy, J. C. Hierso, E. Fouquet, F. X. Felpin, *Adv. Synth. Catal.* **2010**, *352*, 33-79; (l) N. Mejías, R. Pleixats, A. Shafir, M. Medio-Simón, G. Asensio, *Eur. J. Org. Chem.* **2010**, 5090-5099; (m) A. Corma, H. Garcia, *Chem. Soc. Rev.* **2008**, *37*, 2096-2126; (n) M. M. Coulter, J. A. Dinglasan, J. B. Goh, S. Nair, D. J. Anderson, V. M. Dong, *Chem. Sci.* **2010**, *1*, 772-775.

[76] C. Pavia, E. Ballerini, L. A. Bivona, F. Giacalone, C. Aprile, L. Vaccaro, M. Gruttadauria, *Adv. Synth. Catal.* **2013**, *355*, 2007-2018.

[77] V. Campisciano, V. La Parola, L. F. Liotta, F. Giacalone, M. Gruttadauria, *Chem. Eur. J.* **2015**, *21*, 3327-3334.

[78] P. Agrigento, M. J. Beier, J. T. N. Knijnenburg, A. Baiker, M. Gruttadauria, *J. Mater. Chem.* **2012**, *22*, 20728-20735.

[79] (a) D. Zhao, J. Feng, Q. Huo, N. Melosh, G. H. Fredrickson, B. F. Chmelka, G. D. Stucky, *Science* **1998**, *279*, 548-552; (b) D. Zhao, Q. Huo, J. Feng, B. F. Chmelka, G. D. Stucky, *J. Am. Chem. Soc.* **1998**, *120*, 6024-6036.

[80] N. Jiao, Z. Li, Y. Wang, J. Liu, C. Xia, *RSC Adv.* **2015**, *5*, 26913-26922.

[81] R. W. J. Scott, H. Ye, R. R. Henriquez, R. M. Crooks, *Chem. Mater.* **2003**, *15*, 3873-3878.

[82] V. P. Mehta, E. V. Van der Eycken, *Chem. Soc. Rev.* **2011**, *40*, 4925-4936.

[83] (a) T. Beryozkina, P. Appukkuttan, N. Mont, E. Van der Eycken, *Org. Lett.* **2006**, *8*, 487-490; (b) E. J. García-Suárez, P. Lara, A. B. García, M. Ojeda, R. Luque, K. Philippot, *Appl. Catal. A-Gen.* **2013**, *468*, 59-67.

[84] (a) C. Deraedt, D. Astruc, *Acc. Chem. Res.* **2014**, *47*, 494-503; (b) Y. M. A. Yamada, S. M. Sarkar, Y. Uozumi, *J. Am. Chem. Soc.* **2012**, *134*, 3190-3198; (c) Z. Wang, Y. Yu, Y. X. Zhang, S. Z. Li, H. Qian, Z. Y. Lin, *Green Chem.* **2015**, *17*, 413-420; (d) H. Hagiwara, H. Sasaki, N. Tsubokawa, T. Hoshi, T. Suzuki, T. Tsuda, S. Kuwabata, *Synlett* **2010**, *2010*, 1990-1996; (e) M. Chtchigrovsky, Y. Lin, K. Ouchaou, M. Chaumontet, M. Robitzer, F. Quignard, F. Taran, *Chem. Mater.* **2012**, *24*, 1505-1510; (f) J. Lasri, M. F. C. G. da Silva, M. N. Kopylovich, S. Mukhopadhyay, M. A. J. Charmier, A. J. L. Pombeiro, *Dalton Trans.* **2009**, 2210-2216; (g) G. Park, S. Lee, S. J. Son, S. Shin, *Green Chem.* **2013**, *15*, 3468-3473.

[85] (a) M. Ghotbinejad, A. R. Khosropour, I. Mohammadpoor-Baltork, M. Moghadam, S. Tangestaninejad, V. Mirkhani, *J. Mol. Catal. A: Chem.* **2014**, *385*, 78-84; (b) G. Durgun, Ö. Aksın, L. Artok, *J. Mol. Catal. A: Chem.* **2007**, *278*, 189-199.

[86] C. E. Garrett, K. Prasad, *Adv. Synth. Catal.* **2004**, *346*, 889-900.
[87] (a) L. Djakovitch, V. Dufaud, R. Zaidi, *Adv. Synth. Catal.* **2006**, *348*, 715-724; (b) L. Djakovitch, K. Koehler, *J. Am. Chem. Soc.* **2001**, *123*, 5990-5999.
[88] S. Brunauer, P. H. Emmett, E. Teller, *J. Am. Chem. Soc.* **1938**, *60*, 309-319.
[89] H. P. Klug, L. E. Alexander, in *X-ray Diffraction Procedures for Polycrystalline and Amorphous Materials*, Wiley, New York, **1954**.
[90] (a) in *Practical Surface Analysis, Vol. 1* (Eds.: D. Briggs, M. P. Seah), Wiley, New York, **1990**; (b) D. A. Shirley, *Phys. Rev. B* **1972**, *5*, 4709-4714.
[91] (a) J. L. Nallasivam, R. A. Fernandes, *Eur. J. Org. Chem.* **2015**, *2015*, 3558-3567; (b) Y. Lee, M. C. Hong, H. Ahn, J. Yu, H. Rhee, *J. Organomet. Chem.* **2014**, *769*, 80-93; (c) Y.-Y. Peng, J. Liu, X. Lei, Z. Yin, *Green Chem.* **2010**, *12*, 1072-1075.
[92] (a) M. R. Nabid, Y. Bide, *Appl. Catal. A-Gen.* **2014**, *469*, 183-190; (b) S. Gupta, B. Ganguly, S. Das, *RSC Adv.* **2014**, *4*, 41148-41151; (c) A. R. Hajipour, G. Azizi, *RSC Adv.* **2014**, *4*, 20704-20708.
[93] A. Teleki, M. Suter, P. R. Kidambi, O. Ergeneman, F. Krumeich, B. J. Nelson, S. E. Pratsinis, *Chem. Mater.* **2009**, *21*, 2094-2100.
[94] B. R. Buckley, S. P. Neary, *Adv. Synth. Catal.* **2009**, *351*, 71-77.
[95] P. R. Boruah, A. A. Ali, B. Saikia, D. Sarma, *Green Chem.* **2015**, *17*, 1442-1445.

Chapter 2

SWCNT-PAMAM-PdNPs: An Efficient and Recyclable Catalyst for Suzuki and Heck Cross-Coupling Reactions

Part of this chapter has been submitted for publication.

2.1 Introduction

Palladium mediated cross-coupling reactions such as Suzuki, Heck, Sonogashira and Stille reactions, attracted and still attract the interest of the academic and industrial communities.[1] Among carbon-carbon cross coupling reactions, Suzuki and Heck reactions are perhaps the two most important and surely the most deeply studied. The great importance of such reactions is evident when their application fields are taken into account. Suzuki and Heck couplings are indispensable synthetic tools used for the preparation of pharmaceuticals, drugs, agrochemicals but also organic semiconductors.[2]

The field of homogeneous catalysis for the coupling reactions catalyzed by palladium complexes with various ligands (phosphines, amines, carbenes, dibenzylideneacetone, etc.) has experienced a remarkable interest during the years. The promise of a high reaction rate and high turnover numbers (TONs), together with good yields and selectivity were the reasons why many of the earliest catalysts for Heck and Suzuki couplings relied on the use of palladium complexes, mainly based on using of triphenylphosphine as ligand.[3] On the other hand, phosphine ligands are generally moisture and/or air-sensitive. With the aim to seek more environmentally friendly conditions for the coupling reactions, the use of water or aqueous–organic mixtures as reaction media, as well as the development of ligand-free catalytic systems, have received much attention.[4] However, homogeneous catalysis is also characterized by a number of drawbacks. First of all the hard recovery of the catalyst from the reaction mixture is a big problem to solve that leads to contaminated products and to the need of removing residue metals,[5] especially if one takes into account that the metals concentration limits in pharmaceuticals are strictly regulated.[5a] Furthermore, the lack of recovery implies the absence of recyclability of the catalyst.

In order to overcome these problems, heterogeneous catalysts were developed as viable alternative to homogenous catalysts, primarily to facilitate products purification, catalyst recovery and its recyclability, leading to the cost reduction of the overall catalytic process. To cover the gap between heterogeneous and homogeneous catalysis, the use of metal nanoparticles (MNPs) can represent the bridge between these two approaches. MNPs allow reaching a high catalytic activity under mild conditions thanks to their high surface to volume ratio.[6] In order to achieve the recyclability of the catalyst, MNPs can be immobilized on various support materials both organic and inorganic[7] such as metal oxides,[8] polymers,[9] dendrimers[10] and also magnetic nanoparticles-based solid

supports.[11]

Among support materials, carbon nanoforms (CNFs) are gaining more and more importance as promising materials for supporting metal nanoparticles by virtue of the fact that they can be easily tailored to meet specific requirements.[12] In particular carbon nanotubes (CNTs) have intrinsic properties that make them ideal materials for catalysis such as high mechanical and chemical stability, proper pore sizes and relatively high specific area. These characteristics are the reason why CNTs have been exploited as support materials for the deposition of MNPs. Many methods for depositing MNPs onto CNTs were reported in the literature and each of which offering a different degree of control over the size of nanoparticles and their distribution.[13]

Pristine CNTs were successfully employed for the immobilization of palladium for promoting C–C coupling reactions.[14] Regarding the use of pristine CNTs as support material, Karousis *et al.*[14a] reported the synthesis of soluble nanoPd-CNTs hybrids by means the reduction of palladium acetate and the subsequent in situ stabilization and immobilization of PdNPs onto the sodium dodecyl sulfate (SDS) solubilized CNTs (**Scheme 1**).

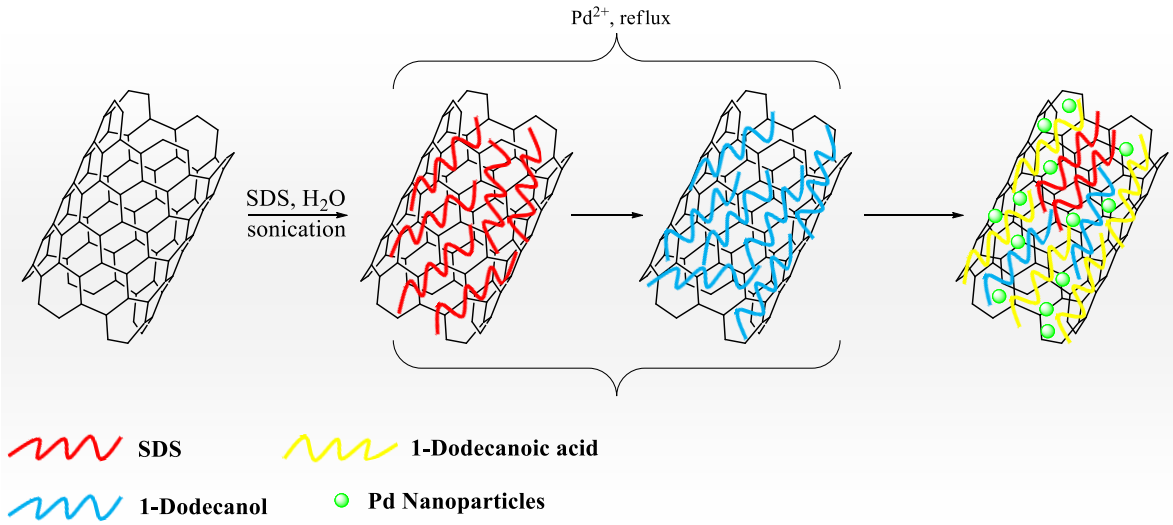

Scheme 1. *Synthetic procedure for decoration of CNTs with palladium nanoparticles.*

The so-obtained catalysts, with a PdNPs size distribution between 2 and 4 nm, were tested in the Suzuki reaction using aryl iodides and phenylboronic acid in DMF at 110 °C for 2 h (Pd loading 0.25 mol%) with good results. In addition, catalysts were also reused up to five times.

Siamaki *et al.*[14d] used both multi-walled carbon nanotubes (MWCNTs) and single-walled

carbon nanotubes (SWCNTs) as support materials for PdNPs. The nanoparticles were prepared by a solventless mechanochemical ball-milling method and a classical thermal procedure. PdNPs prepared by ball-milling at room temperature showed to be more catalytically active toward Suzuki reaction than those prepared by thermal annealing, mainly due to the smaller size of NPs and better dispersion on the surface of CNTs.

Oxidized-CNTs were also used as support material for the deposition of PdNPs.[15] However, all these materials, based on pristine CNTs as well as oxidized-CNTs, often show big palladium nanoparticles (PdNPs) with a broad size distribution and, in many cases, suffer from severe leaching phenomena. This is probably due to the lack of sufficient binding sites on CNTs surface for anchoring MNPs or the parent precursor metal ions, subsequently leading to scarce dispersion and agglomeration of MNPs. In addition, pristine CNTs tend to aggregate to form ropes and bundles decreasing the exposed surface. Thus, the chemical functionalization of CNTs becomes a prerequisite in order to debundle them and to have a better dispersion in solvents in order to improve catalytic performances.[16] In this regard, recently a few examples of CNTs-PdNPs nanocatalysts for Suzuki and Heck reaction were reported in which MWCNTs and SWCNTs were chemically modified with polymers,[17] thiol-containing moieties,[18] ionic liquids,[19] oligo[20] and poly-amidoamine (PAMAM)[21] moieties in order to maximize the interactions between MNPs and the support. Among the above-mentioned MNPs stabilizers used for the chemical modification of CNTs, dendrimers constitute a very interesting class of stabilizing agents.

PAMAM dendrimers is the most common class of dendrimers,[22] they belong to a specific class of dendritic polymers that also includes dendrons, hyperbranched polymers and dendrigrafts. Dendritic polymers can be divided in two major families: monodisperse structures, such as dendrimers and dendrons, and polydisperse structures, such as hyperbranched polymers and dendrigrafts (**Figure 1**).

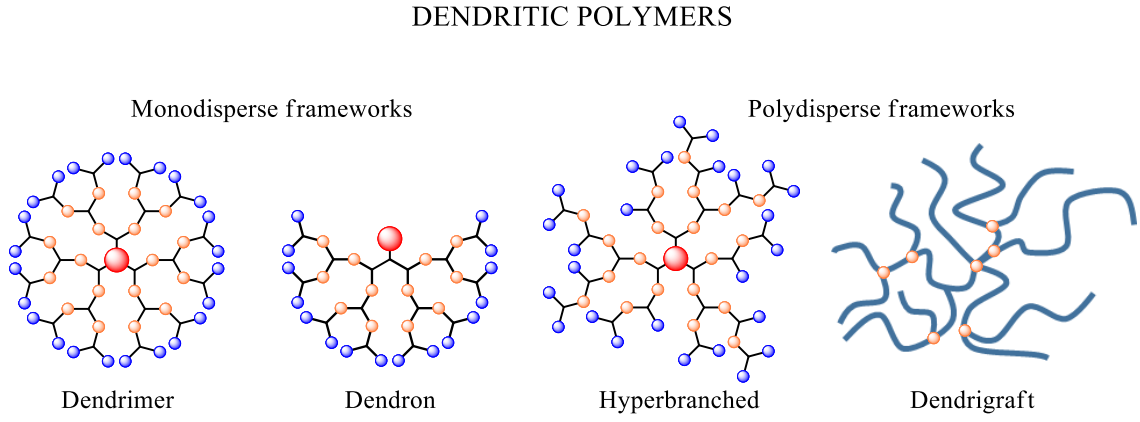

Figure 1. *Classification of dendritic polymers.*

Following a divergent[22] synthetic approach, dendrimers originate from the inner core and ramify outward with each subsequent branching reaction to give higher generation dendrimers, typically named by their generation (e.g. G1, G2, etc.). Dendrimers can also be synthesized following a convergent[23] approach starting from the periphery fragments (**Figure 2**).

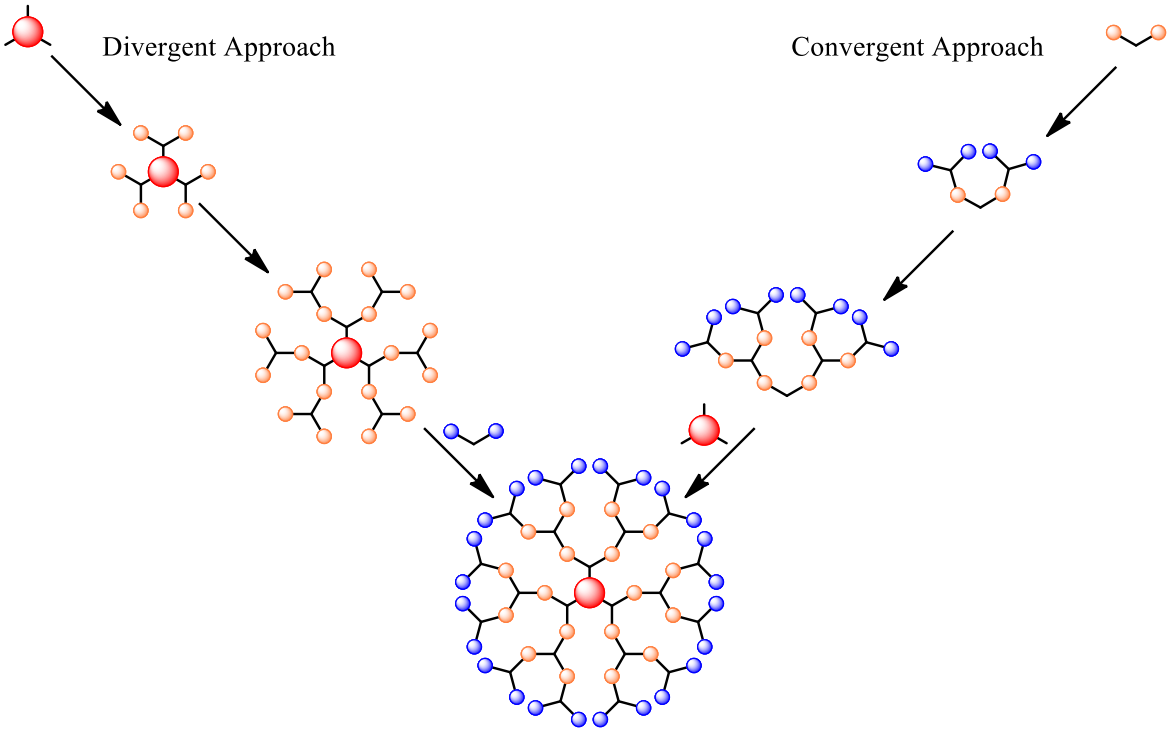

Figure 2. *Schematic representation of divergent and convergent approach for the synthesis of dendrimers.*

Each of these approaches has its advantages and drawbacks. In the divergent approach the easy preparation of high generation dendrimers represents the advantage of adopting this method, whereas the major drawback is the difficulty of controlling the dendrimer quality because of the large number of reaction that take place simultaneously. Commercially available dendrimers such as PAMAM or poly(propyleneimine) (PPI) are usually synthesized by a divergent approach. Conversely, the convergent approach offers a better structure control due to the low number of reaction that take place in each growth step. However, it does not give the possibility of synthesizing high generation dendrimers due to steric hindrances. Polyether dendrimers are an example of dendrimers synthesized by a convergent approach.

The dendritic macromolecular architecture gives rise to structures that adopt a globular shape with a relatively open interior pocket and a porous exterior that makes dendrimers a sort of molecular boxes. In such a way, MNPs can be stabilized in the dendrimer periphery[24] or

encapsulated inside them.[25] Dendrimers are suitable stabilizers for MNPs for several reasons. First, the stabilization of MNPs by dendrimers prevents their agglomeration and, in the case of encapsulated NPs, the stabilization is mainly due to steric effects that leave a substantial fraction of NPs surface unpassivated and thus available to participate in catalytic reactions. Furthermore, the branches of the dendrimers can be used as selective "filters" to limit the access of substrates to encapsulated NPs. Finally, the dendrimers periphery can be tailored to modify the solubility of the hybrid nanocomposite or for facilitating linking to surfaces.[25a] These unique abilities of dendrimers in the stabilization of MNPs, led to the wide use of dendrimers-MNPs hybrids in catalytic applications, imaging, sensing and for electronic devices.[10d, 26]

Functionalization of SWCNTs and MWCNTs with PAMAM dendrimers was reported. In all cases, the synthetic strategies used for the chemical functionalization of CNTs with PAMAM dendrimers involved a multi-step procedure.[27]

An example of this approach was reported by Nabid *et al.*[21] who synthesized a PAMAM-grafted-MWCNTs hybrid material obtained by a divergent method that involved the growth of the 3rd generation PAMAM dendrimer on the surface of MWCNTs and the subsequent immobilization of PdNPs. However, this sequential synthesis in twelve steps is a highly time consuming task.

2.2 Aim of the Chapter

In the search for a suitable support for PdNPs stabilization and immobilization, SWCNTs were used in combination with PAMAM dendrimers. The main motivation of this choice relies in the fact that SWCNTs, among other nanotubes, offer larger surface area and show improved reactivity toward functionalization. In addition, a convergent strategy was adopted for the chemical modification of SWCNTs with cystamine core based PAMAM dendrimers[28] (SWCNTs-PAMAM) by employing a novel approach for the easy functionalization of CNTs with disulfides recently reported in literature.[29] PdNPs, formed by reduction with $NaBH_4$ of $PdCl_4^{2-}$ species complexed in the dendritic shell, were immobilized on the PAMAM functionalized (generation 2.5 and 3.0) SWCNTs obtaining novel heterogeneous palladium nanocatalysts (**Figure 3**).

One of the obtained hybrid materials proved to be an efficient catalyst for promoting the Suzuki and Heck coupling reactions under air and in ligand-free conditions.

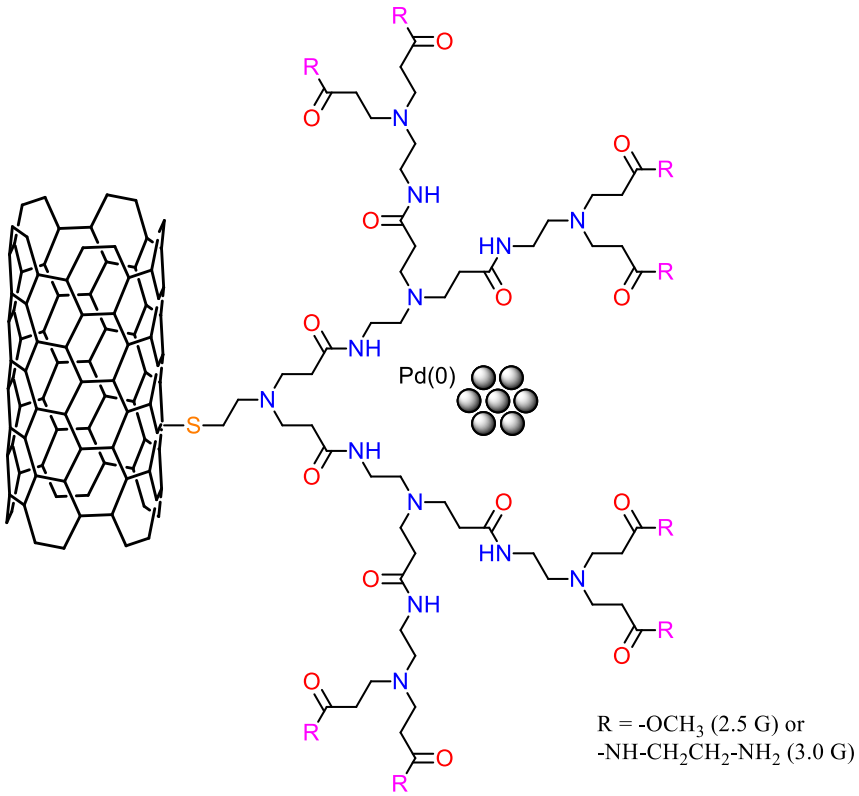

Figure 3. *Representation of the catalysts used in the Suzuki and Heck reactions.*

2.3 Results and Discussion

The preparation of the hybrids SWCNT-PAMAM **3** and **4** has been accomplished by following a convergent strategy through direct reaction of PAMAM dendrimers with cystamine core of generation 2.5 and 3.0 with pristine SWCNTs in refluxing toluene (**Scheme 2**) following a recently reported procedure.[29]

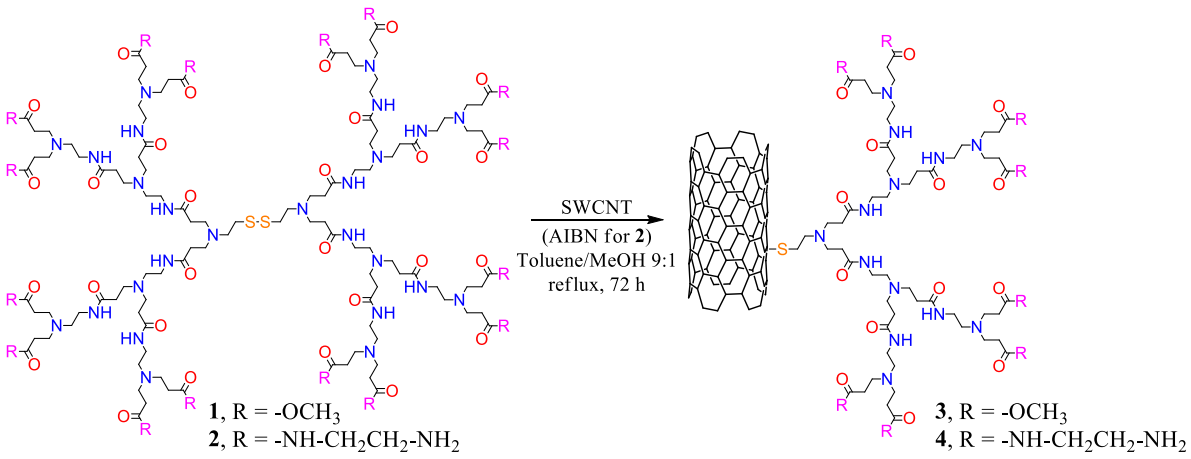

Scheme 2. *Synthesis of SWCNT-PAMAM hybrids **3** and **4**.*

Whereas dendrimer 2.5 G **1** smoothly reacted with the nanotubes, the 3.0 G dendrimer **2** needed the presence of azobisisobutyronitile (AIBN) to proceed properly, accordingly to an analogous reaction between thiols and several CNFs.[30]

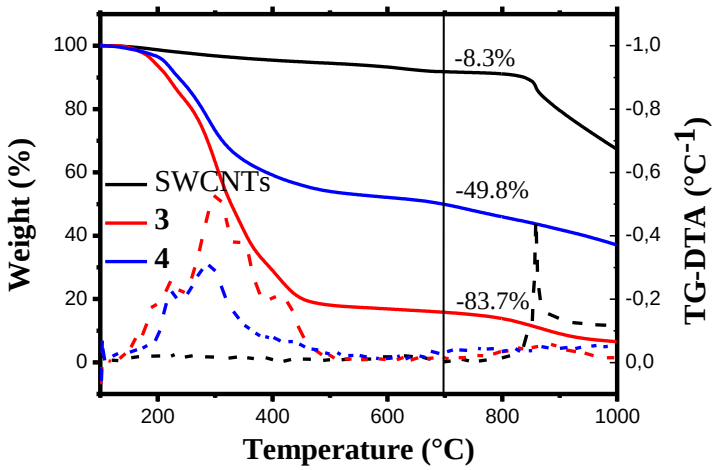

Figure 4. *TGA (solid lines) and TG-Differential Thermal Analysis (dashed lines) of pristine SWCNTs and hybrids **3** and **4**.*

In such a way highly functionalized nanotubes were achieved, as determined by thermogravimetric analysis and Raman spectroscopy. The TGA in nitrogen (**Figure 4**) shows for **3** at 700 °C a net weight loss of 75.4%, corresponding to a 0.52 mmol/g of loading, values in excellent agreement with that obtained previously for the same material.[29a] SWCNT-PAMAM **4** resulted to be less functionalized (net weight loss of 41.5% corresponding to a loading of 0.25 mmol/g) probably due to the low solubility of **2** in the reaction solvent mixture.

In conjunction with TGA, Raman spectroscopy represents a powerful and accurate technique for the characterization of SWCNTs.[31] The covalent functionalization of the CNTs can be detected from the enhancement of the area intensity of D-band with respect to the G-band in the Raman spectrum, due to the rehybridization of the carbon atoms from sp^2 to sp^3. The normalized A_D/A_G ratio from the A_{D0}/A_{G0} ratio can be used as a proof for an effective attachment on the scaffold of CNTs. As shown in **Figure 5**, Raman spectroscopy confirms the effective functionalization of the SWCNTs and the higher degree of functionalization of **3** (with a normalized A_D/A_G of 3.9) with respect to **4** (A_D/A_G = 2.9).

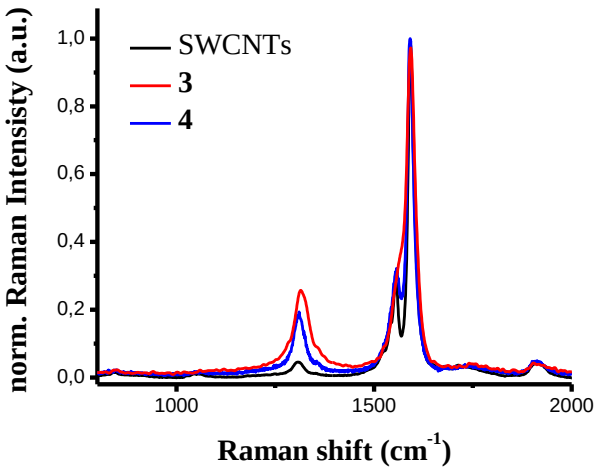

Figure 5. *Raman spectrum of pristine SWCNTs and SWCNT-PAMAM **3** and **4**.*

Next, palladium nanoparticles were immobilized by following an “in situ” strategy (**Scheme 3**). Sodium tetrachloropalladate has been firstly used as Pd(II) precursor for interacting with the dendron moieties, followed by reduction with sodium borohydride.

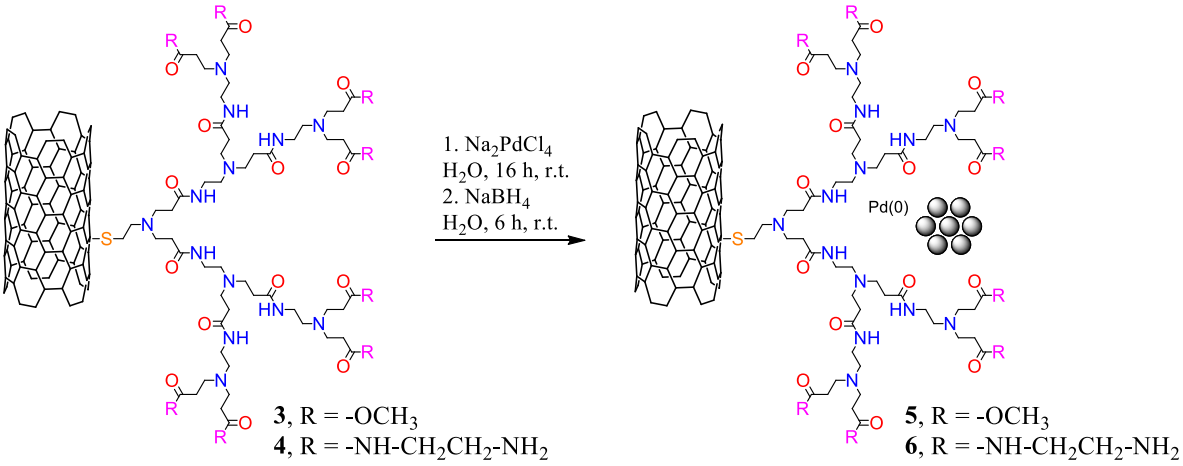

Scheme 3. *Immobilization of PdNPs for the preparation of nanocatalysts **5** and **6**.*

The fine black powders so-obtained have been characterized by means of TGA, DSC, XRD, XPS and HR-TEM. Thermogravimetric analysis coupled with differential scanning calorimetry carried out under air flow resulted to be a very useful technique for the exact quantification of palladium content in the hybrid materials (**Figure 6**).

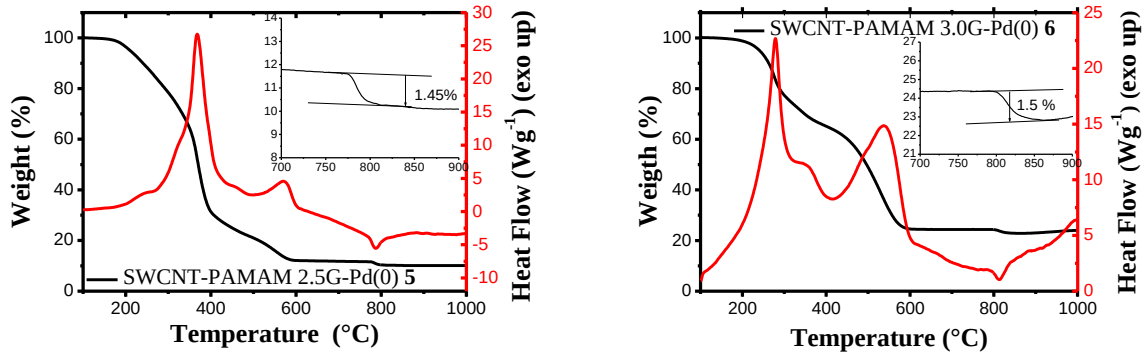

Figure 6. *TGA/DSC analyses of **5** (left), and **6** (right) recorded under air flow (10 °C/min). In the inset, the weight losses due to PdO decomposition are magnified.*

In the 770-840 °C range, the TGA of **5** and **6** presents a small yet defined weight loss (~1.5 wt%) which DSC associates to an endothermic process. These weight losses are caused by the quantitative transformation of PdO to Pd given that the former species is not stable over 800 °C.[32] In this manner a Pd loading of 9.6 and 10.0 wt% can be estimated for **5** and **6**, respectively.

High-resolution transmission electron microscopy has been used in order to shed light on the presence, distribution and dimension of PdNPs. Interestingly, in both materials **5** and **6** the PdNPs are clearly visible and very well dispersed on the nanotube surface (**Figure 7**). The main difference relies in their dimensions given that whereas **6** presents very small

PdNPs with a mean size of 1.6 ± 0.4 nm (n = 245) and a sharp distribution, in the hybrid material **5** the nanoparticles are bigger (3.4 ± 0.6 nm; n = 260) with a broader size distribution. The small dimensions and the good dispersion of the particles were also confirmed by XRD data that did not detect the presence of such nanoparticles. Very likely this difference between the two materials is due to the higher number of stabilizing amino-groups present in SWCNT-PAMAM3.0-Pd **6**. TEM pictures also show that, although the nanotubes are well functionalized, they are still arranged in ropes and bundles and not finely dispersed on the TEM grid.

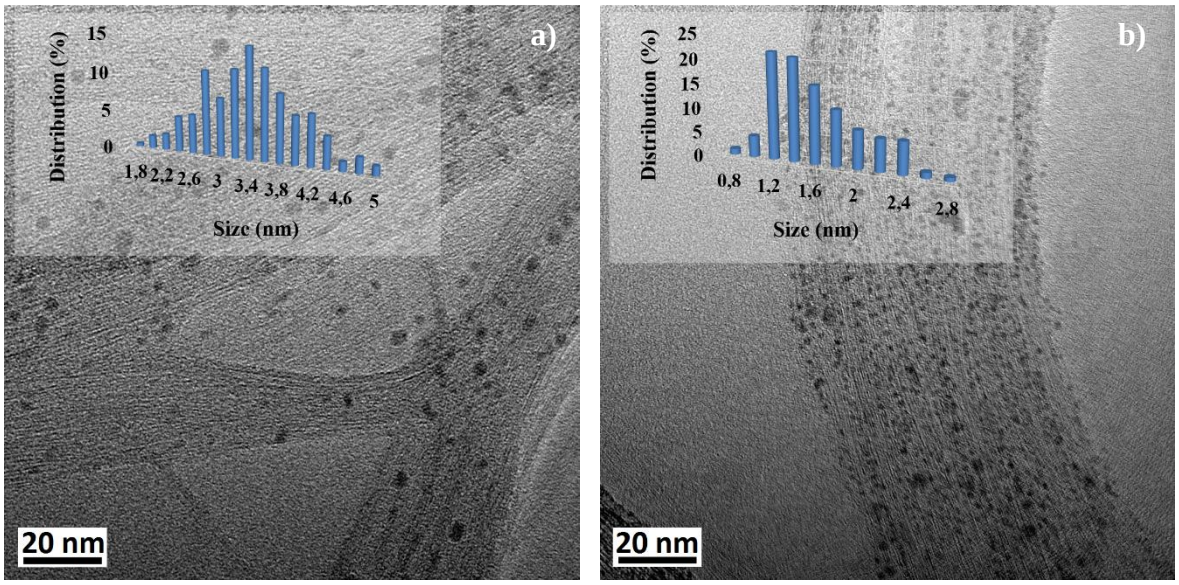

Figure 7. *Representative HR-TEM images of a)* ***5*** *and b)* ***6****. The inset shows PdNPs size distribution.*

XPS analysis was used to evaluate the degree of Pd reduction and the surface concentration of active element. As evidenced by **Figure 8**, showing the Pd3d region for **5** and **6**, Pd is present for both catalysts, mainly as Pd (II) ($Pd3d_{5/2}$ BE = 337.5 eV) with a ca. 20% of reduced Pd ($Pd3d_{5/2}$ BE = 335 eV).[5a, b] The surface atomic ratio of Pd/C is quite different in the two catalysts; in the case of **5** Pd/C = 0.006 while for **6** Pd/C = 0.02. Given that XPS is a surface sensitive technique whose analysis depth is 3-10 nm, the atomic ratio calculated suffer, besides the actual amount of the elements, of segregation, particles size or uneven distributions. Hence, the difference in the Pd/C atomic ratio may be here attributed either to a different Pd loading or to a different Pd particles size. Considering that by TGA the total Pd loading is the same in the two catalysts and by TEM material **5** shows bigger particles, which could account for the lower Pd/C atomic ratio, in case of **6** the higher Pd/C ratio is probably due to an effectively 3.5 higher amount of exposed active sites which is promising for application in catalysis.

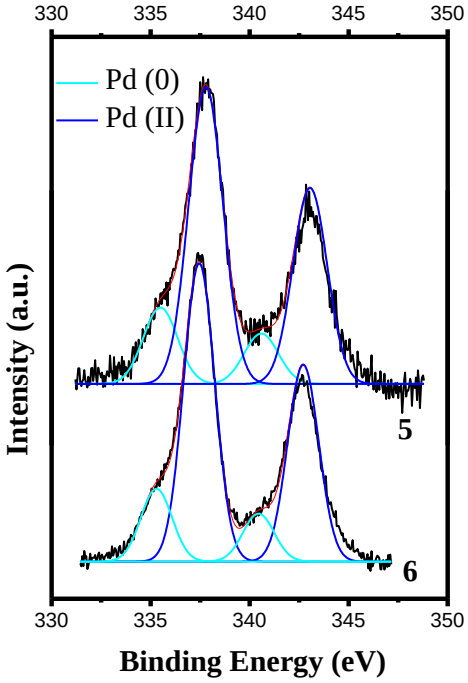

Figure 8. *High-resolution XPS spectra of Pd3d region of **5** and **6**.*

The catalytic activity of the hybrid nanomaterials was tested in C–C cross-coupling reactions. Firstly, **5** and **6** were employed as catalyst at 0.1 mol% loading in the benchmark reaction between phenylboronic acid and 4-bromobenzaldehyde. A quick screening of the reaction conditions indicated a scarce attitude for **5** to promote the title process whilst, in the case of **6**, the mixture of ethanol/water 1:1 was the best medium, allowing nearly full conversion within 5 h at 50 °C (**Table 1,** entry 1). Under such conditions, EtOH guarantees a good solubility of the substrates while water ensures a right dispersion of the catalyst, improving the activity. Very likely, the difference in activity is mainly due to the differences in NPs size in the two catalysts. As a blank experiment, SWCNT-PAMAM3.0-Pd **6** was replaced by colloidal PdNPs stabilized in the presence of PAMAM dendrimer **2** (see Experimental Section ***2.5*** for details), giving rise to no reaction within 5 h at 0.1 mol% and only partial coupling (<6 %) after 16 h with a loading of 0.4 mol%. These attempts highlight the superior activity of SWCNT-PAMAM3.0-Pd hybrid nanocatalyst probably due to the intrinsic nature of the nanotubes. In this regard, beside the fine dispersion and stabilization of the small PdNPs in the polyamidoaminic network, electronic stabilization of palladium species during the catalytic cycle by the SWCNTs may take place.[17d, 33] Interestingly, leaching analyses on the reaction solution as well as on the purified product (4-biphenylcarboxaldehyde) by means of inductively coupled plasma - optical emission spectrometry (ICP-OES) demonstrated the absence, below the limit of detection (LOD, 1

ppm), of Pd species. Hence, the applicability of the reaction has been checked on a set of substituted aryl bromides having either electron-donating or electron-withdrawing groups and boronic acids (**Table 1**). In most of the cases, the conversions were almost quantitative with excellent isolated yields (**Table 1**, entries 1-6). The use of the less reactive 4-formylphenylboronic acid with 4-bromobenzaldehyde led to the corresponding 4-biphenyldicarboxaldehyde with 85% yield (**Table 1**, entry 7) whereas with 1,3-dibromobenzene just a 42% yield has been achieved (**Table 1**, entry 8). The use of very less reactive aryl chlorides gave no conversion.

Table 1. *Suzuki–Miyaura reactions between phenylboronic acids and aryl halides catalyzed by SWCNT-PAMAM3.0-Pd* ***6****.*[a]

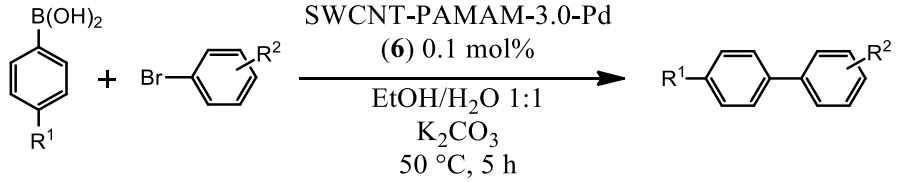

Entry	R^1	R^2	Product	Yield[b] (%)
1	H	4-CHO	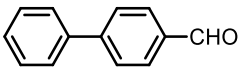	98
2	H	3-CH_3	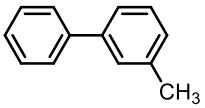	98
3	H	4-CN	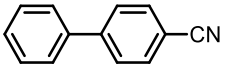	>99
4	H	4-NO_2	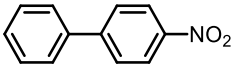	98
5	H	4-OMe	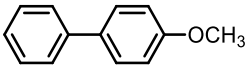	>99
6	H	4-$COCH_3$	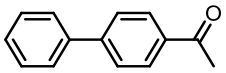	93
7	CHO	4-CHO	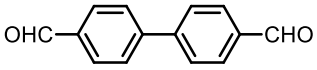	85
8	CHO	3-Br	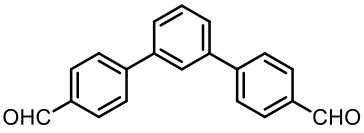	42
9[c]	H	4-CHO	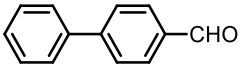	80
10[d]	H	4-CHO	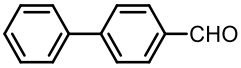	>99

[a] Reaction conditions: phenylboronic acid (0.55 mmol), aryl halide (0.5 mmol), K_2CO_3 (0.6 mmol), EtOH/H_2O (1.2 ml, 1:1), catalyst (0.1 mol%, 0.5 mg), 50 °C, 5 h. [b] Isolated product yields. [c] Catalyst (0.01 mol%), on 3 mmol scale of 4-bromobenzaldehyde, EtOH/H_2O (3.6 ml, 1:1), 16 h. [d] Catalyst (0.005 mol%), on 4 mmol scale of 4-bromobenzaldehyde, EtOH/H_2O (3.2 ml, 1:1). Microwave heating, 120 °C, 5 minutes.

Furthermore, two catalytic tests with a lower catalytic loading were carried out. In the first

one, catalyst was used at 0.01 mol% loading affording 4-biphenylcarboxaldehyde in an 80% yield reaching a TON of 8,000 and a TOF of 500 h^{-1} (**Table1**, entry 9). However, further improving were obtained by the use of microwave irradiation at 120 °C. Just 0.005 mol% of **6** allows to obtain a quantitative yield of the desired product in only 5 minutes (**Table1**, entry 10). In such a way, it was possible to reach a TON of 20,000 and a remarkable TOF value of 240,000 h^{-1}, values that are, to the best of our knowledge, among the highest reported for PdNPs immobilized on nanocarbons.[14b, 14d, 34]

The recyclability of the catalyst was assessed for the reaction between 4-bromobenzaldehyde and phenylboronic acid (0.1 mol%, 5 h). After easy recovery of **6** by centrifugation, it was used for four consecutive runs to give rise to almost complete conversion and yield (92–98%), even though in the fifth cycle the activity dropped (yield 30%) probably due to catalyst loss (just 1.5 mg of **6** has been used during recycling). In order to get some insight about the actual mechanism involved during the catalysis additional experiments were run. In three parallel reactions (4-bromobenzaldehyde and phenylboronic acid) the catalyst was filtered-off after 20 minutes. In the first one, the reaction was stopped and the ^{1}H NMR analysis of the crude mixture showed 32% of the corresponding biaryl compound. The second reaction was quickly filtered still hot (hot filtration) and left to stir (devoid of the nanocatalyst **6**) for additional 4 h 40 min leading to a 55% conversion, still lower with respect the conversion obtained without catalyst removal (**Table 1,** entry 1). On the contrary, the last reaction, which was allowed to cool down to rt prior catalyst removal and left stirring for 4 h 40 min (cold filtration), showed no extra conversion.

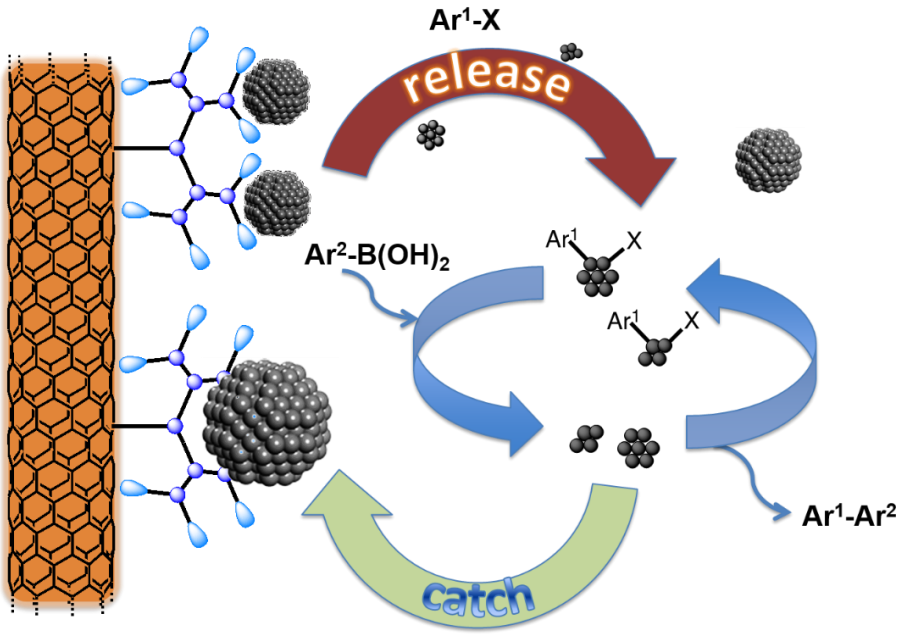

Figure 9. *Sketch of the possible mechanism of "release and catch" involved during the catalytic cycle.*

The above data allow hypothesize a mechanism in which the catalytic species may comprise small soluble clusters of palladium standing close to the catalyst surface that, to some extent, during the catalytic cycle and under a thermal regime can be leached away. However, the "natural" cooling down at the end of the reaction permits the soluble clusters to re-deposit on the immobilized nanoparticles, thus following the "release and catch" mechanism[35] (**Figure 9**).

This hypothesis is strongly supported by TEM analysis of catalyst **6** used for five cycles. **Figure 10** shows a representative TEM picture of the spent catalyst in which PdNPs are clearly discernible. Differently from the fresh catalyst (cfr. **Figure 7b**), in the used one PdNPs are less in number but bigger in size. Statistical estimation of the PdNPs diameter confirms that after catalysis the nanoparticles "grows" reaching a mean diameter of 3.5 ± 1.0 nm (n = 325) with a broad size distribution.

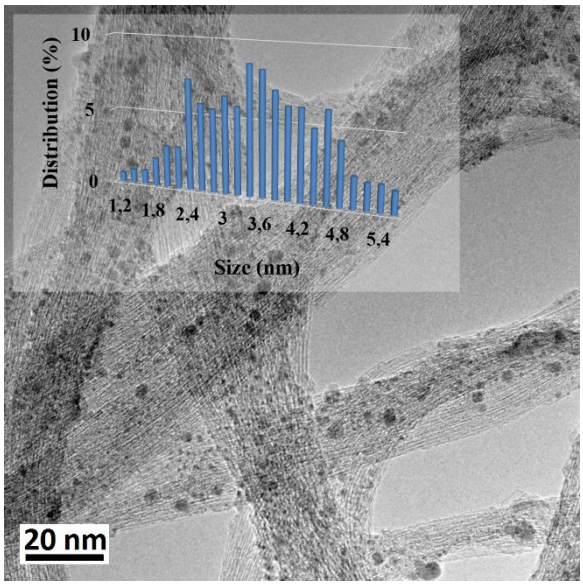

Figure 10. *Representative HR-TEM picture of* ***6*** *after five cycles in Suzuki reaction. The inset shows PdNPs size distribution.*

These data may, to some extent, justify the decreased activity of **6** in the fifth cycle given that the bigger nanoparticles possess sensibly less exposed active sites.

Catalysts **5** and **6** were also tested in Mizoroki-Heck coupling. A quick screening of reaction conditions led to establish DMF/water (4:1 v/v) as the best solvent mixture with triethylamine as the base (**Table 2**). Both catalysts are able to promote the C–C bond formation even if with a remarkably different activity. In fact, SWCNT-PAMAM3.0-Pd **6** is able to work at 0.1 mol% loading, generally faster than SWCNT-PAMAM2.5-Pd **5** whose loading is five times higher. Thus, reactions between several aryliodides endowed with

electron-donating or electron-withdrawing groups and methyl acrylate gave corresponding products in high yields and excellent selectivity (**Table 2**, entries 1–6). In addition, the coupling between 4-iodoacetophenone and methyl acrylate was carried out using catalyst **6** at 0.01 mol% loading to afford the desired product quantitatively after 16 h (**Table 2**,entry 7), with a remarkable TON value of 10,000.

Table 2. *Mizoroki–Heck reactions between methyl acrylate and aryliodides catalyzed by **5** and **6**.*[a]

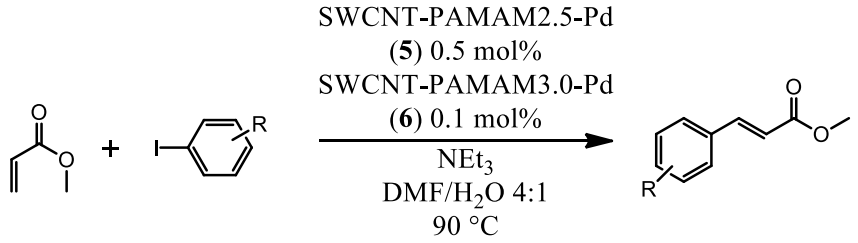

Entry	R	Product	Catalyst	t (h)	Yield[b] (%)
1	H	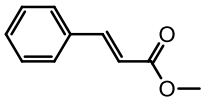	**5**	4	74
			6	5	99
2	4-CH_3	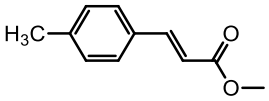	**5**	4	97
			6	5	99
3	4-$COCH_3$	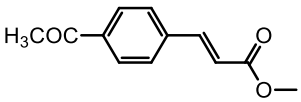	**5**	22	89
			6	5	99
4	4-NO_2	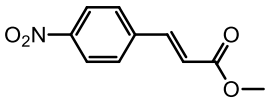	**5**	22	87
			6	16	85
5	4-OCH_3	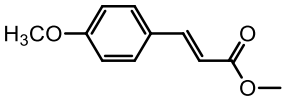	**5**	22	97
			6	5	97
6	3-Br	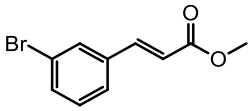	**5**	22	96
			6	5	96
7[c]	4-$COCH_3$	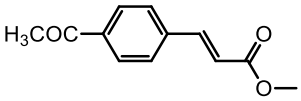	**6**	16	99

[a] Reaction conditions: methyl acrylate (0.75 mmol), aryliodide (0.5 mmol), NEt_3 (1 mmol), catalyst (0.1 mol%, 0.5 mg), DMF/H_2O (1 ml, 4:1), 90 °C, 5 h. [b] Isolated product yield. [c] Reaction conditions: methyl acrylate (2.25 mmol), aryliodide (1.5 mmol), NEt_3 (3 mmol), catalyst (0.01 mol%, 0.15 mg), DMF/H_2O (1.5 ml, 4:1), 90 °C, 16 h.

Next, recyclability of SWCNT-PAMAM3.0-Pd **6** was checked for the reaction between 4-iodoanisole and methyl acrylate (**Figure 11**). It is worth to note that 0.1 mol% of catalyst was enough to yield quantitative conversion of the substrate within 4 h in six consecutive runs. However, the catalytic activity dropped in the 7th cycle. This fact can be ascribed to the combination of several concurrent causes: just 1.5 mg of **6** has been used during recycling and in the last cycles some catalyst has been lost. In addition, TEM analysis showed, at low

magnification, the presence of impurities in the catalyst. Finally, ICP-OES analysis of the reaction mixture displayed the presence of 5 ppm of Pd (9% of Pd present in the catalyst). Nevertheless, no Pd was found in the purified and isolated product (below the LOD of 1 ppm).

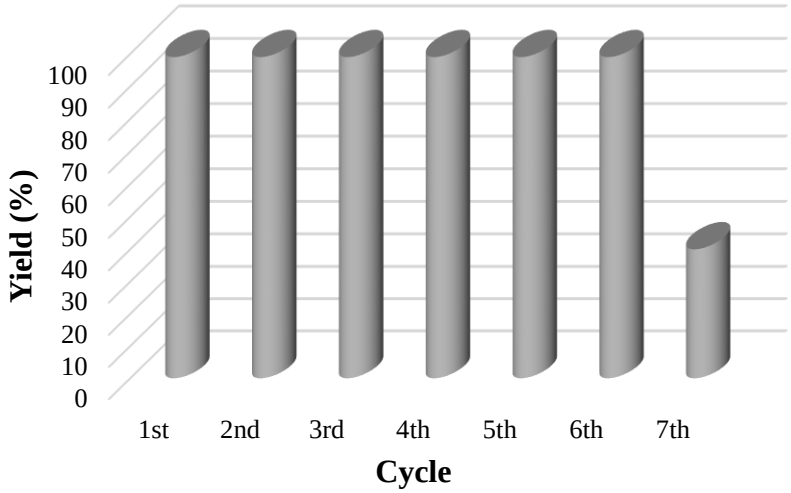

Figure 11. *Recycling tests of catalyst **6** in the Heck reaction between 4-iodoanisole and methyl acrylate.*

TEM analysis of catalyst **6** after seven cycles shows that the PdNPs mean size increases during the recycling to a value of 3.3 ± 0.7 nm (n = 280), significantly higher than that of the fresh catalyst (compare **Figure 7b** with **Figure 12**).

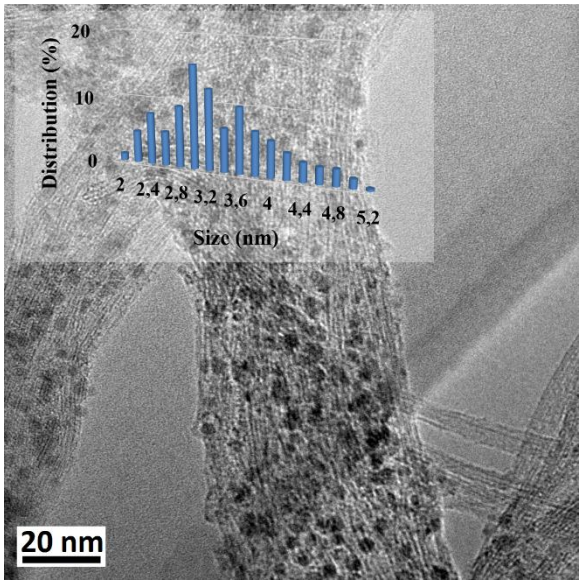

Figure 12. *Representative HR-TEM picture of **6** used in seven consecutive Heck reactions. The inset shows PdNPs size distribution.*

Nevertheless, the reaction temperature of 90 °C is sensibly below the temperature at which

thermal sintering of PdNPs may occur. Hence, additional experiments analogously to those carried out for Suzuki reaction were run. In the case of Mizoroki-Heck coupling, hot and cold filtrations after 20 minutes followed by further stirring for 4 h and 40 minutes gave rise to complete conversion whereas the control reaction blocked after 20 minutes gave 19% conversion. With this data in hand, a possible dual mechanism can be envisaged since the growth of PdNPs during the catalysis indicates that a "release and catch" regime is operative although, in the present case, the main operating mechanism is homogeneous giving that the dissolved Pd species are, very likely, strongly stabilized in solution by the presence of triethylamine and dimethylformamide.[27b, 36]

2.4 Conclusions

In summary, SWCNTs were functionalized with two different PAMAM dendrimers (2.5 G and 3.0 G) with a cystamine core through simple and straightforward convergent protocols. These hybrid materials were characterized by means of TGA and Raman spectroscopy and used for the in situ immobilization of palladium nanoparticles. Characterization of the so-prepared nanocatalysts **5** and **6** by means of TGA, DSC, Raman, XPS, XRD and HR-TEM allowed to establish that both materials are decorated with small PdNPs with mean diameters of 3.2 and 1.6 nm, respectively, in a ~10 wt% loading. Investigations on the catalytic activity of SWCNT-PAMAM2.5-Pd **5** and SWCNT-PAMAM3.0-Pd **6** toward Suzuki-Miyaura and Mizoroki-Heck reactions showed **6** as the best performing material. In both processes, routine substrate scope have been carried out with just 0.1 mol% loading, but reactions with only 0.01 mol% of catalyst were also possible with a slightly larger reaction time, allowing to obtain TON of up to 10,000. Microwave irradiation allowed to achieve complete conversion within 5 minutes with just 0.005 mol% of catalyst. In this manner a remarkable TOF of 240,000 h^{-1} was reached. Nanocatalyst **6** resulted to be recyclable four times in the Suzuki reaction and six times in the Heck coupling with quantitative yields, but showing a loss of catalytic activity in the next cycles. Further experiments permitted to shed light on the two different mechanisms underlying the title processes. In both reactions a "release and catch" mechanism is operative, as pointed out by the PdNPs growth, but whereas during the Suzuki reaction the re-deposition of the small Pd-clusters is highly effective, in the Heck coupling part of the above clusters are stabilized by both the base and the solvent and subsequently leached away.

2.5 Experimental Section

General: Chemicals and solvents were purchased from commercial suppliers or purified by standard techniques. Pristine SWCNTs were obtained from Carbon Nanotechnologies Inc. (HiPco® Single-Wall Carbon Nanotubes, lot number P02772). For thin-layer chromatography (TLC), silica gel plates (Merck 60 F254) were used and compounds were visualized by irradiation with UV light and/or by treatment with a $KMnO_4$ solution. Flash chromatography was carried out using Macherey–Nagel silica gel (0.04–0.063 mm). Petroleum ether refers to the fraction with the boiling range 40–60 °C. MW-assisted catalytic tests were carried out with a CEM DISCOVER monomode system in closed vessel in manual mode (no remote PC control) with infrared sensor for temperature control and with no pressure control. ^{1}H and ^{13}C NMR spectra were recorded with a Bruker 250, Bruker 300 MHz or Bruker Avance II 400 MHz spectrometers. Thermogravimetric analysis (TGA) was performed under oxygen flow from 100 to 1000 °C with a heating rate of 10 °C/min in a Mettler Toledo TGA/DSC STAR System. Raman spectra were acquired with a Renishaw instrument, model InVia reflex equipped with 532, 633, and 785 nm lasers. After acquisition, the spectra were normalized with respect to the G-band and then the area of the D and G peaks were calculated. XRD measurements were carried out with a Bruker D 5000 diffractometer equipped with a Cu Kα anode and a graphite monochromator. A proportional counter and a 0.05° step size in 2θ were used. The assignment of the various crystalline phases in 2θ was based on the JCPDS powder diffraction file cards (JCPDS Powder Diffraction File, International Centre for Diffraction Data, Swarthmore, PA, USA, 1989.). The instrumental broadening was determined by collecting the diffraction pattern of the standard, lanthanum hexaboride LaB6. The X-ray photoelectron spectroscopy (XPS) analyses were performed with a VGMicrotech ESCA 3000Multilab, equipped with a dual Mg/Al anode. The spectra were excited by the unmonochromatized Al Kα source (1486.6 eV) run at 14 kV and 15 mA. The analyzer was operated in the constant analyzer energy (CAE) mode. For the individual peak energy regions, a pass energy of 20 eV set across the hemispheres was used. Survey spectra were measured at 50 eV pass energy. The sample powders were mounted on a double-sided adhesive tape. The pressure in the analysis chamber was in the range of 10^{-8} Torr during data collection. The constant charging of the samples was removed by referencing all the energies to the C1s set at 284.6 eV. The invariance of the peak shapes and widths at the beginning and at the end of the analyses

ensured absence of differential charging. Analyses of the peaks were carried out with the software provided by VG, based on non-linear least squares fitting program using a weighted sum of Lorentzian and Gaussian component curves after background subtraction according to Shirley and Sherwood. Atomic concentrations were calculated from peak intensity using the sensitivity factors provided with the software. The binding energy values are quoted with a precision of ±0.15 eV and the atomic percentage with a precision of ±10%. TEM micrographs were recorded on a high-resolution transmission electron microscope (HR-TEM) JEOL JEM-2100 operating at 200 kV accelerating voltage. Samples were dispersed in water and drop cast onto carbon coated copper TEM grids for HR-TEM analysis. The imaging conditions were carefully tuned by lowering the accelerating voltage of the microscope and reducing the beam current density to a minimum in order to minimize the electron beam induced damage of the sample. Inductively Coupled Plasma - Optical Emission Spectrometry (ICP-OES) analyses were carried out with an Optima 8000, Perkin Elmer, USA. Analyses were conducted using a calibration curve, obtained by dilution.

- **Synthesis of cystamine core PAMAM dendrimers**

The PAMAM dendrimers with cystamine-core (2.5 G and 3.0 G) were prepared following the procedure previously reported in literature.[28a]

- **Synthesis of SWCNTs-PAMAM2.5 – (3)**

Pristine SWCNTs (4.12 mmol, 50 mg) were dispersed in toluene (270 mL). The mixture was sonicated for 20 minutes. PAMAM 2.5G (1.63 mmol, 4.72 g), previously dissolved in 30 mL of methanol, was added to the SWCNTs suspension and the reaction mixture was refluxed and stirred at 115 °C for 72 h. Then, the mixture was cooled and filtered on Millipore PTFE membrane under vacuum. The hybrid solid material was washed with methanol, water, 3.0 M hydrochloric acid, 2% triethylamine solution in THF, THF and diethyl ether. 492.7 mg of SWCNTs-PAMAM2.5 **3** were recovered.

- **Synthesis of SWCNTs-PAMAM3.0 – (4)**

Pristine SWCNTs (3.33 mmol, 40 mg) were dispersed in toluene (220 mL). The mixture was sonicated for 20 minutes. PAMAM 3.0G (1.26 mmol, 4.22 g), previously dissolved in 25 mL of methanol, was added to the SWCNTs suspension. Afterwards, AIBN (0.60 mmol,

100 mg) was added to the reaction mixture which was refluxed and stirred at 115 °C for 72 h. Then, the mixture was cooled and filtered on Millipore PTFE membrane under vacuum. The hybrid solid material was washed with methanol, water, 3.0 M hydrochloric acid, 2% triethylamine solution in THF, THF and diethyl ether. 74.5 mg of SWCNTs-PAMAM3.0 **4** were recovered.

- **Synthesis of SWCNTs-PAMAM2.5-Pd – (5)**

SWCNTs-PAMAM2.5 **3** (180 mg) was suspended and sonicated in distilled water (80 mL) for 30 minutes. In the meanwhile, $PdCl_2$ (0.188 mmol, 33.67 mg) and 20 eq. of NaCl (3.76 mmol, 220.40 mg) in distilled water (6 mL) were stirred at 80 °C for 20 minutes and then cooled to room temperature. The obtained tetrachloropalladate solution was added dropwise to the stirring suspension of SWCNTs-PAMAM2.5 **3**. The reaction mixture was left at room temperature for 19 h. Then, the mixture was filtered under vacuum on Millipore PTFE membrane and washed with water, methanol and diethyl ether. 52 mg of SWCNTs-PAMAM2.5-$PdCl_4^{2-}$ were recovered, suspended in distilled water (15 mL) and sonicated for 5 minutes. A solution of $NaBH_4$ (8 eq. in 10 mL of distilled water) was added to the stirring suspension of SWCNTs-PAMAM2.5-$PdCl_4^{2-}$. The reaction mixture was stirred at room temperature for 17 h. Then, the mixture was filtered on Millipore PTFE membrane under vacuum and washed with water, methanol and diethyl ether. 100.6 mg of SWCNTs-PAMAM2.5-Pd **5** were recovered.

- **Synthesis of SWCNTs-PAMAM3.0-Pd – (6)**

SWCNTs-PAMAM3.0 **4** (63 mg) was suspended and sonicated in distilled water (30 mL) for 30 minutes. In the meanwhile, $PdCl_2$ (0.089 mmol, 15.90 mg) and 20 eq. of NaCl (1.78 mmol, 104.02 mg) in distilled water (6 mL) were stirred at 80 °C for 20 minutes and then cooled to room temperature. The obtained tetrachloropalladate solution was added dropwise to the stirring suspension of SWCNTs-PAMAM3.0 **4**. The reaction mixture was left at room temperature for 19 h. Then, the mixture was filtered on Millipore PTFE membrane under vacuum and washed with water, methanol and diethyl ether. 52 mg of SWCNTs-PAMAM3.0-$PdCl_4^{2-}$ were recovered, suspended in distilled water (15 mL) and sonicated for 5 minutes. A solution of $NaBH_4$ (8 eq in 5 mL of distilled water) was added to the stirring suspension of SWCNTs-PAMAM3.0-$PdCl_4^{2-}$. The reaction mixture was stirred at room temperature for 17 h. Then, the mixture was filtered on Millipore PTFE membrane under

vacuum and washed with water, methanol and diethyl ether. 47.1 mg of SWCNTs-PAMAM3.0-Pd **6** were recovered.

Catalytic tests

- **Suzuki reactions with SWCNTs-PAMAM3.0-Pd (6)**

The catalytic tests were performed in a 3 mL glass vial with screw cap in which aryl bromide (0.5 mmol), phenylboronic acid (0.55 mmol), K_2CO_3 (0.6 mmol) and the catalyst **6** (0.1 mol%, 0.5 mg) were placed. Then, distilled water (0.6 mL) and ethanol (0.6 mL) were placed. The reaction mixture was sonicated for a short time and heated at 50 °C under stirring for 5 h. Then, the reaction mixture was cooled at room temperature and the crude was purified by short flash column chromatography using petroleum ether/ethyl acetate as eluent. Conversions were estimated by ^{1}H NMR analysis. Spectroscopic data are in agreement with those reported in literature.[37]

- **Suzuki reaction with SWCNTs-PAMAM3.0-Pd (6) under microwave irradiation**

In a microwave glass tube 4-bromobenzaldehyde (4.0 mmol), phenylboronic acid (4.4 mmol), K_2CO_3 (4.8 mmol) and catalyst **6** (0.005 mol%,0.2 mg) were placed. Then, distilled water (1.6 mL) and ethanol (1.6 mL) were added. The reaction mixture was sonicated for a short time and heated under microwave irradiation (12 W) at 120 °C for 5 minutes. Then, the reaction mixture was cooled at room temperature and, after confirming the complete conversion by TLC, the crude was poured into water and extracted with diethyl ether. The organic layers were dried with Na_2SO_4 and the solvent evaporated under vacuum to afford the desired product in 100% yield (confirmed by TLC and GC-MS).

- **Preparation of colloidal PdNPs stabilized in the presence of PAMAM3.0G**

A solution of PAMAM3.0G was prepared by dissolving 30 mg of dendrimer in 3 mL of distilled water. Thereafter, $PdCl_2$ (0.028 mmol, 5.05 mg) and 20 eq. of NaCl (0.56 mmol, 33.01 mg) in distilled water (3 mL) were stirred at 80 °C for 20 minutes and then cooled to room temperature. The obtained tetrachloropalladate solution, corresponding to 10 wt% of palladium respect to PAMAM3.0G, was added dropwise to the stirring PAMAM3.0G

solution. The reaction mixture was left at room temperature for 19 h. Then, a solution of $NaBH_4$ (8 eq in 3 mL of distilled water) was added to the stirring PAMAM-3.0-$PdCl_4^{2-}$ solution. The reaction mixture was stirred at room temperature for 16 h.

- **Suzuki reactions with PAMAM3.0G-Pd**

Two catalytic tests were performed in a 4 mL glass vial with screw cap in which 4-bromobenzaldehyde (1.0 mmol), phenylboronic acid (1.1 mmol), K_2CO_3 (1.2 mmol) and PdNPs stabilized in the presence of PAMAM3.0G as catalyst were placed. In the first test, PAMAM3.0-Pd solution (0.3 mL, 0.1 mol%), distilled water (0.9 mL) and ethanol (1.2 mL) were added. The reaction mixture was sonicated for a short time and heated at 50 °C under stirring for 5 h. Then, the reaction mixture was cooled at room temperature and the crude was purified by short flash column chromatography using petroleum ether/ethyl acetate as eluent. ^{1}H NMR analysis detected no conversion.
The second test was carried out in the same conditions as the previous one except for the loading of the catalyst (1.2 mL, 0.4 mol%) and the reaction time (16 h). The reaction mixture was cooled at room temperature and the crude was purified by short flash column chromatography using petroleum ether/ethyl acetate as eluent. By ^{1}H NMR analysis 6% of conversion was estimated.

- **Recycling tests of SWCNTs-PAMAM3.0-Pd (6) in Suzuki reactions**

Recycling tests were performed in a glass vial in which 4-bromobenzaldehyde (1.5 mmol), phenylboronic acid (1.65 mmol), K_2CO_3 (1.8 mmol) and the catalyst **6** (0.1 mol%, 1.5 mg) were placed. Then, distilled water (1.8 mL) and ethanol (1.8 mL) were added. The reaction mixture was sonicated for a short time and heated at 50 °C under stirring for 5 h. Then, the reaction mixture was cooled at room temperature. The catalyst was recovered by centrifugation and washed with ethyl acetate, ethyl acetate/diethyl ether and acetone/diethyl ether. Once dried, the catalyst was used for the next cycle. The crude was purified by short flash column chromatography using petroleum ether/ethyl acetate as eluent. Conversions were estimated by ^{1}H NMR analysis.

- **Heck reactions with SWCNTs-PAMAM2.5-Pd (5) and SWCNTs-PAMAM3.0-Pd (6)**

The catalytic tests were performed in a 3 mL glass vial with screw cap in which catalyst **5** (0.5 mol%, 2.5 mg) or **6** (0.1 mol%, 0.5 mg), aryl iodide (0.5 mmol), methyl acrylate (0.75 mmol), triethylamine (1 mmol) and DMF/H_2O (0.8 mL + 0.2 mL) were placed. The reaction mixture was sonicated for a short time and heated at 90 °C under stirring for the appropriate time. Then, the reaction mixture was cooled at room temperature and the crude was purified by short flash column chromatography using petroleum ether/ethyl acetate as eluent. Conversions were estimated by ^{1}H NMR analysis. Spectroscopic data are in agreement with those reported in literature.[38]

- **Recycling tests of SWCNTs-PAMAM3.0-Pd (6) in Heck reactions**

Recycling tests were performed in a glass vial in which catalyst **6** (0.1 mol%, 1.5 mg), 4-iodoanisole (1.5 mmol), methyl acrylate (2.25 mmol), triethylamine (3 mmol) and DMF/H_2O (2.4 mL + 0.6 mL) were placed. The reaction mixture was sonicated for a short time and heated at 90 °C under stirring for 4 h. Then the reaction mixture was cooled at room temperature. The catalyst was recovered by centrifugation and washed with ethyl acetate, ethyl acetate/diethyl ether and acetone/diethyl ether. Once dried, the catalyst was used for the next cycle. The crude was purified by short flash column chromatography using petroleum ether/ethyl acetate as eluent. Conversions were estimated by ^{1}H NMR analysis.

- **Leaching studies of SWCNTs-PAMAM3.0-Pd (6) in Suzuki reaction**

Three parallel reactions were carried out in three glass vials using 4-bromobenzaldehyde (0.4 mmol), phenylboronic acid (0.44 mmol), K_2CO_3 (0.48 mmol) and catalyst **6** (0.1 mol%, 0.4 mg). Distilled water (0.48 mL) and ethanol (0.48 mL) were employed as solvents. The reaction mixtures were sonicated for a short time and heated at 50 °C under stirring. The catalyst was filtered-off after 20 minutes in all tests. In the first one, the reaction was stopped immediately after catalyst removal. The second reaction was quickly filtered still hot (hot filtration) and left to stir (devoid of the catalyst **6**) for additional 4h 40 min. The last reaction was allowed to cool down to room temperature prior catalyst removal and left stirring for 4h 40 min (cold filtration). All the crude mixtures were purified by short flash column chromatography using petroleum ether/ethyl acetate as eluent. Conversions were estimated

by ^{1}H NMR analysis.

- **Leaching studies of SWCNTs-PAMAM3.0-Pd (6) in Heck reaction**

Three parallel reactions were carried out in three glass vials using iodoacetophenone (0.4 mmol), methyl acrylate (0.6 mmol), triethylamine (0. 8 mmol) and the catalyst **6** (0.1 mol%, 0.4 mg). Distilled water (0.16 mL) and dimethylformamide (0.64 mL) were employed as solvents. The reaction mixtures were sonicated for a short time and heated at 90 °C under stirring. The catalyst was filtered-off after 20 minutes in all tests. In the first one, the reaction was stopped immediately after catalyst removal. The second reaction was quickly filtered still hot (hot filtration) and left to stir (devoid of catalyst **6**) for additional 4h 40 min. The last reaction was allowed to cool down to room temperature prior catalyst removal and left stirring for 4h 40 min (cold filtration). All the crude mixtures were purified by short flash column chromatography using petroleum ether/ethyl acetate as eluent. Conversions were estimated by ^{1}H NMR analysis.

2.6 References

[1] (a) A. De Meijere, F. Diederich, *Metal-Catalyzed Cross-Coupling Reactions, Second Edition*, Wiley-VCH Verlag GmbH & Co. KGaA, Weinheim, Germany, **2004**; (b) E. Negishi, *Handbook of Organopalladium Chemistry for Organic Synthesis*, Wiley-VCH Verlag GmbH & Co. KGaA, Weinheim, Germany, **2002**; (c) K. C. Nicolaou, P. G. Bulger, D. Sarlah, *Angew. Chem* **2005**, *117*, 4516-4563; (d) C. C. C. Johansson Seechurn, M. O. Kitching, T. J. Colacot, V. Snieckus, *Angew. Chem. Int. Ed.* **2012**, *51*, 5062-5085.

[2] (a) C. Torborg, M. Beller, *Adv. Synth. Catal.* **2009**, *351*, 3027-3043; (b) J. Magano, J. R. Dunetz, *Chem. Rev.* **2011**, *111*, 2177-2250; (c) A. Pron, P. Gawrys, M. Zagorska, D. Djurado, R. Demadrille, *Chem. Soc. Rev.* **2010**, *39*, 2577-2632.

[3] (a) H. A. Dieck, R. F. Heck, *J. Am. Chem. Soc.* **1974**, *96*, 1133-1136; (b) A. Suzuki, *Angew. Chem. Int. Ed.* **2011**, *50*, 6723-6733.

[4] (a) J. Qiu, L. Wang, M. Liu, Q. Shen, J. Tang, *Tetrahedron Lett.* **2011**, *52*, 6489-6491; (b) G. Zou, Z. Wang, J. Zhu, J. Tang, M. Y. He, *J. Mol. Catal. A: Chem.* **2003**, *206*, 193-198; (c) L. Liu, Y. Dong, B. Pang, J. Ma, *J. Org. Chem.* **2014**, *79*, 7193-7198; (d) D. N. Korolev, N. A. Bumagin, *Tetrahedron Lett.* **2006**, *47*, 4225-4229; (e) A. Decottignies, A. Fihri, G. Azemar, F. Djedaini-Pilard, C. Len, *Catal. Commun.* **2013**, *32*, 101-107; (f) C. Liu, Q. Ni, F. Bao, J. Qiu, *Green Chem.* **2011**, *13*, 1260-1266.

[5] (a) C. E. Garrett, K. Prasad, *Adv. Synth. Catal.* **2004**, *346*, 889-900; (b) C. J. Welch, J. Albaneze-Walker, W. R. Leonard, M. Biba, J. DaSilva, D. Henderson, B. Laing, D. J. Mathre, S. Spencer, X. Bu, T. Wang, *Org. Process Res. Dev.* **2005**, *9*, 198-205; (c) R. Buscemi, F. Giacalone, S. Orecchio, M. Gruttadauria, *ChemPlusChem* **2014**, *79*, 421-426.

[6] (a) M. Moreno-Mañas, R. Pleixats, *Acc. Chem. Res.* **2003**, *36*, 638-643; (b) D. Astruc, F. Lu, J. R. Aranzaes, *Angew. Chem. Int. Ed.* **2005**, *44*, 7852-7872; (c) A. Roucoux, J. Schulz, H. Patin, *Chem. Rev.* **2002**, *102*, 3757-3778; (d) R. Narayanan, M. A. El-Sayed, *J. Am. Chem. Soc.* **2003**, *125*, 8340-8347; (e) D. Astruc, *Nanoparticles and Catalysis*, Wiley-VCH Verlag GmbH & Co. KGaA, Weinheim, Germany, **2008**.

[7] (a) Á. Molnár, *Chem. Rev.* **2011**, *111*, 2251-2320; (b) A. Fihri, M. Bouhrara, B. Nekoueishahraki, J.-M. Basset, V. Polshettiwar, *Chem. Soc. Rev.* **2011**, *40*, 5181-5203.

[8] (a) F. Hoffmann, M. Cornelius, J. Morell, M. Fröba, *Angew. Chem. Int. Ed.* **2006**, *45*, 3216-3251; (b) S. Mandal, D. Roy, R. V. Chaudhari, M. Sastry, *Chem. Mater.* **2004**, *16*, 3714-3724; (c) V. Polshettiwar, C. Len, A. Fihri, *Coord. Chem. Rev.* **2009**, *253*, 2599-2626; (d) A. Gniewek, J. J. Ziółkowski, A. M. Trzeciak, M. Zawadzki, H. Grabowska, J. Wrzyszcz, *J. Catal.* **2008**, *254*, 121-130; (e) W. Huang, J. H.-C. Liu, P. Alayoglu, Y. Li, C. A. Witham, C.-K. Tsung, F. D. Toste, G. A. Somorjai, *J. Am. Chem. Soc.* **2010**, *132*, 16771-16773; (f) N. Zheng, G. D. Stucky, *J. Am. Chem. Soc.* **2006**, *128*, 14278-14280.

[9] (a) E. Hariprasad, T. P. Radhakrishnan, *ACS Catalysis* **2012**, *2*, 1179-1186; (b) K. Karami, M. Ghasemi, N. Haghighat Naeini, *Catal. Commun.* **2013**, *38*, 10-15; (c) A. Alonso, A. Shafir, J. Macanás, A. Vallribera, M. Muñoz, D. N. Muraviev, *Catal. Today* **2012**, *193*, 200-206; (d) P. Zhang, Z. Weng, J. Guo, C. Wang, *Chem. Mater.* **2011**, *23*, 5243-5249; (e) S. Ogasawara, S. Kato, *J. Am. Chem. Soc.* **2010**, *132*, 4608-4613.

[10] (a) A. K. Diallo, C. Ornelas, L. Salmon, J. R. Aranzaes, D. Astruc, *Angew. Chem. Int. Ed.* **2007**, *46*, 8644-8648; (b) K. Esumi, R. Isono, T. Yoshimura, *Langmuir* **2004**, *20*, 237-243; (c) K. R. Gopidas, J. K. Whitesell, M. A. Fox, *Nano Lett.* **2003**, *3*, 1757-1760; (d) R. Andrés, E. De Jesús, J. C. Flores, *New J. Chem.* **2007**, *31*, 1161-1191; (e) D. Astruc, *Tetrahedron: Asymmetry* **2010**, *21*, 1041-1054.

[11] (a) P. Li, L. Wang, L. Zhang, G.-W. Wang, *Adv. Synth. Catal.* **2012**, *354*, 1307-1318; (b) S. Shylesh, V. Schünemann, W. R. Thiel, *Angew. Chem. Int. Ed.* **2010**, *49*, 3428-3459; (c) V. Polshettiwar, R. Luque, A. Fihri, H. Zhu, M. Bouhrara, J.-M. Basset, *Chem. Rev.* **2011**, *111*, 3036-3075.

[12] (a) D. S. Su, S. Perathoner, G. Centi, *Chem. Rev.* **2013**, *113*, 5782-5816; (b) J. Guerra, M. A. Herrero, *Nanoscale* **2010**, *2*, 1390-1400; (c) G. G. Wildgoose, C. E. Banks, R. G. Compton, *Small* **2006**, *2*, 182-193; (d) P. Serp, B. Machado, *Carbon (Nano)materials for Catalysis* in *Nanostructured Carbon Materials for Catalysis*, The Royal Society of Chemistry, **2015**, pp. 1-45.

[13] (a) L. Shao, B. Zhang, W. Zhang, S. Y. Hong, R. Schlögl, D. S. Su, *Angew. Chem. Int. Ed.* **2013**, *52*, 2114-2117; (b) L. Shao, B. Zhang, W. Zhang, D. Teschner, F. Girgsdies, R. Schlögl, D. S. Su, *Chem. Eur. J.* **2012**, *18*, 14962-14966; (c) S. Kundu, Y. Wang, W. Xia, M. Muhler, *J. Phys. Chem. C* **2008**, *112*, 16869-16878.

[14] (a) N. Karousis, G.-E. Tsotsou, F. Evangelista, P. Rudolf, N. Ragoussis, N. Tagmatarchis, *J. Phys. Chem. C* **2008**, *112*, 13463-13469; (b) M. Cano, A. Benito, W. K. Maser, E. P. Urriolabeitia, *Carbon* **2011**, *49*, 652-658; (c) B. Cornelio, G. A. Rance, M. Laronze-Cochard, A. Fontana, J. Sapi, A. N. Khlobystov, *Journal of Materials Chemistry A* **2013**, *1*, 8737-8744; (d) A. R. Siamaki, Y. Lin, K. Woodberry, J. W. Connell, B. F. Gupton, *Journal of Materials Chemistry A* **2013**, *1*, 12909-12918.

[15] (a) A. Corma, H. Garcia, A. Leyva, *J. Mol. Catal. A: Chem.* **2005**, *230*, 97-105; (b) S. Santra, P. Ranjan, P. Bera, P. Ghosh, S. K. Mandal, *RSC Adv.* **2012**, *2*, 7523-7533; (c) W. Sun, Z. Liu, C. Jiang, Y. Xue, W. Chu, X. Zhao, *Catal. Today* **2013**, *212*, 206-214; (d) L. Zhang, G. Wen, H. Liu, N. Wang, D. S. Su, *ChemCatChem* **2014**, *6*, 2600-2606.

[16] (a) D. Tasis, N. Tagmatarchis, A. Bianco, M. Prato, *Chem. Rev.* **2006**, *106*, 1105-1136; (b) P. Singh, S. Campidelli, S. Giordani, D. Bonifazi, A. Bianco, M. Prato, *Chem. Soc. Rev.* **2009**, *38*, 2214-2230.

[17] (a) S. Mahouche Chergui, A. Ledebt, F. Mammeri, F. Herbst, B. Carbonnier, H. Ben Romdhane, M. Delamar, M. M. Chehimi, *Langmuir* **2010**, *26*, 16115-16121; (b) M. Adeli, E. Mehdipour, M. Bavadi, *J. Appl. Polym. Sci.* **2010**, *116*, 2188-2196; (c) G. M. Neelgund, A. Oki, *Appl. Catal. A-Gen.* **2011**, *399*, 154-160; (d) D. V. Jawale, E. Gravel, C. Boudet, N. Shah, V. Geertsen, H. Li, I. N. N. Namboothiri, E. Doris, *Catal. Sci. Tech.* **2015**, *5*, 2388-2392.

[18] (a) J. A. Sullivan, K. A. Flanagan, H. Hain, *Catal. Today* **2009**, *145*, 108-113; (b) J. Y. Kim, K. Park, S. Y. Bae, G. C. Kim, S. Lee, H. C. Choi, *J. Mater. Chem.* **2011**, *21*, 5999-6005.

[19] L. Rodríguez-Pérez, C. Pradel, P. Serp, M. Gómez, E. Teuma, *ChemCatChem* **2011**, *3*, 749-754.

[20] E. Kim, H. S. Jeong, B. M. Kim, *Catal. Commun.* **2014**, *46*, 71-74.

[21] M. R. Nabid, Y. Bide, S. J. Tabatabaei Rezaei, *Appl. Catal. A-Gen.* **2011**, *406*, 124-132.

[22] (a) J. M. J. Fréchet, D. A. Tomalia, *Dendrimers and Other Dendritic Polymers*, John Wiley & Sons, Ltd, UK, **2001**; (b) G. R. Newkome, C. N. Moorefield, F. Voegtle, *Dendrimers and Dendrons: Concepts, Syntheses, Applications*, Wiley-VCH Verlag GmbH & Co. KGaA, Weinheim, Germany, **2002**.

[23] (a) C. J. Hawker, J. M. J. Frechet, *J. Am. Chem. Soc.* **1990**, *112*, 7638-7647; (b) S. M. Grayson, J. M. J. Fréchet, *Chem. Rev.* **2001**, *101*, 3819-3868.

[24] (a) K. Esumi, A. Suzuki, A. Yamahira, K. Torigoe, *Langmuir* **2000**, *16*, 2604-2608; (b) K. Esumi, A. Suzuki, N. Aihara, K. Usui, K. Torigoe, *Langmuir* **1998**, *14*, 3157-3159.

[25] (a) R. M. Crooks, M. Zhao, L. Sun, V. Chechik, L. K. Yeung, *Acc. Chem. Res.* **2001**, *34*, 181-190; (b) M. Zhao, L. Sun, R. M. Crooks, *J. Am. Chem. Soc.* **1998**, *120*, 4877-4878; (c) L. Balogh, D. A. Tomalia, *J. Am. Chem. Soc.* **1998**, *120*, 7355-7356.

[26] (a) V. S. Myers, M. G. Weir, E. V. Carino, D. F. Yancey, S. Pande, R. M. Crooks, *Chem. Sci.* **2011**, *2*, 1632-1646; (b) L. M. Bronstein, Z. B. Shifrina, *Chem. Rev.* **2011**, *111*, 5301-5344; (c) I. J. Majoros, J. R. Baker, *Biological application of PAMAM dendrimer nanodevices in vitro and in vivo* in *Dendrimer-Based Nanomedicine*, CRC Press, Taylor & Francis Group, **2008**, pp. 175-207; (d) Y. Li, M. A. El-Sayed, *J. Phys. Chem. B* **2001**, *105*, 8938-8943; (e) E. H. Rahim, F. S. Kamounah, J. Frederiksen, J. B. Christensen, *Nano Lett.* **2001**, *1*, 499-501.

[27] (a) M. A. Herrero, F. M. Toma, K. T. Al-Jamal, K. Kostarelos, A. Bianco, T. Da Ros, F. Bano, L. Casalis, G. Scoles, M. Prato, *J. Am. Chem. Soc.* **2009**, *131*, 9843-9848; (b) S. Campidelli, C. Sooambar, E. Lozano Diz, C. Ehli, D. M. Guldi, M. Prato, *J. Am. Chem. Soc.* **2006**, *128*, 12544-12552.

[28] (a) D. A. Tomalia, B. Huang, D. R. Swanson, H. M. Brothers Ii, J. W. Klimash, *Tetrahedron* **2003**, *59*, 3799-3813; (b) B. Huang, D. A. Tomalia, *J. Lumin.* **2005**, *111*, 215-223.

[29] (a) Z. Syrgiannis, V. La Parola, C. Hadad, M. Lucío, E. Vázquez, F. Giacalone, M. Prato, *Angew. Chem. Int. Ed.* **2013**, *52*, 6480-6483; (b) Z. Syrgiannis, A. Bonasera, E. Tenori, V. La Parola, C. Hadad, M. Gruttadauria, F. Giacalone, M. Prato, *Nanoscale* **2015**, *7*, 6007-6013.

[30] (a) B. Iskin, G. Yilmaz, Y. Yagci, *Chem. Eur. J.* **2012**, *18*, 10254-10257; (b) N. D. Luong, L. H. Sinh, L.-S. Johansson, J. Campell, J. Seppälä, *Chem. Eur. J.* **2015**, *21*, 3183-3186; (c) G. Temel, M. Uygun, N. Arsu, *Polym. Bull.* **2013**, *70*, 3563-3574; (d) X. H. Yang, J. W. Guo, S. Yang, Y. Hou, B. Zhang, H. G. Yang, *Journal of Materials Chemistry A* **2014**, *2*, 614-619.

[31] R. Graupner, *J. Raman Spectrosc.* **2007**, *38*, 673-683.

[32] (a) S. Eriksson, M. Boutonnet, S. Järås, *Appl. Catal. A-Gen.* **2006**, *312*, 95-101; (b) V. Campisciano, V. L. Parola, L. F. Liotta, F. Giacalone, M. Gruttadauria, *Chem. Eur. J.* **2015**, *21*, 3327-3334.

[33] (a) M. Melle-Franco, M. Marcaccio, D. Paolucci, F. Paolucci, V. Georgakilas, D. M. Guldi, M. Prato, F. Zerbetto, *J. Am. Chem. Soc.* **2004**, *126*, 1646-1647; (b) G. M. A. Rahman, D. M. Guldi, E. Zambon, L. Pasquato, N. Tagmatarchis, M. Prato, *Small* **2005**, *1*, 527-530.

[34] (a) S. Xu, K. Song, T. Li, B. Tan, *Journal of Materials Chemistry A* **2015**, *3*, 1272-1278; (b) G. M. Scheuermann, L. Rumi, P. Steurer, W. Bannwarth, R. Mülhaupt, *J. Am. Chem. Soc.* **2009**, *131*, 8262-8270; (c) G. Xiang, J. He, T. Li, J. Zhuang, X. Wang, *Nanoscale* **2011**, *3*, 3737-3742; (d) S. Moussa, A. R. Siamaki, B. F. Gupton, M. S. El-Shall, *ACS Catalysis* **2012**, *2*, 145-154; (e) S.-i. Yamamoto, H. Kinoshita, H. Hashimoto, Y. Nishina, *Nanoscale* **2014**, *6*, 6501-6505.

[35] M. Gruttadauria, F. Giacalone, R. Noto, *Green Chem.* **2013**, *15*, 2608-2618.

[36] (a) N. T. S. Phan, M. Van Der Sluys, C. W. Jones, *Adv. Synth. Catal.* **2006**, *348*, 609-679; (b) M. B. Thathagar, J. E. ten Elshof, G. Rothenberg, *Angew. Chem. Int. Ed.* **2006**, *45*, 2886-2890.

[37] (a) J. L. Nallasivam, R. A. Fernandes, *Eur. J. Org. Chem.* **2015**, *2015*, 3558-3567; (b) Y. Lee, M. C. Hong, H. Ahn, J. Yu, H. Rhee, *J. Organomet. Chem.* **2014**, *769*,

80-93; (c) Y.-Y. Peng, J. Liu, X. Lei, Z. Yin, *Green Chem.* **2010**, *12*, 1072-1075; (d) L. Liu, W. Wang, C. Xiao, *J. Organomet. Chem.* **2014**, *749*, 83-87; (e) S. A. R. Mulla, S. S. Chavan, M. Y. Pathan, S. M. Inamdar, T. M. Y. Shaikh, *RSC Adv.* **2015**, *5*, 24675-24680; (f) P. Rajakumar, M. Gayatri Swaroop, S. Jayavelu, K. Murugesan, *Tetrahedron* **2006**, *62*, 12041-12050.

[38] (a) M. R. Nabid, Y. Bide, *Appl. Catal. A-Gen.* **2014**, *469*, 183-190; (b) L. Chen, S. Rangan, J. Li, H. Jiang, Y. Li, *Green Chem.* **2014**, *16*, 3978-3985; (c) M. Scheepstra, L. Nieto, A. K. H. Hirsch, S. Fuchs, S. Leysen, C. V. Lam, L. in het Panhuis, C. A. A. van Boeckel, H. Wienk, R. Boelens, C. Ottmann, L.-G. Milroy, L. Brunsveld, *Angew. Chem. Int. Ed.* **2014**, *53*, 6443-6448.

Chapter 3

Efficient Microwave-Mediated Synthesis of Fullerene Acceptors for Organic Photovoltaics

Part of this chapter has been published in RSC Adv. **2014**, *4*, 63200-63207.

3.1 Introduction

The continuous increase in the request of energy due to the ever-growing world energy consumption, led to the necessity of finding new alternative energy sources. The exploitation of renewable energy sources, such as solar energy, has become, today as never before, a fundamental research topic with a high priority. Solar energy is renewable, clean and so abundant as to be able to meet the word request of energy and for this reason many efforts have been made to develop solar cells with increasingly efficiency.

One of the parameters that establish the performance of a solar cell is the power conversion efficiency (PCE), namely the ratio of generated electricity to incoming solar energy.

Silicon-based solar cells are, currently, the most studied and performing systems available on the market with a PCE of 25% in the case of crystalline silicon and 10% for amorphous silicon ones.[1] On the other hand, the process of making of monocrystalline silicon based solar cells is very expensive and highly time-consuming. Therefore, the high initial cost of such solar cells can be absorbed only with the energy produced over the expected life of the panel. Moreover, the fragility of such solar cells should be take into account not only because the accidental breakage of silicon wafers lead to the loss of its activity, but also because they need to be mounted in a rigid frame making them unfavourable for building flexible devices. All the above-mentioned drawbacks related to the silicon-based photovoltaics modules, in addition to the environmental pollution during their fabrication process, focused research toward the development of alternative techniques.

Bulk heterojunction polymer solar cells (BHJ-PSCs) are characterized by many advantages such as low cost, easy fabrication, simple device structure, light weight and the possibility to use them into flexible devices. Therefore, it is not surprising if, in the last two decades, the organic photovoltaic (OPV) field has witnessed a very impressive momentum in terms of people engaged in and in terms of results.

After the first evidence for photoinduced electron transfer from a conjugated polymer to fullerene,[2] C_{60}-derivatives have been largely employed as n-type organic semiconductors due to their excellent electron-accepting capability.[3] Since then, a number of modified fullerenes have been tested in donor–acceptor BHJ-PSCs,[4] phenyl-C_{61}-butyric acid methyl ester [60]PCBM[5] and its C_{70} analogue, [70]PCBM[6] being the most widely studied (**Figure 1**).

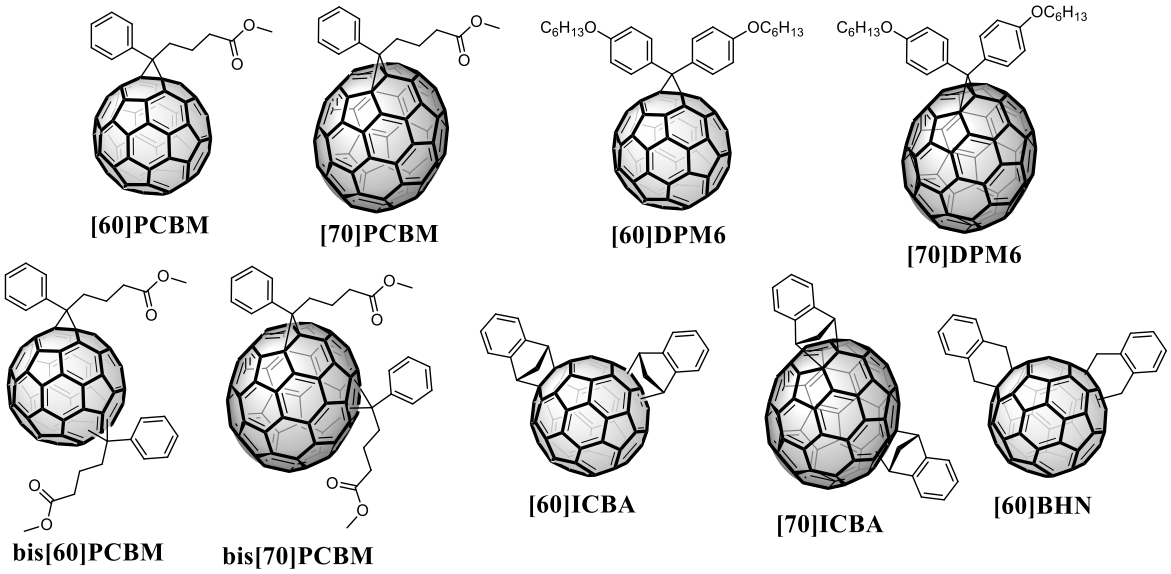

Figure 1. *Chemical structure of some of the most employed fullerene-acceptors for OPV.*

BHJ-PSCs are usually composed by an active layer, constituted of a mixture of a conjugated polymer donor, such as poly(3-hexylthiophene-2,5-diyl) (P3HT), and a fullerene C_{60}- or C_{70}-derivative acceptor sandwiched between two electrodes. Electrodes are constituted of a indium tin oxide (ITO) positive electrode modified with a polymer mixture of poly(3,4-ethylenedioxythiophene) and polystyrene sulfonate (PEDOT:PSS) and a low work function metal negative electrode. Some devices are also characterized by the presence of an additional interlayer on the top of the active layer. This interlayer, usually constituted of hydrophilic fullerene derivatives to avoid intermixing between the layers, acts as an hole blocking and electron selective layer to avoid charge recombination and to improve the performance of the solar cell (**Figure 2**).

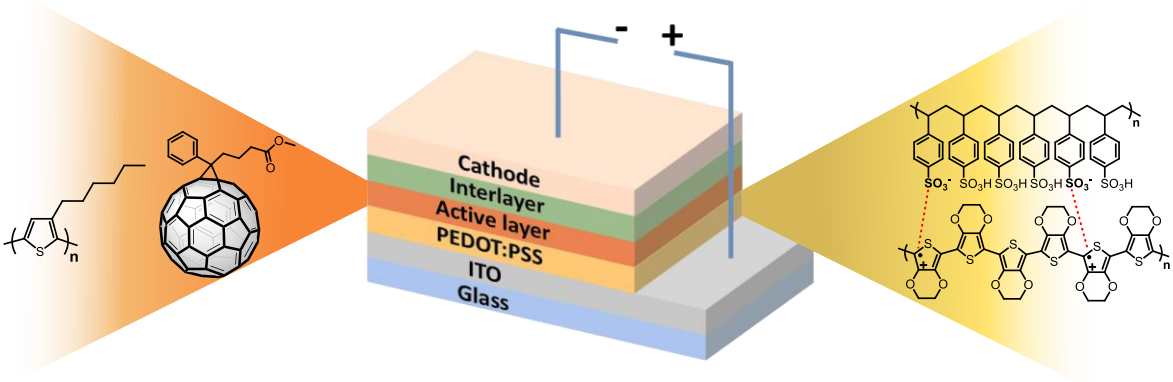

Figure 2. *Schematic representation of the structure of a BHJ-PSC.*

The working principle of a BHJ-PSC is based on photoinduced electron transfer from the

conjugated polymer donor to acceptor species. When the light reaches the photoactive layer through the transparent PEDOT:PSS-ITO electrode, the conjugated polymer donor absorbs photons with specific wavelengths causing the formation of excitons (bound electron-hole pairs). Excitons will move toward donor/acceptor interface where the lowest unoccupied molecular orbital (LUMO) electrons of the donor will be transferred to the LUMO of the acceptor giving rise to the charge separation. At this point, electrons will travel toward the metal cathode, while holes toward the ITO anode producing electric current. Furthermore, acceptor species can also absorb photons promoting a highest occupied molecular orbital (HOMO) electron in its LUMO level and producing an exciton. Charge separation will be produced transferring a hole from the HOMO of the acceptor to the HOMO of the donor (**Figure 3a**).

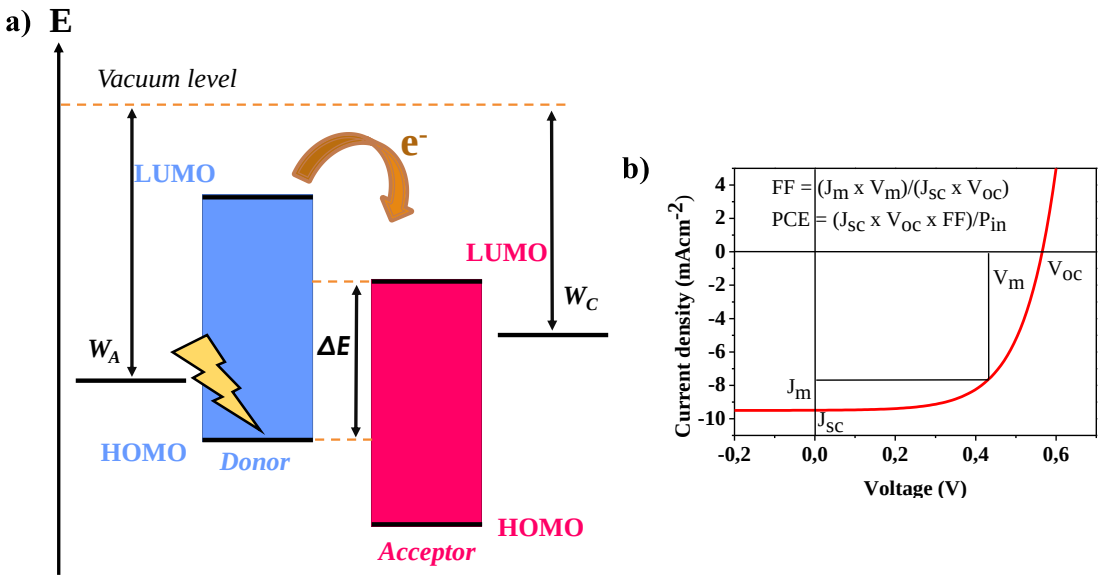

Figure 3. *a) Electronic energy levels of active layer blend and b) typical J-V curve of a BHJ-PSC.*

PCE of BHJ-PSCs is still lower than inorganic semiconductor solar cells, but continuous efforts are made for improving performances of such organic solar cells. Nowadays, the PCE of OPVs has been improved considerably and exceeded 10%.[7] Plotting of a J-V curve of a BHJ-PSC gives information about the PCE of such cell, directly related with short circuit current density (J_{sc}), open circuit voltage (V_{oc}) and fill factor (FF) of the device. Furthermore, J_m and V_m values, corresponding to the J and V values with the maximum J x V value on the J-V curve, are used in the calculation of the FF (**Figure 3b**).

The knowledge of how each of these parameters is influenced by the morphology of the blend active layer or by the nature of the donor and acceptor species is crucial for the fabrication of ever more efficient organic solar cells. In more detail, J_{sc} depends on the light

absorption ability of the active layer and exciton diffusion and dissociation at the donor/acceptor interface, as well as on the charge transportation toward electrodes and the subsequent charge collection. V_{oc} is mainly determined by level offset of the HOMO of the donor and the LUMO of the acceptor species (ΔE in the **Figure 3a**).[8] Therefore, relevant considerations must be made with regard to the optimization of such solar devices. First of all, a broad and strong light absorption of the active layer in the visible and near infrared region, as well as high charge mobility reached with an optimal morphology of the blend layer in which donor and acceptor species constitute an interpenetrating network, contribute to increase the J_{sc} value. Furthermore, the accurate choice of the donor and acceptor species is a key point not only to determine the V_{oc} value given by the energy level difference between the HOMO and LUMO levels of the donor and acceptor species respectively, but also to ensure exciton dissociation at the donor/acceptor interface.

Most used fullerene monoadducts, such as the above mentioned [60]PCBM and [70]PCBM but also [60]DPM and [70]DPM,[9] have a LUMO at a relatively low energy level, which gives rise to a small V_{oc} when P3HT is used as donor species. The introduction of electron-donating groups in the fullerene acceptor species, as well as the use of bisadducts of fullerene, lead to an increase of the LUMO energy level.[10] In this regard, it has been shown that the further functionalization of fullerene to reach production of bisadducts does not have a great influence on the charge-carrier properties of the fullerene and moreover the isomer mixture of bisadducts can be directly used giving rise to cells with greater performances than those constituted by corresponding monoadducts.[10-11] Another important feature of bisadducts is their higher solubility in common organic solvents compared to corresponding monoadducts.[12] This improved solubility may ensure a better morphology of the blend film, which constitutes an important factor in the PSCs fabrication.[13] Among the fabrication technologies developed for the production of PSCs, solution process such as spin-coating is surely the most popular. This process require a good solubility of the donor and acceptor species of the photovoltaic device to ensure a good morphology and a uniform coating. Moreover, in an attempt to further reduce the fabrication costs, other technologies for the manufacturing of PSCs are developed such as the printing/coating based processes, namely roll-to-roll printing, inkjet printing, screen printing, brush painting and spray coating.[14]

Recently, novel C_{60} bisadducts such as [60]BHN (bishydronaphthyl-C_{60})[12d, 15] and [60]ICBA (indene-C_{60} bisadduct)[16] emerged as key acceptors in high performing BHJ-PSCs. Nevertheless, taking advantage of two decades of optimization in OPV, [60]PCBM and [70]PCBM are still able to afford tandem devices with outstanding power conversion

efficiencies in the 6.0–10.6% range.[7, 17]

However, in order to ensure a large-scale diffusion of PSCs, it is necessary to have a facile and convenient access to all substances employed in the fabrication of such solar cells. It was estimated that the active layer (mixture of conjugated polymer donor and fullerene-derivative acceptor) contributes to over 25% of the total material cost for the fabrication of PSCs (**Figure 4**).[18]

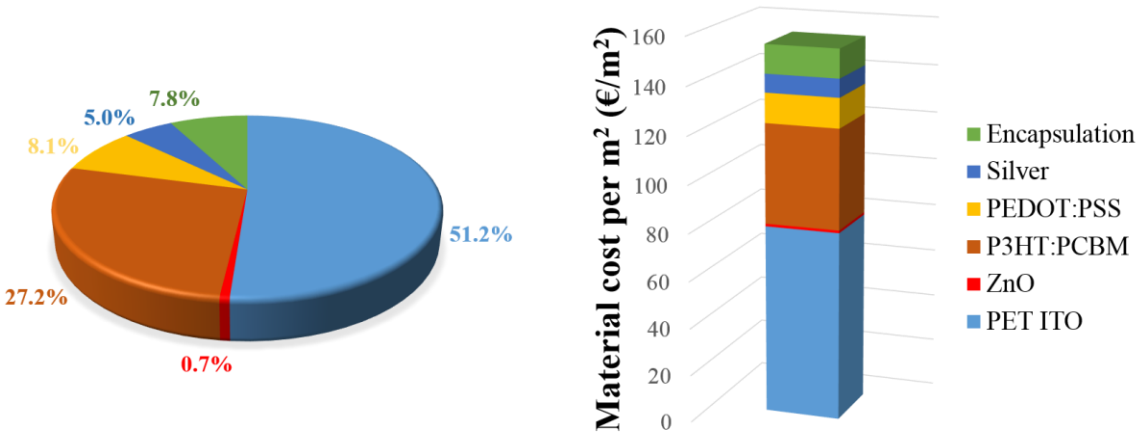

Figure 4. *Estimation of the material cost of a PSC.*[18]

Especially regarding the synthesis of different acceptor species, one of the main drawback in the synthesis of fullerene derivatives is that the reported examples show from low to moderate yields often below 40% and/or long reaction time, which in several cases reach up to 72 h.[11, 12d, 15a, b, 16e, 19] These weak points strongly contribute to a higher final price for the fullerene acceptors and led to address many efforts toward the synthesis optimization of such acceptor species.

Recently, using a continuous flow approach, various fullerene derivatives acceptors, namely [60]PCBM, [70]PCBM, [60]ICBA and [70]ICBA, were synthesized via cycloaddition reactions.[20] By varying experimental parameters, such as residence time, temperature, and equivalents of cycloaddition reagents, acceptor species were obtained in improved yields and in a shorter reaction time in comparison with conventional batch processes. The results obtained were very promising; [60]PCBM, [70]PCBM, [60]ICBA and [70]ICBA were obtained in 59, 49, 54 and 49% conversion (determined via HPLC) respectively, opening the way for the large-scale production of such fullerene derivatives. However, this approach

requires the use of very specific micro-flow reactors setup that may be not available in all laboratories.

Conversely, nowadays the use of microwave irradiation in organic synthesis, which was introduced about thirty years ago by Gedye and by the group of Giguere and Majetich,[21] has become a common use technique applied in almost all laboratories as an alternative to conventional heating processes to carry out a large number of reactions in different fields of chemistry.[22]

The so-called microwave-assisted organic synthesis (MAOS) is an ever-growing field owing to its many benefits.[23] There are many examples reported in the literature in which the use of microwave irradiation led to a drastic reduction of reaction time, an improving of yields and a diminishing of side reactions.[24] Furthermore, an interesting approach to MAOS consists in the possible use of solvent-free conditions.[24a, 24d, 25] The absence of solvent to carry out chemical transformations under MW irradiation is a good method to optimize efficiency (in this case, absorption of MW radiation is limited only to reactants) and simplify clean procedures of such chemical reactions.

In the light of these considerations, microwave mediated functionalization of fullerenes, and more in general of carbon nanoforms (CNFs), which interact strongly with microwaves,[26] may overcome the problem of both productivity and efficiency in terms of reaction time.

First examples on use of microwave irradiation for functionalization of fullerenes are due to Langa and Martín.[27] Their works showed, through a direct comparison, as microwave irradiation was more efficient than conventional conductive heating to perform various chemical functionalizations in a shorter time and in improved yield.

3.2 Aim of the Chapter

Taking into account the above, herein simple and very efficient synthetic procedures based on MW irradiation were optimized in order to obtain mono-, bis-, and tris-adducts of the most common C_{60}- and C_{70}-derivatives, namely PCBM, DPM6, BHN and ICBA, employed in OPV in good yields and in a short time.[28] Results obtained in terms of yields are in almost all cases the best reported so far.

3.3 Results and Discussion

The first process to be investigated was the modified Bamford–Stevens reaction for the synthesis of [60]PCBM and [70]PCBM mono-, bis- and trisadducts (**Scheme 1**), firstly reported by Hummelen and Wudl.[29]

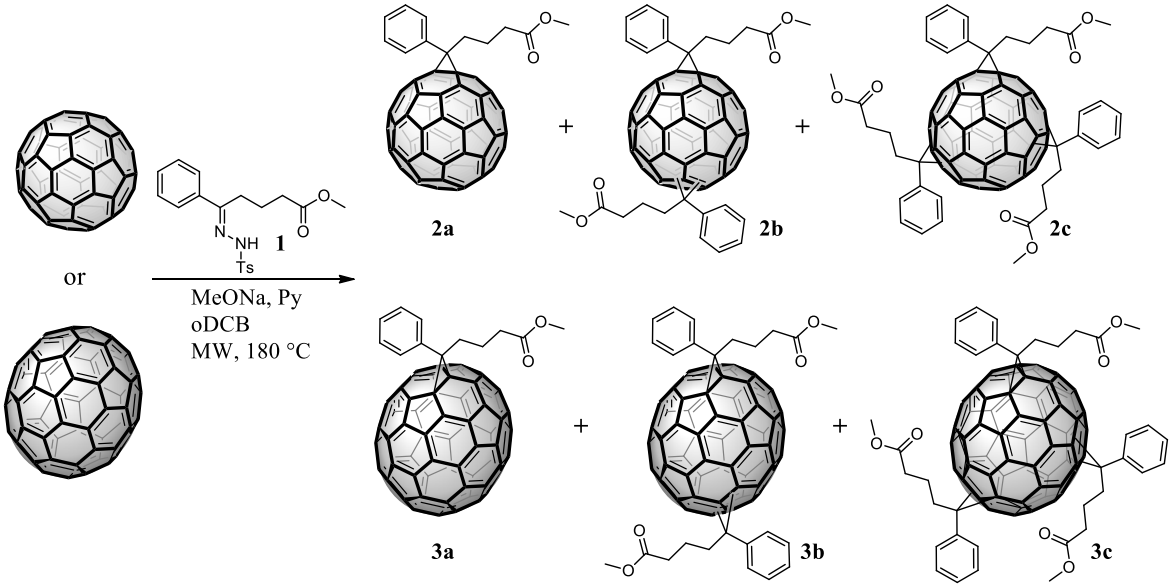

Scheme 1. *Synthesis of PCBM derivatives.*

This procedure involves the base-induced decomposition of a tosylhydrazone derivative to achieve the *in situ* generation of a diazo compound that readily reacts with fullerene by means of a [3+2] cycloaddition that occurs at a [6,6] double bond, giving rise to a pyrazoline intermediate. After the subsequent N_2 extrusion, the title transformation leads to the formation of both [6,6]-closed methanofullerene and [5,6]-open fulleroid stereoisomers (**Scheme 2**), being the latter the kinetically favoured and the former the most stable.[30]

Table 1. *Conditions optimization for the synthesis of* ***2a–c*** *and* ***3a–c****.*[a]

Entry	C_x	$1/C_x$	Mono[b]-(%)	Bis[b]-(%)	Tris[b]-(%)
1	C_{60}	0.66	65	27	<5
2	C_{60}	2.5	29	37	20
3	C_{60}	3.0	22	43	31
4	C_{60}	4.0	5	36	47
5	C_{70}	0.66	83	14	–
6	C_{70}	1.0	48	23	–
7	C_{70}	3.0	3	50	44

[a] Reaction conditions: 50 mg of fullerene, and the indicated amount of tosylhydrazone **1** (after conversion in the corresponding diazoderivative with MeONa in dry pyridine) were stirred under microwave irradiation (48 W) for 1 h at 180 °C. [b] Isolated yield.

The key factor for the right outcome of the reaction is the tosylhydrazone **1**/fullerene ratio, which will direct the process toward the preferential formation of the monoadduct or to the bis- and trisadducts, and the temperature at which the reaction is carried out. In this regard, usually the rearrangement of the [5,6]-open to the [6,6]-closed form can be achieved by means of photochemical irradiation[6e, 31] or by thermal treatment in refluxing 1,2-dichlorobenzene (oDCB) for several hours.[30, 32] In **Table 1**, the microwave-mediated optimization of the synthesis of PCBM derivatives is reported.

The reaction was carried out in oDCB at 180 °C with the aim to work under thermodynamic control and concomitantly pursue the isomerization of the [5,6]-open isomer possibly produced (**Scheme 2**).

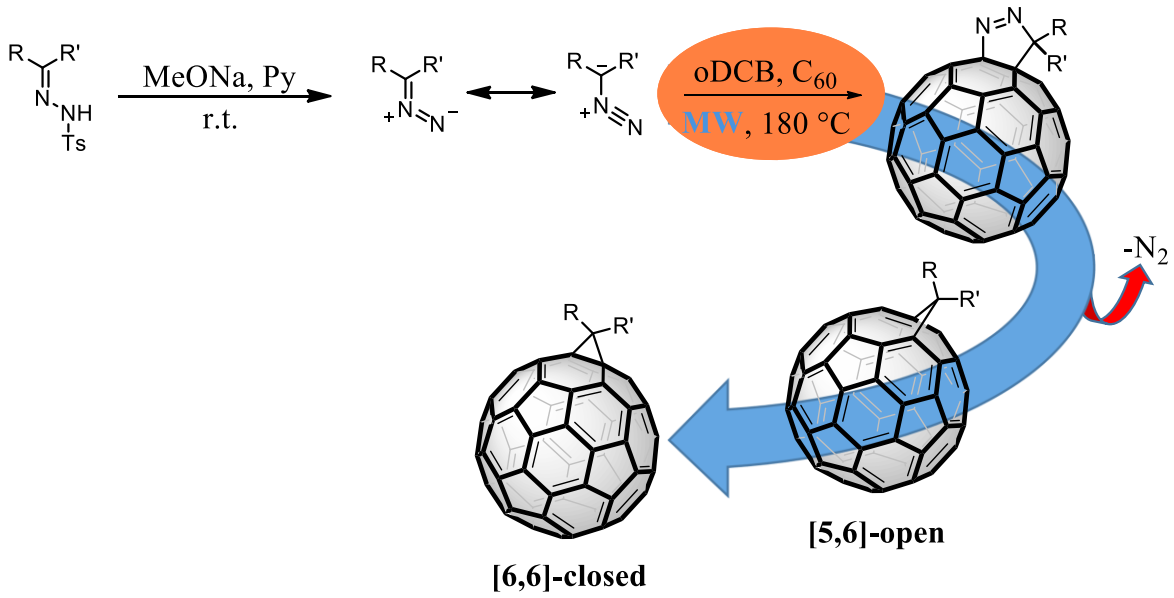

Scheme 2. *Synthetic route of a diazo derivative, its reaction with C_{60} and subsequent in situ isomerization of the [5,6]-open fulleroid in the [6,6] closed fullerene adduct under microwave irradiation.*

The microwave oven (closed vessel CEM DISCOVER monomode system in manual mode with no pressure control) was set to 180 °C, temperature reached within 2 minutes and an observed power of 150 W. Afterwards, the oven kept the above temperature automatically supplying 100 W, which in 30 minutes decreased to a constant power supply of 48 W. To our delight, 1 hour is sufficient to the reaction smoothly proceed to the excellent formation of [60]PCBM **2a** with a 65% yield when **1**/C_{60} ratio of 0.66 is employed (**Table 1**, entry 1). To our knowledge, this is the highest yield reported so far, being the precedent value 59% obtained under continuous flow conditions (conversion determined by HPLC, isolated yield 35%).[20b] It is worth to note that ^{1}H and ^{13}C NMR spectra confirmed the exclusive presence

of [6,6]-closed form (**Figure 5**).

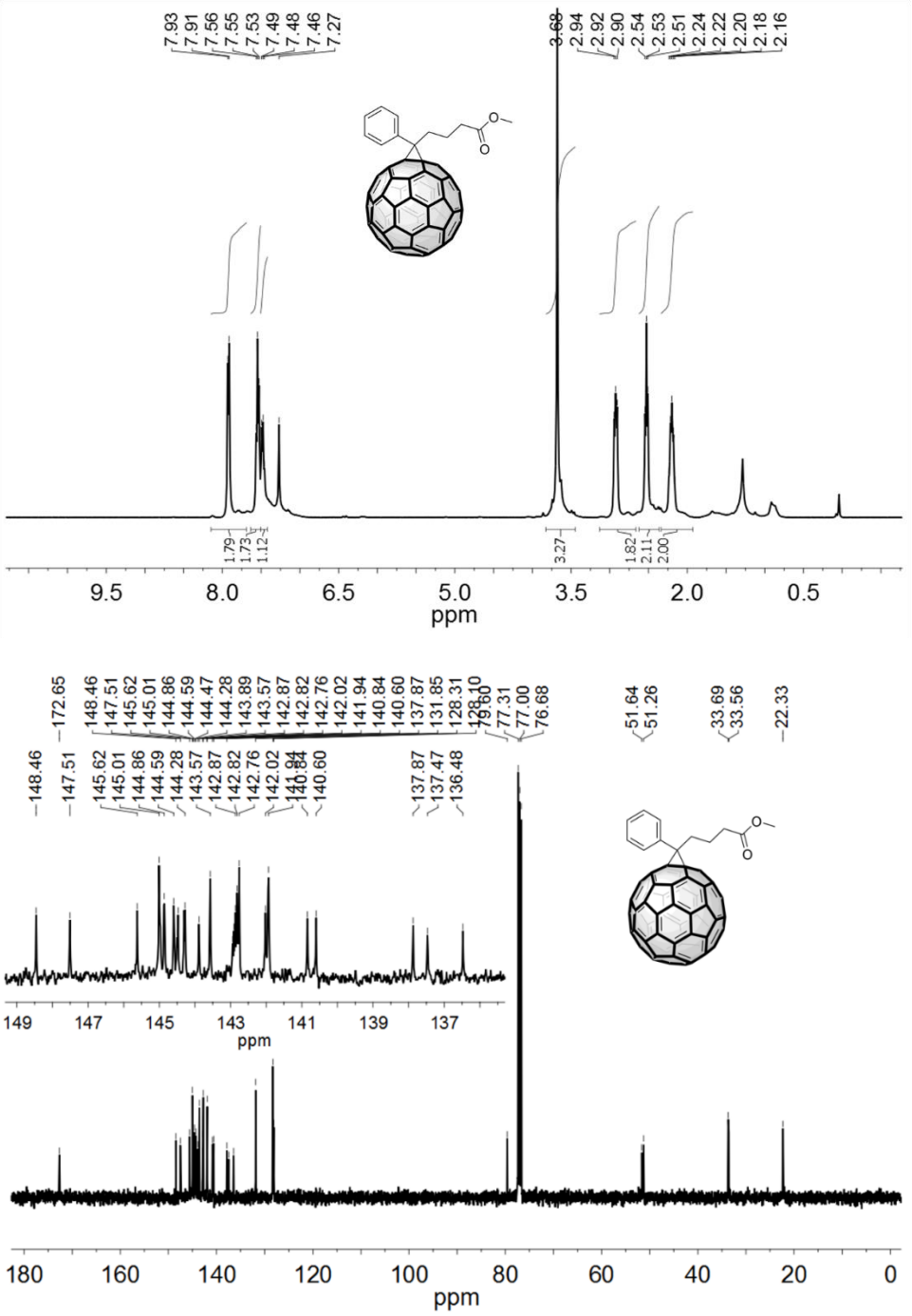

Figure 5. *^{1}H (top) and ^{13}C NMR (bottom) in $CDCl_3$ of compound **2a**, showing the exclusive presence of the [6,6]-closed form. Spectroscopic data are in agreement with those reported in literature.*[19c]

Hence, tosylhydrazone **1**/fullerene ratio was varied in order to maximize the production of bisadducts **2b** and trisadducts **2c** (entries 2–4).

Interestingly, when the ratios were >2.5 the fullerene conversion was complete affording, in the case of **1**/C_{60} ratio 3, **2b** in 43% yield (**Table 1**, entry 3) and **2c** in 47% yield when the

ratio was 4 (**Table 1**, entry 4). Unfortunately, in the literature bis- and trisadducts yields are not reported since they are collected as "byproducts" of the synthesis of [60]PCBM, however these obtained represent very good values taking into account that even higher adducts could be produced during the process.

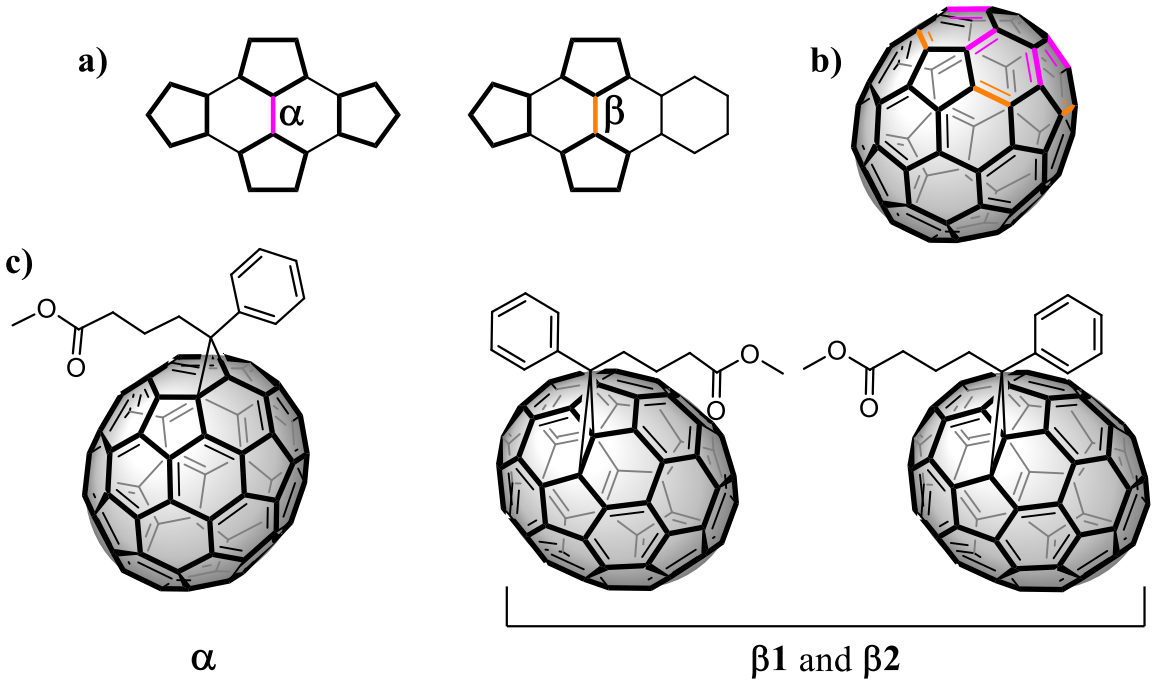

Figure 6. *a) The most curved fullerene bonds, b) their location in the fullerene C_{70} and c) the structure of the possible isomers.*

Finally, also the syntheses of [70]PCBM **3a** and bis [70]PCBM **3b** was optimized (entries 5–7). In the former case, the **1**/C_{70} ratio of 0.66 led to the outstanding yield of 83% for **3a** which is unprecedented (**Table 1**,entry 5; the previous record was 59%).[6e]. Differently from C_{60}, which possess a single kind of [6,6] bond, [70]fullerene has four different [6,6] bonds with different reactivity based on the local spheroid curvature of the fullerene C_{70}. The most strained fullerene bonds, type α, are located near at the poles surrounded by less strained type β bonds (**Figure 6a-b**). The flatter and less curved equatorial region of fullerene C_{70} contains the less curved and then less reactive bonds.[33] In such a way, the reaction of the different bonds give rise to different isomers.

^{1}H NMR spectrum of monoadduct **3a** (**Figure 7**) revealed the presence of three isomers of [70]PCBM in a 9/80/11 ratio for α, β1 and β2 (**Figure 6c**), respectively as indicated by the methoxy groups signals at 3.75, 3.68, and 3.52 ppm.

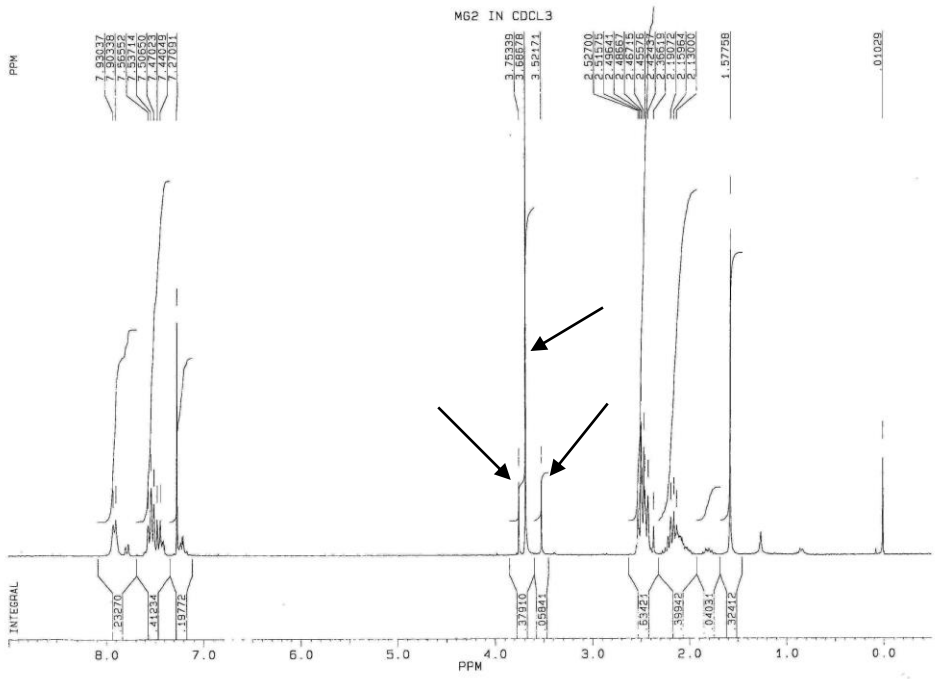

Figure 7. *^{1}H NMR spectrum of compound **3a** in $CDCl_3$ (250 MHz)*

Total conversion and a substantially equal distribution of **3b** and **3c** are achieved with **1**/C_{70} ratio of 3.0 (**Table 1**, entry 7).

The general applicability of the microwave-mediated protocol for the Bamford–Stevens reaction was checked through the synthesis of the series of diphenylmethanofullerene-derivatives with the hexyloxy-chains (DPM6 – **Scheme 3**).

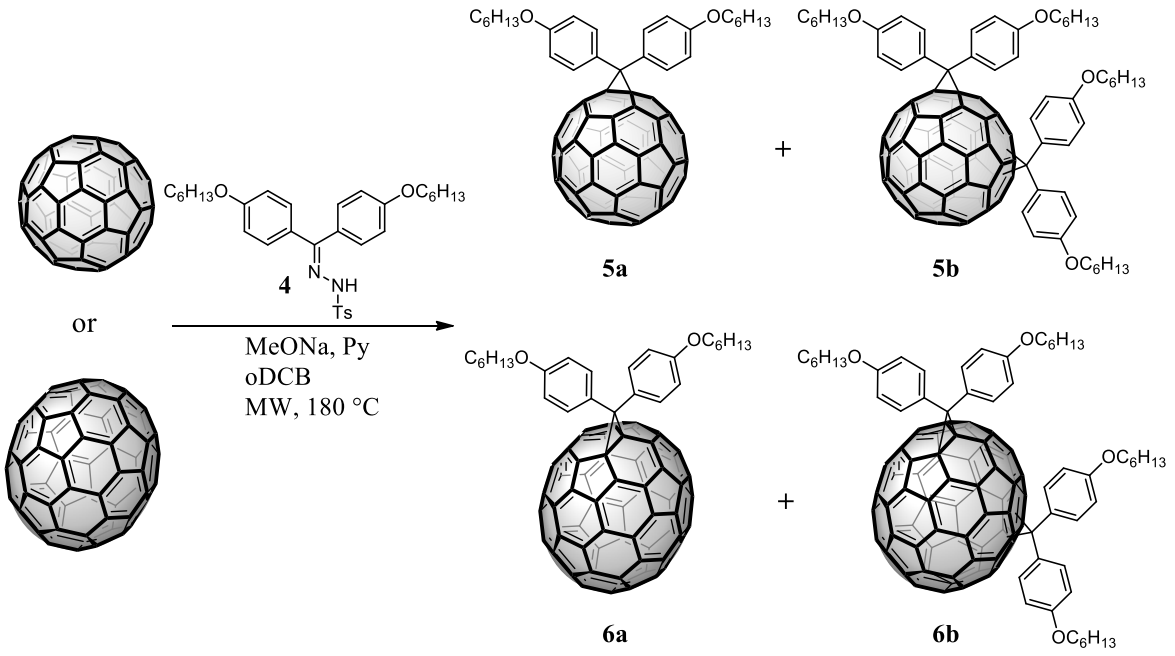

Scheme 3. *Synthesis of DPM6 derivatives.*

This class of acceptors is of interest due to higher V_{oc} showed by the devices in which they are employed in the active layer in comparison with those containing PCBM derivatives.[9a] In **Table 2**, the microwave-mediated optimization of the synthesis of DPM6 derivatives is reported. The same conditions used for PCBM derivatives were applied also for DPM6, generally resulting in a minor conversion to the products.

Table 2. *Conditions optimization for the synthesis of* ***5a–b*** *and* ***6a–b****.*[a]

Entry	C_x	4/C_x	Time (h)	Mono[b]-(%)	Bis[b]-(%)
1	C_{60}	0.66	1	40	<3
2	C_{60}	0.66	1 + 1	48	16
3	C_{60}	2.0	1	25	45
4	C_{60}	4.0	1	30	41
5	C_{60}	4.0	1 + 1	26	61
6	C_{60}	4.0	1 + 1 + 1	28	59
7	C_{70}	0.66	1 + 1	57	2
8	C_{70}	4.0	1 + 1	19	50
9	C_{70}	4.0	1 + 1 + 1	27	59

[a] Reaction conditions: 50 mg of fullerene, and the indicated amount of tosylhydrazone **4** (after conversion in the corresponding diazoderivative with MeONa in dry pyridine) were stirred under microwave irradiation (55 W) for the indicated time at 180 °C. [b] Isolated yield.

This finding is clearly reflected in the case of a **4**/C_{60} ratio of 0.66 which gave rise to a conversion of 42% (yield of **5a** 40%) after 1 h of irradiation at 180 °C whereas for the PCBM the conversion was >92% (compare **Table 2**, entry 1 with **Table 1**, entry 1). Once again, the exclusive presence of [6,6]-closed form can be confirmed by ^{1}H and ^{13}C NMR spectra. An increase in the irradiation time to 2 h resulted in an enhanced conversion with 48% yield for **5a** (**Table 2**, entry 2). On the other hand, in order to maximize the yield of **5b**, **4**/C_{60} ratio as well as reaction time was varied (**Table 2**, entries 3–6).

Interestingly, in none of these reaction trisadducts were produced above 5%, likely due to the bulkiness of DPM substituent. An increase in the reaction time from 1 to 2 h had a remarkable effect on the yield of [60]DPM6 bisadducts (from 41 to 61%) when a **4**/C_{60} ratio of 4.0 was used (**Table 2**, entries 4 and 5). A more prolonged reaction time had no additional beneficial effect (**Table 2**, entry 6). Applying the best conditions found for **5a**, [70]DPM6 **6a** was synthesized in 57% of yield being the two isomers α and β in a 9/1 ratio (**Table 2**, entry 7), whereas 3 h of irradiation led to the best results for [70]DPM6 bisadducts **6b**, which was obtained in 59% yield (**Table 2**, entry 9).

Microwave-assisted Diels–Alder [4 + 2] cycloadditions were the first transformations investigated for fullerenes with the help of microwave irradiation.[27a, 27e, 34] As stated, recently C_{60} and C_{70} bisadducts such as [60]BHN (bishydronaphthyl-C_{60})[12d, 15a, b] and [60]ICBA (indene-C_{60} bisadduct),[16] prepared through [4 + 2] cycloadditions, attracted the

interest as novel acceptor materials for OPV due to their excellent performances in terms of PCE. Hence, the attention was focused on the optimization of BHN-derivatives synthesis employing the sultine **7** as ideal precursor of the o-quinodimethane intermediate **7'**, since it decomposes with chelotropic extrusion of sulfur dioxide at around 80 °C, not producing additional organic or inorganic byproducts (**Scheme 4**).

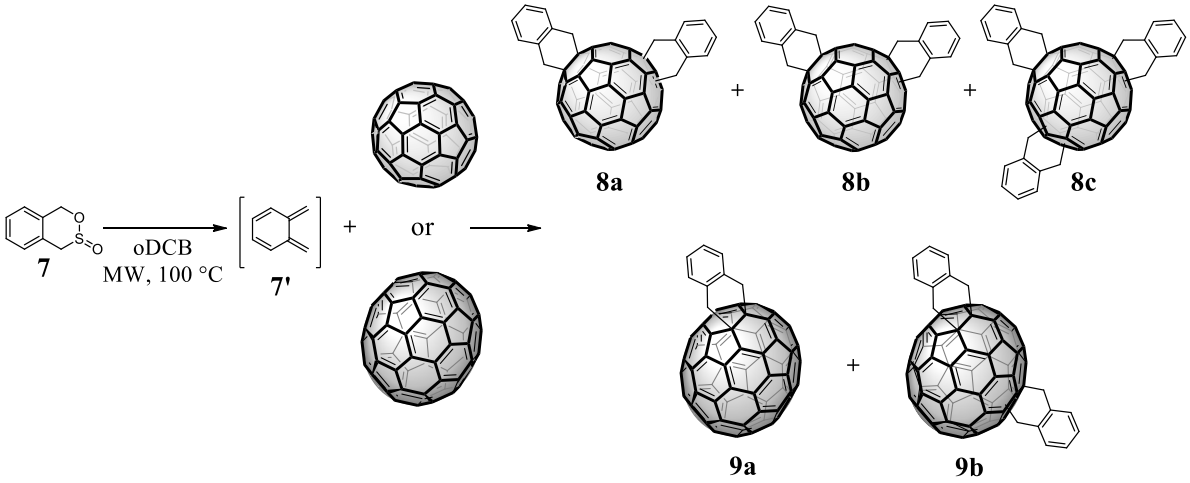

Scheme 4. *Synthesis of BHN derivatives.*

Initially, a **7**/C_{60} ratio equal to 3 has been chosen, using oDCB as solvent and the temperature was set to 100 °C leaving the reaction for 1 h (**Table 3**, entry 1).

Table 3. *Conditions optimization for the synthesis of **8a–b** and **9a–b**.*[a]

Entry	C_x	7/C_x	(W/°C)	Mono[b]-(%)	Bis[b]-(%)	Tris[b]-(%)
1	C_{60}	3.0	7/100	38	54	5
2	C_{60}	3.0	10/130	32	58	7
3	C_{60}	4.0	7/100	18	63	16
4	C_{70}	4.0	7/100	29	68	1

[a] Reaction conditions: 50 mg of fullerene, and the indicated amount of sultine **7** were stirred under microwave irradiation for 1 h at 100 °C. [b] Isolated yield.

Under these conditions, an equilibrium power of 7 W was reached which was sufficient to afford the total conversion of fullerene, giving rise to a yield of 54% for the desired bis-adduct **8b**. Raising the temperature to 130 °C just had a marginal beneficial effect on the yield of **8b** (**Table 3**, entry 2), whereas a **7**/C_{60} ratio of 4 allowed to obtain a remarkable yield of 63% (**Table 3**, entry 3). This value is exactly the same obtained by us carrying out the reaction under classical thermal conditions in refluxing toluene for 15 h that slightly differs from the 72% reported (conversion determined by HPLC).[15a]

Hence, the same conditions were successfully applied in the synthesis of the C_{70} analogue **9b** achieving the outstanding yield of 68% (**Table 3**, entry 4), higher than the best reported

value (64%).[19a]

Finally, by means of microwave-assisted [4 + 2] Diels–Alder cycloadditions, the syntheses of ICBA-derivatives reacting fullerenes and *in situ* thermally converted isoindene **10'** was optimized (**Scheme 5**).

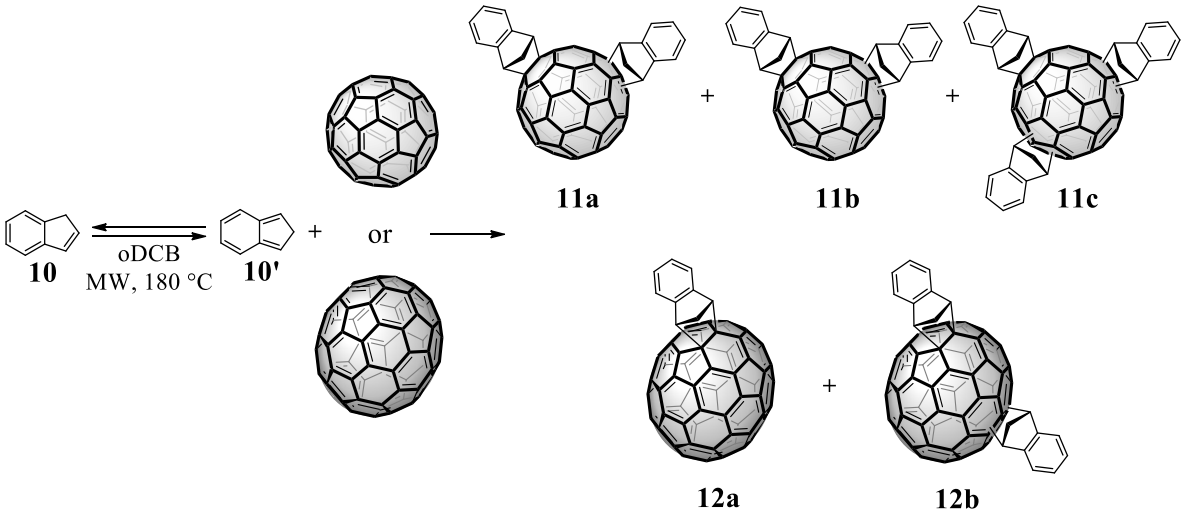

Scheme 5. *Synthesis of ICBA derivatives.*

Differently from the reactions previously investigated, ICBA-derivatives require higher indene/fullerene ratio (10–36 equivalents). In our case, adopting a **10**/C_{60} ratio of 12 in oDCB at 180 °C irradiating for 1 h, resulted in the formation of 49% of monoadduct **11a** (**Table 4**, entry 1), which has not utility in OPV due to its scarce solubility.

Table 4. *Conditions optimization for the synthesis of **11a–b** and **12a–b**.*[a]

Entry	C_x	10/C_x	Time (h)	Mono[b]-(%)	Bis[b]-(%)	Tris[b]-(%)
1	C_{60}	12	1	49	29	–
2	C_{60}	24	1	36	54	<5
3	C_{60}	24	1 + 1	11	62	24
4	C_{60}	36	1	18	61	18
5	C_{60}	36	0.75 + 0.75	9	58	29
6	C_{60}	36	1 + 1	7	52	33
7	C_{70}	36	1	40	40	–
8	C_{70}	36	1 + 1	35	62	–
9	C_{70}	36	1 + 1 + 1	38	50	9

[a] Reaction conditions: 50 mg of fullerene, and the indicated amount of indene **10** were stirred under microwave irradiation (25 W) for the indicated time at 180 °C. [b] Isolated yield.

Then, the use of 24 equivalents irradiated for 1 h led to an improved yield in **11b** (54%), even though the not complete conversion of C_{60} (**Table 4**, entry 2) suggested the possibility to irradiate for a longer time. Hence, 2 h of irradiation had a beneficial effect both on the total conversion as well as in the yield of [60]ICBA, which reached the remarkable value of

62% with the concomitant decrease to 11% of yield for the monoadduct (**Table 4**, entry 3). Almost the same result gave the employment of 36 equivalents of indene irradiated for 1 h (**Table 4**, entry 4), whereas no improvements were achieved with longer reaction times (**Table 4**, entries 5 and 6). On the contrary, with a **10**/C_{70} of 36, 2 h of reaction was found as optimum for obtaining a 62% yield of [70]ICBA **12b** (**Table 4**, entries 7–9). It is worth to note that, once again, for bisadduct **11b** and **12b**, the yields obtained are the higher reported so far, being the previous 54%[20b] and 58%,[16c] respectively. It is worth to note that under solvent-free conditions the reaction was hard to control, giving rise to a mixture of higher adducts. Probably the presence of a solvent able to partially absorb microwaves and to transfer the heat (tan δ oDCB: 0.28[35]), helps to have a better control on the reaction.

3.4 Conclusions

In conclusion, [4 + 2] Diels Alder cycloaddition and, for the first time, modified Bamford–Stevens reaction, were optimized under microwave irradiation for the functionalization of fullerenes. Such protocols were applied to the improved synthesis of C_{60}- and C_{70}-based acceptor derivatives for OPV such as PCBM, DPM, BHN and ICBA (mono-, bis-, and in some case trisadducts). In almost all cases the acceptors were obtained in high yields (48–82% range), which were increased or at least paired with respect to those reported in literature. One of the main advantages of the reported microwave-assisted protocols is that often the complete fullerene conversion is achieved within 1–3 hours, sensibly less than the reaction times required under classical conditions (16–72 h), and with high selectivity toward the target acceptor. Thus, the higher yields of a selected acceptor are accompanied by a less waste production (side products) and a sensitive energy and time saving. As a whole, acceptors molecules can be produced with strong cost abatement, which will represent a step forward toward the wide production of cheaper organic solar cells.

3.5 Experimental Section

General: Chemicals and solvents were purchased from commercial suppliers or purified by standard techniques. For thin-layer chromatography (TLC), silica gel plates (Merck 60 F254) were used and compounds were visualized by irradiation with UV light and/or by treatment with a $KMnO_4$ solution. Flash chromatography was carried out using Macherey–Nagel silica gel (0.04–0.063 mm). MW-assisted syntheses were carried out with a CEM DISCOVER monomode system in closed vessel in manual mode (no remote PC control) with infrared sensor for temperature control and with no pressure control. Petroleum ether refers to the fraction with the boiling range 40–60 °C. ^{1}H and ^{13}C NMR spectra were recorded with a Bruker 250, Bruker 300 MHz or Bruker Avance II 400 MHz spectrometers. HRMS spectra were recorded on $MeOH/CH_2Cl_2$ or in CH_2Cl_2 with a Waters Q-TOF Premier, with atmospheric pressure chemical ionization (APCI) as ion source.

- ***Synthesis of [70] and [60]PCBM derivatives***

Synthesis of methyl 4-benzoylbutyrate. This compound was prepared on 5 g scale starting from 4-benzoylbutyric acid and MeOH using HCl gas, following a procedure previously reported in literature.[32a] Methyl 4-benzoylbutyrate was obtained as a colourless oil (yield: 88%).

Synthesis of methyl 4-benzoylbutyrate p-tosylhydrazone (1). Methyl 4-benzoylbutyrate (4.5 g, 21.8 mmol) and p-toluenesulfonyl hydrazide (5.0 g, 1.2 eq) were placed in a round bottom flask and methanol was added (15 mL). The mixture was stirred and refluxed for 6 h and then stirred overnight at room temperature and lastly cooled to -15 °C. The product was collected by filtration, washed with cold methanol and dried under vacuum to obtain 4-benzoylbutyrate p-tosylhydrazone as white crystals (yield: 92 %).

General procedure for preparation of 1-phenyl-1-(3-(methoxycarbonyl)propyl)-diazomethane. Sodium methoxide (3.73 mg, 0.069 mmol) was added in a microwave glass tube sealed with a teflon cap containing a solution of 4-benzoylbutyrate p-tosylhydrazone **1** (17.20 mg, 0.046 mmol) in dry pyridine (2 mL). The mixture was stirred at room temperature for 15 minutes.

Synthesis of PCBM derivatives (2a-c, 3a-c). A solution of C_{60} or C_{70} (50.00 mg) in 3 mL of oDCB (previously sonicated for about 15 minutes) was added to a previously prepared mixture containing the appropriate quantity of 1-Phenyl-1-(3-(methoxycarbonyl)propyl)diazomethane in dry pyridine. The resulting mixture was kept under MW irradiation at 180 °C (48 W) for appropriate time. After cooling down, pyridine was removed under vacuum and the remaining reaction mixture was directly poured into a chromatographic column without removal of the remaining solvent (silica gel column conditions for C_{60}-derivatives: 3:1 hexane/toluene up to 9:1 toluene/hexane for monoadduct recovery, then dichloromethane for bisadducts. Column conditions for C_{70}-derivatives: 3:1 hexane/toluene up to 2:1 toluene/hexane for monoadduct recovery, then dichloromethane for bisadducts recovery). Both mono- and bis-adducts were solubilized and transferred to a centrifuge tube using a minimal amount of chloroform and subsequently precipitated with methanol. (**2a**) ^{1}H NMR (400 MHz, $CDCl_3/CS_2$) δ: 7.92 (d, *J* = 7.2 Hz, 2H; o-H arom), 7.55 (t, *J* = 7.3 Hz, 2H; m-H arom), 7.51-7.41 (m, 1H; p-H arom), 3.68 (s, 3H; O***C***H_3), 2.92 (t, *J* = 7.3Hz, 2H; PhC***C***H_2), 2.53 (t, *J* = 7.3 Hz, 2H; ***C***H_2CO_2Me), 2.20 (q, *J* = 7.3 Hz, 2H; ***C***$H_2CH_2CO_2Me$). ^{13}C NMR (100 MHz, $CDCl_3/CS_2$) δ: 172.65 (***C***=O), 148.46, 147.51, 145.62, 145.01, 144.86, 144.59, 144.50, 144.47, 144.30, 144.28, 143.89, 143.57, 142.94, 142.91, 142.87, 142.82, 142.76, 142.02, 141.94, 140.84, 140.60, 137.87, 137.47, 136.48, 131.85, 128.31, 128.10, 79.60 (C_{60} sp^3), 51.64 (O***C***H_3), 51.26 (Ph***C***CH_2), 33.69, 33.56 (PhC***C***H_2 and ***C***H_2CO_2Me), 22.33 (***C***$H_2CH_2CO_2Me$). HRMS calculated: 933.0891; found: 933.2404 $[M\text{-}Na]^+$. (**2b**) ^{1}H NMR (400 MHz, $CDCl_3$) δ: 8.24-7.31 (m, 10H; H arom), 3.81-3.52 (m, 6H; O***C***H_3), 3.23-1.85 (m, 12H; PhC***C***H_2, ***C***H_2CO_2Me and ***C***$H_2CH_2CO_2Me$). HRMS calculated: 1123.1885; found: 1123.3757 $[M\text{-}Na]^+$. (**2c**) ^{1}H NMR (250 MHz, $CDCl_3$) δ: 8.23-7.29 (m, 15H; H arom), 3.89-3.35 (m, 9H; O***C***H_3), 3.23-1.85 (m, 18H; PhC***C***H_2, ***C***H_2CO_2Me and ***C***$H_2CH_2CO_2Me$). HRMS calculated: 1314.2878; found: 1314.6711 $[M\text{-}Na]^+$. (**3a**) ^{1}H NMR (250 MHz, $CDCl_3/CS_2$) δ: 7.93-7.19 (m, 5H; H arom), 3.75, 3.69, 3.52 (s, 3H; O***C***H_3 isomers mixture), 2.53-2.37 (m, 4H; PhC***C***H_2 and ***C***H_2CO_2Me), 2-19-1.75 (m, 2H; ***C***$H_2CH_2CO_2Me$). HRMS calculated: 1053.0891; found: 1053.0590 $[M\text{-}Na]^+$. (**3b**) ^{1}H NMR (400 MHz, $CDCl_3$) δ: 7.96-7.00 (m, 10H; H arom), 4.10-3.22 (m, 6H; O***C***H_3), 2.71-1.93 (m, 12H; PhC***C***H_2, ***C***H_2CO_2Me and ***C***$H_2CH_2CO_2Me$). HRMS calculated: 1245.1963; found: 1245.1877 $[M\text{-}Na]^+$. (**3c**) HRMS calculated: 1433.2878; found: 1433.6976 $[M\text{-}Na]^+$.

- ***Synthesis of [70] and [60]DPM6 derivatives***

Synthesis of 4,4'-dihexyloxybenzophenone-p-tosylhydrazone (4). The synthesis of this compound was carried out following procedures previously reported in literature.[19d, e, 36] This compound was prepared starting from commercially available 4,4'-dihydroxy-benzophenone in two synthetic steps and on 5 g scale.

General procedure for preparation of 4,4'-(diazomethylene)bis(hexyloxybenzene). Sodium methoxide (3.73 mg, 0.069 mmol) was added in a microwave glass tube sealed with a teflon cap containing a solution of 4,4'-dihexyloxybenzophenone-p-tosylhydrazone **4** (25.30 mg, 0.046 mmol) in dry pyridine (2 mL). The mixture was stirred at room temperature for 15 minutes.

Synthesis of DPM6 derivatives (5a-b, 6a-b). A solution of C_{60} or C_{70} (50.00 mg) in 3 mL of oDCB (previously sonicated for about 15 minutes) was added to a previously prepared mixture containing the appropriate quantity of 4,4'-(diazomethylene)bis(hexyloxybenzene) in dry pyridine. The resulting mixture was kept under MW irradiation at 180 °C (48 W) for appropriate time. After cooling down, pyridine was removed under vacuum and the remaining reaction mixture was directly poured into a chromatographic column without removal of the remaining solvent (silica gel column conditions for C_{60}-derivatives: CS_2 to recover unreacted C_{60}, then hexane/toluene 4:1 and 3:1 for monoadduct recovery and finally 1:1 hexane/toluene for bisadducts recovery. Column conditions for C_{70}-derivatives: CS_2 to recover unreacted C_{70}, then hexane/toluene 6:1 and 4:1 for monoadduct recovery and finally 2:1 hexane/toluene for bisadducts recovery). Both mono and bis-adducts were solubilized and transferred to a centrifuge tube using a minimal amount of chloroform and subsequently precipitated with methanol. (**5a**) ^{1}H NMR (250 MHz, $CDCl_3$) δ: 7.97 (d, *J* = 8.6 Hz, 4H), 6.98 (d, *J* = 8.6 Hz, 4H), 3.98 (t, *J* = 6.5 Hz, 4H; O***C***H_2), 1.97-1.68 (m, 4H; OCH_2***C***H_2), 1.54-1.19 (m, 12H; -***C***H_2-), 0.91 (t, *J* = 6.6 Hz, 6H; CH_2***C***H_3). ^{13}C NMR (62.5 MHz, $CDCl_3/CS_2$) δ: 158.68 (***C***$_{Ar}$-O), 148.48, 145.34, 145.10, 145.02, 144.63, 144.52, 144.18, 143.78, 142.92, 142.85, 142.23, 142.05, 140.76, 138.17, 131.75, 131.20, 114.60, 79.57 (C_{60} sp^3), 68.00 (O***C***H_2), 57.30 (C_{DPM}), 31.67, 29.35, 25.85, 22.73, 14.09. HRMS calculated: 1087.2637; found: 1087.2247 $[M-H]^+$. (**5b**) ^{1}H NMR (250 MHz, $CDCl_3$) δ: 8.20-7.50 (m, 8H), 7.12-6.60 (m, 8H), 4.08-3.78 (m, 8H; O***C***H_2), 2.04-1.1 (m, 32H, -***C***H_2-), 1.1-0.64 (m, 12H; CH_2***C***H_3). HRMS calculated: 1453.5195; found: 1453.4471 $[M-Na]^+$. (**6a**) ^{1}H NMR (250 MHz, $CDCl_3$) δ: 7.95, 7.83, 7.46 (d, *J* = 7.9 Hz, 4H), 6.95, 6.65 (d, *J* = 7.9 Hz, 4H), 3.99, 3.80 (m, 4H;

isomers mixture), 2.09-1.12 (m, 16H; $OCH_2\boldsymbol{C}H_2$ and -$\boldsymbol{C}H_2$-), 1.12-0.68 (m, 6H; $CH_2\boldsymbol{C}H_3$). ^{13}C NMR (100 MHz, $CDCl_3/CS_2$) δ: 158.42, 155.69, 155.41, 151.83, 150.95, 150.61, 150.30, 149.18, 148.99, 148.90, 148.26, 148.05, 147.77, 147.29, 147.19, 146.85, 146.73, 145.82, 145.49, 145.25, 144.26, 143.71, 143.53, 143.11, 142.38, 141.42, 141.35, 139.81, 138.57, 137.16, 136.58, 133.74, 132.56, 131.52, 131.14, 130.99, 130.60, 130.38, 114.53, 114.19, 106.59, 71.72, 69.62, 67.83, 67.65, 65.46, 43.03, 40.73, 31.65, 29.31, 25.83, 22.76, 14.11. HRMS calculated: 1208.2637; found: 1208.2496 $[M-H]^+$. (**6b**) ^1H NMR (250 MHz, $CDCl_3$) δ: 8.21-7.33 (m, 8H), 7.21-6.49 (m, 8H), 4.26-3.60 (m, 8H; $O\boldsymbol{C}H_2$), 2.03-1.08 (m, 32H, -$\boldsymbol{C}H_2$-), 1.08-0.73 (m, 12H; $CH_2\boldsymbol{C}H_3$). HRMS calculated: 1570.5195; found: 1570.5037 $[M-H]^+$.

- ***Synthesis of [70] and [60]BHN derivatives***

Synthesis of sultine (7). The synthesis of this compound was carried out following a procedure previously reported in literature.[15a] To a solution in DMF (75 mL) of 1,2-bis(bromomethyl)benzene (1.15 g, 4.230 mmol), sodium hydroxymethanesulfinate (rongalite; 2.60 g, 16.902 mmol) and tetrabutylammonium bromide (413.00 mg, 1.268 mmol) were added. The mixture was stirred at 0 °C under argon atmosphere for 4 h. Then water was added and the mixture was extracted three times with dichloromethane. The combined organic layers were dried over Na_2SO_4, and the solvent was evaporated at 25 °C under vacuum to give colourless oil (627.35 mg, 88.2%). The crude product was used in the next reaction step without further purification.

Synthesis of BHN derivatives (8a-c, 9a-b). To a solution of C_{60} or C_{70} (50.00 mg) in 4 mL of oDCB (previously sonicated for about 20 minutes), the appropriate amount of sultine was added. The resulting mixture was kept under MW irradiation at appropriate temperature (7-10 W) for appropriate time. After cooling down, the reaction mixture was precipitated with methanol. The recovered residue was solubilized in a minimal amount of chloroform and precipitated again with methanol. Methanol was removed and the residue was solubilized in dichloromethane, adsorbed on silica and purified by flash column chromatography (silica gel column conditions for C_{60}-derivatives: hexane/toluene from 15:1 to 5:1 for mono- and bisadducts and finally 2:1 for trisadducts. Column conditions for C_{70}-derivatives: hexane/toluene from 15:1 to 5:1 for mono- and bisadducts and finally 2:1). Both mono- and bisadducts were solubilized and transferred to a centrifuge tube using a minimal amount of chloroform and subsequently precipitated with methanol. (**8a**) ^{1}H NMR (250 MHz, $CDCl_3$) δ: 7.68 (m, 2H), 7.57 (m, 2H), 4.81 (m, 2H), 4.72 (m, 2H). (**8b**) ^{1}H NMR (250 MHz, $CDCl_3$) δ: 8.00-7.30 (m, 8H), 5.18-3.36 (m, 8H). HRMS calculated: 929.1330; found: 929.0865 $[M-H]^+$. (**9b**) ^{1}H NMR (250 MHz, $CDCl_3$) δ: 7.95-6.96 (m, 8H), 4.74-3.10 (m, 8H). HRMS calculated: 1049.1331; found: 1049.0826 $[M-H]^+$.

- ***Synthesis of [70] and [60]ICBA derivatives***

Synthesis of ICBA derivatives (11a-c, 12a-b). To a solution of C_{60} or C_{70} (50.00 mg) in 4 mL of oDCB (previously sonicated for about 20 minutes), the appropriate amount of indene (**10**) was added. The resulting mixture was kept under MW irradiation at 180 °C (25 W) for appropriate time. After cooling down, the reaction mixture was precipitated with methanol. The recovered residue was solubilized in a minimal amount of chloroform and precipitated again with methanol. Methanol was removed and the residue was solubilized in dichloromethane, adsorbed on silica and purified by flash column chromatography (silica gel column conditions for C_{60}-derivatives: hexane/chloroform 25:1, then 20:1 for monoadduct, 10:1 for bisadducts mixture and finally 1:1 for trisadducts. Column conditions for C_{70}-derivatives: hexane/chloroform 30:1 and 25:1 for monoadducts, 15:1 and 9:1 for bisadducts and finally 5:1 for trisadducts). Both mono- and bisadducts were solubilized and transferred to a centrifuge tube using a minimal amount of chloroform and subsequently precipitated with methanol. (**11b**) ^{1}H NMR (250 MHz, $CDCl_3$) δ: 8.01-7.12 (m, 8H), 5.41-2.34 (m, 8H). HRMS calculated: 953.1252; found: 953.0886 $[M-H]^+$. (**11c**) HRMS calculated: 1068.1877; found: 1068.1566 $[M-H]^+$. (**12a**) ^{1}H NMR (400 MHz, $CDCl_3$) δ: 8.32-7.28 (m, 3H), 7.24-6.88 (m, 1H). 4.94-2.10 (m, 4H; isomers mixture). (**12b**) ^{1}H NMR (400 MHz, $CDCl_3$) δ: 7.87-6.72 (m, 8H), 5.19-1.97 (m, 8H). HRMS calculated: 1072.1252; found: 1072.0819 $[M-H]^+$.

3.6 References

[1] M. A. Green, K. Emery, Y. Hishikawa, W. Warta, E. D. Dunlop, *Prog. Photovolt: Res. Appl.* **2015**, *23*, 1-9.

[2] N. S. Sariciftci, L. Smilowitz, A. J. Heeger, F. Wudl, *Science* **1992**, *258*, 1474-1476.

[3] G. Yu, J. Gao, J. C. Hummelen, F. Wudl, A. J. Heeger, *Science* **1995**, *270*, 1789-1791.

[4] (a) C. J. Brabec, N. S. Sariciftci, J. C. Hummelen, *Adv. Funct. Mater.* **2001**, *11*, 15-26; (b) A. Mishra, P. Bäuerle, *Angew. Chem. Int. Ed.* **2012**, *51*, 2020-2067; (c) S. Günes, H. Neugebauer, N. S. Sariciftci, *Chem. Rev.* **2007**, *107*, 1324-1338; (d) M. T. Lloyd, J. E. Anthony, G. G. Malliaras, *Mater. Today* **2007**, *10*, 34-41; (e) G. Dennler, M. C. Scharber, C. J. Brabec, *Adv. Mater.* **2009**, *21*, 1323-1338; (f) C. J. Brabec, S. Gowrisanker, J. J. M. Halls, D. Laird, S. Jia, S. P. Williams, *Adv. Mater.* **2010**, *22*, 3839-3856; (g) A. W. Hains, Z. Liang, M. A. Woodhouse, B. A. Gregg, *Chem. Rev.* **2010**, *110*, 6689-6735; (h) O. Inganäs, F. Zhang, K. Tvingstedt, L. M. Andersson, S. Hellström, M. R. Andersson, *Adv. Mater.* **2010**, *22*, E100-E116; (i) C. J. Brabec, S. Gowrisanker, J. J. M. Halls, D. Laird, S. Jia, S. P. Williams, *Adv. Mater.* **2010**, *22*, 3839-3856.

[5] (a) S. E. Shaheen, C. J. Brabec, N. S. Sariciftci, F. Padinger, T. Fromherz, J. C. Hummelen, *Appl. Phys. Lett.* **2001**, *78*, 841-843; (b) F. Zhang, E. Perzon, X. Wang, W. Mammo, M. R. Andersson, O. Inganäs, *Adv. Funct. Mater.* **2005**, *15*, 745-750; (c) C. Shi, Y. Yao, Y. Yang, Q. Pei, *J. Am. Chem. Soc.* **2006**, *128*, 8980-8986; (d) F. B. Kooistra, J. Knol, F. Kastenberg, L. M. Popescu, W. J. H. Verhees, J. M. Kroon, J. C. Hummelen, *Org. Lett.* **2007**, *9*, 551-554; (e) J. Hou, M. H. Park, S. Zhang, Y. Yao, L. M. Chen, J. H. Li, Yang, *Macromolecules* **2008**, *41*, 6012-6018; (f) F. Silvestri, A. Marrocchi, M. Seri, C. Kim, T. J. Marks, A. Facchetti, A. Taticchi, *J. Am. Chem. Soc.* **2010**, *132*, 6108-6123; (g) G. Zhao, Y. He, Z. Xu, J. Hou, M. Zhang, J. Min, H. Y. Chen, M. Ye, Z. Hong, Y. Yang, Y. Li, *Adv. Funct. Mater.* **2010**, *20*, 1480-1487; (h) J. Hou, Z. Tan, Y. Yan, Y. He, C. Yang, Y. Li, *J. Am. Chem. Soc.* **2006**, *128*, 4911-4916; (i) W. Ma, C. Yang, X. Gong, K. Lee, A. J. Heeger, *Adv. Funct. Mater.* **2005**, *15*, 1617-1622.

[6] (a) D. H. Wang, D. Y. Kim, K. W. Choi, J. H. Seo, S. H. Im, J. H. Park, O. O. Park, A. J. Heeger, *Angew. Chem. Int. Ed.* **2011**, *50*, 5519-5523; (b) C. M. Amb, S. Chen, K. R. Graham, J. Subbiah, C. E. Small, F. So, J. R. Reynolds, *J. Am. Chem. Soc.* **2011**, *133*, 10062-10065; (c) L. Huo, J. Hou, H.-Y. Chen, S. Zhang, Y. Jiang, T. L. Chen, Y. Yang, *Macromolecules* **2009**, *42*, 6564-6571; (d) Y. Liang, Z. Xu, J. Xia, S.-T. Tsai, Y. Wu, G. Li, C. Ray, L. Yu, *Adv. Mater.* **2010**, *22*, E135-E138; (e) M. M. Wienk, J. M. Kroon, W. J. H. Verhees, J. Knol, J. C. Hummelen, P. A. Van Hal, R. A. J. Janssen, *Angew. Chem. Int. Ed.* **2003**, *42*, 3371-3375; (f) S. H. Park, A. Roy, S. Beaupré, S. Cho, N. Coates, J. S. Moon, D. Moses, M. Leclerc, K. Lee, A. J. Heeger, *Nature Photon.* **2009**, *3*, 297-303; (g) J. Peet, J. Y. Kim, N. E. Coates, W. L. Ma, D. Moses, A. J. Heeger, G. C. Bazan, *Nat. Mater.* **2007**, *6*, 497-500.

[7] J. You, L. Dou, K. Yoshimura, T. Kato, K. Ohya, T. Moriarty, K. Emery, C.-C. Chen, J. Gao, G. Li, Y. Yang, *Nat Commun* **2013**, *4*, 1446.

[8] M. C. Scharber, D. Mühlbacher, M. Koppe, P. Denk, C. Waldauf, A. J. Heeger, C. J. Brabec, *Adv. Mater.* **2006**, *18*, 789-794.

[9] (a) I. Riedel, E. Von Hauff, J. Parisi, N. Martín, F. Giacalone, V. Dyakonov, *Adv. Funct. Mater.* **2005**, *15*, 1979-1987; (b) A. Sánchez-Díaz, M. Izquierdo, S. Filippone,

N. Martin, E. Palomares, *Adv. Funct. Mater.* **2010**, *20*, 2695-2700; (c) H. J. Bolink, E. Coronado, A. Forment-Aliaga, M. Lenes, A. La Rosa, S. Filippone, N. Martín, *J. Mater. Chem.* **2011**, *21*, 1382-1386; (d) F. Piersimoni, S. Chambon, K. Vandewal, R. Mens, T. Boonen, A. Gadisa, M. Izquierdo, S. Filippone, B. Ruttens, J. D'Haen, N. Martin, L. Lutsen, D. Vanderzande, P. Adriaensens, J. V. Manca, *J. Phys. Chem. C* **2011**, *115*, 10873-10880; (e) D. Fernández, A. Viterisi, J. W. Ryan, F. Gispert-Guirado, S. Vidal, S. Filippone, N. Martín, E. Palomares, *Nanoscale* **2014**, *6*, 5871-5878; (f) I. Riedel, N. Martin, F. Giacalone, J. L. Segura, D. Chirvase, J. Parisi, V. Dyakonov, *Thin Solid Films* **2004**, *451-452*, 43-47.

[10] M. Lenes, G. Wetzelaer, F. Kooist, S. Veenstra, J. Hummelen, P. Blom, *Adv. Mater.* **2008**, *20*, 2116-2119.

[11] M. Lenes, S. W. Shelton, A. B. Sieval, D. F. Kronholm, J. C. Hummelen, P. W. M. Blom, *Adv. Funct. Mater.* **2009**, *19*, 3002-3007.

[12] (a) Y. Li, *Acc. Chem. Res.* **2012**, *45*, 723-733; (b) J. L. Delgado, P. A. Bouit, S. Filippone, M. A. Herranz, N. Martín, *Chem. Commun.* **2010**, *46*, 4853-4865; (c) Y. Li, *Chem. Asian J.* **2013**, *8*, 2316-2328; (d) E. Voroshazi, K. Vasseur, T. Aernouts, P. Heremans, A. Baumann, C. Deibel, X. Xue, A. J. Herring, A. J. Athans, T. A. Lada, H. Richter, B. P. Rand, *J. Mater. Chem.* **2011**, *21*, 17345-17352; (e) Y. He, Y. Li, *PCCP* **2011**, *13*, 1970-1983.

[13] F. Liu, Y. Gu, J. W. Jung, W. H. Jo, T. P. Russell, *J. Polym. Sci., Part B: Polym. Phys.* **2012**, *50*, 1018-1044.

[14] H. Youn, H. J. Park, L. J. Guo, *Small* **2015**, *11*, 2228-2246.

[15] (a) X. Meng, W. Zhang, Z. a. Tan, C. Du, C. Li, Z. Bo, Y. Li, X. Yang, M. Zhen, F. Jiang, J. Zheng, T. Wang, L. Jiang, C. Shu, C. Wang, *Chem. Commun.* **2012**, *48*, 425-427; (b) K.-H. Kim, H. Kang, S. Y. Nam, J. Jung, P. S. Kim, C.-H. Cho, C. Lee, S. C. Yoon, B. J. Kim, *Chem. Mater.* **2011**, *23*, 5090-5095; (c) E. Voroshazi, K. Vausseur, T. Aernouts, P. Heremans, A. Baumann, C. Deibel, X. Xue, A. J. Herring, A. J. Athans, T. A. Lada, H. Richter, B. P. Rand, *J. Mater. Chem.* **2011**, *21*, 17345-17352.

[16] (a) H. Kang, C.-H. Cho, H.-H. Cho, T. E. Kang, H. J. Kim, K.-H. Kim, S. C. Yoon, B. J. Kim, *ACS Appl. Mater. Interfaces* **2011**, *4*, 110-116; (b) E. T. Hoke, K. Vandewal, J. A. Bartelt, W. R. Mateker, J. D. Douglas, R. Noriega, K. R. Graham, J. M. J. Fréchet, A. Salleo, M. D. McGehee, *Adv. Energy Mater.* **2013**, *3*, 220-230; (c) G. Zhao, Y. He, Y. Li, *Adv. Mater.* **2010**, *22*, 4355-4358; (d) H. Xin, S. Subramaniyan, T.-W. Kwon, S. Shoaee, J. R. Durrant, S. A. Jenekhe, *Chem. Mater.* **2012**, *24*, 1995-2001; (e) Y. He, H.-Y. Chen, J. Hou, Y. Li, *J. Am. Chem. Soc.* **2010**, *132*, 1377-1382; (f) P. P. Khlyabich, B. Burkhart, B. C. Thompson, *J. Am. Chem. Soc.* **2011**, *133*, 14534-14537.

[17] (a) Z. He, C. Zhong, X. Huang, W.-Y. Wong, H. Wu, L. Chen, S. Su, Y. Cao, *Adv. Mater.* **2011**, *23*, 4636-4643; (b) L. Dou, J. You, J. Yang, C.-C. Chen, Y. He, S. Murase, T. Moriarty, K. Emery, G. Li, Y. Yang, *Nat Photon* **2012**, *6*, 180-185; (c) J. Y. Kim, K. Lee, N. E. Coates, D. Moses, T.-Q. Nguyen, M. Dante, A. J. Heeger, *Science* **2007**, *317*, 222-225.

[18] S. Beaupre, M. Leclerc, *J. Mater. Chem. A* **2013**, *1*, 11097-11105.

[19] (a) X. Meng, W. Zhang, Z. a. Tan, Y. Li, Y. Ma, T. Wang, L. Jiang, C. Shu, C. Wang, *Adv. Funct. Mater.* **2012**, *22*, 2187-2193; (b) Y. He, G. Zhao, B. Peng, Y. Li, *Adv. Funct. Mater.* **2010**, *20*, 3383-3389; (c) J. C. Hummelen, B. W. Knight, F. LePeq, F. Wudl, *J. Org. Chem.* **1995**, *60*, 532-538; (d) H. J. Bolink, E. Coronado, A. Forment-Aliaga, M. Lenes, A. La Rosa, S. Filippone, N. Martin, *J. Mater. Chem.* **2011**, *21*, 1382-1386; (e) R. Gómez, J. L. Segura, *Tetrahedron* **2009**, *65*, 540-546.

[20] (a) E. Rossi, T. Carofiglio, A. Venturi, A. Ndobe, M. Muccini, M. Maggini, *Energy Environ. Sci.* **2011**, *4*, 725-727; (b) H. Seyler, W. W. H. Wong, D. J. Jones, A. B. Holmes, *J. Org. Chem.* **2011**, *76*, 3551-3556.

[21] (a) R. Gedye, F. Smith, K. Westaway, H. Ali, L. Baldisera, L. Laberge, J. Rousell, *Tetrahedron Lett.* **1986**, *27*, 279-282; (b) R. J. Giguere, T. L. Bray, S. M. Duncan, G. Majetich, *Tetrahedron Lett.* **1986**, *27*, 4945-4948.

[22] (a) A. de la Hoz, A. Loupy, *Microwaves in Organic Synthesis: Third Edition, Vol. 1-2*, Wiley-VCH Verlag GmbH, Weinheim, Germany, **2013**; (b) M. Baghbanzadeh, L. Carbone, P. D. Cozzoli, C. O. Kappe, *Angew. Chem. Int. Ed.* **2011**, *50*, 11312-11359; (c) A. de la Hoz, A. Diaz-Ortiz, A. Moreno, *Chem. Soc. Rev.* **2005**, *34*, 164-178.

[23] (a) D. Dallinger, C. O. Kappe, *Chem. Rev.* **2007**, *107*, 2563-2591; (b) C. Oliver Kappe, *Chem. Soc. Rev.* **2008**, *37*, 1127-1139; (c) S. Caddick, *Tetrahedron* **1995**, *51*, 10403-10432; (d) P. Lidström, J. Tierney, B. Wathey, J. Westman, *Tetrahedron* **2001**, *57*, 9225-9283.

[24] (a) C. O. Kappe, D. Dallinger, *Mol Divers* **2009**, *13*, 71-193; (b) C. O. Kappe, *Angew. Chem. Int. Ed.* **2004**, *43*, 6250-6284; (c) L. Perreux, A. Loupy, *Tetrahedron* **2001**, *57*, 9199-9223; (d) M. B. Gawande, V. D. B. Bonifácio, R. Luque, P. S. Branco, R. S. Varma, *ChemSusChem* **2014**, *7*, 24-44.

[25] (a) A. de la Hoz, A. Loupy, in *Microwaves in Organic Synthesis, Vol. I*, Wiley-VCH Verlag GmbH, Weinheim, Germany, **2012**, pp. 427-486; (b) K. Tanaka, *Solvent-free Organic Synthesis*, Wiley-VCH Verlag GmbH, Weinheim, **2006**; (c) C. Strauss, R. Varma, *Microwaves in Green and Sustainable Chemistry* in *Microwave Methods in Organic Synthesis, Vol. 266* (Eds.: M. Larhed, K. Olofssonq), Springer Berlin Heidelberg, **2006**, pp. 199-231; (d) A. Loupy, A. Petit, J. Hamelin, F. Texier-Boullet, P. Jacquault, D. Mathé, *Synthesis* **1998**, *1998*, 1213-1234.

[26] (a) S. P. Economopoulos, N. Karousis, G. Rotas, G. Pagona, N. Tagmatarchis, *Curr. Org. Chem.* **2011**, *15*, 1121-1132; (b) E. Vázquez, M. Prato, *ACS Nano* **2009**, *3*, 3819-3824; (c) F. Langa, P. de la Cruz, *Comb. Chem. High Throughput Screening* **2007**, *10*, 766-782; (d) E. Vazquez, F. Giacalone, M. Prato, *Chem. Soc. Rev.* **2014**, *43*, 58-69.

[27] (a) F. Langa, P. de la Cruz, E. Espíldora, J. J. García, M. C. Pérez, A. de la Hoz, *Carbon* **2000**, *38*, 1641-1646; (b) P. de la Cruz, A. de la Hoz, L. M. Font, F. Langa, M. C. Pérez-Rodríguez, *Tetrahedron Lett.* **1998**, *39*, 6053-6056; (c) U. M. Fernández-Paniagua, B. Illescas, N. Martín, C. Seoane, P. de la Cruz, A. de la Hoz, F. Langa, *J. Org. Chem.* **1997**, *62*, 3705-3710; (d) P. de la Cruz, A. de la Hoz, F. Langa, B. Illescas, N. Martin, *Tetrahedron* **1997**, *53*, 2599-2608; (e) B. Illescas, N. Martín, C. Seoane, P. de la Cruz, F. Langa, F. Wudl, *Tetrahedron Lett.* **1995**, *36*, 8307-8310.

[28] V. Campisciano, S. Riela, R. Noto, M. Gruttadauria, F. Giacalone, *RSC Adv.* **2014**, *4*, 63200-63207.

[29] J. C. Hummelen, B. W. Knight, F. LePeq, F. Wudl, *J. Org. Chem.* **1995**, *60*, 532-538.

[30] M. Prato, V. Lucchini, M. Maggini, E. Stimpfl, G. Scorrano, M. Eiermann, T. Suzuki, F. Wudl, *J. Am. Chem. Soc.* **1993**, *115*, 8479-8480.

[31] (a) P. Ceroni, F. Conti, C. Corvaja, M. Maggini, F. Paolucci, S. Roffia, G. Scorrano, A. Toffoletti, *J. Phys. Chem. A* **1999**, *104*, 156-163; (b) R. A. J. Janssen, J. C. Hummelen, F. Wudl, *J. Am. Chem. Soc.* **1995**, *117*, 544-545.

[32] (a) J. C. Hummelen, B. W. Knight, F. LePeq, F. Wudl, J. Yao, C. L. Wilkins, *J. Org. Chem.* **1995**, *60*, 532-538; (b) A. B. Smith, R. M. Strongin, L. Brard, G. T. Furst, W. J. Romanow, K. G. Owens, R. J. Goldschmidt, R. C. King, *J. Am. Chem. Soc.* **1995**, *117*, 5492-5502.

[33] A. Hirsch, *The Higher Fullerenes: Covalent Chemistry and Chirality* in *Fullerenes and Related Structures* (Eds.: C. Thilgen, F. Diederich), Springer-Verlag, Berlin — Heidelberg, Germany, **2000**, pp. 135-172.
[34] A. de la Hoz, A. Díaz-Ortis, A. Moreno, F. Langa, *Eur. J. Org. Chem.* **2000**, *2000*, 3659-3673.
[35] B. L. Hayes, in *Microwave Synthesis: Chemistry at the Speed of Light*, CEM Publishing, Matthews NC, **2002**.
[36] M.-P. Hernández, F. Monroy, F. Ortega, R. G. Rubio, Á. Martín-Domenech, E. M. Priego, L. Sánchez, N. Martín, *Langmuir* **2001**, *17*, 3317-3328.

List of Publications

- A. M. P. Salvo, V. Campisciano, H. A. Beejapur, F. Giacalone, M. Gruttadauria, *"A Simple Procedure for Oxidation of Alcohols using [Bis(acetoxy)iodo]benzene and a Catalytic Amount of Bromide Ions in Ethyl Acetate"*, *Synlett* **2015**; *26*, 1179-1184.

- V. Campisciano, V. La Parola, L. F. Liotta, F. Giacalone, M. Gruttadauria, *"Fullerene-ionic liquids conjugates: a new class of hybrid materials with unprecedented properties"*, *Chem. Eur. J.* **2015**, *21*, 3327-3334.

- H. A. Beejapur, V. Campisciano, F. Giacalone, M. Gruttadauria, *"Catalytic synergism in a $C_{60}IL_{10}TEMPO_2$ hybrid in the efficient oxidation of alcohols"*, *Adv. Synth. Catal.* **2015**, *357*, 51-58.

- V. Campisciano, S. Riela, R. Noto, M. Gruttadauria, F. Giacalone, *"Efficient Microwave-mediated synthesis of fullerene acceptors for Organic Photovoltaics"*, *RSC Adv.*, **2014**, *4*, 63200-63207.

- H. A. Beejapur, V. Campisciano, P. Franchi, M. Lucarini, F. Giacalone, M. Gruttadauria, *"Fullerene as a Platform for Recyclable TEMPO Organocatalysts for the Oxidation of Alcohols"*, *ChemCatChem* **2014**, *6*, 2419-2424.

- F. Giacalone, V. Campisciano, C. Calabrese, V. La Parola, Z. Syrgiannis, M. Prato, M. Gruttadauria, *"SWCNT-PAMAM-PdNP: An Efficient and Recyclable Catalyst for Suzuki and Heck Cross-Coupling Reactions"*, submitted.

Communications to Congress

- 6th CIS-GIC-AIZ Congress, Amantea (Italy) 14-17 June 2015.
  Poster communication: V. Campisciano, C. Calabrese, V. La Parola, L. F. Liotta, C. Aprile, F. Giacalone, M. Gruttadauria, *"Supported fullerene C_{60}-ionic liquid hybrids as new catalytic materials".*

- Convegno congiunto delle sezioni Sicilia e Calabria della Società Chimica Italiana, Palermo (Italy) 1-2 December 2014.
  Poster communication: V. Campisciano, S. Riela, R. Noto, M. Gruttadauria, F. Giacalone, *"Sintesi efficiente mediata da microonde di derivati di fullerene per dispositivi fotovoltaici organici"*.

- XXV congresso nazionale della Società Chimica Italiana, Università della Calabria, Rende (Italy) 7-12 September 2014.
  Oral communication: V. Campisciano, F. Giacalone, M. Gruttadauria, *"Nuovi ibridi [60]fullerene-liquido ionico"*.

- 6th ORCA-COST Meeting, Mondello (Italy) 7-10 May 2014.
  Poster communication: V. Campisciano, H. A. Beejapur, F. Giacalone, M. Gruttadauria, *"C_{60}-TEMPO-IL hybrid: "release and catch" organocatalyst for the oxidation of alcohols".*

- 6th ORCA-COST Meeting, Mondello (Italy) 7-10 May 2014.
  Poster communication: H. A. Beejapur, V. Campisciano, F. Giacalone, M. Gruttadauria, *"Organocatalytic Alcohol Oxidation Catalyzed by Recyclable TEMPO-functionalized [60]fullerene"*.

- Convegno congiunto delle sezioni Sicilia e Calabria della Società Chimica Italiana, Catania (Italy) 2-3 December 2013.
  Oral communication: F. Giacalone, H. A. Beejapur, V. Campisciano, R. Noto, M. Gruttadauria, "*Sistemi Tempo-C_{60} come catalizzatori riciclabili attivi nell'ossidazione di alcoli"*.

Period Abroad

Three months stay as visiting PhD student at the University of Namur (Belgium), under supervision of Prof. Carmela Aprile – Laboratory of Applied Material Chemistry (CMA) Unit of Nanomaterial Chemistry (CNano), Chemistry Department.

Glossary of Terms

BHJ-PSCs	Bulk Heterojunction Polymer Solar Cells
CNFs	Carbon Nanoforms
CNTs	Carbon Nanotubes
DSC	Differential Scanning Calorimetry
ESI	Electrospray Ionization
FF	Fill Factor
HOMO	Highest Occupied Molecular Orbital
HPLC	High Performance Liquid Chromatography
HR-TEM	High Resolution Transmission Electron Microscopy
ICP-OES	Inductively Coupled Plasma – Optical Emission Spectrometry
ILs	Ionic Liquids
ITO	Indium-Tin Oxide
J_{sc}	Short Circuit Current Density
LUMO	Lowest Unoccupied Molecular Orbital
MNPs	Metal Nanoparticles
MP-AES	Microwave Plasma – Atomic Emission Spectroscopy
MW	Microwave
MWCNTs	Multi-Walled Carbon Nanotubes
oDCB	1,2-Dichlorobenzene
OPV	Organic Photovoltaic
PAMAM	Poly-Amidoamine
PCE	Power Conversion Efficiency
PEDOT:PSS	Poly(3,4-ethylenedioxythiophene):polystyrene Sulfonate
SAXS	Small-Angle X-ray Scattering
SEM-EDAX	Scanning Electron Microscopy–Energy-Dispersive X-ray Analysis
SILLP	Supported Ionic Liquid-Like Phase
SILP	Supported Ionic Liquid Phase
SSA	Specific Surface Area
SWCNTs	Single-Walled Carbon Nanotubes
TEA	Triethylamine
TGA	Thermogravimetric Analysis

TOF	Turnover Frequency
TON	Turnover Number
TSILs	Task Specific Ionic Liquids
$\boldsymbol{V_{oc}}$	Open Circuit Voltage
XPS	X-ray Photoelectron Spectroscopy
XRD	X-ray Diffraction